

**THE EXTRACELLULAR MATRIX REGULATES MYOBLAST
MIGRATION DURING WOUND HEALING**

by

Kyle Peter Goetsch

BSc. Hons (*cum laude*)

Submitted in fulfillment of the academic requirements for the degree of Philosophy of Science in the

Discipline of Biochemistry

School of Life Sciences

University of KwaZulu-Natal

Pietermaritzburg

November 2012

As the candidate's supervisor I have approved this thesis for submission.

Signed: _____ Name: Dr. C. U. Niesler Date: _____

As the candidate's co-supervisor I have approved this thesis for submission.

Signed: _____ Name: Prof. K. H. Myburgh Date: _____

ABSTRACT

Mammalian skeletal muscle can regenerate after injury and this response is primarily mediated by the satellite cell, a muscle stem cell. Following injury, satellite cells are activated to myoblasts, undergo rapid proliferation, migrate towards the injury site, and subsequently differentiate into myotubes in order to facilitate functional muscle repair. Fibrosis, caused by the secretion of structural extracellular matrix (ECM) proteins such as collagen I and fibronectin, by fibroblasts, impairs complete functional repair of the muscle. In this study, the role of the microenvironment during wound conditions was assessed by analysing the effect of specific extracellular matrix and growth factors on myoblast migration. The role of the Rho/ROCK pathway as a possible mechanism in mediating the effects seen was investigated. In order to analyse wound repair in an *in vitro* setting, we optimised and improved a wound healing model specifically designed for skeletal muscle repair. To this end we also developed a co-culture assay using primary myoblasts and fibroblasts isolated from the same animal.

The studies showed that collagen I and fibronectin both increased myoblast migration in a dose-dependent manner. Decorin displayed opposing effects on cellular movement, significantly increasing collagen I-stimulated, but not fibronectin-stimulated, migration of myoblasts. ROCK inhibitor studies revealed a significant increase in migration on uncoated plates following inhibition with Y-27632 compared to untreated control. When cells were cultured on ECM components (Matrigel, collagen I, or fibronectin), the inhibitory effect of Y-27632 on migration was reduced. Analysis of ROCK and vinculin expression, and localization at the leading front, showed that ROCK inhibition resulted in loosely packed focal adhesion complexes (matrix dependent). A reduced adhesion to the ECM could explain the increased migration rates observed upon inhibition with Y-27632.

We also investigated the role of TGF- β and decorin during wound repair, as TGF- β is a known pro-fibrotic agent. TGF- β treatment decreased wound closure rates; however, the addition of decorin with TGF- β significantly increased wound closure. The addition of ECM components, Matrigel and collagen I enhanced the effect seen in response to TGF- β and decorin; however, fibronectin negated this effect, with no increase in migration seen compared to the controls.

In conclusion, the importance of extracellular matrix components in regulating myoblast migration and therefore skeletal muscle wound repair was demonstrated. We emphasize that, in order to gain a better understanding of skeletal muscle wound repair, the combination of ECM and growth factors released during wounding need to be utilised in assays which mimic the *in vivo* environment more closely.

PREFACE

The experimental work described in this dissertation was carried out in the Discipline of Biochemistry, School of Life Sciences, University of KwaZulu-Natal, Pietermaritzburg, from January 2009 to November 2012, under the supervision of Dr. C. U. Niesler and Prof. K. H. Myburgh.

These studies represent original work by the author and have not otherwise been submitted in any form for any degree or diploma to any tertiary institution. Where use has been made of the work of others it is duly acknowledged in the text.

Signed:

.....

Date:

.....

DECLARATION 1 - PLAGIARISM

I, Kyle Peter Goetsch, declare that:

1. The research reported in this thesis, except where otherwise indicated, is my original research.
2. This thesis has not been submitted for any degree or examination at any other university.
3. This thesis does not contain other persons' data, pictures, graphs or other information, unless specifically acknowledged as being sourced from other persons.
4. This thesis does not contain other persons' writing, unless specifically acknowledged as being sourced from other researchers. Where other written sources have been quoted, then:
 - a. Their words have been re-written but the general information attributed to them has been referenced
 - b. Where their exact words have been used, then their writing has been placed in italics and inside quotation marks, and referenced.
5. This thesis does not contain text, graphics or tables copied and pasted from the Internet, unless specifically acknowledged, and the source being detailed in the thesis and in the References sections.

Signed:

.....

Date:

.....

DECLARATION 2 – PUBLICATIONS

DETAILS OF CONTRIBUTION TO PUBLICATIONS that form part and/or include research presented in this thesis (include publications in preparation, submitted, *in press* and published and give details of the contributions of each author to the experimental work and writing of each publication)

K.P. Goetsch, K. Kallmeyer & C.U. Niesler (2011) Decorin modulates collagen I-stimulated, but not fibronectin-stimulated, migration of C2C12 myoblasts, *Matrix Biology*, 30, pp 109-117 – **PUBLISHED**

K.P. Goetsch & C.U. Niesler (2011) Optimisation of the scratch assay for *in vitro* skeletal muscle wound healing analysis, *Analytical Biochemistry*, 411, pp 158-160 - **PUBLISHED**

K.P. Goetsch, C. Snyman, E. Elliott, C.U. Niesler (2012) Y-27632 modulates mesenchymal and epithelial cell migration in a matrix-dependent manner, *Matrix Biology* – **SUBMITTED**

K.P. Goetsch, K.H. Myburgh, C.U. Niesler (2012) Simultaneous isolation of enriched myoblasts and fibroblasts for migration analysis within a novel co-culture assay – *Stem Cell Research* – **IN REVISION**

K.P. Goetsch, K.H. Myburgh, C.U. Niesler (2013) The TGF- β /decorin complex differentially influences myoblast migration in a ECM dependant manner– **IN PREPARATION**

K.P. Goetsch, K.H. Myburgh, C.U. Niesler (2013) The evolution of skeletal muscle migration assays – **IN PREPARATION**

Signed:

.....

Date:

.....

ACKNOWLEDGEMENTS

I would like to start off by thanking God, as without Him this project would not have been possible to begin with. He has been the guiding force throughout my life and has been my rock.

Dr. Niesler you have been an unending source of motivation, encouraging me to pursue my own ideas and have given me the confidence to believe in my abilities as a young scientist.

Prof. Myburgh for all your support during my PhD and for helping me with primary culture isolation and training in the use of small laboratory animals.

Celia Snyman; for your vast reservoir of knowledge and your passion which feeds my own. I really enjoy our discussions and debates and look forward to many more. Without your training on the confocal microscope this project would never be what it has become. I owe you many many thanks.

Thanks to the Microscopy and Micro-analysis Unit, for their assistance in sample preparation and use of the scanning electron and confocal microscopes. I would especially like to thank Shirley for her assistance and for always being willing to help. We both learnt a lot from each other.

Prof. Goldring and Prof. Coetzer, for always offering guidance when I need it, and for instilling a pride in me for the work that I do.

Thanks to lab 39 which has been my lab, office, home and prison. Dennis, for always keeping my methods in check and for helping me with ECL, your singing is improving. Scott, for his excellent admin skills and making sure that there is always coffee when it is needed.

Bridget Cumming for helping me with my stats, without you I would have been lost for a very long time.

I would like to thank my family for their constant prayers and encouragement, for showing an interest in my work even though they do not get most of it and for instilling in me the attitude that I can do anything I set my mind to. Each and every one of you has shaped me into the person I am today and these simple thanks are not enough to convey my gratitude.

To Rachel, who has been my inspiration and constant source of encouragement, as well as my support when times get tough. Thank you Angel.

Finally, I would like to thank Charmaine and Robyn for putting up with my constant interruptions. Your smiles in the morning can turn a bad day into a good one. Thanks for that. To TIA, NRF and UKZN for their financial support and to everyone else I have not mentioned. There are so many it is hard to keep track.

“The financial assistance of the Technology Innovation Agency towards this research is hereby acknowledged. Opinions expressed and conclusions arrived at, are those of the author and are not necessarily to be attributed to TIA.”

CONTENTS

ABSTRACT	<i>Page</i>
PREFACE	i
DECLARATIONS	iii
ACKNOWLEDGEMENTS	iv-v
LIST OF FIGURES & TABLES	vi
ABBREVIATIONS	xiv
	xviii

CHAPTER 1 – LITERATURE REVIEW 1

1.1	<i>SATELLITE CELLS</i>	1
1.2	<i>EXTRACELLULAR MATRIX COMPONENTS & GROWTH FACTORS</i>	3
1.2.1	<i>Extracellular Matrix</i>	3
1.2.2	<i>Growth Factors</i>	3
1.2.2.1	<i>Hepatocyte Growth Factors (HGF)</i>	3
1.2.2.2	<i>Fibroblast Growth Factors (FGF)</i>	4
1.2.2.3	<i>Transforming Growth Factor beta (TGF-β)</i>	5
1.2.2.4	<i>Insulin-like Growth Factor-I (IGF-I)</i>	5
1.2.3	<i>Skeletal Muscle ECM Components, Receptors and Proteases</i>	6
1.2.4	<i>Integrins</i>	7
1.2.5	<i>Collagens</i>	9
1.2.6	<i>Tenascins</i>	9
1.2.7	<i>Fibronectin</i>	10
1.2.8	<i>Laminins</i>	10
1.2.9	<i>Glycans</i>	10
1.2.10	<i>Proteases involved in ECM Degradation</i>	12
1.3	<i>MYOBLAST MIGRATION MECHANISMS</i>	13
1.3.1	<i>Migration</i>	13
1.3.1.1	<i>Cell Shape during Migration</i>	14
1.3.2	<i>Intracellular Signal Transduction</i>	16
1.3.2.1	<i>Rho-GTPases Role in Cellular Migration</i>	18

1.3.2.3	<i>Rho/ROCK Activation</i>	20
1.3.2.3	<i>ROCK Structure</i>	21
1.4	<i>SKELETAL MUSCLE GROWTH & REPAIR</i>	22
1.4.1	<i>Muscle Injury & Wound Repair</i>	22
1.4.1.1	<i>In Situ Necrosis</i>	22
1.4.1.2	<i>Shear Type Injuries</i>	24
1.4.2	<i>Fibrosis</i>	26
1.4.3	<i>Myoblast Transplantation Challenges</i>	27
1.5	<i>SUMMARY AND AIMS</i>	29

CHAPTER 2 – *IN VITRO* MODEL DEVELOPMENT & OPTIMIZATION 31

2.1	INTRODUCTION	31
2.2	EXPERIMENTAL PROCEDURES	35
2.2.1	<i>Animals</i>	35
2.2.2	<i>Culture Conditions</i>	35
2.2.3	<i>Scratch Assay</i>	35
2.2.4	<i>Live Cell Imaging</i>	36
2.2.5	<i>Preparation of Primary Cultures</i>	36
2.2.6	<i>Isolation of Myoblasts and Fibroblasts</i>	37
2.2.7	<i>Enrichment of Primary Cultures</i>	38
2.2.8	<i>Immunofluorescence of Isolated Primary Cultures</i>	38
2.2.9	<i>Co-culture Assay</i>	39
2.2.10	<i>Statistics</i>	40
2.3	RESULTS	41
2.3.1	<i>Scratch Assay Development</i>	41
2.3.2	<i>Isolation and Enrichment of Murine Myoblasts & Fibroblasts</i>	44
2.3.3	<i>Lineage Confirmation for use in the Co-Culture Assay</i>	46

2.3.4	<i>Validation and Application of Co-Culture Assay to determine the effect of Fibroblasts on Myoblast Migration</i>	48
2.4	DISCUSSION	51
 CHAPTER 3 – THE EXTACELLULAR MATRIX AFFECTS C2C12 MYOBLAST MIGRATION		 54
<hr/>		
3.1	INTRODUCTION	54
3.2	EXPERIMENTAL PROCEDURES	57
3.2.1	<i>Cell Culture</i>	57
3.2.2	<i>Collagen I Coating</i>	57
3.2.3	<i>Fibronectin Coating</i>	57
3.2.4	<i>Scratch Assay</i>	58
3.2.5	<i>Immunocytochemical analysis of ROCK -1 & -2</i>	58
3.2.6	<i>Western Blot Analysis of ROCK-1 & -2</i>	58
3.2.7	<i>Scanning Electron Microscopy (SEM)</i>	59
3.2.8	<i>Statistical Analysis</i>	59
3.3	RESULTS	60
3.3.1	<i>Dose responses for decorin, fibronectin and collagen I</i>	60
3.3.2	<i>Decorin facilitates collagen I-stimulated wound closure</i>	62
3.3.3	<i>Effect of Collagen & Decorin on Myoblast Migration in Differentiated Myotubes</i>	63
3.3.4	<i>Effect of Decorin and Collagen I on Primary Cultured Murine Myoblast Migration</i>	65
3.3.5	<i>Decorin does not Increase Fibronectin Facilitated Migration</i>	66
3.3.6	<i>Total ROCK-2 Expression is Higher than ROCK-1 Expression in C2C12 myoblasts</i>	67
3.3.7	<i>ROCK 2, but not ROCK 1, localizes to focal adhesions in C2C12 myoblasts</i>	68

3.3.8	<i>Increased number of ROCK-2-containing focal adhesions during decorin & collagen I facilitated migration</i>	68
3.3.9	<i>Fibronectin does not increase active ROCK-2 focal adhesions during migration</i>	70
3.4	DISCUSSION	71

CHAPTER 4 – ROCK INHIBITOR (Y-27632) MODULATES MYOBLAST MIGRATION IN A MATRIX-DEPENDENT MANNER **74**

4.1	INTRODUCTION	74
4.2	EXPERIMENTAL PROCEDURES	76
4.2.1	<i>Collagen & Matrigel Coating</i>	76
4.2.2	<i>Scratch Assay</i>	76
4.2.3	<i>Live Cell Imaging</i>	76
4.2.4	<i>Immunocytochemical Analysis of ROCK-2 & Vinculin</i>	77
4.2.5	<i>Statistics</i>	77
4.3	RESULTS	78
4.3.1	<i>Y-27632 differentially affects myoblast morphology and velocity</i>	78
4.3.2	<i>Effect of Y-27632 on migration of C2C12 myoblasts cultured on Matrigel</i>	80
4.3.3	<i>Effect of Y-27632 on C2C12 myoblast migration cultured on collagen I</i>	81
4.3.4	<i>Localization of ROCK-2 & vinculin within migrating C2C12 myoblasts cultured on Matrigel and collagen I</i>	82
4.3.5	<i>Y-27632 increases the total area of ROCK-2-containing focal adhesion clusters in C2C12 myoblasts</i>	84
4.4	DISCUSSION	88

CHAPTER 5 – THE TGF-β/DECORIN COMPLEX DIFFERENTIALLY INFLUENCES MYOBLAST MIGRATION IN A ECM DEPENDANT MANNER		92
<hr/>		
5.1	INTRODUCTION	92
5.2	EXPERIMENTAL PROCEDURES	94
5.2.1	<i>General</i>	94
5.2.2	<i>Cell Culture</i>	94
5.2.3	<i>Scratch Assay</i>	94
5.2.4	<i>Immunocytochemical Analysis of ROCK-2 & Vinculin</i>	95
5.2.5	<i>Statistics</i>	95
5.3	RESULTS	96
5.3.1	<i>Decorin modulates the inhibitory effect of TGF-β on myoblast migration</i>	96
5.3.2	<i>Decorin and TGF-β promote HSKM cell migration in the presence of Matrigel</i>	99
5.3.3	<i>Decorin and TGF-β promote HSKM cell migration in the presence of collagen I, but not fibronectin</i>	101
5.4	DISCUSSION	105

CHAPTER 6 – 3D SKELETAL MUSCLE TISSUE DEVELOPMENT

	& FUTURE WORK	108
6.1	INTRODUCTION	108
6.2	EXPERIMENTAL PROCEDURES	110
6.2.1	<i>General</i>	110
6.2.2	<i>Cell Culture</i>	110
6.2.3	<i>MC-8 chamber</i>	110
6.2.4	<i>Silicone chamber</i>	111
6.2.5	<i>Collagen I Gel Construct</i>	111
6.2.6	<i>Collagen I/Matrigel Construct</i>	111
6.2.7	<i>Fibrin Gel Construct</i>	112
6.2.8	<i>Hydrogel Construct</i>	112
6.3	RESULTS	113
6.3.1	<i>Development of an in vitro 3-Dimensional Skeletal Muscle Tissue Model</i>	113
6.3.2	<i>MC-8 Chamber</i>	115
6.3.3	<i>Silicone Chamber</i>	117
6.3.4	<i>Conclusion</i>	120
CHAPTER 7 – CONCLUDING REMARKS		121
PUBLICATIONS		123
CONFERENCE ABSTRACTS		124
REFERENCES		130

LIST OF FIGURES & TABLES

CHAPTER 1 – LITERATURE REVIEW		Page
<i>Figure 1.1</i>	<i>Satellite cell activation, proliferation, and differentiation and concomitant transcription factor expression</i>	2
<i>Table 1.1</i>	<i>ECM components and proteases within the interstitial ECM and basement membrane of skeletal muscle</i>	7
<i>Figure 1.2</i>	<i>The structural components of an integrin indicating the specific domains</i>	8
<i>Figure 1.3</i>	<i>Two distinct mechanisms for the binding of decorin to the $\alpha2\beta1$ integrin</i>	12
<i>Figure 1.4</i>	<i>Specific ECM interactions that facilitate 2D and 3D migration</i>	15
<i>Figure 1.5</i>	<i>The major members of the Rho-GTPases and their respective functions</i>	17
<i>Figure 1.6</i>	<i>The effect of GTPases on cellular migration with particular focus on the Rho/ROCK pathway</i>	19
<i>Figure 1.7</i>	<i>Mechanism of Rho activation and subsequent ROCK phosphorylation</i>	20
<i>Figure 1.8</i>	<i>The specific domains and regions of ROCK-1 and -2</i>	21
<i>Figure 1.9</i>	<i>Myofiber regeneration following necrosis</i>	23
<i>Figure 1.10</i>	<i>Myofiber regeneration after shear injury</i>	25
<i>Figure 1.11</i>	<i>Overview of growth factors and ECM components that affect basal myoblast migration along with their respective signaling pathways</i>	30

CHAPTER 2 - *IN VITRO* MODEL DEVELOPMENT & OPTIMIZATION

Table 2.1	<i>Summary of widely utilized migration assays and variations on these models</i>	31
Figure 2.1	<i>Pre- and post- cellular migration within different migration assays</i>	33
Figure 2.2	<i>Isolation of primary cultured fibroblasts and myoblasts</i>	37
Figure 2.3	<i>Co-culture assay utilizing isolated primary culture myoblasts and fibroblasts</i>	39
Figure 2.4	<i>Scratch assay optimization for C2C12 myoblast cell line</i>	41
Figure 2.5	<i>Wound front at 0 and 7 hours depicting a classically migrating C2C12 myoblast</i>	42
Figure 2.6	<i>Live cell tracking of migrating C2C12 myoblasts</i>	43
Figure 2.7	<i>Primary cultured myoblasts from PPI-PP5</i>	45
Figure 2.8	<i>Percentage desmin⁺/Pax7⁺ cells (PPI-PP5) of the total cellular population</i>	46
Figure 2.9	<i>Validation of co-culture wound healing assay</i>	47
Figure 2.10	<i>Preliminary findings of co-culture assay versus scratch assay</i>	48
Figure 2.11	<i>Dose response of fibroblast cell number on myoblast migration</i>	50

CHAPTER 3 – THE EXTRACELLULAR MATRIX AFFECTS C2C12 MYOBLAST MIGRATION

Figure 3.1	<i>Decorin, fibronectin, and collagen I dose optimization</i>	61
Figure 3.2	<i>Effects of decorin on collagen I-stimulated myoblast migration</i>	62
Figure 3.3	<i>Effect of collagen type I and decorin on myoblast migration amongst differentiated C2C12 myotubes</i>	64
Figure 3.4	<i>Effect of collagen type I and decorin on primary cultured murine myoblast migration</i>	65
Figure 3.5	<i>Effects of decorin and fibronectin on the percentage wound closure and rate of C2C12 myoblast migration</i>	66
Figure 3.6	<i>ROCK-1 and -2 protein expression in C2C12 myoblasts</i>	67

<i>Figure 3.7</i>	<i>ROCK-1 and -2 localization in C2C12 myoblasts</i>	68
<i>Figure 3.8</i>	<i>ROCK-2 localization in response to incubation with decorin and collagen I during C2C12 myoblast migration</i>	69
<i>Figure 3.9</i>	<i>ROCK-2 localization within C2C12 myoblasts migrating on fibronectin</i>	70

CHAPTER 4 – ROCK INHIBITOR (Y-27632) MODULATES MYOBLAST MIGRATION IN A MATRIX-DEPENDENT MANNER

<i>Figure 4.1</i>	<i>Effect of Y-27632 on morphology and migration patterns of C2C12 myoblasts on uncoated plates</i>	79
<i>Figure 4.2</i>	<i>Effect of Y-27632 on C2C12 myoblast wound closure when cultured on Matrigel</i>	80
<i>Figure 4.3</i>	<i>Effect of Y-27632 on C2C12 myoblast wound closure when cultured on collagen I</i>	81
<i>Figure 4.4</i>	<i>Cellular expression of ROCK-2 and vinculin in response to Matrigel and collagen I \pm Y-27632</i>	83
<i>Figure 4.5</i>	<i>Effect of Matrigel and collagen I \pm Y-27632 on the number of ROCK-2 containing focal adhesion clusters in C2C12 myoblasts</i>	85
<i>Figure 4.6</i>	<i>Effect of Matrigel and collagen I \pm Y-27632 on the area of focal adhesion clusters in C2C12 myoblasts</i>	87
<i>Figure 4.6</i>	<i>Effect of Y-27632 on myoblast migration in relation to untreated ECM-coated plates</i>	90

CHAPTER 5 – THE TGF- β /DECORIN COMPLEX DIFFERENTIALLY INFLUENCES MYOBLAST MIGRATION IN A ECM DEPENDANT MANNER

<i>Figure 5.1</i>	<i>Decorin and TGF-β2 enhance C2C12 myoblast migration</i>	95
<i>Figure 5.2</i>	<i>Decorin and TGF-β2 in combination promote the migration of HSKM myoblasts</i>	97
<i>Figure 5.3</i>	<i>Decorin and TGF-β2 in combination promote the migration of HSKM myoblasts on matrigel coated plates</i>	99
<i>Figure 5.4</i>	<i>Decorin and TGF-β2 in combination promote the</i>	

	<i>migration of HSKM myoblasts on collagen I coated plates</i>	101
Figure 5.5	<i>Decorin and TGF-β2 in combination do not promote the migration of HSKM myoblasts on fibronectin coated plates</i>	103
CHAPTER 6 – 3D SKELETAL MUSCLE TISSUE DEVELOPMENT & FUTURE WORK		
Figure 6.1	<i>MC-8 and customized silicone chamber for the development of in vitro 3D skeletal muscle</i>	111
Table 6.1	<i>Optimization of 3D construct model within two different chamber systems</i>	112
Figure 6.2	<i>Development of a 3D in vitro muscle tissue model utilizing the MC-8 chamber system</i>	114
Figure 6.3	<i>Skeletal muscle formation using a silicone tube model</i>	116
Figure 6.4	<i>Development of a 3D in vitro muscle tissue model utilizing the silicone tube system</i>	117

ABBREVIATIONS

ADAM	a disintegrin and metalloproteinase domain
ATP	adenosine triphosphate
BMP	bone morphogenetic proteins
cDNA	complimentary deoxyribonucleic acid
CR	cysteine-rich domain
DMD	Duchenne/Becker muscle dystrophy
DMEM	Dulbecco's Modified Eagle Serum
EGF	epidermal growth factor
ECM	extracellular matrix
FCS	fetal calf serum
FGF	fibroblast growth factor
FGFR	fibroblast growth factor receptor
GAG	glycosaminoglycan chain
GAP	GTPase-activating protein
GAPDH	Glyceraldehyde-3-Phosphate Dehydrogenase
GEF	guanine nucleotide exchange factor
GDF	growth differentiation factor
GDI	guanine nucleotide dissociation inhibitor
GDP	guanosine diphosphate
GTP	guanosine triphosphate
HGF	hepatocyte growth factor
HS	horse serum
HsKM	human skeletal myoblasts
IGF(s)	insulin-like growth factor(s)
IGF-IR	insulin-like growth factor-I receptor
LIF	leukemia inhibitory factor
LIMK	LIM Kinase
LM	laminin
MAPK	mitogen-activated protein kinase
M-cadherin	myogenic cadherin
MyHC	myosin heavy chain
MLC	myosin light chain
MMP	matrix metalloproteinase
MRCK	myotonic dystrophy kinase-related Cdc42-binding kinase
mRNA	messenger ribonucleic acid
MT1-MMP	membrane type-1 matrix metalloproteinase

MRF(s)	myogenic regulatory factor(s)
Myf5	myogenic factor 5
PAK	p21-activated kinase
PAR	protease activated receptor
PAX	paired box gene
PBS	phosphate buffered saline
PH	Pleckstrin homology
PDGF	platelet-derived growth factor
PI3K	phosphatidylinositol 3-kinase
RBD	Rho-binding domain
ROCK	Rho-associated protein kinase
Serpin	serine protease inhibitor
SDF-1	stromal derived factor-1
SDS	sodium dodecyl sulfate
Smad	“mother against decapentaplegic homolog”
TGF-β	transforming growth factor- β
WASP	Wiskott Aldrich syndrome protein

CHAPTER 1

LITERATURE REVIEW

1.1 SATELLITE CELLS

Skeletal muscle regeneration is facilitated by satellite cells, a group of muscle-derived stem cells first discovered in 1961 between the sarcolemma and basal lamina of the myofiber (Mauro 1961). Other stem cells, such as hematopoietic stem cells from the bone-marrow or endothelial cells, have been shown to enter the satellite cell niche and contribute to skeletal muscle regeneration (Peault *et al.*, 2007). However, satellite cells are thought to be the primary contributors to the postnatal growth, maintenance and repair of skeletal muscle (Figure 1.1).

Previously satellite cells could only be identified by their location between the sarcolemma and basal lamina; however markers are now used to identify them. These include M-cadherin, myogenic factor 5 (Myf5), paired box gene 3/7 (Pax 3/7), SMC 2.6 and CD34 (Irintchev *et al.*, 1994; Beauchamp *et al.*, 2000; Seale *et al.*, 2000; Nagata *et al.*, 2006). Satellite cells are found in a mitotically quiescent state within their niche; however in response to certain stimuli (e.g. injury or stress) they can be activated to enter the cell cycle (Zammit *et al.*, 2004). Once activated, satellite cells up-regulate the expression of Pax7 and myogenic regulatory factors, such as myogenic factor 5 (Myf5) and myoblast determination protein (MyoD) (Figure 1.1) (Cornelison and Wold 1997; Zammit *et al.*, 2004), and divide asymmetrically into two myogenic daughter cells (Moss and Leblond 1971). One daughter cell re-enters the quiescent state, maintaining a constant satellite cell population via self-renewal, while the other, now termed a myoblast, begins to proliferate (Peault *et al.*, 2007 6294)).

The myogenic regulatory factors (MRFs) are the main transcription factors involved in satellite cell activation and differentiation. The expression of these MRFs is regulated by Pax3/7 which bind to proximal promoters of MyoD and distal enhancer promoters of Myf5, thereby regulating their expression (Bentzinger *et al.*, 2012). Although Pax3 and Pax7 are paralogues with conserved amino acid sequences and almost identical sequence-specific DNA-binding motifs, studies using knockout mice of either Pax3 or Pax7 have yielded distinct phenotypes, suggesting that Pax3 has specific functions during embryonic

development whereas Pax7 is more involved in post-natal satellite cell specification (Seale and Rudnicki 2000). MyoD and Myf5 are the dominant MRFs and are required for myogenic determination, which is established when these genes are activated in progenitors at sites of myogenesis (Pownall *et al.*, 2002). In contrast, the secondary MRFs, myogenin and MRF4, promote terminal differentiation (Figure 1.1) (Seale and Rudnicki 2000). Myogenin and MRF4 are expressed in differentiating muscle and regulate contractile protein target gene expression (Nicolas *et al.*, 2000). Muscle contractile protein genes are controlled by muscle-specific transcription enhancers which contain essential E-box sites for binding MRFs. One such muscle transcription factor is MEF2, which cooperatively interacts with MRFs and their associated histone acetyltransferases and deacetylases (Puri *et al.*, 2001).

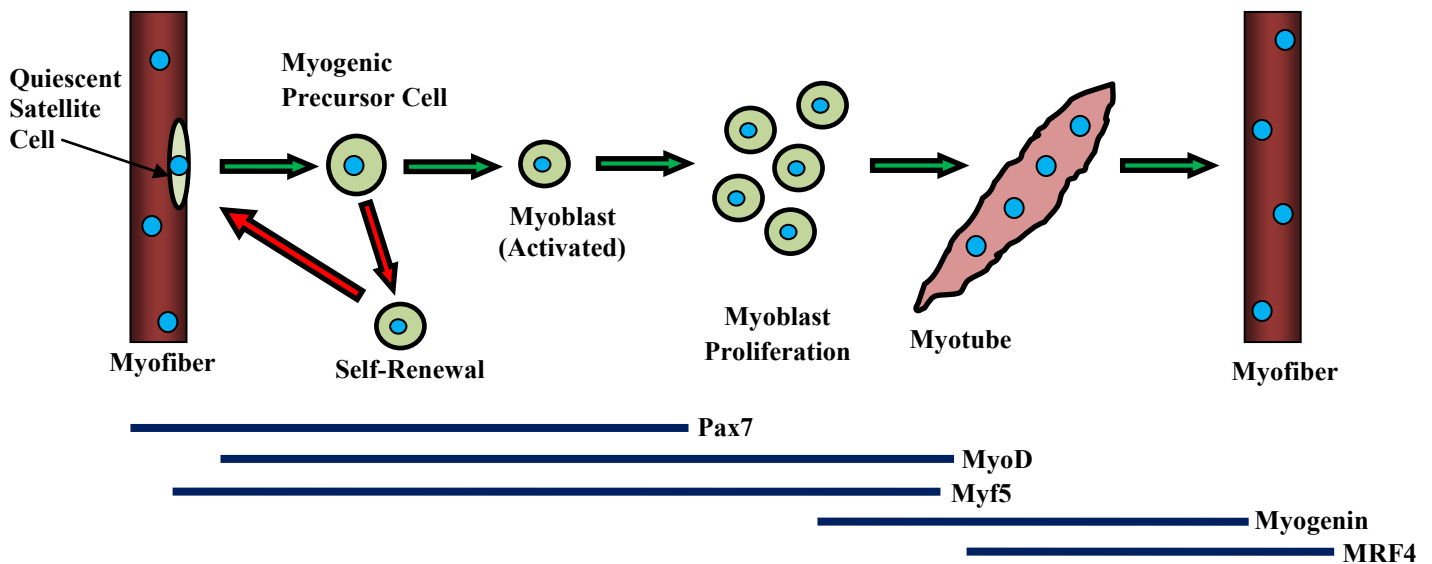


Figure 1.1: Satellite cell activation, proliferation, differentiation and concomitant transcription factor expression. Pax7 is expressed within quiescent satellite cells, and is unregulated during activation of the satellite cell. This is followed by the expression of the primary MRFs, MyoD and Myf5. The secondary MRFs, myogenin and MRF4, are expressed during differentiation and subsequent fusion of the myotube to the myofiber. Diagram compiled from references within Section 1.1.

1.2 EXTRACELLULAR MATRIX COMPONENTS & GROWTH FACTORS

1.2.1 Extracellular Matrix

Skeletal muscle myofibers are surrounded by an extracellular matrix (ECM) which was initially thought to act only as a scaffold for maintaining tissue structure. It has since been shown to regulate many cellular processes, including survival, proliferation, migration, and differentiation of precursor cells (Bretscher 1996; Heino 1996; Friedl and Brocker 2000). The ECM is a complex meshwork of many different types of proteins, proteoglycans, and polysaccharides and differs in the ratio of these components depending on the tissue type. Specific spatial orientation of individual ECM components can facilitate directional migration and cellular orientation during proliferation. The ECM components are remodeled by proteases which degrade the ECM surrounding the cell (Bernal *et al.*, 2005). These are activated and secreted following cell surface interactions with the ECM via specific receptor binding. The ECM has a complex relationship with cells located within it; on the one hand the cells control the matrix degradation (via secretion of proteases) and assembly, and on the other the ECM controls many vital cellular processes. In the following sections we will look at this relationship in more depth.

1.2.2 Growth Factors

Growth factors play a role in nearly every aspect of myogenesis, from activating quiescent cells, controlling proliferation and aspects of migration, to terminal differentiation and fusion of myoblasts into myotubes during muscle repair. The growth factors which contribute the most to these processes are: Hepatocyte Growth Factor (HGF), Fibroblast Growth Factor (FGF), Transforming Growth Factor beta (TGF- β), Insulin-like Growth Factors (IGFs) (Booth 2006), and Platelet-derived Growth Factors (PDGFs) (Kawada *et al.*, 2009).

1.2.2.1 Hepatocyte Growth Factors (HGF)

HGF is particularly important in muscle repair (Birchmeier and Gherardi 1998), tissue development, and regeneration and exists in two isoforms, pro-HGF and mature HGF (Matsumoto and Nakamura 1997). Pro-HGF is secreted as a single chain and binds to ECM components until it is cleaved and activated by a serine protease (Catlow *et al.*, 2003). Mature HGF consists of a heavy α -chain and light β -chain of 69 kDa and 34 kDa, respectively. The α -chain consists of an N-terminal hairpin domain and four-kringle domains, whereas the β -domain contains a serine protease-like domain (Matsumoto and

Nakamura 1997). Once activated, HGF binds to its cell surface receptor c-met (a heterodimeric tyrosine kinase) (Catlow *et al.*, 2003). Binding of HGF to the c-met receptor will cause auto-phosphorylation of tyrosine residues within the intracellular domain of the receptor, initiating downstream signaling of the Ras and PI3-Kinase pathways (Leshem *et al.*, 2002). The binding of HGF to the c-met receptor also results in the silencing of MyoD and myogenin gene expression and inhibits the synthesis of muscle-specific structural proteins, such as MyHC, as well as myotube formation; this is thought to occur via the Twist protein, an inhibitor of MyoD expression (Karalaki *et al.*, 2009). HGF is expressed during the early phases of muscle regeneration and its expression levels have been shown to be proportional to the extent of the injury (Kastner *et al.*, 2000; Suzuki *et al.*, 2002). HGF also plays a unique role during satellite cell activation by shortening the time the cell requires to re-enter the cell cycle, this is either via the MAPK or PI3K signaling pathways or by HGF down-regulating caveolin-1 protein expression, which results in the up-regulation of the ERK pathway required for satellite cell activation (Tatsumi *et al.*, 1998). HGF signaling can also be enhanced through the addition of co-receptors, such as heparan sulfate which increases the potency of HGF downstream signaling effects (Kemp *et al.*, 2006).

1.2.2.2 Fibroblast Growth Factors (FGF)

FGFs are known to play a role in apoptosis, as well as tissue and organ development (Ornitz 2005). FGFs are defined by two key features; a strong affinity for heparan sulfate proteoglycans (Kiselyov *et al.*, 2006), and a core protein that is highly homologous in all FGFs and serves as the binding site to the FGF receptor (Ornitz and Itoh 2001). FGFs activate signaling pathways by a dual receptor system consisting of tyrosine kinase trans-membrane FGF receptors (FGFR1- 4) and heparan sulfate proteoglycans which are required for the proper activation and binding of FGFs to their receptors (Ornitz and Itoh 2001). FGF-6 expression is stimulated after skeletal muscle injury and induces strong morphological changes, alters satellite cell adhesion, and compromises their ability to differentiate into myotubes. FGF-6 also stimulates the proliferation and migration of satellite cells and induces the expression of genes required for terminal differentiation (i.e. MyoD and myogenin). This biphasic effect of promoting both proliferation and differentiation is possibly explained by a dose dependent mechanism of FGF-6, whereby FGF-6 up-regulates and down-regulates the expression of FGFR1 and FGFR4 depending on the concentration utilised (Armand *et al.*, 2006; Karalaki *et al.*, 2009).

1.2.2.3 Transforming Growth Factor beta (TGF- β)

The TGF- β superfamily contains more than 40 different members including TGF- β isoforms, growth differentiation factors (GDFs), and bone morphogenetic proteins (BMPs) (Shi and Massague 2003). These members have important roles in tissue homeostasis, differentiation, migration, proliferation, and bone morphogenesis (Massague and Wotton 2000; Attisano and Wrana 2002). TGF- β binds to and causes dimerization of the type I and II serine/threonine kinase TGF- β receptors on the cell surface. This allows for the type II receptor to phosphorylate the type I receptor kinase domain, which facilitates the phosphorylation of downstream Smad proteins and affects various cellular processes, such as proliferation and differentiation (Shi and Massague 2003). TGF- β 1, 2, and 3 have all been shown to delay differentiation into myotubes while significantly increasing cellular proliferation of C2C12 myoblasts (Schabort *et al.*, 2009), indicating a similar effect to FGF-6 (Section 1.2.2.2). The proteoglycan, decorin, has been shown to bind TGF- β through interaction with the lipoprotein related protein (LRP-1) and activate the PI3K dependent pathway. In a study by Cabello-Verrugio & Brandan, decorin null cells had a decreased responsiveness to TGF- β , indicating that decorin is required for optimal activation of the TGF- β signaling pathway (Cabello-Verrugio and Brandan 2007; Zhang *et al.*, 2009).

1.2.2.4 Insulin-like Growth Factor-I (IGF-I)

During muscle regeneration IGF-I stimulates both proliferation and differentiation of muscle cells. It does this by enhancing the expression of intracellular mediators, such as cyclin-D, which increases the proliferation potential of satellite cells (Chakravarthy *et al.*, 2000); whereas for terminal differentiation IGF-1 induces myogenin gene expression. This dual regulatory mechanism (shown to be dose dependent) is important as during muscle regeneration, IGF-1 initially reduces myogenic factor expression and induces proliferation, after which myogenin gene expression is up-regulated and differentiation is induced (Engert *et al.*, 1996). Decorin has also been shown to bind to both IGF-1 and its receptor (IGF-1R), thereby regulating this pathway in endothelial and fibroblast cells. The binding of decorin results in IGF-1R phosphorylation and activation, followed by receptor down-regulation (Brandan *et al.*, 2008). It is thought that decorin may regulate the ability of IGF-I to modulate mitotic and myogenic activity of skeletal muscle, thereby playing an important role in skeletal muscle regeneration. Fiedler and colleagues demonstrated that

the decorin core protein binds to the IGF-IR and modulates cellular migration of endothelial cells as well as increasing affinity of integrins for their specific ligands, such as collagen I and the $\alpha 2\beta 1$ integrin, through “inside-out” signaling (Fiedler *et al.*, 2008).

1.2.3 Skeletal Muscle ECM Components, Receptors and Proteases

Satellite cells and activated myoblasts are located between the sarcolemma of the muscle fiber and the basement membrane. The basement membrane is further surrounded by interstitial connective tissue. The interstitial connective tissue provides a scaffold and support for blood vessels and nerves which surround the muscle fibers, as well as the elasticity to transfer mechanical force needed to move the skeletal frame (Kjaer 2004). Skeletal muscle is made up of different layers of interstitial connective tissue, The first layer outside individual myofibers is composed of random collagen fibrils to allow for movement during contraction; each myofiber is surrounded by an endomysium layer. Bundles of fibers are held together by the perimysium which contains the blood vessels and nerves that extend into the epimysium. The epimysium covers an entire muscle and is composed of two layers of collagen fibrils to form a sheet-like structure (Kjaer 2004). The intramuscular connective tissue is dominated by collagens, but contains other important components such as fibronectin, tenascins, laminins, and proteoglycans. These ECM components and related proteases, as well as their ECM location are summarized in Table 1.1.

Table 1.1: ECM components and proteases within the interstitial ECM and basement membrane of skeletal muscle

ECM Components	Subtypes	Interstitial ECM	Basement Membrane	References
Collagen	Col I, IV, VI, XV, XVIII, IX, XI	Mainly Collagen I	Collagen IV, VI, I	Ricard-Blum & Rugeiro, 2005; Kjaer, 2004; Gelse <i>et al.</i> , 2003
Tenascin	Tenascin C, X, R, W	Tenascin C	-	Chiquet-Ehrismann, 2004; Chiquet-Ehrismann & Tucker, 2004
Fibronectin	Fibronectin	Fibronectin	-	Jarvinen <i>et al.</i> , 2007
Laminin	Laminin 211, 221, 411, 421, 511, 521	-	Laminin 211, 411, 511	Grounds <i>et al.</i> , 2005
Proteoglycans	Chondroitin Sulfates Heparan Sulfates Dermatan Sulfates	Heparan sulfates (decorin), Dermatan sulfates	Heparan sulfates (biglycan), Syndecans	Jenniskens <i>et al.</i> , 2006; Bishop <i>et al.</i> , 2007
Proteases	MMPs, plasmin, Trypsin, Calpain	MMP-2, MMP-9	-	Kherif <i>et al.</i> , 1999; Bernal <i>et al.</i> , 2005

1.2.4 Integrins

Integrins are the major transmembrane receptors that allow cell adhesion to ECM proteins and indirect interactions with other cells. Integrins are dimers composed of α - and β -subunits which can combine to form 24 different integrin heterodimers, each with unique ligand specificities (Humphries *et al.*, 2006). The α -chain is composed of two calf domains and a thigh domain linked to a β -propeller (Figure 1.2). The β -chain consists of a cystatin-like domain bound to epidermal growth factor (EGF) repeats, which in turn are linked to the hybrid and $\beta\alpha$ -domains (Figure 1.2). The intracellular domains of integrins are associated with the actin cytoskeleton which allows for direct control of cell shape and rapid responses to environmental changes (Hynes *et al.*, 2002). Integrins accumulate in clusters at the leading edge of the cell during migration, forming a stable platform or focal adhesion with an increased affinity for the ECM. These focal adhesions result in the formation of intracellular adhesion complexes which assist in signaling and cell-fate determination, by allowing direct interaction of the ECM with the intracellular actin cytoskeleton.

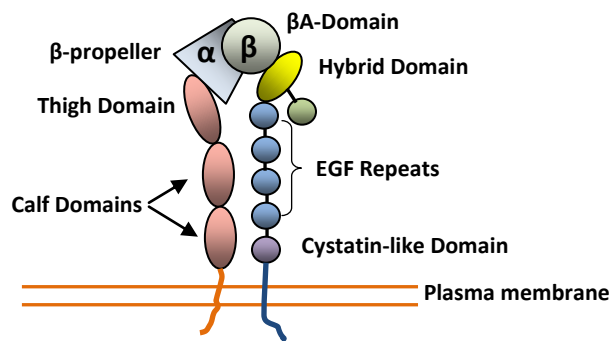


Figure 1.2: The structural components of an integrin indicating the specific domains. The α -chain is made up two calf domains and a thigh domain linked to a β -propeller. The β -chain consists of a cystatin-like domain linked to epidermal growth factor (EGF) repeat. These in turn are bound to the hybrid and $\beta\alpha$ -domains. Each ECM component will bind to a specific $\alpha\beta$ integrin combination (i.e. collagen binds to the $\alpha2\beta1$ integrin via a critical GFOGER motif within the collagen I domain (Emsley *et al.*, 2000)).

The interaction of integrins with the ECM can be enhanced by either the direct binding of growth factors or other ligands to the integrin, or the binding of ligands to their specific receptors, which in turn enhances the affinity of the integrin for its specific ligand. Beside conformational changes, integrin-ECM interaction can be enhanced by increased gene expression of integrin subunits. For example fibroblast growth factor-2 (FGF-2) increases $\alpha5\beta1$ expression in endothelial cells and transforming growth factor- $\beta1$ (TGF- $\beta1$) increases $\beta1$ and $\beta5$ integrin levels (Moissoglu and Schwartz 2006; Streuli and Akhtar 2009). The engagement of integrins and growth factor/cytokine receptors in parallel can increase the signal output for a longer sustained synergistic signal via inside-out signaling (Figure 1.3) (Streuli and Akhtar 2009).

In the early 1990's it was discovered that certain integrin heterodimers are internalized from the plasma membrane into endosomal compartments and are recycled back to the cell surface (Bretscher 1996; Caswell and Norman 2006). This endo-exocytic cycle occurs at a relatively rapid pace with cycling being reported once every 30 minutes. This type of integrin trafficking has been observed in neural crest cells, as well as in fibroblasts and macrophages (Fabbri *et al.*, 1999; Strachan and Condic 2004). Integrin trafficking is a selective process whereby specific integrins are trafficked rapidly and at a higher frequency than others depending on the cellular process being undertaken by the cell. This suggests that integrin presentation is reliant on specific cues and that cellular migration can be regulated with precision, in response to the changing environment (Strachan and Condic 2004).

1.2.5 Collagens

Collagens are important structural proteins which facilitate many functions within the ECM (Gelse *et al.*, 2003; Abd-Elgaliel and Tung 2012). They are all composed of three polypeptide α -chains coiled into a triple helix structure rich in glycine. Twenty seven different collagens, each with their own distinct α -chains have been identified to date (Ricard-Blum and Ruggiero 2005). The fibrillar collagens are divided into collagen I, II, III, IV, V, VI and XI. Collagen I is the most abundant collagen and is the major component of the interstitial ECM surrounding skeletal muscle fibers (Kjaer 2004). In culture, collagen I increases β 1-integrin expression in fibroblasts, which become clustered at the leading edge where they interact with the collagen fibers. Friedl and colleagues showed that after addition of the anti- β 1 integrin antibody to block ligand binding, integrin clustering, fiber traction, and cell polarization were lost (Friedl *et al.*, 1998). This demonstrated the importance of α 2 β 1 integrin engagement with collagen I for the development of polarized morphology and migration. Collagen IV is the major structural component of the basement membrane and interacts with laminins and proteoglycans. The interstitial ECM is joined to the basement membrane via a microfilament network rich in collagen VI (Bonnemann and Laing 2004). Over time, collagens form increasing intermolecular cross-links leading to stiffness and reduced function in aged tissues (Avery and Bailey 2005). This is important to note for the repair of injured skeletal muscle.

1.2.6 Tenascins

Tenascins are glycoproteins which are involved in weak cell adhesion events and do not promote cell spreading (Chiquet-Ehrismann 2004). Tenascins consist of a large complex of six polypeptide chains attached to a central core by disulfide bonds. There are four members of the tenascin family; tenascin C, X, R and W. During muscle repair, tenascin C is expressed in skeletal muscle in close proximity to fibronectin and is up-regulated, especially during the inflammation phase (Fluck *et al.*, 2003). Tenascin C counteracts the effects of fibronectin by acting as an anti-adhesive. This is achieved through syndecan-1 and -4 expression, which subsequently prevents the binding of cells to fibronectin. Syndecans are ECM molecules which modulate cell adhesion, cell-cell interactions and ligand receptor interactions (Chiquet-Ehrismann and Tucker 2004; Midwood and Orend 2009).

1.2.7 Fibronectin

Fibronectin is a glycoprotein which exists in 3 different forms: a soluble dimeric form (located within the blood stream), cell surface fibronectin oligomers, and insoluble fibronectin fibrils which make up part of the ECM. Fibronectin is able to bind to other ECM components such as collagen and tenascin (Hocking *et al.*, 2008). Fibronectin along with tenascin C are among the first ECM components to be produced by fibroblasts within a damaged muscle fiber. Fibronectin forms multimeric fibrils which aid in the formation of a super fibronectin molecule with strong adhesive properties. Fibronectin together with fibrin, forms a cross-linked structure in early granulation tissue, which is required to act as a scaffold for invading inflammatory cells. The anti-adhesive effect of tenascin C, via syndecan-4 expression, could help to prevent myoblasts from becoming attached to the fibronectin. This would be important during myoblast migration and subsequent wound repair (Jarvinen *et al.*, 2007; Midwood and Orend 2009).

1.2.8 Laminins

Laminins are found almost exclusively in the basement membrane and are composed of multiple heterodimers consisting of α , β and γ chains. Laminin-2 (LM-211) is found around the sarcolemma of muscle fibers whereas laminin-4 (LM-221) is located at neuromuscular junctions (Grounds *et al.*, 2005). Laminins bind to the collagen IV network in the basement membrane as well as the proteoglycan, perlecan. Laminins are key molecules which connect the myofiber directly to the basement membrane; without them the contractile force created by the myofiber cannot be transferred effectively to the interstitial connective tissue (Jenniskens *et al.*, 2006). Loss of laminin or mutations of laminin result in congenital muscular dystrophies.

1.2.9 Glycans

Three main proteoglycan groups are involved in the skeletal muscle ECM; heparan sulfates, chondroitin sulfates, and dermatan sulfates. Chondroitin and dermatan sulfates fall under the name of galactosaminoglycans as they have N-acetyl-D-galactosamine and glucuronic acid disaccharides linked to their backbones (Bishop *et al.*, 2007). Heparan sulfates are complex macromolecules consisting of a protein core with one or more glycosaminoglycan (GAG) chains attached. Heparan sulfate proteoglycans play a major part in the regulation of the basement membrane and bind to underlying ECM molecules

due to their negative charge (Jenniskens *et al.*, 2006). Perlecan (a heparan sulfate) is important in the assembly and integrity of the basal lamina. Two other heparan sulfates, syndecan-3 and -4, are abundant on the surface of skeletal muscle fibers where they play roles in regeneration and cell adhesion (Kanagawa *et al.*, 2005).

Decorin, a component of the ECM, is a member of the small leucine-rich repeat heparan sulfate family, which is composed of a leucine-rich repeat core protein, consisting of 12-folded repeats, each containing a 24 amino acid residue. It also has a single covalently-linked GAG chain at its NH₂-terminus which can vary in length and composition (Scott and Haigh 1985). Decorin plays a key role in collagen fibrillogenesis (Fiedler *et al.*, 2008; Dunkman *et al.*, 2013). It binds to collagen via its core protein, at the peptide sequence SYIRIADTNIT, causing a delay in the collagen fibril assembly which results in the reduction of the average fibril diameter (Kresse *et al.*, 1997; Kalamajski *et al.*, 2007). In the absence of decorin the collagen network is loosely packed and exhibits irregular collagen contours where the fibrils are abnormally fused to larger collagen shafts (Weber *et al.*, 1996; Keene *et al.*, 2000). Keene and colleagues investigated the binding site of decorin to the collagen fibril and also whether this binding could affect the structure and cross-linking of collagen. They determined that decorin binds 25nm from the C-terminus in the region of the C₁ band on the collagen fibril D-period. This binding area is located in close proximity to one of the major intermolecular cross-linking sites of collagen I, indicating that decorin possesses a unique binding specificity which can regulate collagen fibril stability (Keene *et al.*, 2000).

Fiedler and colleagues investigated the regulatory effects of decorin on the ability of collagen I to regulate endothelial cell motility. They discovered that decorin promotes $\alpha 2\beta 1$ integrin-dependent binding of collagen I, which in turn enhanced cell adhesion and migration in endothelial cells. Decorin modulates cell-matrix interactions by stimulating focal adhesion reorganization via binding and activating the IGF-IR (Insulin-like Growth Factor I Receptor) and interacts with the $\alpha 2\beta 1$ integrin via its GAG chain at a site distinct from that where collagen I binds the integrin (Figure 1.3A) (Fiedler *et al.*, 2008). It has also been suggested that decorin, while bound to collagen I, may bind to the $\alpha 2\beta 1$ integrin via its GAG chain, subsequently enhancing the signaling of the integrin (Figure 1.3B). In skeletal muscle decorin is located within the interstitial ECM. Collagen bound decorin within skeletal muscle is able to interact with TGF- β , with decorin still maintaining an active site within the core protein (Brandan *et al.*, 2008); suggesting decorin is able to bind

multiple proteins at different active sites. These findings suggest that decorin plays a large role in cell-ECM regulation and that these roles are not distinct to one mechanism, but encompass a highly sophisticated array of binding mechanisms (Fiedler and Eble 2009). The combination of decorin and collagen during skeletal muscle repair may play an important role in cell migration into the wound and reduce fibrotic scar tissue formation (Sato *et al.*, 2003).

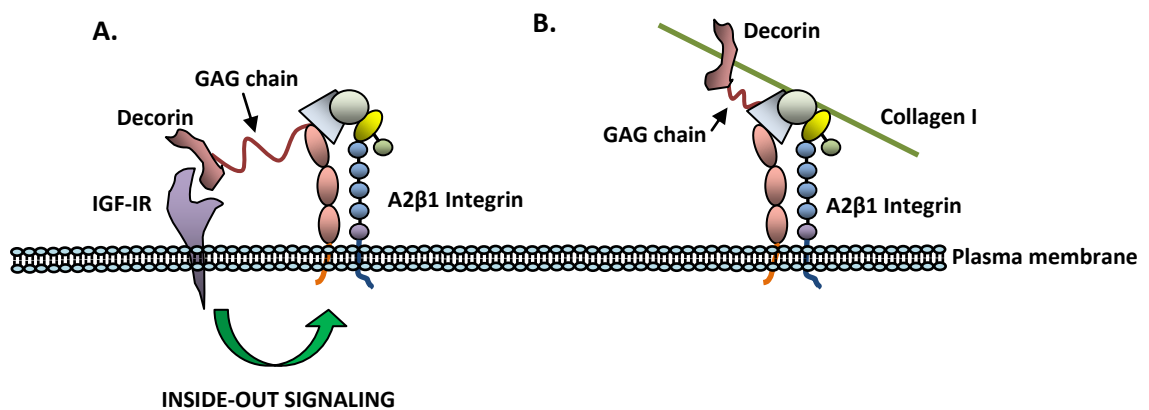


Figure 1.3: Two distinct mechanisms for the binding of decorin to the $\alpha 2\beta 1$ integrin. **A)** Decorin can bind to IGF-IR and enhance signaling of integrin via inside-out signaling. **B)** Decorin can also bind to collagen and may be able to bind directly to the integrin via its GAG chain while bound to collagen. Diagram compiled from references within *Section 1.2.9*.

1.2.10 Proteases Involved in ECM Degradation

Proteolysis is essential for ECM maintenance and facilitates the constant turnover and remodeling of the ECM environment. Matrix metalloproteases (MMPs) are secreted enzymes which degrade components of the ECM, and cleave cellular receptors and cytokines. MMPs are produced as inactive zymogens and are activated extracellularly, either upon secretion or by other proteases such as MT1-MMP and plasmin (Bernal *et al.*, 2005; Suelves *et al.*, 2005). MMP-2 and -9 degrade many connective tissue components, including collagen I, II, III, IV, V, fibronectin, and many proteoglycans. MMP-2 has been shown to be essential for the degeneration of damaged myoblasts as well as for the regeneration of new myofibers. It has been proposed that MMP-9 expression is related to the inflammatory response and subsequent activation of satellite cells, since its expression is induced within 24 hours post damage and remains present for several days. (Kherif *et*

al., 1999; Chen and Li 2009). These metalloproteinases appear to be differentially expressed at various stages of the degeneration and regeneration process within damaged skeletal muscle. A recent study has highlighted a relationship between MT1-MMP, MMP-2 and ROCK inhibition in an endothelial cell line. When ROCK is inhibited there is an increase in cell surface localization of MT1-MMP, as well as an increase in PI3Kinase activity which is required for MMP-2 activation. These findings suggest an important role of these MMPs in regulating cellular migration (Ispanovic *et al.*, 2008).

1.3 MYOBLAST MIGRATION MECHANISMS

1.3.1 Migration

Cellular migration is essential for tissue development, wound repair, the inflammatory response, immune surveillance, and plays a role in pathological processes such as metastasis (Friedl and Brocker 2000). Cellular migration can be integrin-dependent (where re-organization of the matrix takes place) or independent (whereby the cell moves swiftly over the matrix, makes only minor adhesion contacts, and does not remodel the ECM). This second method is not directionally controlled by the ECM; however, chemokines can regulate the direction of migration in an integrin-independent manner.

The migration of myoblasts, which plays an integral role in repair of a damaged myofiber, occurs both in a 2D manner (along the basement membrane in skeletal muscle myofibers) and in a 3D manner (into the interstitial tissue surrounding muscle myofibers). 2D migration on the basement membrane occurs in three parts. Firstly, the extension of the leading edge of the cell into lamellipodia and adhesion to the ECM, followed by the contraction of the main body of the cell through action of the actin fibers within the cell, and, lastly the detachment of the tail at the rear of the cell (Friedl and Brocker 2000).

During 3D migration the cell has to interact with matrix ligands to produce a forward movement force and also has to overcome the biomechanical resistance created by the matrix network. This is evident in fibroblasts and myoblasts, which need to migrate through the interstitial ECM into the muscle wound to facilitate muscle repair (Friedl *et al.*, 1998). 3D migration includes, to a greater extent than in 2D migration, proteolysis of ECM components by serine proteases and metallo-proteinases, such as membrane type-1 matrix metalloproteinase (MT1-MMP) and matrix metalloproteinase-2 (MMP-2) (Birkedal-Hansen 1995; Shapiro 1998).

1.3.1.1 Cell Shape During Migration

At the leading edge of the cell, ruffling will occur followed by the protrusion of the lamellipodia. These are “arm-like” protrusions used to extend the cell forward during migration and form new attachments to the ECM surface (McLennan *et al.*, 2012). The process of lamellipodia extension and cell ruffling involves actin polymerization, which is initiated and maintained mainly by the integrin receptor family as well as by cell surface proteoglycans, such as phosphacan and CD44 (Humphries *et al.*, 2006). Filopodia on the other hand are used to probe the ECM and are not directly involved in the actual mechanism of migration (Figure 1.4) (Nobes and Hall 1995).

During migration a “gradient” is established between the front and rear of the cell in terms of binding and traction factors resulting in forward movement in the direction of chemokine signaling. The forward motion is facilitated by the contraction of stress fibers, which consist of actin fibers containing myosin-motors between them. The contraction of the actin filaments is regulated by the GTPase family.

In order for cell contraction and migration to occur, the focal contacts at the trailing edge of the cell have to be resolved so that the rear of the cell is released from the ECM. This is brought about by integrin detachment from the ECM, followed by endocytosis and recycling of integrins to the leading edge of the cell (Bretscher 1996). Alternatively the integrins may be released into the ECM where they are degraded (Figure 1.4A).

Within a 3D environment the migration process follows a similar three step process as mentioned above. However, specific aspects of migration will differ in a 3D environment, e.g. cell polarity, to compensate for the addition of the extra dimension of depth. This can be seen in shape change (i.e. probing the ECM in all directions) and in the arrangement of receptors and proteases within the cell membrane (Figure 1.4B).

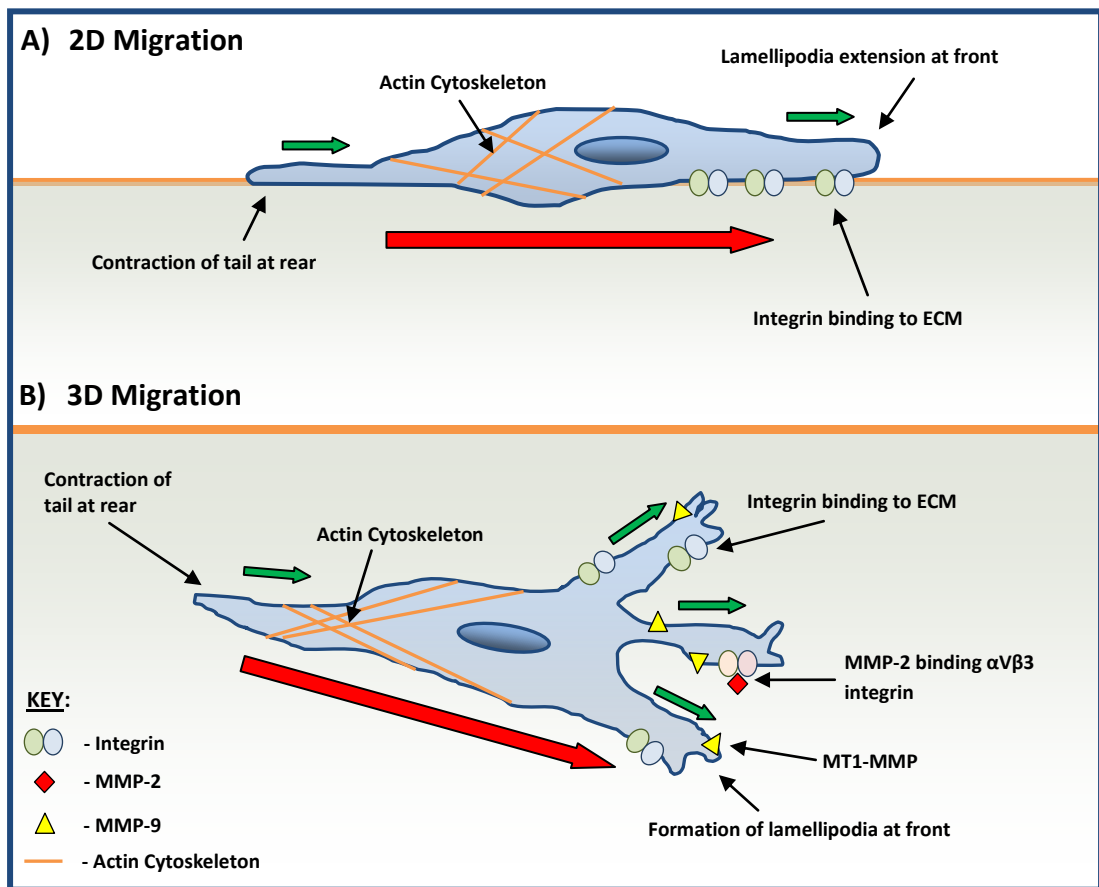


Figure 1.4: Specific ECM interactions that facilitate 2D and 3D migration. **A)** 2D migration on the ECM. Integrin clustering will occur at the front of the cell followed by the extension of the lamellipodia. The actin fibers will contract pulling the cell forward. This is then followed by the release of the tail at the rear of the cell. **B)** 3D migration occurs along the same basic migration principles as 2D migration. However, proteolysis can play a larger role in actively degrading the ECM and allowing for forward cell movement. MT1-MMP can actively degrade the ECM as well as activate pro-MMP-2. Integrins such as $\alpha\beta 3$ can also bind activated MMP-2 located within the ECM. MMP-2 and MT1-MMP are good proteases of collagen degradation, which is the main constituent of the skeletal muscle ECM. Diagram compiled from references within *Section 1.3*. Red arrow – migration direction, green arrow – lamellipodia extension.

During migration the cell will adapt morphologically to the ECM and follow the path of least resistance. Friedl *et al.*, demonstrated that in 3D collagen matrices, dendritic cell migration occurred along the existing matrix strands, and areas consisting of dense collagen fiber networks were circumnavigated rather than being directly penetrated by the cells (Friedl *et al.*, 1998). These findings showed that migration can occur independently of matrix remodeling *in vitro*. However, this is highly unlikely in *in vivo* situations where the ECM is densely packed. During migration, secreted and membrane-bound proteases are essential for proteolytic remodeling of the ECM, as cells will need to lower the level of

obstruction caused by the ECM if alterations in morphology of the cell are unable to adapt to the existing matrix gaps. For instance, invasive melanoma cells can degrade the ECM as they have active MMP-2, which is bound to their cell surface via the integrin $\alpha\beta3$, as well as MT1-MMP, which is localized on the leading edge of the migrating cell (Brooks 1996).

Protease localization on the cell surface is brought about either by the binding of extracellular proteases (e.g. pro-MMP-2) to membrane receptors or by the expression of endogenous transmembrane proteases (e.g. MT1-MMP). MMP-2 and MMP-9 facilitate localized proteolysis of collagens and fibronectin, respectively. MT1-MMP cleaves collagen I, cartilage, proteoglycans, fibronectin and laminins, as well as pro-MMP-2, resulting in its activation (Ohuchi *et al.*, 1997). Another family of transmembrane proteases termed, 'a disintegrin and metalloproteinase' (ADAMs), contains both a disintegrin and metalloproteinase domain which allows for the attachment and proteolysis to occur in a close proximity to each other. ADAMs can therefore play a role in cellular adhesion as well as in matrix remodeling by cleaving ECM components and shedding growth factors from membrane-anchored precursors (Black and White 1998). Specifically, ADAM17 is required for the growth of cultured vascular smooth muscle cells *in vitro* and has been implicated in angiogenesis and fibrosis (Takaguri *et al.*, 2011).

1.3.2 Intracellular Signal Transduction

Cell migration is controlled by a vast array of intracellular signaling molecules, including phospholipases, serine/threonine and tyrosine kinases, and scaffold proteins. However, one particular group of proteins, the Rho GTPases, appear to outshine the rest in the regulation of cytoskeletal organization and thus cellular migration. Rho GTPases are frequently over-expressed in invading tumor cells when the tumor cells increase cell motility to cross tissue boundaries during invasion (Sahai and Marshall 2003).

Rho GTPases were first highlighted as key players in cytoskeleton shaping in 1992 and since then the intricate signaling and functioning of these proteins has been more clearly described and understood (Ridley and Hall 1992a; Ridley and Hall 1992b). To date, twenty genes encoding proteins that contain a small GTPase domain have been characterized in mammals. These include the Ras GTPases (*H-Ras*, *K-Ras*, *N-Ras* and *R-Ras*) (Ridley 2001), and the Ras-homologous (Rho) GTPases which are divided into 5 subfamilies (Rho,

Rac, Cdc42, Rnd, and RhoBTB) (Figure 1.5). Rho, Rac, and Cdc42 are the most prevalent GTPases and will be discussed in detail (Burrige and Wennerberg 2004). The Rho-like subfamily contributes to actin fiber formation and contraction during migration and includes RhoA, B, and C. RhoA plays a large role in migration by activating the downstream effector, Rho kinase (ROCK) (Wennerberg *et al.*, 2003). The Cdc42-like subfamily plays a large role in cell polarization via the organization of the orientation of the nucleus and Golgi apparatus at the front of the cell during myoblast migration, and binds to the Wiskott Aldrich syndrome protein (WASP) or N-WASP proteins which mediate the formation of filopodia (Kozma *et al.*, 1995). Rac-like GTPases stimulate membrane ruffling at the leading edge of myoblasts and contribute to the formation of lamellipodia (Machesky and Hall 1997). Little is known about the Rnd and RhoBTB subfamilies, except that Rnd GTPases are highly expressed in the brain and contribute to neurite growth and branching and RhoBTB GTPases are down-regulated in breast cancer cells (Wennerberg *et al.*, 2003).

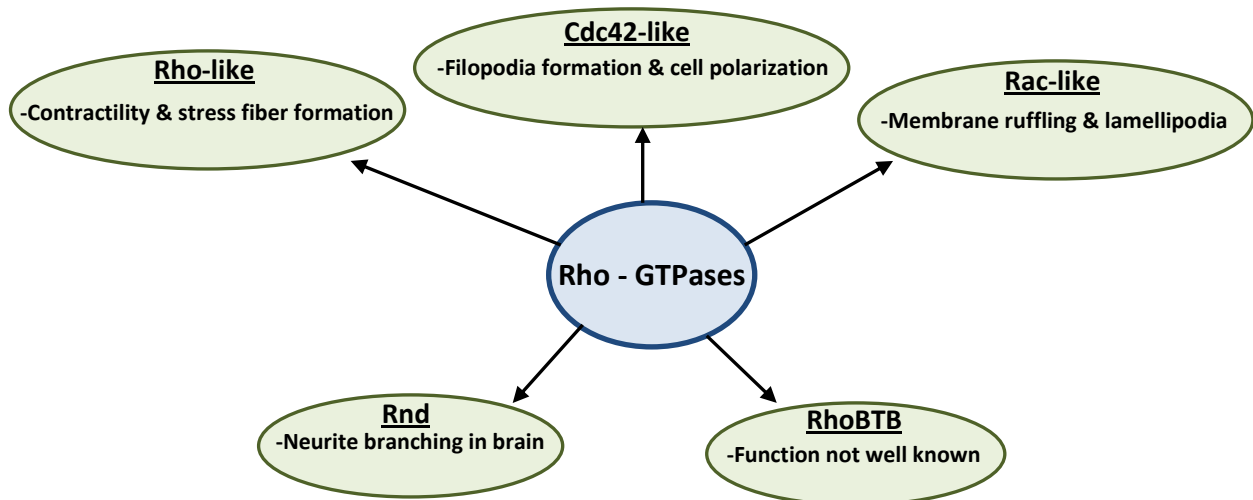


Figure 1.5: The major members of the Rho-GTPases and their respective functions. The five subfamilies of the Ras-homologous GTPase family are Rho, Rac, Cdc42, Rnd and RhoBTB. The Rho, Cdc42 & Rac subfamilies regulate cellular migration and will be focused on in detail within the text. Diagram adapted from (Wennerberg *et al.*, 2003; Burrige and Wennerberg 2004).

1.3.2.1 *Rho-GTPases Role in Cellular Migration*

Rho activity is associated with focal adhesion assembly and cell contractility via myosin light chain phosphorylation (Figure 1.6) (Chrzanowska-Wodnicka and Burridge 1996). This occurs at the rear of the cell where Rho facilitates the cell body contraction as well as cell retraction. The downstream effector of Rho is ROCK (also termed p160ROCK or ROK). Once activated by Rho, ROCK can phosphorylate LIM-kinase (LIMK), which in turn can phosphorylate and inactivate cofilin. This will lead to actin filament stabilization within the actin:myosin filament bundles, as active cofilin degrades the actin filaments via subunit dissociation at the ends of the filaments (Figure 1.6) (Schmitz *et al.*, 2000). In addition, ROCK phosphorylates the myosin binding subunit (MBS) of the myosin light chain (MLC) phosphatase resulting in its inactivation (Kawano *et al.*, 1999).

The inactivation of the MLC phosphatase leads to increased levels of myosin phosphorylation which enables the actin filaments to cross-link generating contractile force (Figure 1.7). Another downstream effector of Rho is mDia which also cooperates with ROCK in the assembly of actin:myosin filaments within the cytoskeleton of the myoblast, but to a lesser extent than that of ROCK alone (Watanabe *et al.*, 1999).

Both Rac and Cdc42 are required near the leading edge (front) of the cell. Rac has been shown to be spatially restricted to the leading edge of the cell where it is required for the regulation of membrane ruffling and for the formation of lamellipodia (Figure 1.6). Cdc42 induces actin polymerization via the effectors WASP and myotonic dystrophy kinase-related Cdc42-binding kinase (MRCK) and aids in the generation of filopodia (Figure 1.6), as well as regulating the direction of cellular migration. This was shown by Kozma *et al.*, whereby a Swiss 3T3 fibroblast cell line was transfected with Cdc42 and a subsequent increase in filopodia formation was observed (Kozma *et al.*, 1995). P21-activated kinase (PAK) is a downstream kinase for both Rac and Cdc42 and causes the localization of membrane ruffles and cytoskeletal rearrangement (Sanders *et al.*, 1999). PAK can also phosphorylate and activate LIM kinase (LIMK), which in turn can phosphorylate and inactivate cofilin (Raftopoulou and Hall 2004), preventing actin fiber degradation during cytoskeletal rearrangement. PAK also facilitates the de-phosphorylation of the myosin light chain allowing for myoblast spreading (ruffling) to occur, as well as inhibiting Rho during this process at the cell front (Liu *et al.*, 2011).

The spatial orientation of Rho GTPase activation is important for cytoskeletal organization that will support forward movement of the cell. Therefore, mechanisms must be put in place to inhibit Rho activity at the leading edge of the cell. This is achieved by means of Rac, as Rho and Rac are antagonists of each other ensuring that their specific mechanisms do not compete against each other and thus inhibit cell migration (Machesky 1997).

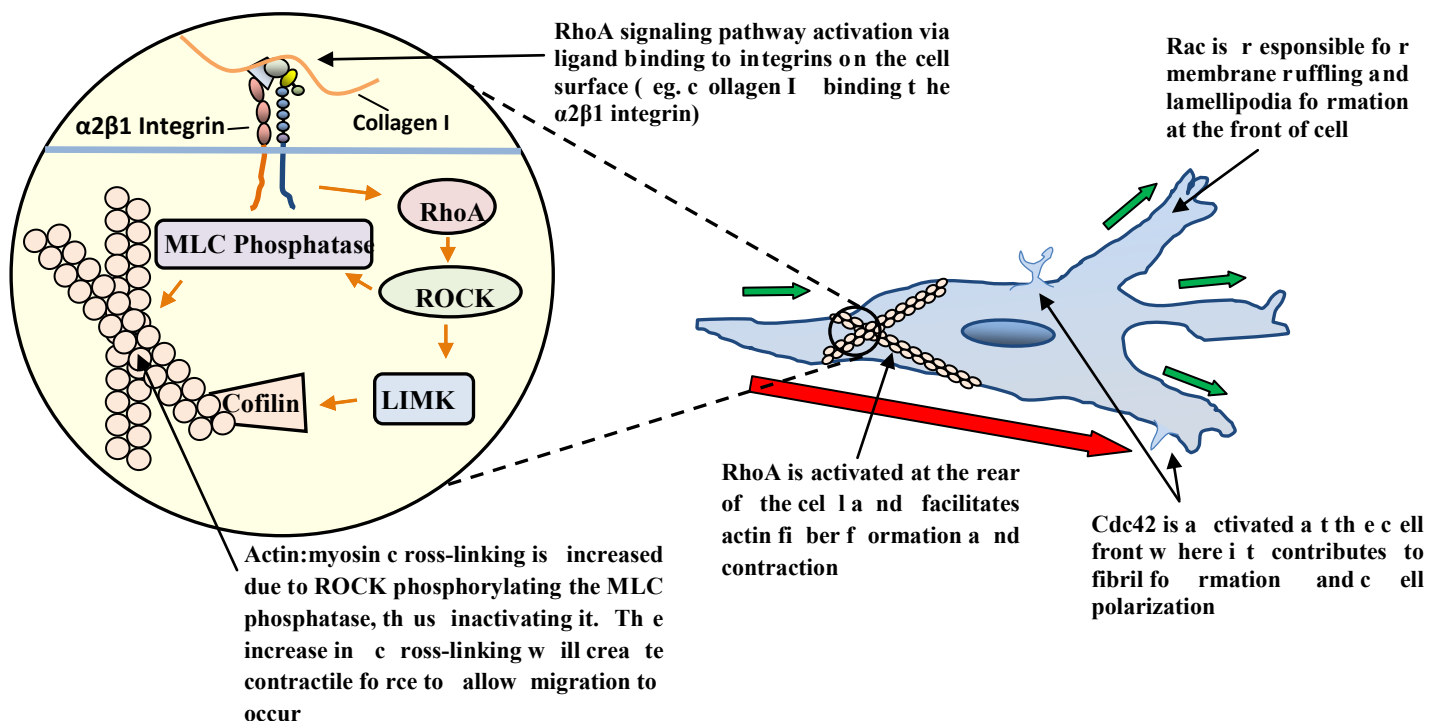


Figure 1.6: The effect of GTPases on cellular migration with particular focus in the Rho/ROCK pathway. Activated Rac and Cdc42, localized near the front of the cell, regulate lamellipodia formation and cell polarization, respectively. Activated Rho on the other hand is localized at the rear end of the cell. Rho is activated by ECM components, such as collagen I. Once activated Rho will signal via ROCK. ROCK leads to the phosphorylation of the myosin binding unit located on the MLC phosphatase. This inactivates the MLC phosphatase allowing for actin:myosin cross-linking of the actin filaments to occur. ROCK can also phosphorylate LIM-kinase which in turn will phosphorylate cofilin and thus inactivate it. This will lead to actin fiber stabilization as cofilin usually degrades the actin filaments. All of these effects create a network of actin fibers which create contractile strength to enable the cell to move forward. Diagram compiled from references within *Section 1.3.2.1*.

1.3.2.2 *Rho/ROCK Activation*

As with all GTPases, Rho-GTPases have the ability to control signal transduction pathways by cycling between an inactive guanine di-phosphate (GDP)-bound form and an active guanine tri-phosphate (GTP)-bound form (Figure 1.7). This Rho-GTPase activation cycle is regulated by guanine nucleotide exchange factors (GEFs), GTPase-activating proteins (GAPs), and guanine nucleotide dissociation inhibitors (GDIs). GEFs promote the activation of the Rho-GTPase by promoting the exchange of GDP for GTP (Figure 1.7). This cycle is negatively regulated by GAPs which increase the intrinsic GTPase activity of Rho-GTPases to return it to the inactive form. GDIs block the GTPase cycle by solubilising the GDP-bound form of the Rho-GTPase (Moon and Zheng 2003). Extracellular signals appear to promote the activation of Rho-GTPases via modification of the GEFs. The activated Rho-GTPases will then interact with downstream effectors (e.g. ROCK) to stimulate a number of responses including actin cytoskeletal rearrangements, gene transcription regulation, membrane trafficking, cell cycle regulation, and the control of apoptosis (Ridley 2001).

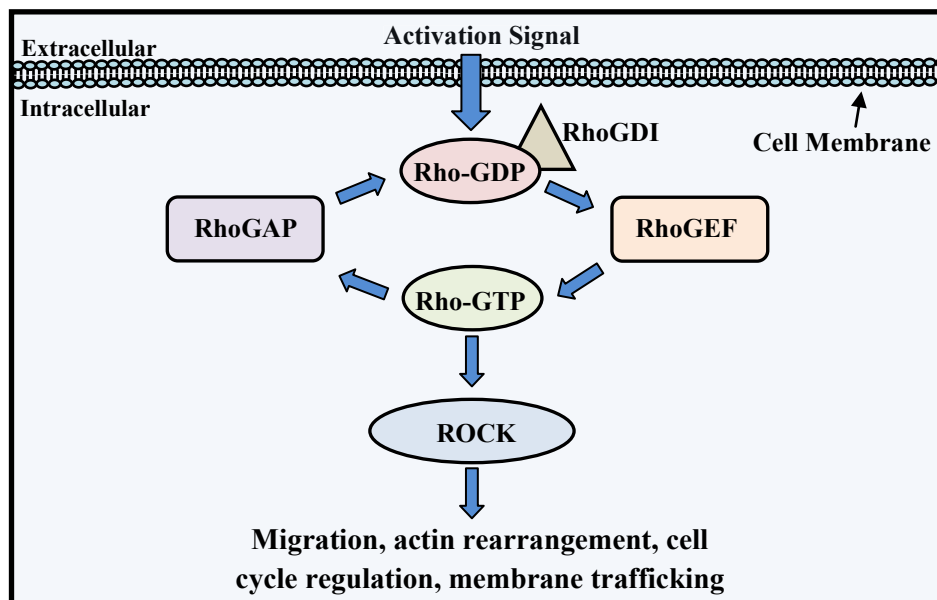


Figure 1.7: Mechanism of Rho activation and subsequent ROCK phosphorylation. (Detailed mechanism described in text above – Section 1.3.2.2). Diagram adapted from (Moon and Zheng 2003)

1.3.2.3 ROCK Structure

ROCK consists of a serine/threonine kinase domain located at the amino-terminus, a coiled-coil domain forming the middle region, and a pleckstrin homology (PH) domain region, which contains a cysteine-rich zinc finger-like motif at the carboxyl terminus (Figure 1.8). Nakagawa and colleagues isolated cDNA from two distinct mouse libraries (Nakagawa *et al.*, 1996). The first was the mouse counterpart of the human ROCK-1 and the second was a novel ROCK-related kinase (ROCK-2). They also demonstrated that the two similar, yet distinct, kinases were expressed in different tissues. ROCK-1 mRNA was expressed quite ubiquitously, with only low levels expressed within the brain and muscle, whereas ROCK-2 mRNA was found in abundance specifically in the brain, muscle, heart, lungs, and placenta (Shi and Wei 2007). These results suggest that the roles of ROCK-1 and -2 should be examined independently as well as in combination to fully understand the downstream mechanisms involved in migration of different cell types.

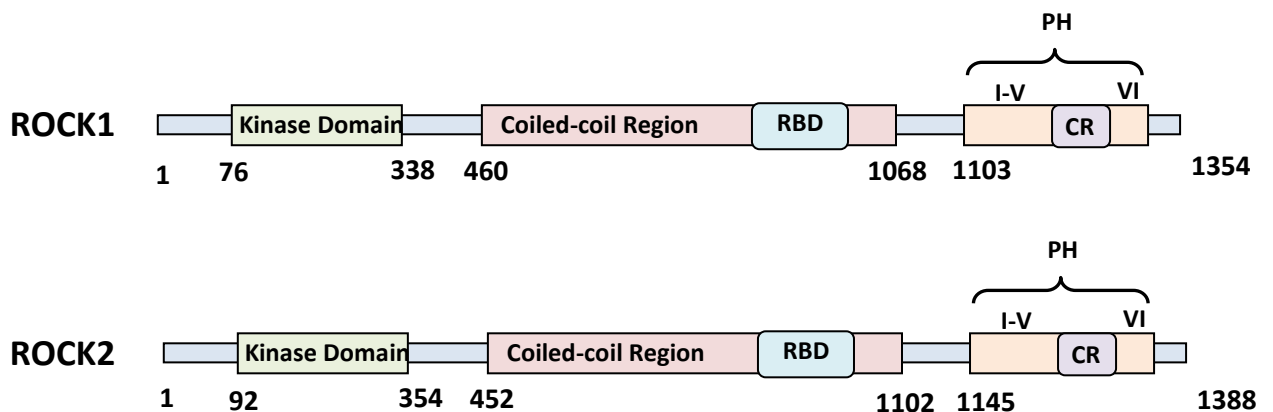


Figure 1.8: The specific domains and regions of ROCK-1 and -2. ROCK sequences have a serine/threonine kinase domain located at the amino-terminus of the protein, followed by a central coiled-coil domain containing a Rho-binding domain (RBD) and a carboxyl terminal pleckstrin homology (PH) domain with an internal cysteine-rich domain (CR). Diagram adapted from (Nakagawa *et al.*, 1996)

1.4 SKELETAL MUSCLE GROWTH & REPAIR

The optimal restoration of skeletal muscle tissue is critical for normal function of the repaired tissue. Growth factors, cytokines and ECM components regulate myogenic processes during muscle repair and regeneration; certain factors are known to be pro-fibrotic and cause scar tissue formation in severe muscle injuries.

1.4.1 Muscle Injury & Wound Repair

Most common forms of muscle injury occur as a result of physical activities and can be divided into two types. During *in situ* necrosis the myofibers are degraded via specific necrotic mechanisms, while the basement membrane remains unbroken. However, following lacerations, severe muscle strain, and contusions, a shear type injury may result (Ehrhardt and Morgan 2005). Shear injuries are a severe form of muscle injury that results in the tearing or breaking of the basement membrane and allows for components of the interstitial ECM to enter the muscle fiber (Moyer and Wagner 2011).

1.4.1.1 In Situ Necrosis

Necrosis involves the rapid cell death of the skeletal muscle fiber. However, only a segment of the fiber is degraded, and the length of the segment depends upon the nature of the injury. At the onset of necrosis, both loss of sarcolemma integrity and myonuclear dissolution will occur. This is followed by the degradation of organelles with resultant debris within the necrotic segment (Moyer and Wagner 2011). Macrophages invade the segment and assist in phagocytosis and removal of the debris. This is essential for optimal regeneration to occur in the damaged area (Figure 1.9A). Satellite cells are activated by cytokines and growth factors, such as HGF, and migrate along the intact basement membrane (also termed basal lamina) to the site of injury where they differentiate into myotubes (Figure 1.9B) (Ehrhardt and Morgan 2005). The myotubes finally fuse with undamaged myofibers to facilitate complete repair (Figure 1.9C). Necrosis is triggered in many forms of muscle dystrophies and inflammatory myopathies such as Duchenne/Becker muscle dystrophy (DMD) resulting in a constant degradation-regeneration state (Jarvinen *et al.*, 2007).

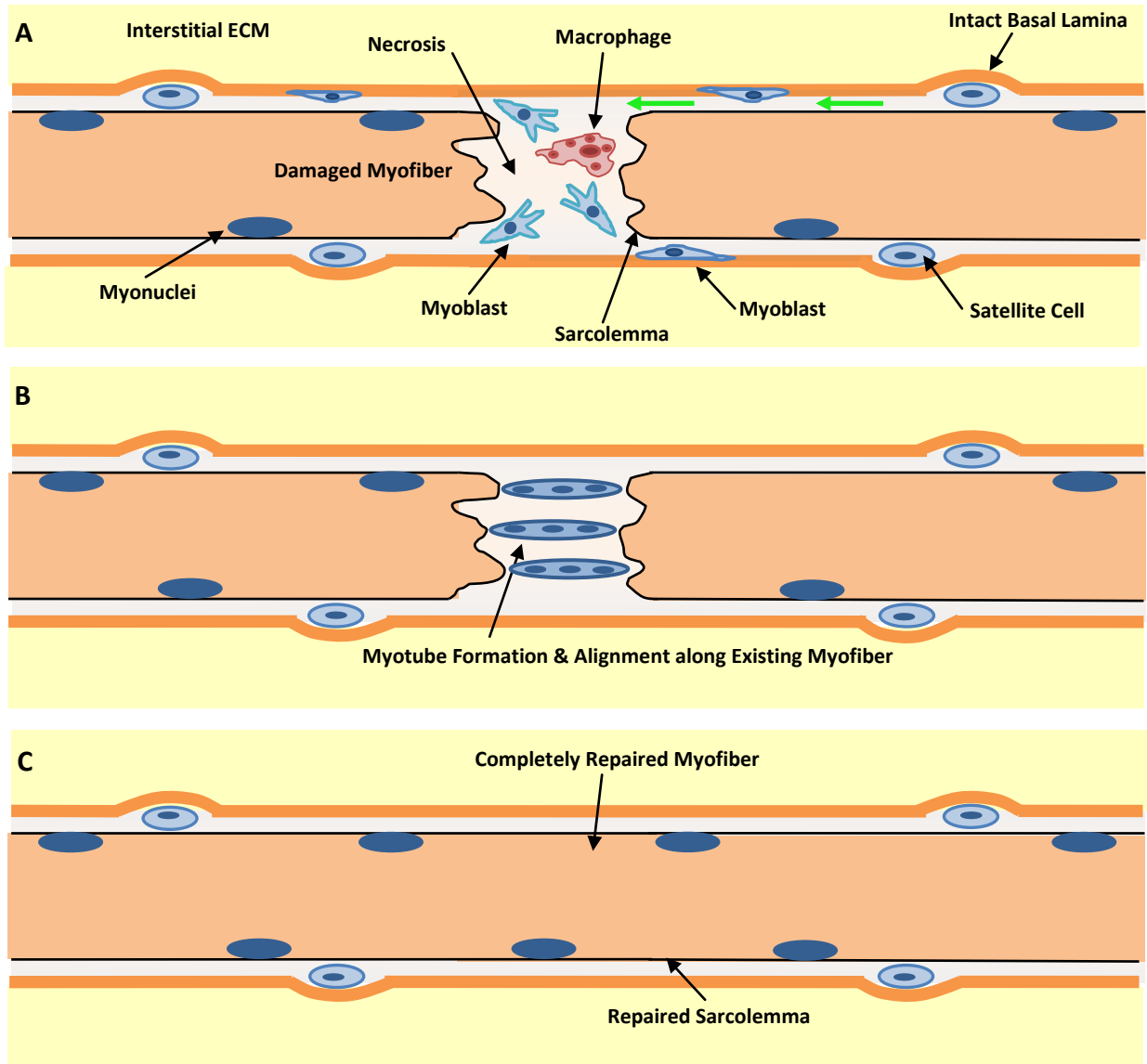


Figure 1.9: Myofiber regeneration following necrosis. During *in situ* necrosis, macrophages remove debris, while myotube formation and fusion with the original myofiber allows healing of the myofiber. During this process the basement membrane (basal lamina) remains intact. Diagram compiled from references within Section 1.4.

1.4.1.2 *Shear Type Injuries*

Following a shear type injury, the myofibers, surrounding blood vessels, myelin sheaths surrounding bundled myofibers, as well as the basal lamina, are all ruptured (Jarvinen *et al.*, 2004). Regeneration following contusions and lacerations occurs in a 3 step process; degradation of debris, repair and remodeling (Figure 1.10) (Rushton *et al.*, 1997).

i) Degradation of Debris

The degradation process begins with necrosis of the damaged myofiber segment, followed several hours after the injury by establishment of a new sarcolemma to seal off the damaged segment (Figure 1.10A). The remaining myofibers then contract leaving a gap between them which is filled by red blood cells and platelets due to damaged blood vessels. This is followed by the invasion of macrophages and monocytes to phagocytose the necrotic debris (Tidball 2005).

ii) Repair

Satellite cells in the surrounding myofibers assist in the subsequent repair process (Figure 1.10B). Satellite cells begin to proliferate and form a myoblast population which will differentiate into myotubes. At the same time that the satellite cells are beginning to proliferate, fibroblasts within the interstitial ECM become activated to myofibroblasts by growth factors, in particular HGF. The myofibroblasts migrate into the wound area and begin to secrete ECM components such as fibronectins and collagens to provide structural support for the damaged myofiber (Mackey *et al.*, 2012). The newly formed myotubes will fuse with the existing segments, but rarely fuse with each other, due to scar tissue. The myofibers then begin to penetrate the connective scar tissue formed between the two myofiber segments, but are unable to penetrate entirely through the dense scar tissue.

iii) Remodeling

The remodeling process (Figure 1.10C) involves the formation of new contractile segments within the existing myofiber, and the attachment of these ends to the connective scar tissue. The scar tissue will contract, pulling the two ends of the myofiber closer together. However, the two ends will always be separated by the connective scar tissue and the optimal linear contractile force of the muscle is hampered. Fibrosis inhibits the complete repair of the myofiber and subsequently results in a loss of function of the damaged myofiber after repair (Rushton 2007).

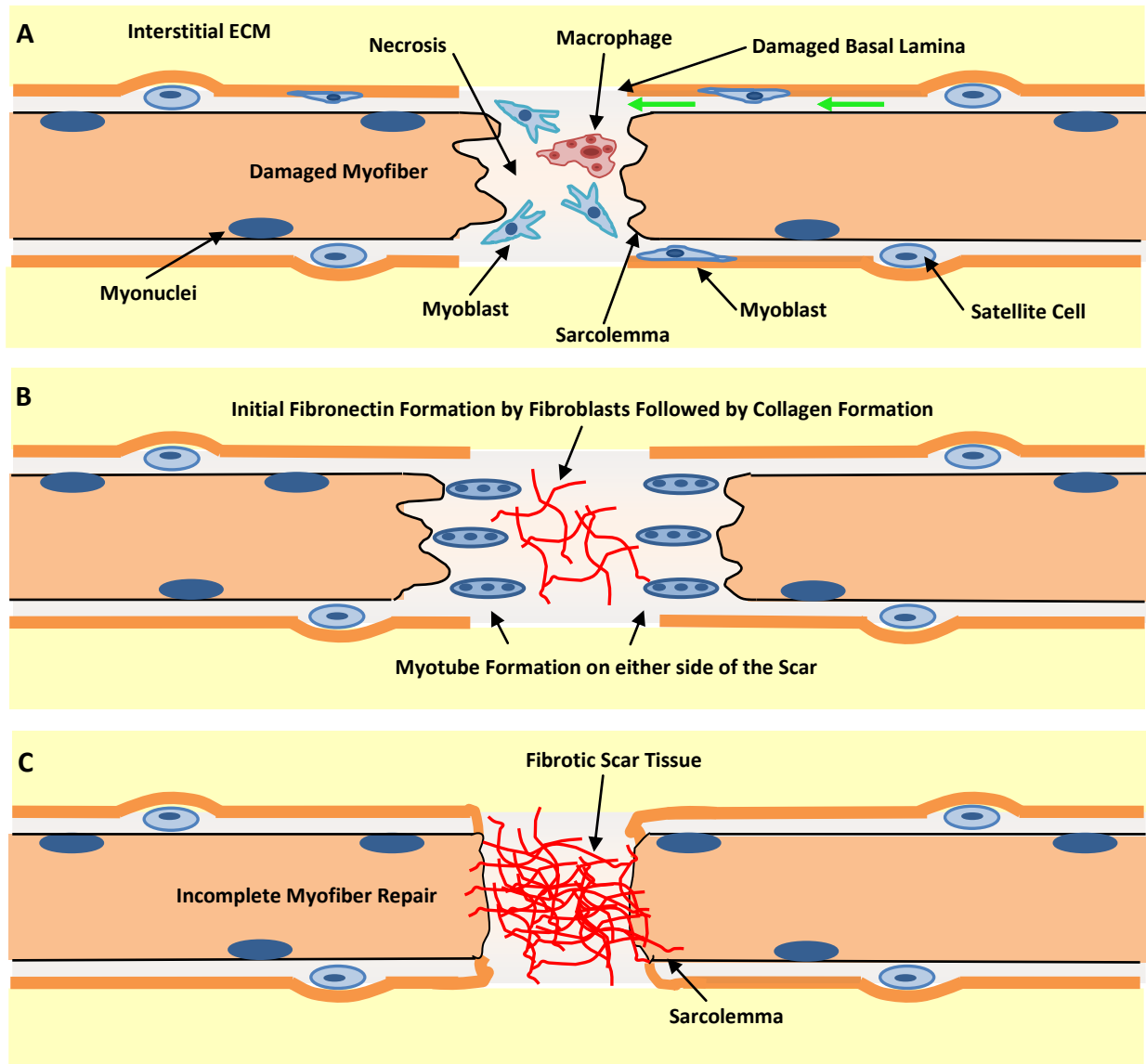


Figure 1.10: Myofiber regeneration after shear injury. During a shear type injury the basement membrane (basal lamina) is broken. This allows for fibroblasts located within the interstitial ECM to enter into the damaged myofiber and secrete ECM components. Myoblasts facilitate repair by fusing with the damaged myofibers. However, they are unable to transverse the dense fibrotic scar tissue. The scar tissue laid down by the fibroblasts initially consists of fibronectin, but is later replaced by collagen I which is a stronger scaffold. After repair the scar tissue remains, reducing the contractile force of the muscle. Diagram compiled from references within *Section 1.4*.

1.4.2 Fibrosis

Fibroblasts are activated during injury of the skeletal muscle and are subsequently termed myofibroblasts. As mentioned above, the myofibroblasts migrate into the wound and synthesize ECM proteins to strengthen the connective tissue framework during muscle repair (Sheffer *et al.*, 2007).

The first ECM components to be synthesized and laid down by the myofibroblasts are fibronectin and tenascin-C. These components create an elastic-type framework to support the mechanical load being applied to the injured muscle, as well as to provide support for the early granulation tissue, which was formed from the blood cells and was deposited in the wound. Collagen I and III are then synthesized to create a more permanent support scaffold. Collagen I is the major component of the connective scar tissue which remains after the muscle fiber has been regenerated (Ehrhardt and Morgan 2005). The tensile strength created by the collagen I is attributed to intermolecular cross-linking between the collagen I molecules during scar tissue maturation. Once the scar tissue has fully matured, the repaired area is no longer the weakest point in the muscle fiber, but it has lost the major part of its contractile function (Jarvinen *et al.*, 2007). This suggests a survival mechanism of rapid, compromised repair predominates over slow, full repair of the muscle to ensure a quick return to functionality and ultimately the survival of the organism.

A delay in inflammation or an impaired activation of satellite cells has been shown to result in excessive fibrotic tissue deposition. This may be due to factors and enzymes secreted by inflammatory cells and myoblasts, such as decorin and proteases (MT1-MMP and MMP-2) which possess anti-fibrotic characteristics. Fibrosis occurs in many muscular dystrophies and is enhanced by the growth factor TGF- β , which is regarded as the key mediator in tissue fibrosis. (Chua *et al.*, 2005; Zanotti *et al.*, 2005). TGF- β is contained in high concentrations within platelets and is released into the tissue at the site of injury. Inactive TGF- β is also found within the ECM and is released upon injury. An increased concentration of active TGF- β triggers fibroblasts to differentiate into myofibroblasts, migrate to the injured area and synthesize ECM components. TGF- β production in surrounding cells is also triggered in an autocrine fashion due to increased TGF- β found within the wound area (Border and Noble 1994; Li *et al.*, 2004).

Decorin has been shown to act as an anti-fibrotic agent in mouse skeletal muscle by binding to TGF- β and resulting in reduced fibrosis (Sato *et al.*, 2003). In a study conducted

by Fukushima and colleagues, decorin was injected into a laceration created within murine muscle at 0, 5, 10, 15 days post-injury. The results demonstrated a decreased level of fibrotic tissue formation, as well as complete regeneration of the muscle to a level similar to that of non-injured muscle at all time points. However, addition at day 10 and 15 showed the best reduction in fibrotic scar tissue. Decorin also reduced myofibroblasts proliferation when added separately or with TGF- β (Fukushima *et al.*, 2001; Fukushima *et al.*, 2006). This indicates that decorin may be used to counteract the fibrotic effect of TGF- β resulting in optimal skeletal muscle wound healing with minimal scar tissue formation.

1.4.3 Myoblast Transplantation Challenges

Myofibers are mitotically inactive and cannot regenerate when damaged. Satellite cells and myoblasts within the myofiber are the primary means by which repair occurs and in the event of a major injury, they often cannot cope with the demands required to successfully repair the damaged muscle. Myoblast transplantation could aid in severe muscle injuries as the number of satellite cells able to divide and proliferate into myoblasts will be significantly increased upon transplantation (Usas *et al.*, 2011). However, a number of challenges exist and have prevented successful myoblast transplantation and subsequent improved wound healing. These include the rejection of the transplanted myoblasts, an inability of the myoblasts to migrate to and penetrate the wound area successfully, and the death of a large number of myoblasts after transplantation (Guerette *et al.*, 1997).

The concept of myoblast rejection was largely overlooked in early human transplantation experiments as many of the mouse models used were nude mice, which have a deficient immune system (Usas *et al.*, 2011). It was also thought that rejection would not be an issue in muscle transplantation as muscle cells were initially thought not to contain MyHC molecules. However, this theory was abandoned as it was shown that myoblasts do in fact express MyHC (Huard *et al.*, 1994). Autologous transplantation of cultured human myoblasts isolated from muscle biopsies may circumvent this problem. However, the generation of sufficient cell numbers is still a hurdle to be overcome (Saijara *et al.*, 2009).

The low success rate of transplanted myoblasts is also due to the limited migration seen following injection into the wound (Rando *et al.*, 1995). This may be due to the myoblasts becoming trapped within the interstitial connective tissue surrounding the myofiber, as well as negative effects of pro-fibrotic cytokines and ECM factors, such as TGF- β and collagen I. Kinoshita *et al.*, showed that addition of bFGF, a MMP activating factor, to

myoblast cultures prior to transplantation increased migration and the success of myoblast transplantation four-fold, as increased MMP secretion aided in degradation of the surrounding interstitial ECM (Kinoshita *et al.*, 1995).

The third issue in myoblast transplantation is that 95-99% of myoblasts transplanted into a wound die within the first week after transplantation (Beauchamp *et al.*, 1999). The cell death is accredited to the inflammatory response following myoblast transplantation. A method to overcome this high percentage of cell death is to enhance the proliferation of the surviving myoblasts within the wound. However, pre-treating the myoblasts with bFGF increases the proliferation of the myoblasts, but decreases their ability to fuse (Guerette *et al.*, 1997). Leukemia inhibitory factor (LIF) and TGF- β have also been shown to increase the proliferation of myoblasts (Austin and Burgess 1991); however, TGF- β concomitantly decreases differentiation (Schabort *et al.*, 2009). Therefore, stimuli that promote proliferation may decrease differentiation potential which is problematic for the technique of myoblast transplantation, indicating the need for further knowledge in this area.

Aging also negatively affects the ability of muscle to repair as the deposition of ECM components changes in older muscle (Jasper and Kennedy 2012). Non-enzymatic glycation of collagen I occurs during aging and diabetes, affecting polymerization and intermolecular interactions (Young *et al.*, 2006). A study conducted by Reigle and colleagues showed that not only was glycated collagen I less likely to form normal helical conformations, but that the binding of proteoglycans (such as decorin and biglycan) to collagen I was diminished, resulting in matrix integrity disruptions, decreased cell-collagen interactions and subsequent decreased cellular migration (Melrose *et al.*, 2008; Reigle *et al.*, 2008). Another key regulator of fibrosis within aged muscle is the Wnt family of secreted proteins, which have been shown to modulate myogenic, fibrogenic and adipogenic activity within regenerating adult muscle (Wagers 2008). Age-dependent increases in Wnt signaling promote the transdifferentiation of activated myogenic satellite cells to fibrogenic cells and thereby contribute to deficient repair of aged muscle (Brack *et al.*, 2007; Chakkalakal *et al.*, 2012). These issues highlight the importance of cell-matrix interactions on cell migration and wound repair.

1.5 SUMMARY AND AIMS

Throughout this chapter we have highlighted the components and mechanisms involved in regulating skeletal muscle migration to facilitate wound repair. Collagen, fibronectin, laminin, decorin and TGF- β are key ECM components found in the extracellular matrix which regulate aspects of myogenesis and fibrotic scar tissue formation (Figure 1.11). ROCK, a downstream effector of the Rho GTPase migratory pathway, is an important facilitator of cellular migration (Figure 1.11).

Our objective within this study was to determine the effect of decorin, TGF- β , Matrigel (collagen IV and laminin), fibronectin and collagen I on myoblast migration. To achieve this we first needed to establish an assay best suited specifically for analyzing myoblast migration. Our specific aims were therefore to:

Chapter 2:

- 1) Optimize a scratch assay for our myoblast migration and analysis.
- 2) Develop a co-culture assay utilizing isolated primary culture murine myoblasts and fibroblasts to mimic *in vivo* conditions more closely.

Chapters 3-5:

- 1) Determine the effect of decorin, Matrigel, collagen I, fibronectin on murine and human myoblast migration
- 2) Determine the role of ROCK in myoblast migration under the above-mentioned conditions
- 3) Investigate the role of the TGF- β 2/decorin complex on myoblast migration under different ECM conditions.

Chapter 6:

- 1) Develop a 3-dimensional skeletal muscle tissue model for analysis of ECM components within a 3D micro-environment.

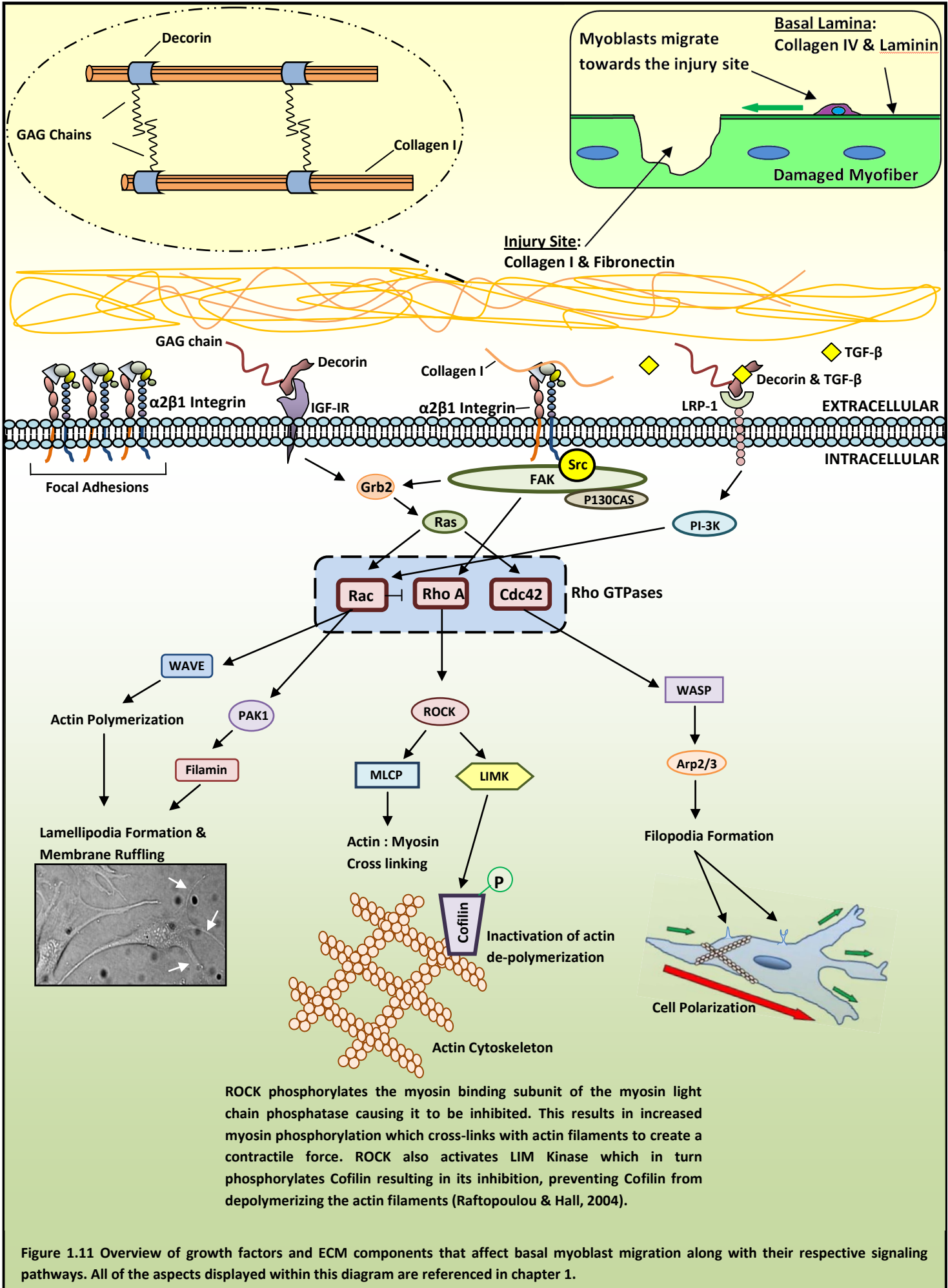


Figure 1.11 Overview of growth factors and ECM components that affect basal myoblast migration along with their respective signaling pathways. All of the aspects displayed within this diagram are referenced in chapter 1.

CHAPTER 2

IN VITRO MODEL DEVELOPMENT & OPTIMIZATION

Includes data from:

Goetsch, K. P. & Niesler, C. U. (2011) Optimization of the scratch assay for *in vitro* skeletal muscle wound healing analysis, *Anal Biochem*, vol. 411, no. 1, pp 158-160.

Goetsch, K. P., Myburgh, K., Niesler, C. U. (2012) Simultaneous isolation of enriched myoblasts and fibroblasts for migration analysis within a novel co-culture assay, *Stem Cell research – in Revision*

2.1 INTRODUCTION

Skeletal muscle repair requires the activation of satellite cells to myoblasts and their migration to the region of injury. Initially myoblasts migrate along the basal lamina, in a 2-dimensional manner and subsequently enter the injury site where they facilitate repair by fusing into myotubes (Ranzato *et al.*, 2009). Currently, a range of assays (Table 2.1) are available to researchers who wish to study 2-dimensional migration, however the problem with several of these migration assays is they do not take into account many of the *in vivo* conditions which would be present during muscle regeneration.

Table 2. 1: Summary of widely utilized migration assays and variations upon these models

Migration Assay	Assay Variation	References
Chemotaxis Assay	• Boyden chamber – top & bottom chambers	Boyden, 1962
	• Zigmond chamber – side by side chambers	Zigmond, 1988
	• Dunn chamber – concentric ring chambers	Zicha <i>et al.</i> , 1991
	• Microfluidic chambers	Meyvantsson & Beebe, 2008
	• μ -slide Chemotaxis assay	Zengel <i>et al.</i> , 2011
Stopper-Based Assay	• Oris™ assay – silicone stopper	Nizamutidnova <i>et al.</i> , 2007
	• Cell exclusion zone assay	Poujade <i>et al.</i> , 2007
Scratch/Wound Assay	• Scratch assay with chemotactic gradient	Smith <i>et al.</i> , 2010
	• Scratch assay – photoablation	Tamada <i>et al.</i> , 2007
	• Electrical wound assay	Keese <i>et al.</i> , 2004
	• ECIS (electric cell-substrate impedance sensing) - fully automated	Gorshkova <i>et al.</i> , 2008

Depending on the cell type and aspect of migration under investigation, three migration assays are utilized routinely by researchers. These are the chemotaxis, stopper-based and scratch/wound healing assays (Table 2.1) (Goetsch and Niesler 2011). Chemotaxis assays involve the establishment of a temporary gradient, normally between two chambers separated by a microporous membrane. This is followed by the analysis of the movement of cells from one chamber to the other (Figure 2.1A & 2.1D) (Boyden 1962; Zigmond 1988; Zicha *et al.*, 1991; Meyvantsson and Beebe 2008; Zengel *et al.*, 2011). However, for the study of adherent cells such as myoblasts, accurate quantification of migration using this system is difficult since migrated cells adhere to the underside of the membrane. Furthermore, the established gradient is short-lived, the use of the assay for analysis of the effect of ECM factors is limited, and morphological changes cannot be detected easily. In addition, using the traditional Boyden chamber, the mode of migration is not representative of the migration of myoblasts in response to injury *in vivo*, where myoblasts have to migrate *along* the basal lamina of the myofiber towards the injury site (Siegel *et al.*, 2009).

The stopper-based and scratch/wound healing assays are both two-dimensional assays and monitor the migration of a monolayer of adherent cells into an area which does not contain any cells (Figure 2B, C, E, F) (Keese *et al.*, 2004; Liang *et al.*, 2007; Poujade *et al.*, 2007; Tamada *et al.*, 2007; Gorshkova *et al.*, 2008; Nizamutdinova *et al.*, 2009; Smith *et al.*, 2010; Goetsch and Niesler 2011). The advantage of this strategy is that the rate of migration can be determined and visual changes in cell morphology can be observed via time-lapse microscopy. In addition, the wells can be coated with different ECM substrates allowing analysis of migration under conditions which mimic the *in vivo* environment more closely (Goetsch and Niesler 2011). When comparing the scratch/wound healing assay to the stopper-based assay, the scratch assay has the advantage that it incorporates the actual wounding of cells, and therefore to an extent, a response that would be elicited *in vivo* due to this “wounding”.

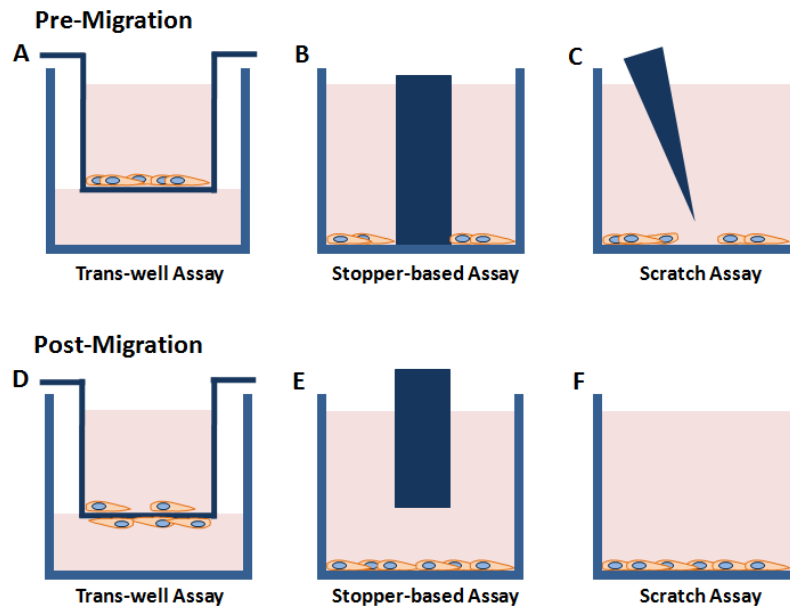


Figure 2.1 Pre- and post- cellular migration within different migration assays. The effects of migration depicted are that of adherent cells such as myoblasts. Initial seeding of cells prior to migration within the trans-well (A), stopper-based (B) and scratch assays (C). Post-migration effect for the trans-well (D), stopper-based (E) and scratch assays (F). The cells are seeded within the trans-well chamber which has a porous base to allow for migrating cells to pass through due to the chemotactic gradient. For the stopper-based assay the stopper is removed and the number of cells that migrate within the area which contained the stopper are counted. The scratch assay is analyzed by taking a series of images throughout the migration period and calculating the percentage wound closure from the area of the scratch.

Despite these advantages, the scratch assay still fails to account for key migration regulatory signals secreted by other cells, such as fibroblasts, during the repair process (Cornelison 2008; Velnar *et al.*, 2009; Ten Broek *et al.*, 2010). The majority of *in vitro* assays used to study skeletal muscle cell migration within the healing context focus solely on the movement of myoblasts in response to various growth or extracellular matrix factors (Cooper and Isacson 2004; Goetsch *et al.*, 2011). The addition of exogenous stimuli (e.g. growth factors) and substrates (e.g. collagen, laminin) to these systems represents an effort to mimic *in vivo* conditions. However, failure to include interstitial cells, such as fibroblasts (usually present in the wound post-injury) within the assay, prevents the researcher from establishing an accurate reflection of the replacement process occurring *in vivo* (Cornelison 2008; Ten Broek *et al.*, 2010). Fibroblasts contribute to the milieu by secreting growth and extracellular matrix (ECM) factors which influence the migration of myoblasts (Murphy *et al.*, 2011). For instance, following injury, satellite cells express the

functional CXCR4 receptor. This binds to stromal-derived factor-1 (SDF-1), a chemokine secreted by fibroblasts during muscle repair and facilitates the homing of satellite cells to the injury site (Ratajczak *et al.*, 2003; Miller *et al.*, 2008). Furthermore, hepatocyte growth factor (HGF), an important satellite cell activation factor, and fibroblast growth factor (FGF), a key regulator of myogenic proliferation, migration and terminal differentiation, are both secreted by fibroblasts and are required for muscle regeneration (Fedorov *et al.*, 1998; Neuhaus *et al.*, 2003). It is therefore necessary to take into account the effect of the factors these cells secrete during myoblast migration.

In this chapter we present the optimization of a scratch assay specifically designed for myoblast migration, the development of a primary culture isolation protocol for murine fibroblasts and myoblasts, and a unique co-culture assay utilizing these isolated cells. We also show that the isolation of highly pure cultures of myoblasts and fibroblasts from the same muscle slurry can be achieved consistently, rapidly and inexpensively. Furthermore, the co-culture assay is designed to better mimic *in vivo* wound healing conditions, as both myoblasts and fibroblasts from the same animals are incorporated into one assay. This is unique to a wound healing assay as it allows for secreted factors from the fibroblasts to interact with the migrating myoblasts during wound repair and provides an *in vitro* environment which is closer to that of actual wound healing conditions *in vivo*.

2.2 EXPERIMENTAL PROCEDURES

2.2.1 Animals

BALB/c mice were bred and maintained at the University of KwaZulu-Natal (UKZN) animal house, Pietermaritzburg. Mice were utilized for skeletal muscle primary culture isolation at 3-6 weeks of age. All animals were handled in accordance with guidelines of the UKZN Animal Ethics Research Committee (Ethics number: 068/11/animal).

2.2.2 Culture Conditions

C2C12 myoblasts were used for initial scratch assay optimization experiments. The cells were maintained in a humidified incubator at 37°C, 5% CO₂ in growth medium consisting of Dulbecco's Modified Eagle's Medium (DMEM, Highveld, cat. CN3193-9) supplemented with 2% L-glutamine (Cambrex, cat. 17-605E), 2% PenStrep (Cambrex, cat. 17-602E) and 10% fetal calf serum (FCS, Invitrogen, cat. 10108165). Primary culture media consisted of Ham's F-10 nutrient mixture (Gibco, cat. 31550) supplemented with 20% FCS (Gibco, cat. 10108165), 2% penstrep (Gibco, cat. 15140), 50 µg/ml Gentamicin (Gibco, cat. 15750-037) and 2.5 ng/ml fibroblast growth factor (rhFGF, Promega, cat. G507A). The 6-well plates, T25 flasks and co-culture chambers (IVF center well dish, Nunc, cat. 1019411) used in the pre-plating, enrichment and co-culture steps were coated with 50 µg/ml rat tail collagen I (a gift from Dr. E. Elliott, Discipline of Biochemistry, University of KwaZulu-Natal). Enrichment media used after the initial pre-plating isolation consisted of a 1:1 Ham's F-10 nutrient mixture with Dulbecco's Modified Eagle's Medium (DMEM) (Sigma, cat. D5648), 20% FCS, 2% penstrep, 2.5 ng/ml rhFGF. All cells were maintained in a humidified incubator at 37°C, 5% CO₂.

2.2.3 Scratch Assay

C2C12 cells were plated at 5×10^4 cells per well in a 24-well plate (TPP, cat. 92024) and were incubated at 37°C until 80% confluent. The cultures were "wounded" with a loading tip (1-200µl, Whitehead Scientific, cat. 010), washed with PBS, and re-incubated with 250µl growth media. Wounds were photographed at hours 0, 1, 3, 5, & 7 with the *Motic 3* megapixel camera (40 X magnifications, Olympus CKX41) and were analyzed via the *Motic 2.0* image analysis software. All experiments were performed in triplicate and repeated three times. The following equation was used to determine the percentage wound closure:

$$\frac{[Wound\ area(0\ h) - Wound\ area\ (n\ h)]}{Wound\ area\ (0\ h)} \times 100 = Percentage\ wound\ closure$$

2.2.4 Live Cell Imaging

Cells were seeded onto a glass-bottom tissue dish (cat. *P35G-1.5-14-C*, Matek Corporation) and the scratch assay was performed, as previously described. Real-time visualization was determined by differential interference contrast (DIC) microscopy, utilizing the Zeiss LSM 710 confocal microscope, within an incubated chamber at 37°C and 5% CO₂. Images were taken at 2 minute intervals for 3 hours. Live cell analysis was done with the manual cell tracker plug-in for ImageJ (available as freeware at rsbweb.nih.gov/ij/) which calculates distance and velocity of the cell migration.

2.2.5 Preparation of Primary Cultures

The isolation protocol was adapted from Rando and Blau (Rando and Blau, 1994). Briefly, 3-6 week old mice (two mice per isolation; a single animal did not yield sufficient cells), were euthanized and submerged in 70% ethanol for 5 minutes within a sterile level II biological safety cabinet. The hindlimbs were removed and the muscle was dissected away from the bone and placed within a few drops of warm phosphate buffered saline (PBS, pH 7.2). The muscle from both mice was minced into a coarse slurry using a razor blade. The cells were enzymatically dissociated by the addition of 2 ml of a 1 mg/ml collagenase/dispase solution (Roche, cat. *10269638001*). The slurry was incubated at 37°C on a shaker for 40 minutes, with titration of the slurry every 10 minutes to dislodge the cells. The slurry solution was filtered through a sterile tea sieve and washed thoroughly with PBS (20 ml). The filtrate was then centrifuged at 350 g to pellet the cells. Finally, the supernatant was discarded and the pellet was re-suspended in 2 ml primary culture media and plated in one well of a 6-well plate coated with 50 µg/ml collagen I; this well was referred to as pre-plate 1 (PP1; Passage 0).

2.2.6 Isolation of Myoblasts and Fibroblasts

Isolated cells went through a series of five pre-plating steps (PP1-PP5), all plates were coated with 50 $\mu\text{g/ml}$ collagen I, in order to isolate both fibroblasts and myoblasts (Figure 2.2). After 1 hour the cell suspension solution was moved from the PP1 well to the PP2 well. Remaining PP1 cells (Passage 0) were washed with PBS and 2 ml new primary media was added to the well. This wash step with PBS and the addition of new primary media was repeated whenever the cell suspension was moved to a new well for PP2, PP3, PP4 and PP5. The incubation times for each pre-plate were 1 h (PP1), 2 h (PP2), 18 h (PP3), 24 h (PP4), 24 h (PP5). Following each subsequent incubation time, the non-adherent cells transferred to a new well contained more myoblasts (green cells, Figure 2.2) and fewer fibroblasts (orange cells, Figure 2.2). Conversely, the adherent cells remaining behind consisted of fewer myoblasts and more fibroblasts in PP1; compared to PP5, which contained predominantly myoblasts. The media was replaced every day with two PBS wash steps prior to the addition of 2 ml primary media. Once the cells reached a density of approximately 70% within the wells of the 6-well plate they were transferred to collagen I coated T25 flasks (Passage 1) for enrichment. (Note: it was important to check for contaminants at this point to ensure optimal cell viability).

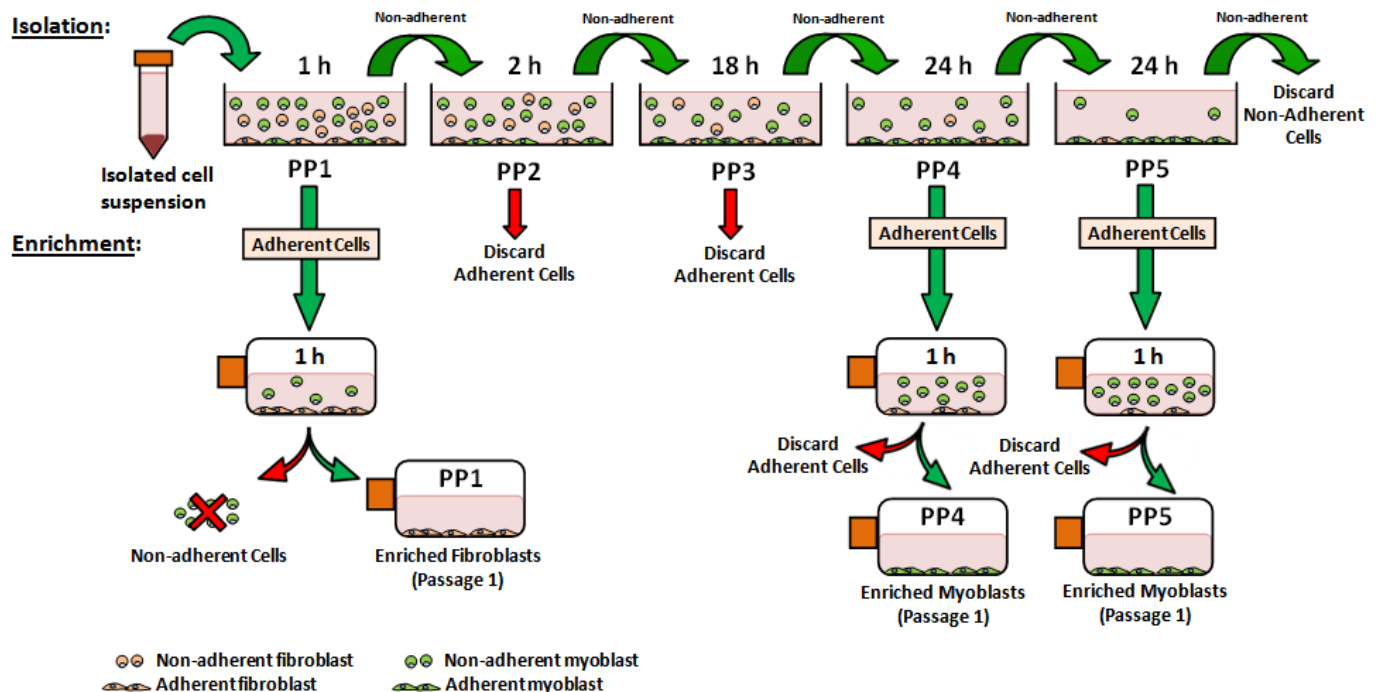


Figure 2.2 Isolation of primary cultured fibroblasts and myoblasts. Diagram of the isolation procedure which utilizes consecutive pre-plating steps for the isolation and enrichment of myoblasts and fibroblasts. PP1-PP5 refers to consecutive pre-plates 1-5. PP2 & PP3 flasks were tested for desmin positive cells before being discarded.

2.2.7 Enrichment of Primary Cultures

Only PP1, PP4 and PP5 (all Passage 0) were utilized for the enrichment of cells (Figure 2.2). Enrichment of fibroblasts and myoblasts by pre-plating was adapted from Richler and Yaffe (Richler and Yaffe 1970). For fibroblast enrichment, adherent cells from PP1 (Passage 0) in the initial isolation well were trypsinized (1 ml of 0.25% trypsin, Highveld Biological, cat. *CN3649*) and transferred with the addition of 5 ml enrichment media to a T25 flask. The flask was incubated for 1 hour after which the media, along with any non-adherent cells was discarded and replaced with 5 ml enrichment media. This allowed for the enrichment of fibroblasts (now Passage 1), which have a shorter adhesion time compared to myoblasts. For PP4 and PP5 the opposite was carried out for enrichment. The cell suspension which did not adhere to the flask within the first hour was placed in a new T25 flask (now Passage 1), eliminating the majority of fibroblasts and resulting in myoblast enrichment due to the difference in cell adhesion times. The enriched populations were grown to a density of 70%. At this point the PP1, PP4 and PP5 cell populations were either frozen down (1 ml enrichment media containing 1% DMSO, 20% FCS) in liquid nitrogen or plated for experimental purposes.

2.2.8 Immunofluorescence of Isolated Primary Cultures

Cells were grown on glass coverslips coated with 50 µg/ml collagen I within a 24 well plate. The cells were fixed with a 4% paraformaldehyde solution for 10 minutes and washed twice with PBS for 5 minutes. For blocking, a 5% donkey serum solution (Sigma, cat. *D9663*) was added for 1 hour at room temperature (RT), followed by the addition of the following primary antibodies for 2 hours at room temperature: polyclonal rabbit anti-human desmin (1/500, Abcam, cat. *AB15200*) and monoclonal mouse anti-human Pax7 (1/500, Abcam, cat. *AB55494*). The coverslips were then washed three times with PBS for 5 minutes. Secondary antibodies, Dylight488 donkey anti-rabbit (1/1000, Jackson, cat. *711-485-152*) and Dylight594 donkey anti-mouse (1/1000, Jackson, cat. *715-515-151*), were added for 1 hour at room temperature in the dark. This was followed by three washes with PBS (5 min), the addition of Hoechst (1/4000, Sigma, cat. *B2261*) for 5 minutes, and finally, four PBS wash steps. Coverslips were then mounted onto slides with moviol mounting media. The slides were viewed, directly after labelling, with a Zeiss 710 confocal microscope at 40X magnification.

2.2.9 Co-Culture Assay

Enriched fibroblasts (PP1, Passage 1) were seeded in 2 ml enrichment media onto the outer-ring of collagen I-coated co-culture chambers, with 10 000, 20 000, 40 000, 80 000 cells per dish. Enriched myoblasts (PP4/5, Passage 1) were seeded in 2 ml enrichment media in the inner chamber, at 70 000 cells per dish (Figure 2.2). Control conditions consisted of a co-culture chamber seeded only with enriched myoblasts in the inner chamber and media in the outer-ring. The seeded chambers were incubated for 16 hours at 37°C, 5% CO₂. A scratch was then performed as previously described (Goetsch and Niesler, 2011). Overflow of media between the outer-ring and inner chamber occurred directly after the scratch had been performed, with the addition of 13 ml enrichment media (Figure 2.3, blue arrows). Images were captured at initial “wounding” and at hours 3.5 and 7 post-“wounding” with the Motic Image Plus 2.0 software.

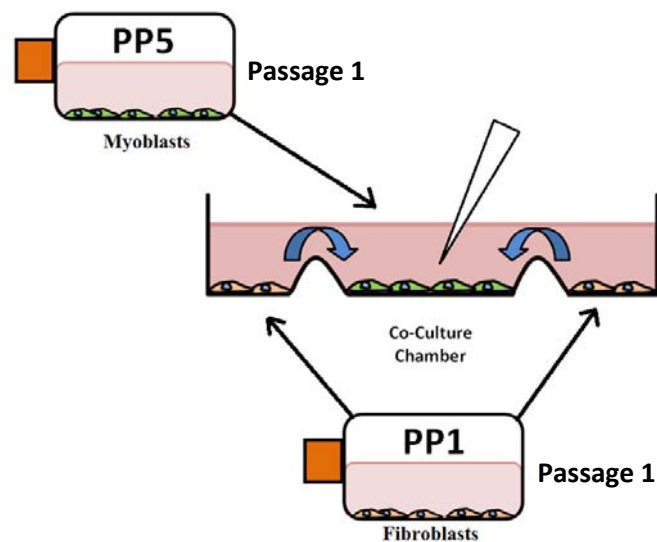


Figure 2.3 Co-culture assay utilizing isolated primary culture myoblasts and fibroblasts.

Diagram of the co-culture assay which utilizes a two-chamber culture dish with myoblasts seeded in the center and fibroblasts seeded in the outer ring. PP1 & PP5 refers to pre-plates 1 & 5, respectively.

2.2.10 Statistics

Statistical evaluations were performed for the scratch assay by non-parametric Mann-Whitney U tests for all experiments. For the co-culture assay and isolation procedure, triplicate data points were obtained for each condition and a *Student's t-test* was performed to calculate *p*-values for the differences between the means of experimental conditions and control. *Genstat* was used for all statistical tests and significance was determined as $p < 0.05$. Results are presented as the mean +/- standard error of the mean (SEM) for three or more individual experiments.

2.3 RESULTS

Initial migration analysis was carried out utilizing the Oris™ stopper-based assay (Nizamutdinova *et al.*, 2009; Park *et al.*, 2012), but it was found that only a few myoblasts moving around the edge of the area blocked originally by the stopper leading to inconsistent results (*data not shown*). This was attributed to the lack of signalling factors to promote the migration of myoblasts into the open area. The only promoting factor for migration was the lack of contact of surrounding cells (i.e. an open area for the cells to expand and proliferate into). We therefore, decided to adopt the scratch assay as our model of choice for myoblast migration as we could coat the flasks with different ECM components at varying concentrations, “wound” cells to release signalling molecules and monitor migration over an optimal time period to avoid proliferative effects. This specific regulation while monitoring myoblast migration allowed us to better mimic *in vivo* conditions specific for myoblast migration.

2.3.1 Scratch Assay Development

We first needed to establish the best way to perform the scratch in order to ensure and remove the very minimal quantity of ECM coating as possible within the well. We initially tried a rigid tip (yellow pipette tip) and a flexible tip (loading pipette tip). Wounds created via the loading and yellow tip methods were analyzed and the percentage wound closure equation over a 7 hour period was assessed (Figure 2.4B). The loading tip, along with a streaking action (Figure 2.4ii), demonstrated the best method as smaller consistent wounds could be achieved and a greater wound closure over the twisting yellow tip method was observed (Figure 2.4B).

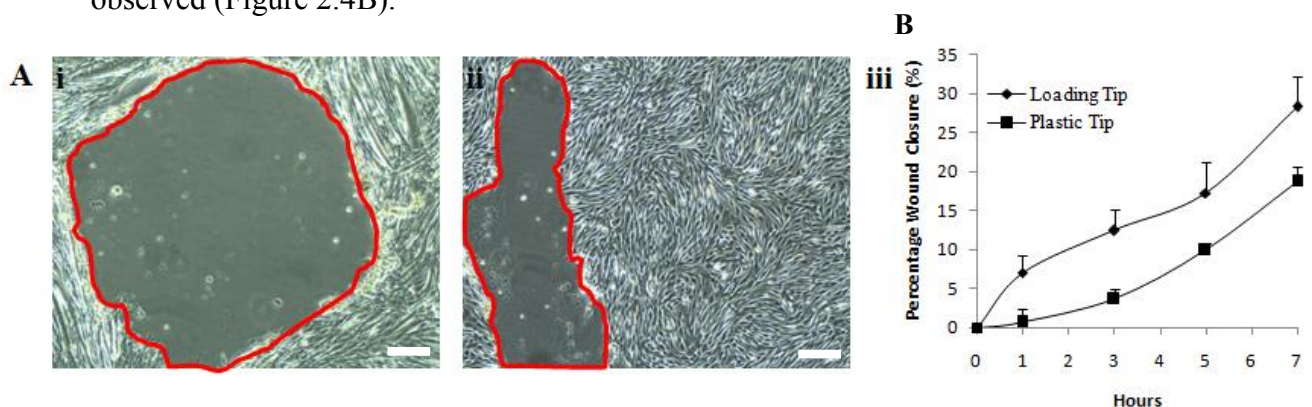


Figure 2.4 Scratch assay optimization for C2C12 myoblast cell line. Scratches were performed in a 24-well plate containing C2C12 myoblasts at a 80% confluence level. **A)** Photos depicting the differences between the two scratch sizes of the yellow tip (**i**) and the loading tip (**ii**). **B)** Percentage wound closure for the plastic and loading tips over a 7 hour period. Images were taken with the Motic 3 megapixel camera at 4X magnification. All data shown as \pm SEM.

To ensure that the C2C12 cells were migrating into the wound area instead of encroaching on the wound area via proliferation, the cells moving across the wound edge were monitored for the classical migration shape. Migrating C2C12 cells will extend a number of lamellipodia at their front with the tapering off of the tail at the rear of the cell. This classical myoblast migration shape was witnessed throughout the scratch assay experiments ensuring that the results reflected migrating cells (Figure 2.5, black arrow). To determine the optimal time period, myoblast migration was monitored over a 24 hour period via live cell imaging (Figure 2.6). After ± 8 hours the proliferative effects of the myoblasts begin to affect the percentage wound closure results and after 9-12 hours depending on treatment the “wound” area reached 100% wound closure. A 7 hour period was therefore determined as the optimal time period to monitor myoblast migration.

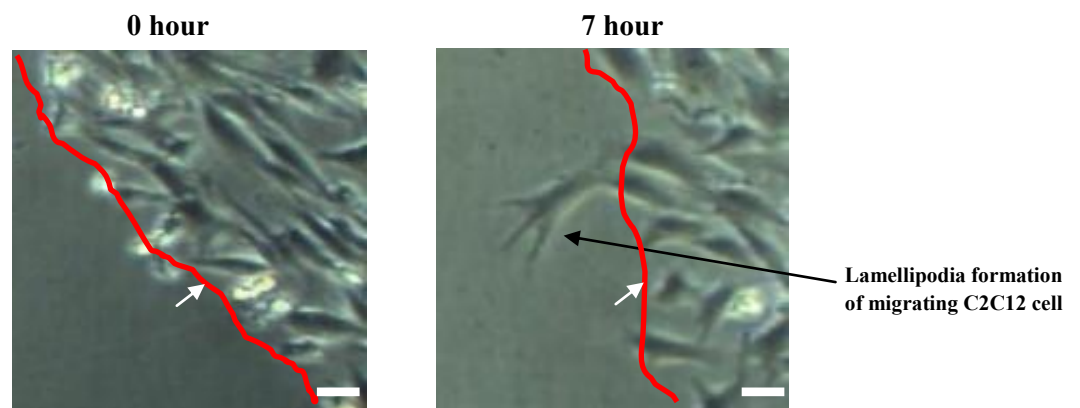


Figure 2.5 Wound front at 0 and 7 hours depicting a classically migrating C2C12 myoblast. Scratches were performed, using a loading tip, on collagen-coated 12-well plates containing C2C12 myoblasts at a 90% confluence level. Images were taken at 0, 1, 3, 5, & 7 hours with the *Motic 3* megapixel camera at 100x magnification. The white arrow shows the wound front. The black arrow depicts a C2C12 myoblast in the classical migration shape with lamellipodia extending into the wounded area.

Live cell tracking was also performed to monitor the movement of migrating cells into the “wound” area in terms of directionality and velocity. The outline of the lamellipodia as well as the nucleus was traced for each migrating myoblast (Figure 2.6). This allowed for individual cell tracking of migrating cells and up to 8 cells per field of view could be individually tracked at the same time utilizing this method of live cell imaging.

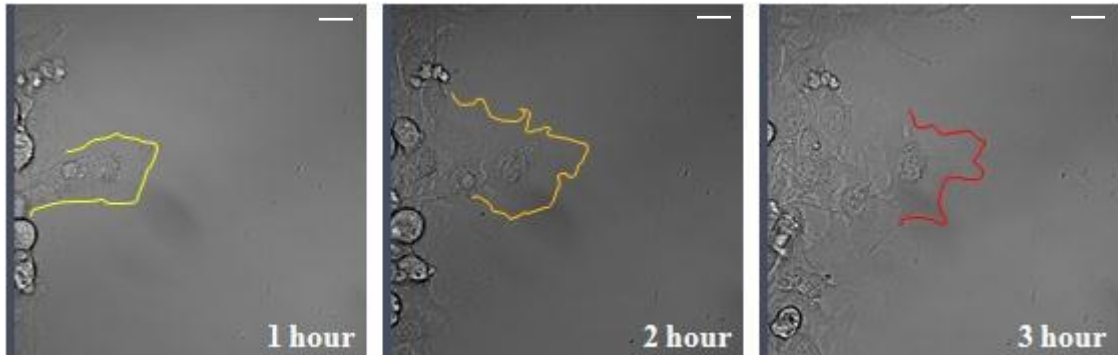


Figure 2.6 Live cell tracking of migrating C2C12 myoblasts. C2C12 myoblasts were grown to 80% confluency on glass coverslips prior to the scratch assay. Live cell tracking of a migrating C2C12 myoblast at the wound front. Images were taken at 1 hour (yellow), 2 hour (orange) and 3 hour (red) post-wounding. Images were taken with the LSM 710 confocal microscope at 40X magnification. Scale bar = 10 μ m.

2.3.2 Isolation and enrichment of murine myoblasts and fibroblasts

The isolation protocol of primary fibroblasts and myoblasts utilized a serial pre-plating technique specifically optimized for the enrichment of both cell types. To determine the percentage of myoblasts present at each pre-plate level (PP1-PP5), cells were fixed and immuno-labelled for desmin (a subunit of the intermediate filaments in skeletal muscle tissue commonly used to identify primary isolated myoblasts) and Pax7 (a satellite cell transcription factor). Although PP6 was isolated during initial experiments, it was not utilized further, as too few cells remained in the cell suspension to contribute to a viable cell population.

After the establishment of an isolation protocol, myoblasts were identified as cells staining positive for desmin and Pax7 (Figure 2.7). The percentage cells positive for desmin/Pax7 was then determined (Figure 2.8). PP1 (Passage 0), which was subsequently utilized for fibroblast enrichment, contained an average myoblast population of $36 \pm 7.53\%$. An increase in the percentage myoblasts present in each subsequent pre-plate was evident, with PP2, PP3, PP4 and PP5 (all Passage 0) containing a myoblast purity of $47 \pm 6.64\%$, $62\% \pm 0.27\%$, $80 \pm 8.12\%$ and $96 \pm 0.9\%$, respectively (Figure 2.8). PP4 and PP5 were selected for myoblast enrichment due to the significantly higher percentage of myoblasts within these pre-plates when compared to PP1-PP3 ($p < 0.05$ and $p < 0.005$; Figure 2.8).

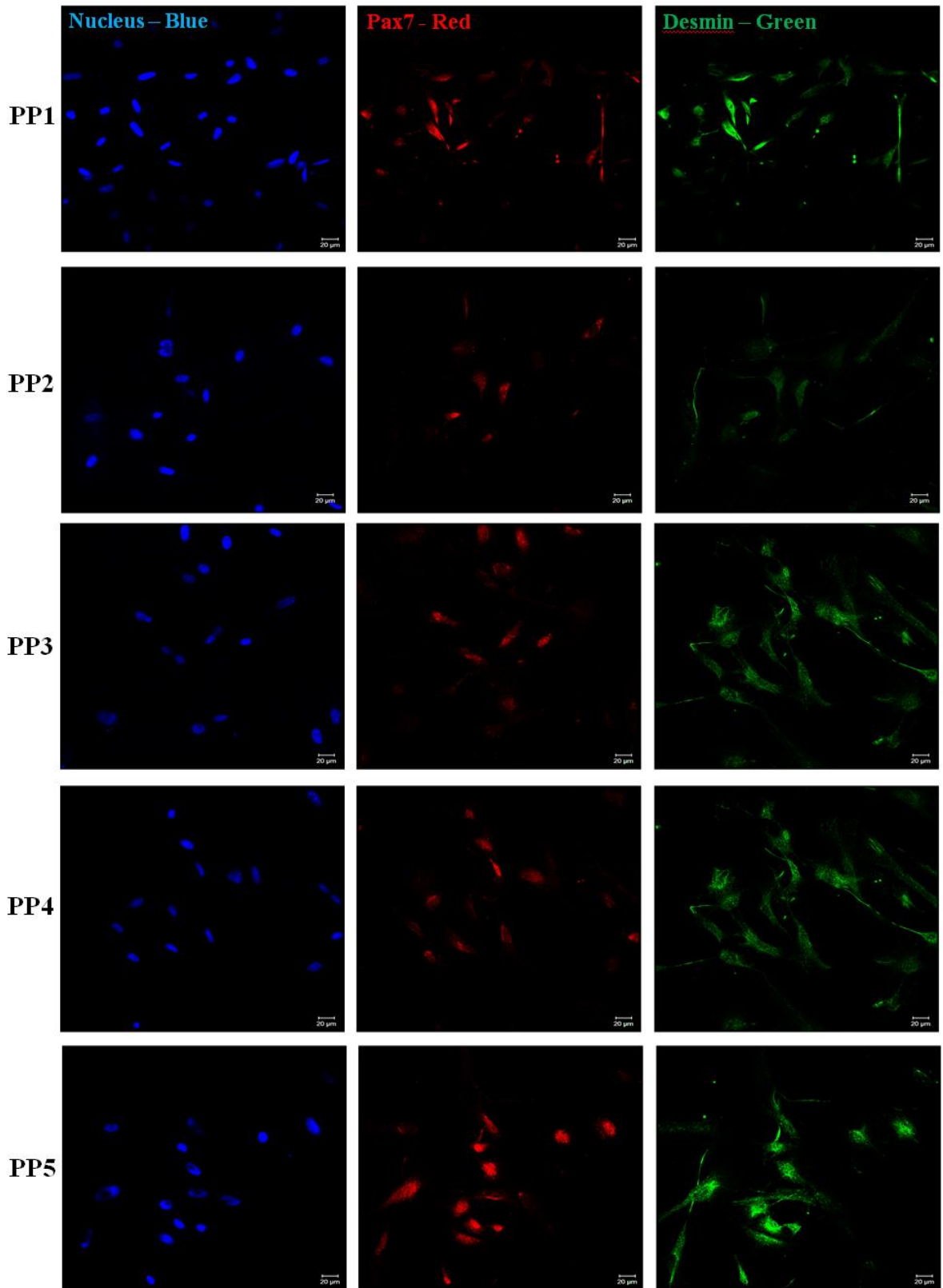


Figure 2.7 Primary cultured myoblasts from PP1-PP5.

Micrographs of cell populations from PP1 through to PP5 immuno-labelled with mouse monoclonal anti-desmin (green) and mouse monoclonal anti-Pax7 (red) antibodies. Hoechst (blue) was used as the nuclear stain. The cells were seeded on coverslips coated with 50 µg/ml collagen I and images captured using a Zeiss 710 confocal microscope at 40X magnification. Scale bar = 20µm. n=3 (5 random fields of view per n).

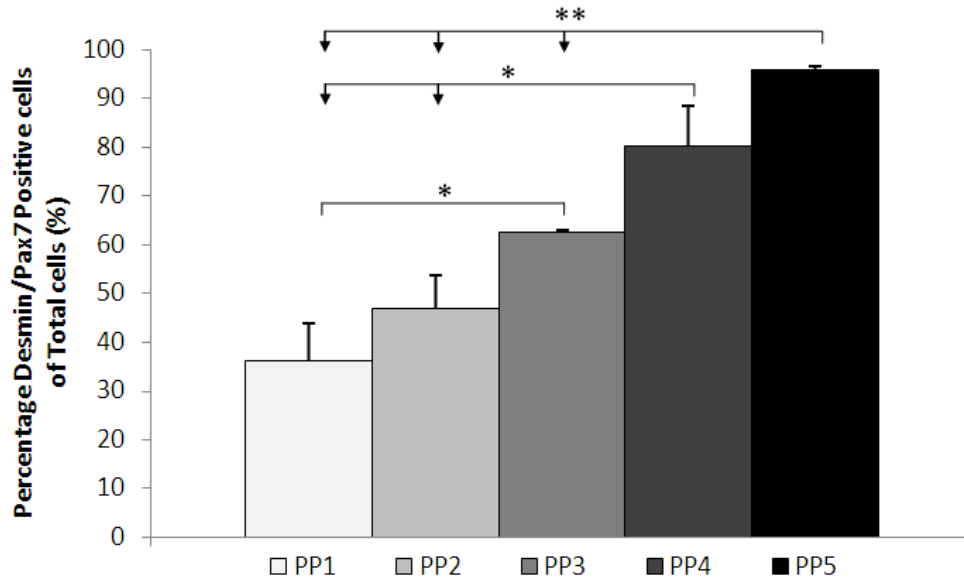


Figure 2.8 Percentage desmin⁺/Pax7⁺ cells (PP1-PP5) of the total cellular population.

Bar graph showing the percentage desmin and Pax7 positive cells (compared to total number of cells stained with Hoechst). Pre-plate 1 (PP1) through to pre-plate 5 (PP5) were isolated as previously described (Figure 2.2). * $p < 0.05$, ** $p < 0.005$, $n = 3$ (5 random fields of view per n), data = Mean \pm SEM.

2.3.3 Lineage confirmation for use in the co-culture assay

Following the enrichment of fibroblasts and myoblasts, cells (Passage 1) were plated out into a co-culture dish. Myoblasts (PP4/5; Passage 1) were tested for their ability to migrate using the scratch assay (Figure 2.9Ai). Cells migrating into the “wound” area were immuno-labelled for desmin to ensure that myoblasts, and not any residual fibroblasts, migrated into the “wound” area (Figure 2.9Aii). Expression of Pax7 and desmin in PP1 (Passage 1) was compared to the control myoblast C₂C₁₂ cell line (Figure 2.9B).

Consistent scratches were readily reproducible within the primary myoblast cultures and a relatively low amount of debris was observed on the migration front (Figure 2.9Ai), resulting in consistent “wound” areas for all experimental groups and controls. All the cells on the migrating front at 7 hours post-“wounding” labelled positive for desmin, indicating the PP4/5 cells migrating into the “wound” area were myoblasts and that observations drawn from the co-culture assay would be a true reflection of myoblast migration (Figure 2.9Aii). C₂C₁₂ cells were used as a positive control and labelled strongly for desmin and Pax7. (Figure 2.9Bi). The PP1 population which had been enriched for fibroblasts was not found to express either Pax7 or desmin (Figure 2.9Bii). Given the culture conditions employed, this suggested a population of predominantly fibroblasts. PP5 enriched for myoblasts showed desmin/Pax7 positive labelling for all cells (Figure 2.9Biii).

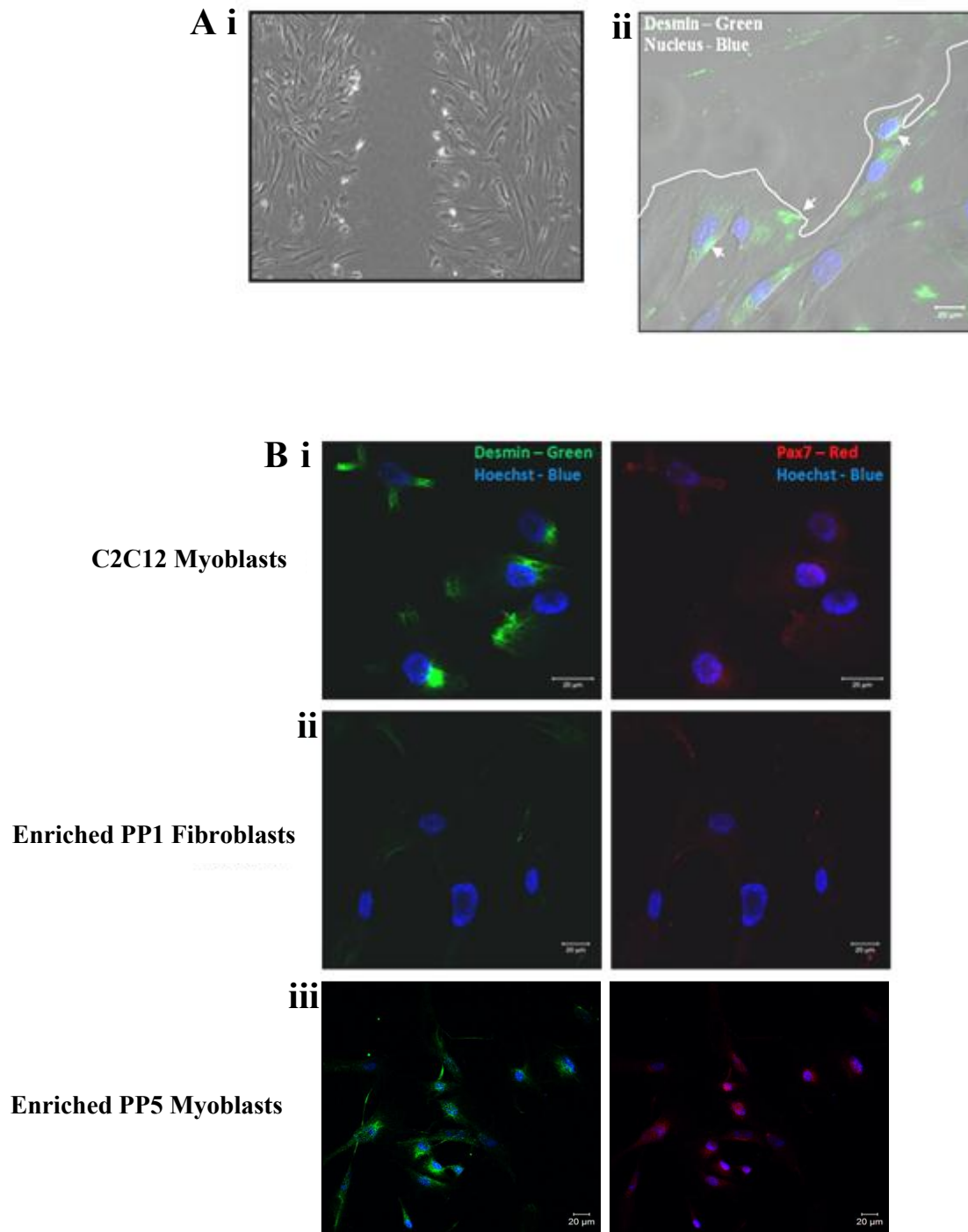


Figure 2.9 Validation of co-culture wound healing assay. (Ai) Micrograph of the scratch area within the myoblast-seeded inner chamber. All scratches were performed on 50 $\mu\text{g}/\text{ml}$ collagen I-coated co-culture chambers. (ii) Micrographs of desmin positive cells (green) at the leading front of the “wound” area. (B) Fibroblast purity within the outer-ring was determined by comparison between the C₂C₁₂ myoblast cell line (i), PP1 enriched fibroblasts (ii), and PP5 enriched myoblasts (iii). Desmin (green) and Pax7 (red) were used to distinguish myoblasts from fibroblasts. Hoechst (blue) was used as the nuclear stain. Images were captured using the Zeiss 710 confocal microscope at 40X magnification. Scale bar = 20 μm .

2.3.4 Validation and application of co-culture assay to determine the effect of fibroblasts on myoblast migration

To validate the newly developed co-culture assay, the percentage wound closure following myoblast injury was compared over time in the presence and absence of fibroblasts. It was found that, in the presence of fibroblasts (60 000 cells), the percentage wound closure negatively affected migration after 1 hour compared to control. However, after hours 5 and 7 there was a significant increase (7 hour: $69.3 \pm 5.2\%$; $p < 0.001$) when compared with control (7 hour: $40.4 \pm 2.4\%$), which lacked fibroblasts (Figure 2.10B). The rate of myoblast migration was also significantly increased in the presence of fibroblasts ($10.0 \pm 0.8 \%$ /hr; $p < 0.025$) compared to control ($5.4 \pm 0.6 \%$ /hr) conditions (Figure 2.10C).

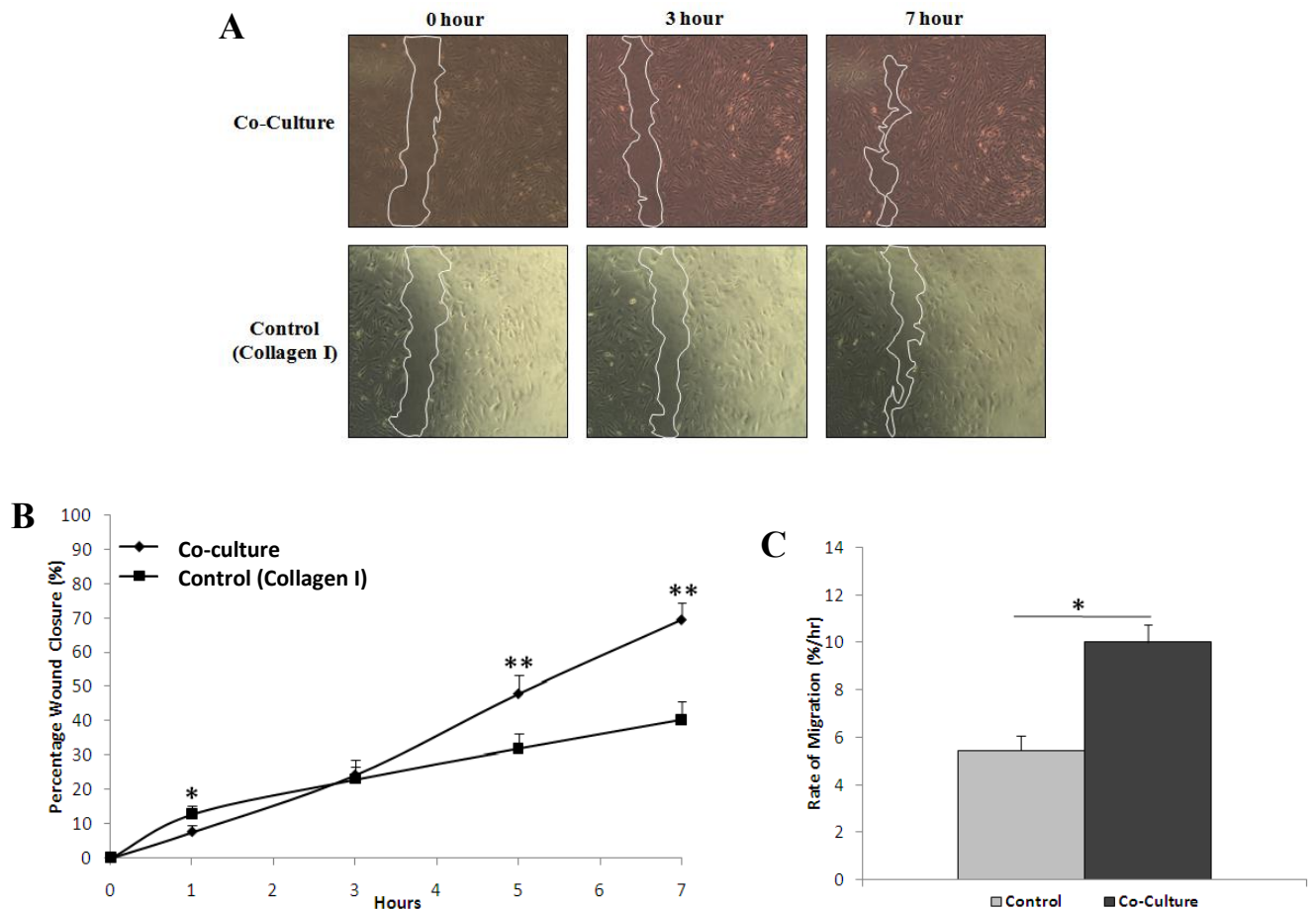


Figure 2.10 Preliminary findings of co-culture assay versus scratch assay.

(A) Micrographs of scratch assay control (collagen I 50 µg/ml) versus co-culture assay (collagen I 50 µg/ml) at initial wounding and, 3 and 7 hours post-wounding. (B) Line graph showing the percentage wound closure at 0, 1, 3, 5 and 7 hours post-“wounding” for control (without fibroblasts) and co-culture (containing fibroblasts). All scratches were performed on 50 µg/ml collagen I coated co-culture chambers. Images were captured with the 3MP *Motic* camera and analysed with the *Motic Plus 2.0* software. (C) Plot of the rate of migration of myoblasts for control and co-culture assay at 7 hours post-“wounding”. * $p < 0.05$, ** $p < 0.005$, $n = 3$, error bars = \pm SEM.

A dose response was then carried out to determine the exact effect of fibroblast *number* on myoblast migration. 10 000 - 80 000 enriched fibroblasts from PP1 (Passage 1) were seeded in the outer-ring and enriched myoblasts from PP4/5 (Passage 1) were seeded within the inner chamber (at 70% confluence). A co-culture dish containing PP4/5 myoblasts within the inner chamber and only media within the outer-ring was used as the control for all co-culture experiments. Consistently sized scratches were induced for all experiments and the “wound” area was calculated at hours 3.5 and 7 (Figure 2.11A).

The percentage wound closure was calculated and a noticeable effect was observed, whereby the increase in fibroblast number led to an increase in the percentage wound closure (Figure 2.11B). The percentage wound closure changed from 51.6 \pm 5.1% (no fibroblasts), 48.3 \pm 2.7% (10 000 fibroblasts), 60.0 \pm 5.9% (20 000 fibroblasts), 67.4 \pm 7.9% (40 000 fibroblasts; $p < 0.05$) to 87.1 \pm 8.2% (80 000 fibroblasts; $p < 0.005$). Co-culture with 80 000 fibroblasts had the greatest significant effect compared to control ($p < 0.007$) at 7 hours post-“wounding”. At 3.5 hours post-“wounding” no significant difference in the percentage wound closure was observed for all experimental groups compared to the control (Figure 2.11B). The rate of migration was also consistent with the results observed above, with an increase in the rate of migration as fibroblast number increased. The rate (% per hour) of myoblast migration in response to co-culture with 80 000 fibroblasts was 12.4 \pm 1.2, a significant increase compared to the other 3 conditions: control 7.4 \pm 0.7 ($p < 0.011$), 10 000 fibroblasts, 6.9 \pm 0.4 ($p < 0.006$), and 20 000 fibroblasts 8.6 \pm 0.8 ($p < 0.028$) (Figure 2.11C).

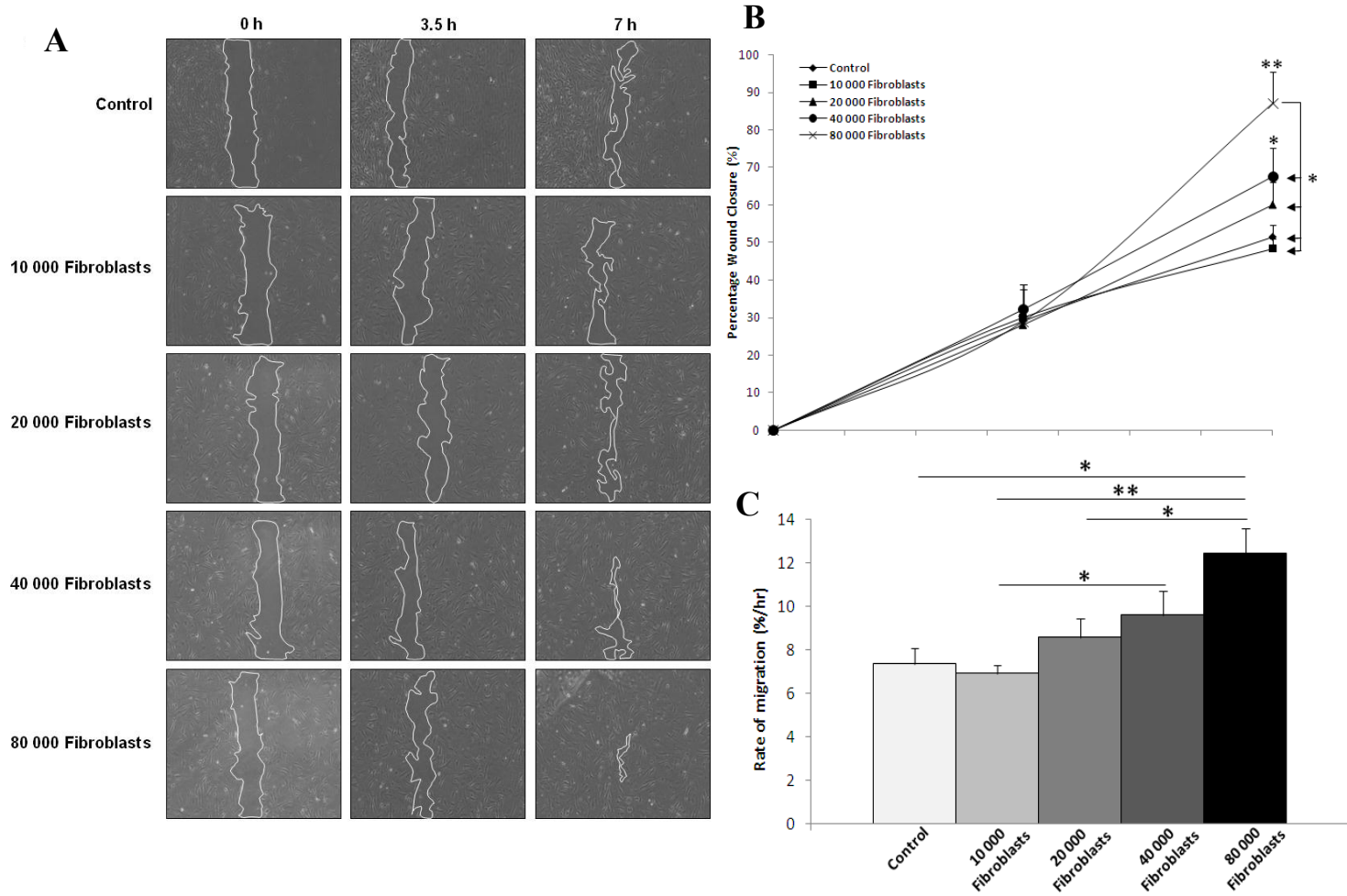


Figure 2.11 Dose response of fibroblast cell number on myoblast migration.

(A) Micrographs of the “wounded” area within the myoblast monolayer (imaged at 0, 3.5 and 7 hours post-“wounding”) in response to control, 10 000, 20 000, 40 000, 80 000 fibroblasts. All scratches were performed on 50 $\mu\text{g/ml}$ collagen I coated co-culture chambers. Images were captured with the 3MP *Motic* camera and analysed with the *Motic Plus 2.0* software. The white outline represents the calculated “wound” area. (B) Line graph showing the percentage wound closure at 3.5 and 7 hours post-“wound” in response to increasing number of fibroblasts initially seeded. (C) Graph of the rate of migration of myoblasts for control, 10 000, 20 000, 40 000, 80 000 fibroblasts at 7 hour post-“wounding”. * $p < 0.05$, ** $p < 0.005$ compared to control, $n=3$, Mean \pm SEM.

2.4 DISCUSSION

In this chapter we report the development of an optimized scratch assay protocol specifically for the analysis of myoblast migration, as well as a novel co-culture assay which utilizes primary cultured myoblasts and fibroblasts from the same animal. The optimized scratch assay has numerous benefits over existing migration models including that it: a) is ideal for migratory studies of adherent monolayer cell types, b) is versatile; as it allows modification of the ECM coating on which the myoblasts migrate, c) mimics the *in vivo* situation, as the “wound” releases cytokines, d) allows for the analysis of both undifferentiated myoblasts and differentiated myotubes, e) can be adjusted to discount proliferation as a confounding factor, f) allows simultaneous microscopic analysis of morphology and protein distribution, g) permits accurate assessment of the percentage wound repair, and h) is cost effective and relatively simple to set up in a basic tissue culture lab (Goetsch and Niesler 2011).

Numerous protocols for the isolation of primary myoblasts using culture procedures have been published, however, most protocols focus on acquiring significant myoblast numbers following consecutive pre-plate passages. To our knowledge, none of these isolate both myoblasts and fibroblasts simultaneously from the same animal to establish an *in vitro* co-culture wound healing assay. Our optimised protocol efficiently generates low passage, pure myoblast and fibroblast populations. Furthermore, we were able to utilise it to establish a novel wound healing protocol which uses the co-culture of these two cell types to mimic the *in vivo* environment more closely.

One of the major concerns with primary myoblast isolation relates to the purity and late passage number utilized in experimental designs. To address this we ensured our purity level was greater than 80%. It has been demonstrated that after passage three, isolated myogenic cells display a decrease in myogenic marker expression (Desmin, MyoD and Pax7) and lose a significant ability to differentiate (Machida *et al.*, 2004). Due to this we have focused on maintaining a low passage number; we were consistently able to utilise cells at Passage 1 or 2 (for both fibroblasts and myoblasts).

The inclusion of fibroblasts within our co-culture assay allows for multiple fibroblast-secreted factors to bind to and stimulate myoblasts. In addition, fibroblasts and myoblasts are isolated simultaneously from the same muscle slurry, further ensuring a profile closer to *in vivo* conditions. This model is ideal for drug discovery and potentially myoblast

transplantation studies as it gives the researcher a better representative model of myoblast migration triggered by signals present under *in vivo* injury/wound conditions (Tremblay *et al.*, 1997). Importantly, our newly optimised method is also relatively inexpensive and uncomplicated in comparison to other previously published methods (Rando and Blau 1994; Gharaibeh *et al.*, 2008; Musaro and Barberi 2010).

The term “co-culture” is often used to describe a setup where two different cell populations are combined within the same dish, such as dermal fibroblasts and endothelial cells described in the study by Oberringer *et al.* (Oberringer *et al.*, 2007). However, in our study we use this term to refer to the simultaneous culture of two cell types in distinct compartments, but where the media, and therefore secreted soluble factors (e.g. chemokines and growth factors), is shared. In this way myoblasts can be exposed to signals released from fibroblasts, and vice versa, enabling some simulation of *in vivo* wound conditions (Ratajczak *et al.*, 2003; Ten Broek *et al.*, 2010). Our model mimics *in vivo* repair during the proliferative phase of repair, at approximately three weeks after initial injury (i.e. after hemostasis and the inflammatory phase) (Huard *et al.*, 2002; Valluru *et al.*, 2011). Under these conditions we found that an eight-fold increase in fibroblast cell number resulted in significantly faster wound closure over seven hours. This is most likely due to known chemokine factors secreted by the fibroblasts, such as HGF, FGF and IGF-1, which contribute to regulation of myoblast migration (Neuhaus *et al.*, 2003). Interestingly, analysis at 3.5 hours showed no significant differences, suggesting that a threshold time is needed for production and secretion of relevant factors required for myogenic migration.

In this chapter, a specific fibroblast marker, such as TE-7 or Tcf4, to unambiguously prove the presence of fibroblasts in PP1 (Passage 1), was not used (Goodpaster *et al.*, 2008; Mathews *et al.*, 2011). However, the isolated muscle slurry contains primarily myoblasts and fibroblasts which can be distinguished morphologically from each other. Furthermore, the inability of the PP1 cells to differentiate into myotubes, and the lack of myogenic marker expression did prove the fibroblast nature of this population. These measures are currently accepted methods for fibroblast determination during myoblast isolation protocols.

In conclusion, we have optimized the scratch assay, specifically for myoblast migration (Goetsch and Niesler 2011) and developed a novel co-culture wound healing assay which uses an optimised protocol for the isolation and enrichment of both myoblasts and fibroblasts from the same muscle slurry (Goetsch *et al.*, 2011). Future characterisation of these assays could include the analysis of the factors secreted by fibroblasts, followed by the use of antibodies to remove secreted factors from the media. Adaptation of the assay to low oxygen tensions would mimic the skeletal muscle environment even more closely. These could all be applied in order to more fully understand the factors critical to optimal myoblast migration during skeletal muscle regeneration and effective repair. In the subsequent chapters the scratch assay was utilized, however future work will involve the expansion of these chapters to incorporate the co-culture assay.

CHAPTER 3

THE EXTRACELLULAR MATRIX AFFECTS C2C12 MYOBLAST MIGRATION

Includes data from:

Goetsch, K. P., Kallmeyer, K., Niesler, C. U. (2011) Decorin modulates collagen I-stimulated, but not fibronectin-stimulated, migration of C2C12 myoblasts, *Matrix Biol*, 30 (2): 109-117.

3.1 INTRODUCTION

Skeletal muscle contains satellite cells which are located between the basal lamina and sarcolemma, and can be activated following injury to initiate muscle fibre regeneration (Thorrez *et al.*, 2008). Skeletal myofibers are surrounded by extracellular matrix (ECM) which was initially thought to act only as a scaffold for maintaining tissue structure. It has since been shown to regulate many cellular processes, including survival, proliferation, migration, and differentiation of satellite cells (Bretscher 1996; Heino 1996; Friedl and Brocker 2000). The ECM is a complex meshwork of many different types of proteins (i.e. collagens, laminins and fibronectins), proteoglycans (i.e. biglycan and decorin), and polysaccharides and differs in the ratio of these components depending on the tissue type. Following a severe shear-type muscle injury, platelets within the damaged area secrete cytokines and growth factors and, along with blood derived fibrin and fibronectin, form early cross-linked granulation tissue (Ranzato *et al.*, 2009). This creates a scaffold for the invading inflammatory cells and fibroblasts (Ehrhardt and Morgan 2005).

Fibroblasts are activated to myofibroblasts and migrate into the wound to synthesize more ECM proteins and restore the strength of the connective tissue framework (Sheffer *et al.*, 2007). The first ECM components to be synthesized and laid down by the myofibroblasts are fibronectin and tenascin C. These components create an elastic type framework to support the mechanical load being applied to the injured muscle, as well as to provide support for the early granulation tissue. Collagen I and III are then synthesized to create a more permanent support scaffold. Collagen I is the major component of the connective scar tissue which remains after the muscle fiber has been regenerated (Ehrhardt and Morgan 2005). The tensile strength created by the collagen I is attributed to intermolecular cross-linking between the collagen molecules during scar tissue maturation. Once the scar tissue has fully matured the repaired area is no longer the weakest point in the muscle fiber, but it has lost the major part of its contractile function (Jarvinen *et al.*, 2007).

In response to a severe skeletal muscle injury, the activated satellite cell (now termed a myoblast) will migrate along the basal lamina, which consists primarily of laminin and collagen IV (Bonnemann and Laing 2004), and enter the wound site. Concomitantly, myofibroblasts from the interstitial space will move into the site of injury and secrete fibronectin, tenascin C and collagen I & III, thereby creating a ECM scaffold for structural support (Ehrhardt and Morgan 2005). As a result, migrating myoblasts are exposed to the ECM components of the developing wound scaffold; this influences their ability to facilitate repair.

The migration process can be seen to occur in three parts: extension of lamellipodia, contraction of the cellular body, and detachment from the ECM at the rear of the cell (Friedl and Brocker 2000). At the leading edge of the cell, ruffling will occur followed by the protrusion of the lamellipodia. These are “arm-like” protrusions used to extend the cell forward during migration and form new attachments to the ECM surface it encounters. This process of the lamellipodial extension and cell ruffling involves actin polymerization, which is initiated and maintained primarily by the integrin receptor in concert with cell surface proteoglycans, such as phosphacan and CD44 (Nobes and Hall 1995; Humphries *et al.*, 2006). A key kinase within the Rho-GTPase family which regulates myoblast migration is Rho-kinase (ROCK). Two isoforms of ROCK, ROCK-1 and -2 have been described. ROCK-1 is localized throughout the cytoplasm of the cell, whereas ROCK-2 exhibits both cell membrane and intense perinuclear distributions in fibroblasts (Shi and Wei 2007; Jayo *et al.*, 2012). ROCK-2 has been shown to be a crucial regulator of adhesion formation and release, as well as rear-end retraction in migrating NIH 3T3 fibroblasts (Iwanicki *et al.*, 2008). ROCK-1 is up-regulated at the onset of differentiation and down-regulated during fusion of C2C12 myoblasts (Fortier *et al.*, 2008). This suggests potentially distinct roles for ROCK-1 and -2 in differentiation versus migration.

Collagens are important structural proteins which facilitate many functions within the ECM (Gelse *et al.*, 2003). They are all composed of three polypeptide α -chains coiled into a triple helix rich in glycine (Ricard-Blum and Ruggiero 2005). Collagen I is the most abundant fibrillar collagen and the major component of the interstitial ECM surrounding skeletal muscle fibers and binds to myoblasts via the $\alpha 2\beta 1$ integrin receptor (Kjaer 2004). Collagen I increases $\beta 1$ -integrin expression in fibroblasts; these receptors then become clustered at the leading edge and increase the interaction of the cell with collagen fibers. Friedl and colleagues have shown that, after addition of an anti- $\beta 1$ integrin antibody to

block ligand binding, integrin clustering and fiber traction, as well as cell polarization were lost (Friedl *et al.*, 1998). This demonstrated the importance of $\alpha 2\beta 1$ integrin engagement with collagen I for the development of a polarized morphology and ensuing migration.

Fibronectin is a glycoprotein which exists in 3 different forms. A soluble dimeric form is located within the blood stream, whereas cell surface fibronectin oligomers and insoluble fibronectin fibrils form part of the ECM. Fibronectin, secreted by fibroblasts, forms multimeric fibrils which aid in the formation of a super fibronectin molecule with strong adhesive properties. Fibronectin, together with fibrin, forms a cross-linked structure in early granulation tissue, which is required to act as a scaffold for invading inflammatory cells. Fibronectin is also able to bind to other ECM components such as collagen and tenascin-C (Hocking *et al.*, 2008).

Decorin is a member of the small leucine-rich repeat heparan sulfate family. It is composed of a leucine-rich repeat core protein consisting of 12-folded repeats, each containing a 24 amino acid residue. It also has a single covalently-linked GAG chain at its NH₂-terminus which can vary in length and composition (Scott and Haigh 1985). Decorin binds to collagen via its core protein, at the peptide sequence SYIRIADTNIT (Kresse *et al.*, 1997; Kalamajski *et al.*, 2007). Decorin also binds to fibronectin via a pentapeptide sequence, NKISK, located within its core protein (Schmidt *et al.*, 1991). Decorin has been shown to act as an anti-fibrotic agent in skeletal muscle by binding to TGF- β decreasing its interaction with its receptors (Droguett *et al.*, 2006) and reducing fibrosis (Fukushima *et al.*, 2001; Sato *et al.*, 2003; Fukushima *et al.*, 2006).

In this chapter we investigate the effect of decorin, collagen I, and fibronectin on myoblast migration utilizing the *in vitro* wound healing assay. We demonstrate that decorin significantly increased myoblast migration rates when added in combination with collagen I; whereas with fibronectin no noticeable effect was observed. We also compared the roles of ROCK-1 and ROCK-2 to investigate which isoform plays a predominant role in myoblast migration.

3.2 EXPERIMENTAL PROCEDURES

All chemicals used were of an analytical grade and were purchased from either Sigma or Merck unless otherwise stipulated. All cell culturing was carried out under sterile conditions in a level II laminar flow hood (ESCO class II BSC) and incubated in a CO₂ incubator (Innova CO-170) at 37°C, 5% CO₂. Brightfield images were captured using the Motic 3.0 MP camera on the Olympus CKX41 microscope. The Zeiss 710 confocal microscope was utilized for all fluorescence microscopy.

3.2.1 Cell Culture

The C2C12 cell line was donated by the Cape Heart Center, University of Cape Town. Growth media contained Dulbecco's Modified Eagle Serum (DMEM) (Highveld, cat. CN3193-9), L-glutamine (2 % v/v) (Cambrex, cat. 17-605E), PenStrep (2 % v/v) (Cambrex, cat. 17-602E), Fetal calf serum (10 % v/v) (Invitrogen, cat. 10108165). Differentiation media contained DMEM, L-glutamine (2 % v/v), PenStrep (2 % v/v) and Horse serum (HS; 1 % v/v) (Invitrogen cat. 16050-130).

3.2.2 Collagen I Coating

Calf skin collagen I (Sigma, Cat. no. C9791) was utilized for all 2D collagen coating. Collagen I (1.5 mg) was added to 1.5 ml acetic acid (0.1 % w/v) for 2 hours at 4 °C. Chloroform (10 % w/v) was layered at the bottom of the collagen solution and stored at 4 °C overnight. The collagen stock concentration was then diluted, for the dose response, to a range of 6.25-100 µg/ml with distilled water. The collagen solution was added to 24-well and 6-well plates and incubated at 37 °C for 4 hours, after which the excess collagen solution was removed and plates allowed to air dry overnight under a U.V. light.

3.2.3 Fibronectin Coating

Bovine plasma fibronectin (1 mg/ml, Sigma) was diluted with PBS to a concentration range of 2.5-20 µg/ml for the dose response. The fibronectin was added to 24 or 6 well plates and incubated for 2 hours at 37 °C, 5% CO₂. The excess fibronectin was removed and plates were allowed to air dry overnight under a U.V. light. The plates were subsequently stored at 4 °C and washed with PBS prior to use.

3.2.4 Scratch Assay

C2C12 cells were plated at 5×10^4 cells per well in a 24-well plate (TPP, Cat. no. 92024) and were incubated at 37 °C, 5% CO₂ until 90% confluent. Wells were pre-coated with either collagen I or fibronectin at the required concentrations, ranging from 6.25-100 µg/ml for collagen I and 2.5-20 µg/ml for fibronectin, prior to the addition of the cells. The cultures were “wounded” with a loading tip (1-200 µl, Whitehead Scientific, Cat. no. 010), washed with PBS and re-incubated with 250 µl growth media. Decorin was added to the growth media at a concentration range of 5-20 µg/ml. Images of the scratch area were captured at initial wounding and hours 1, 3, 5, & 7 with the *Motic* 3 megapixel camera (40 X magnifications, Olympus CKX41) and were analyzed via the *Motic 2.0* image analysis software. All experiments were performed in triplicate.

3.2.5 Immunocytochemical analysis of ROCK -1 & -2

Cells were seeded on non-coated, as well as collagen I-coated or fibronectin-coated, glass coverslips and wounded as described above. Fixation was performed with a 4% paraformaldehyde solution followed by a blocking step with 5% donkey serum. Cells were incubated with monoclonal mouse anti-human ROCK-1 (1/500, IMGENEX, Cat. no. IMG-383A) and polyclonal goat anti-rat ROCK-2 (1/500, Santa Cruz, Cat. no. Sc-1851) primary antibodies for 2 hours. This was followed by incubation with a FITC-conjugated donkey anti-mouse secondary antibody for ROCK-1 (1/4000, Jackson Scientific) or a Cy5-conjugated donkey anti-goat secondary antibody for ROCK-2 (1/8000, Jackson Scientific) for 1 hour. A Phalloidin-TRITC conjugated cytoskeletal stain (1/15 000, Sigma) was added with the secondary antibody followed by the nuclear stain Hoechst (1/4000, Sigma). Images were captured and analyzed by use of the Zeiss LSM 710 confocal microscope.

3.2.6 Western Blot Analysis of ROCK-1 & -2

Cells were grown in 6-well plates (non-coated and coated) until 80% confluent. Plates were coated with either collagen I (25µg/ml) or fibronectin (5µg/ml). Decorin (10µg/ml) was then added and lysates harvested 8 hours later using RIPA buffer (Sigma, pH 8) containing a protease inhibitor cocktail (Sigma). Proteins (25µg) were separated on a 10% SDS-PAGE gel and transferred to nitrocellulose. Blots were probed separately using a polyclonal goat anti-human ROCK-1 primary antibody (1/2000, Santa Cruz, Cat. Sc-6055) and a polyclonal goat anti-rat ROCK-2 antibody (1/2000, Santa Cruz, Cat. Sc-1851). The

polyclonal rabbit anti-human GAPDH primary antibody (1/4000, Cell Signalling, Cat. 2118) or monoclonal mouse anti-human alpha tubulin primary antibody (1/400, Santa Cruz, Cat. no.Sc5286) were utilized as internal controls. A HRP-conjugated donkey anti-goat secondary antibody (1/20 000, Santa Cruz, Sc-5286) was used for ROCK-1 and -2, and an HRP-conjugated goat anti-rabbit secondary antibody (1/4000, Dako, Cat. P0448) and HRP-conjugated rabbit anti-mouse secondary antibody (1/16 000, Dako, Cat. P0260) for GAPDH and alpha tubulin, respectively. Enhanced chemiluminescence (ECL) was used to detect protein expression (Immun-Star WesternC, BioRad). Densitometry analysis was carried out using Quantity One 2.6 (BioRad).

3.2.7 Scanning Electron Microscopy (SEM)

Scanning electron microscopy (SEM) was performed on a collagen I (25 µg/ml) and fibronectin (5 µg/ml) coated coverslips. The samples were fixed with a 0.05 M cacodylate buffer containing 3 % glutaraldehyde (pH 7) for 1 hour and then washed with distilled water. A series of 5 minute ethanol washes to dehydrate the samples was performed in the following order; 50 %, 75 %, 90 %, and 100 % ethanol dilutions. The coated coverslips were then air dried and sputter coated with gold particles (2 minutes) before being viewed at high vacuum with the Zeiss EVO LSM 15 VPSEM microscope.

3.2.8 Statistical Analysis

Statistical evaluations were performed by non-parametric Mann-Whitney U tests for all experiments. All statistical analysis was performed using *Genstat*. Significant differences were taken as $p < 0.05$. All data is expressed as Mean \pm S.E.M.

3.3 RESULTS

3.3.1 Dose responses for decorin, fibronectin and collagen I

To determine the concentrations at which decorin, collagen I and fibronectin influence wound closure, a dose response was carried out for each. Decorin (range 5-20 $\mu\text{g/ml}$) at a concentration of 10 $\mu\text{g/ml}$ had the greatest effect, increasing the percentage wound closure from 30.2% to 35.4%, over a 7 hour period when compared to the control, a 1.2 fold increase (Figure 3.1A). Interestingly, at a concentration of 20 $\mu\text{g/ml}$, decorin decreased the percentage wound closure compared to control by 8.1%. Fibronectin (range 5-20 $\mu\text{g/ml}$) significantly increased the percentage wound closure at all doses and time points analysed (5, 10, and 20 $\mu\text{g/ml}$, $p < 0.001$) compared to the control, with 5 $\mu\text{g/ml}$ demonstrating the highest percentage wound closure at 49.3% representing a 3.5 fold increase compared with the control (Figure 3.1B, $p < 0.001$). Collagen I (range 6.25-100 $\mu\text{g/ml}$), at 25 $\mu\text{g/ml}$ and 50 $\mu\text{g/ml}$, significantly increased the percentage wound closure (Figure 3.1C, $p < 0.05$) at 7 hours with an increase of 27.3% and 12.4% respectively over and above that of the control (20.1%). At 25 $\mu\text{g/ml}$ the effect of collagen I on wound closure represented the largest increase at 2.4 fold compared to control. Analysis of collagen I and fibronectin coated coverslips by SEM confirmed successful fibril formation that coated the entire surface of the coverslips (Figure 3.1D). As a result of these studies, optimal doses of decorin, fibronectin and collagen I (10 $\mu\text{g/ml}$, 5 $\mu\text{g/ml}$ and 25 $\mu\text{g/ml}$, respectively) were utilised for all subsequent experiments.

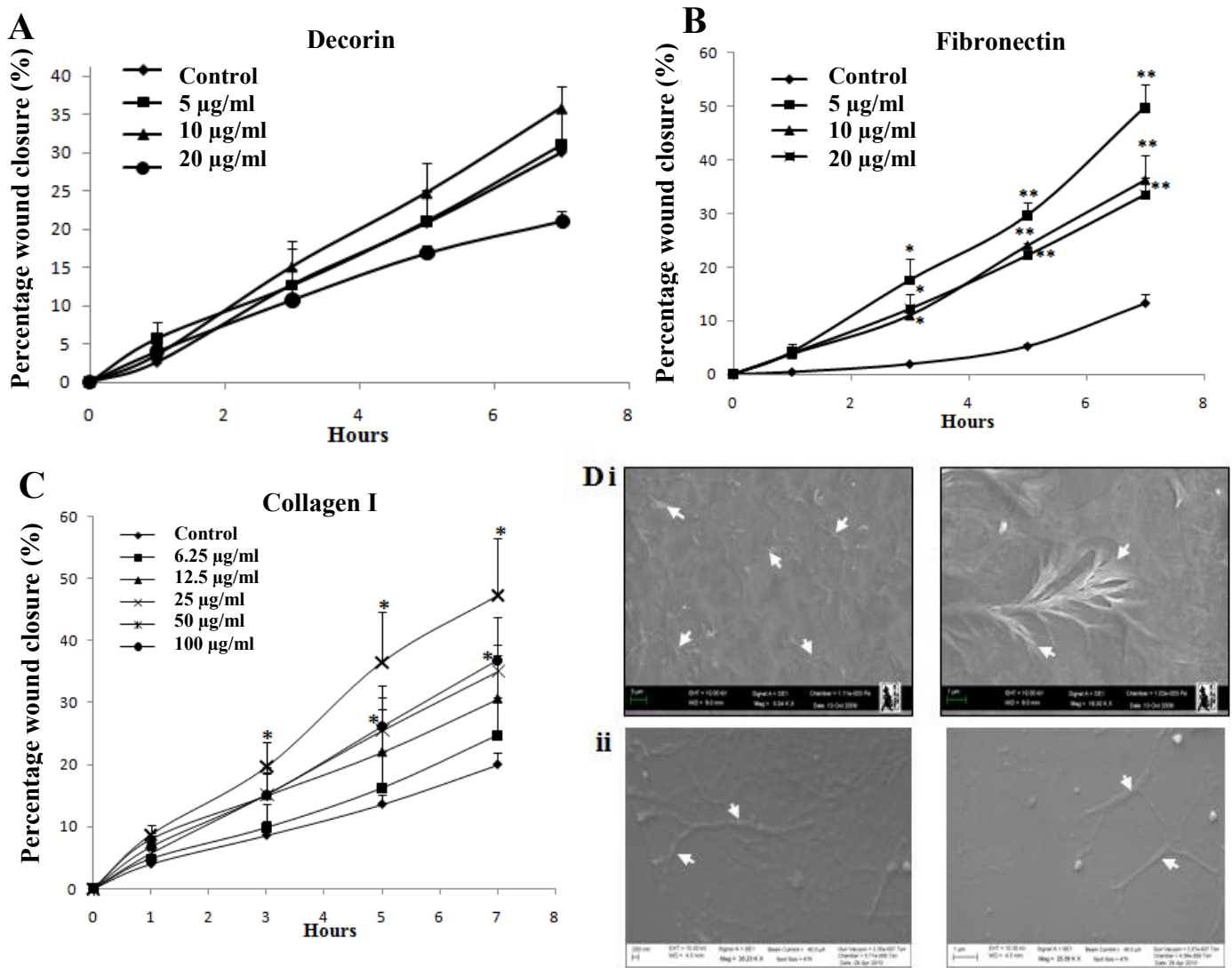


Figure 3.1 Decorin, fibronectin, and collagen I dose optimization. **A)** Decorin dose response (5, 10 and 20 $\mu\text{g/ml}$). **B)** Fibronectin dose response (5, 10 and 20 $\mu\text{g/ml}$). **C)** Collagen I dose response (6.25, 12.5, 25, 50, and 100 $\mu\text{g/ml}$). The scratch assay was utilized with photos taken at hours 0, 1, 3, 5, and 7. Growth media on non-coated wells was used as control for all experimental procedures. Percentage wound closure was calculated by determining the area of the wound. **D)** Scanning electron microscopy micrographs of fibril formation for collagen I (**i**, left $5.04 \times 10^6 \times$, right $18.30 \times 10^6 \times$) and fibronectin (**ii**, left $30.23 \times 10^6 \times$, right $25.59 \times 10^6 \times$). * $p < 0.05$, ** $p < 0.005$, $n = 3$. All data shown as Mean \pm SEM.

3.3.2 Decorin facilitates collagen I-stimulated wound closure

To determine whether the decorin modulates collagen I-stimulated migration, myoblasts were seeded on collagen I-coated plates (25 μ g/ml) and treated with decorin (10 μ g/ml). The percentage wound closure was monitored over a 7 hour period. Decorin and collagen type I in combination, significantly ($39.79 \pm 5.79\%$, $p < 0.005$) increased the percentage wound closure compared with control ($15.73 \pm 1.87\%$) and decorin ($21.03 \pm 3.07\%$) at all time points measured, with a 2.54 fold and 1.9 fold increase in wound closure at 7 hours compared with control and decorin, respectively (Figure 3.2i). The rate of wound closure, as calculated from the change in percentage wound closure over 7 hours, revealed that decorin and collagen I ($5.55 \pm 0.87\%/hr$) in combination showed a significantly ($p < 0.005$) higher rate of wound closure compared to control ($2.17 \pm 0.28\%/hr$), decorin ($2.83 \pm 0.41/hr$), and collagen ($4.10 \pm 0.92\%/hr$) (Figure 3.2ii). Furthermore, decorin significantly increased the rate of collagen-stimulated migration by 1.5 %/hr, whereas in the absence of collagen I, the increase in response to decorin was not significant and only 0.6 %/hr.

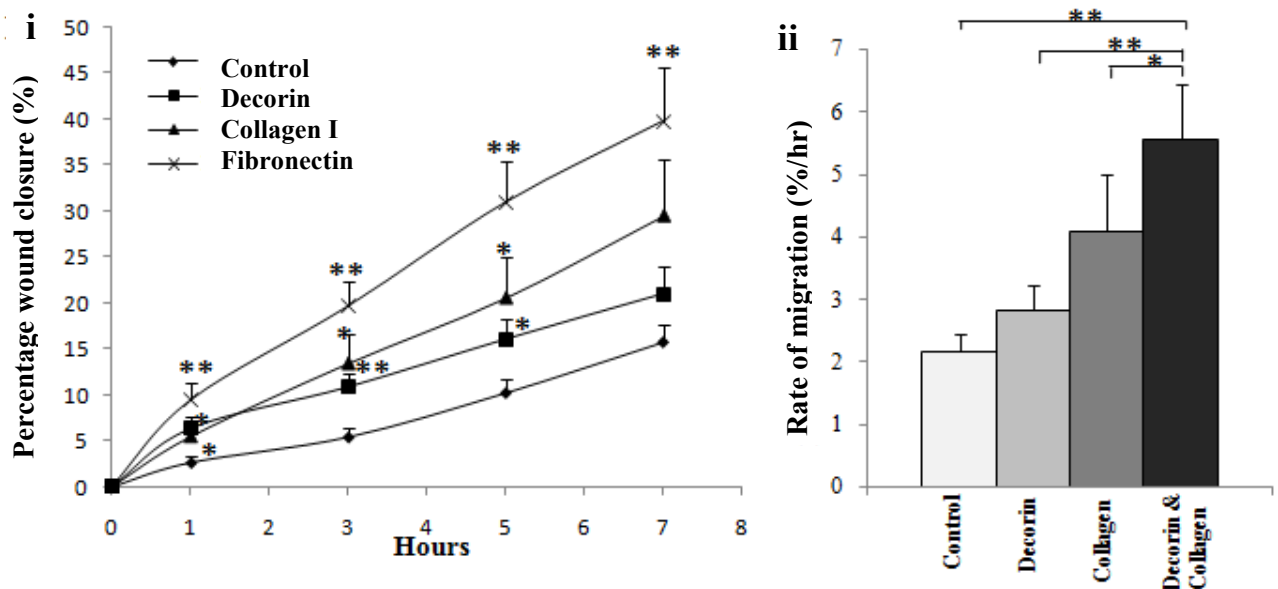


Figure 3.2 Effects of decorin on collagen I-stimulated myoblast migration. i) Effect of decorin (10 μ g/ml) and collagen I (25 μ g/ml) on the percentage wound closure of C2C12 myoblasts. ii) Rate of wound closure for decorin and collagen I. The scratch assay was utilized with photos taken at hours 0, 1, 3, 5, and 7. Growth media on non-coated wells was used as control for all experimental procedures. Percentage wound closure calculated by determining the area of the wound (Section 4.1.5). * $p < 0.05$, ** $p < 0.005$, $n = 9$. All data shown as Mean \pm SEM.

3.3.3 Effect of Decorin and Collagen I on Myoblast Migration in Differentiated C2C12 Myotubes

Skeletal muscle segments are composed of differentiated myoblasts that have fused into multinucleated myotubes. These myotubes are unable to divide, therefore for regeneration to occur, satellite cells are activated and create a myoblast population which can differentiate and fuse to the existing skeletal muscle segments, facilitating repair. Not all the myoblasts differentiate into myotubes. A population of myoblasts remains as satellite cells within their niche and are the main source of cells during muscle regeneration. We modeled this type of skeletal muscle regeneration by creating scratches in differentiated C2C12 myotubes and monitoring the migration rates of the undifferentiated population of myoblasts (mimic *in vivo* satellite cells to a certain extent) (Figure 3.3A).

The myoblasts were grown until 80% confluent and were differentiated for 9 days (Figure 3.3A). Scratches were created and analyzed as the previous described. Decorin and collagen in combination significantly ($19.19 \pm 1.48\%$, $p < 0.05$) increased the percentage wound closure compared to control ($5.87 \pm 1.96\%$) at hour 7 by 6.2% (Figure 3.3B). Decorin ($15.41 \pm 2.05\%$) and collagen ($14.39 \pm 2.27\%$) had no significant effect on wound closure over the control at hour 7. Analysis of migration rates confirmed that decorin and collagen in combination significantly ($2.67 \pm 0.24\%/hr$, $p < 0.05$) increased the rate of migration into the scratch area compared only to the control ($1.76 \pm 0.28\%/hr$) (Figure 3.3C).

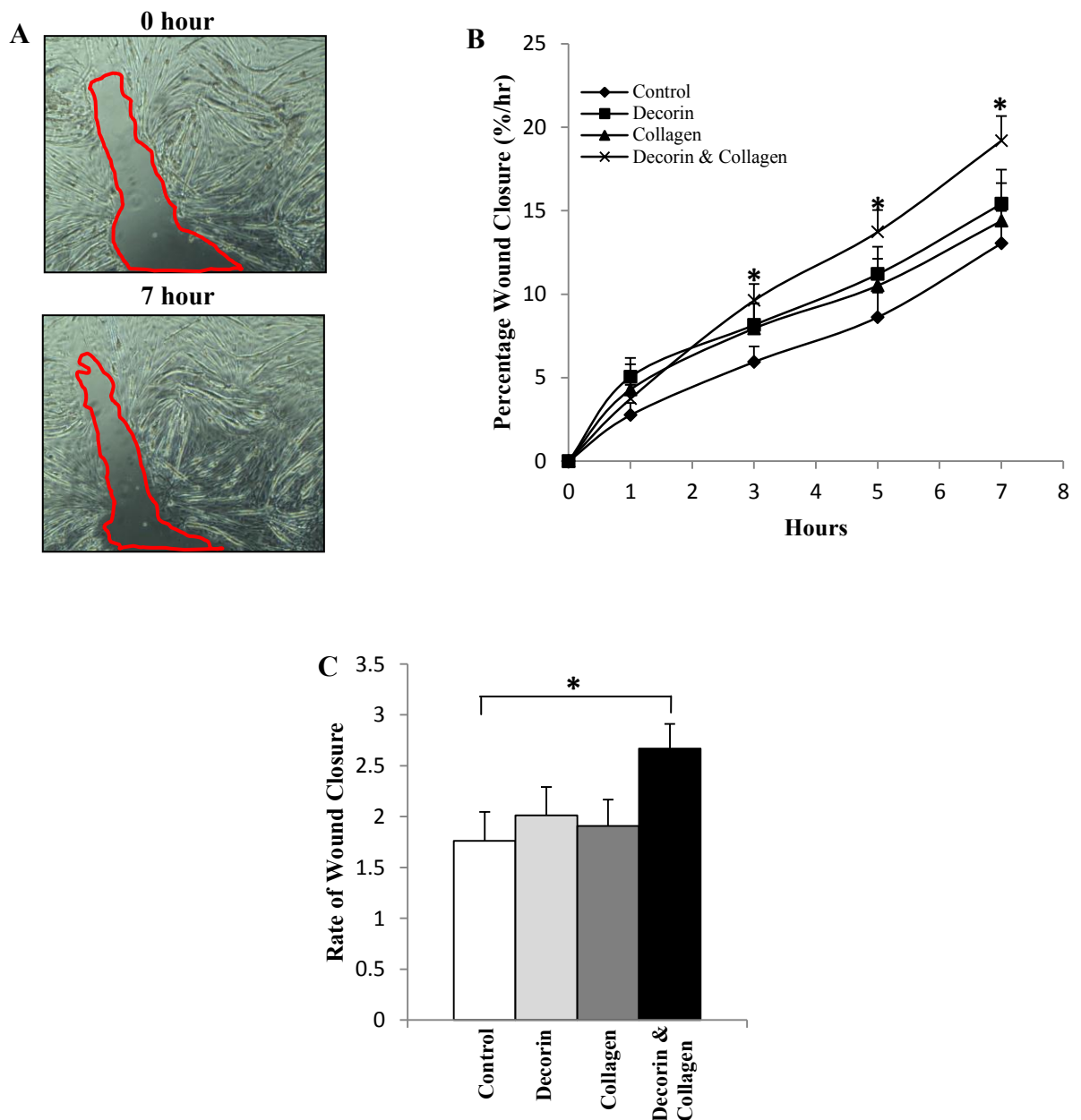


Figure 3.3 Effect of collagen type I and decorin on myoblast migration amongst differentiated C2C12 myotubes. **A)** Photos depicting the wound size at 0 and 7 hours on collagen coated 24-well plates. Cells were allowed 9 days to differentiate and fuse into myotubes. The red line indicates the wound front. **B)** The percentage wound closure was calculated for the control, decorin and collagen separately, as well as decorin & collagen in combination. **C)** The rate of wound closure. The scratch assay was utilized. Decorin and collagen concentrations of 10 and 25 μ g/ml respectively, were used as determined by the dose response assays. Cells were analyzed at 0, 1, 3, 5, & 7 hours. Growth media containing 10% fetal calf serum served as the control. Photos were taken using the *Motic 3* megapixel camera at 40x magnification. * $p < 0.05$, ** $p < 0.005$, $n = 6$. All data shown as Mean \pm SEM.

3.3.4 Effect of Decorin and Collagen I on Primary Cultured Murine Myoblast Migration

The isolation and propagation of primary cultured murine myoblasts provided cells which better mimicked *in vivo* cellular responses due to the lack of modifications required to immortalize a cell line. A similar trend was observed for the percentage wound closure between primary culture myoblasts (Figure 3.4A) and C2C12 myoblasts (Figure 3.2A). Decorin and Collagen I significantly increased the percentage wound closure compared to the control at hours 5 (45.70% \pm 7.01) and 7 (53.48% \pm 8.55), respectively. Collagen I also significantly increased the percentage wound closure at hour 7 (40.40% \pm 5.19) compared to the control (32.32 \pm 3.07). Collagen I increased the percentage wound closure by 8% compared to the control, whereas collagen I and decorin increased it by 21%, a 2.63 fold increase. Interestingly, when comparing the rate of migration no significant trends were observed even though decorin and collagen I increased the rate of migration over that of control, decorin, and collagen I (Figure 3.4).

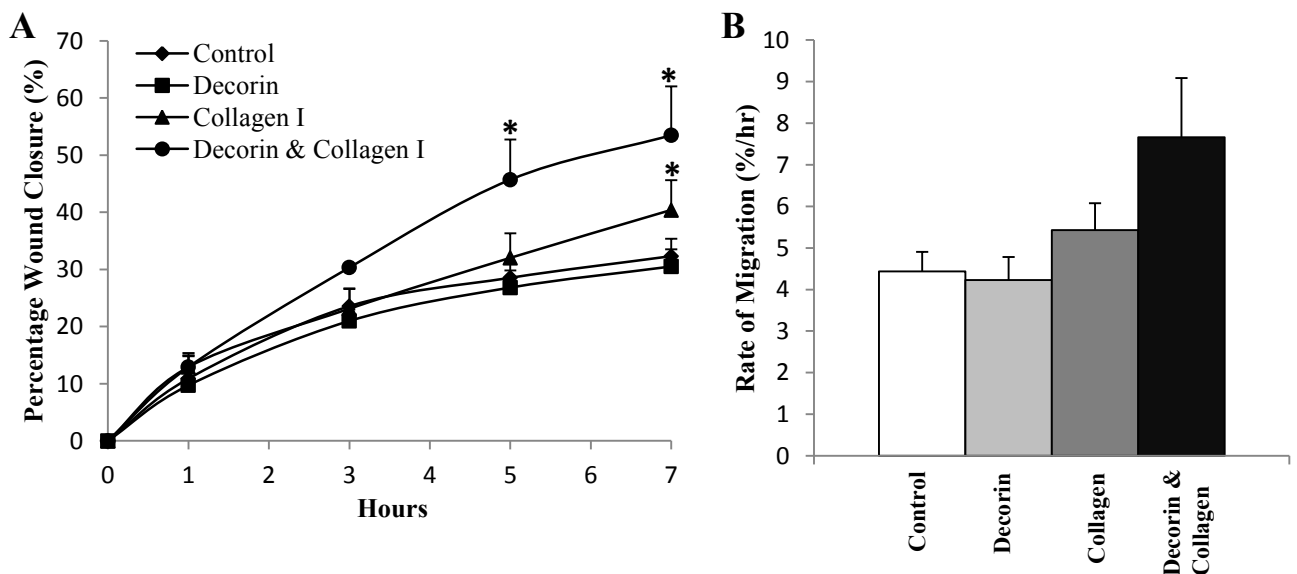


Figure 3.4 Effect of collagen type I and decorin on primary cultured murine myoblast migration. **A)** The percentage wound closure was calculated for the control, decorin and collagen separately, as well as decorin & collagen in combination. **B)** The rate of wound closure. The scratch assay was utilized. Decorin and collagen concentrations of 10 and 25 μ g/ml respectively, were used as determined by the dose response assays. Cells were analyzed at 0, 1, 3, 5, & 7 hours. Growth media containing 10% fetal calf serum served as the control. Photos were taken using the *Motic* 3 megapixel camera at 40x magnification. * $p < 0.05$, $n = 4$. All data shown as Mean \pm SEM.

3.3.5 Decorin does not increase fibronectin facilitated migration

To determine whether the interaction of fibronectin and decorin modulate migration compared with control, decorin (10 μ g/ml) was added to myoblasts seeded on fibronectin-coated plates (5 μ g/ml) and wound closure monitored over a 7 hour period (Figure 3.5A). As expected, decorin showed no significant increase in wound closure compared to the control. Fibronectin demonstrated a 44% increase in the percentage wound closure compared to control and when combined with decorin, a 36% increase was observed (Figure 3.5A, $p < 0.005$). Although decorin decreased fibronectin-stimulated migration, this effect was not significant. The rate of wound closure further supported these findings where both fibronectin, and fibronectin plus decorin, significantly increasing the rate of migration by 2.3 fold and 2.1 fold, respectively (compared with control), however, there was no significant difference between these two interventions (Figure 3.5B).

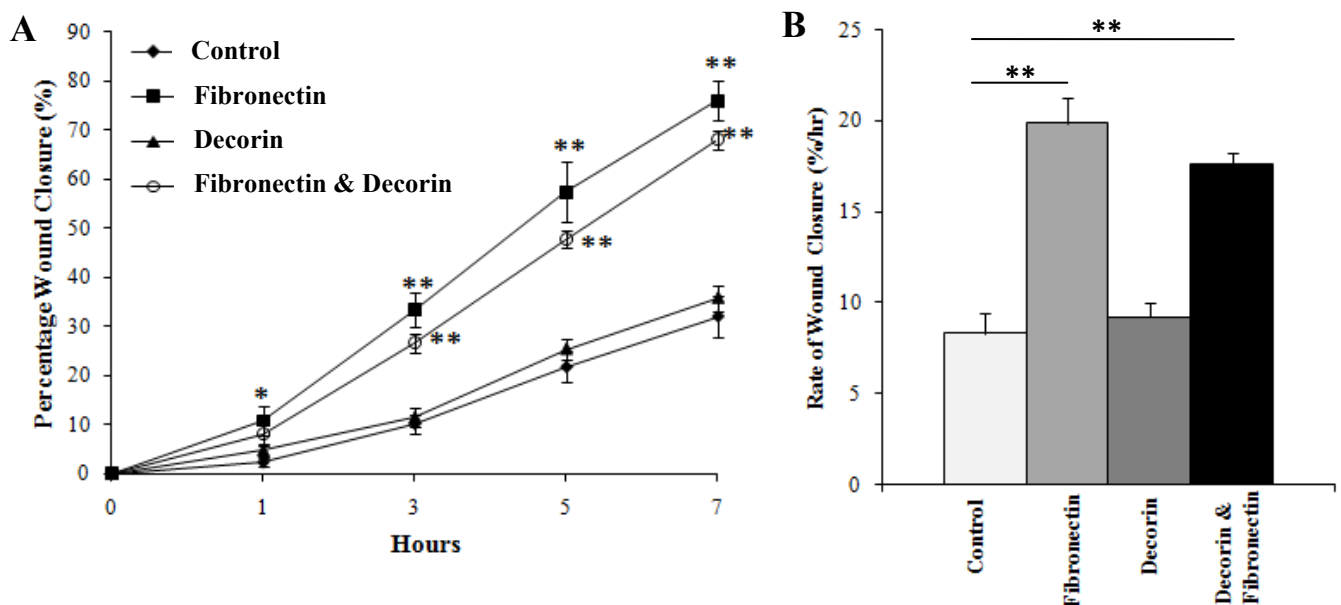


Figure 3.5 Effects of decorin and fibronectin on the percentage wound closure and rate of C2C12 myoblast migration. **A)** Effect of decorin (10 μ g/ml) and fibronectin (5 μ g/ml) on the percentage wound closure of C2C12 myoblasts. **B)** Rate of wound closure for decorin and fibronectin. The scratch assay was utilized with photos taken at hours 0, 1, 3, 5, and 7. Growth media on non-coated wells was used as control for all experimental procedures. Percentage wound closure calculated by determining the area of the wound. * $p < 0.05$, ** $p < 0.005$, $n = 3$. All data shown as Mean \pm SEM.

3.3.6 Total ROCK-2 expression is higher than ROCK-1 expression in C2C12 myoblasts

We next determined total ROCK-1 and -2 protein expression levels in non-wounded C2C12 myoblasts under control conditions and in response to decorin (10 $\mu\text{g/ml}$) and collagen I (25 $\mu\text{g/ml}$). ROCK-2 expression was also analysed in response to fibronectin (5 $\mu\text{g/ml}$). ROCK-2 was expressed at higher levels than ROCK-1 for all experimental groups analyzed (Figure 3.6B). No stark difference in expression of total ROCK-2 in response to decorin, collagen I, or fibronectin was detected (Figure 3.6ii and iii, Figure 3.6B).

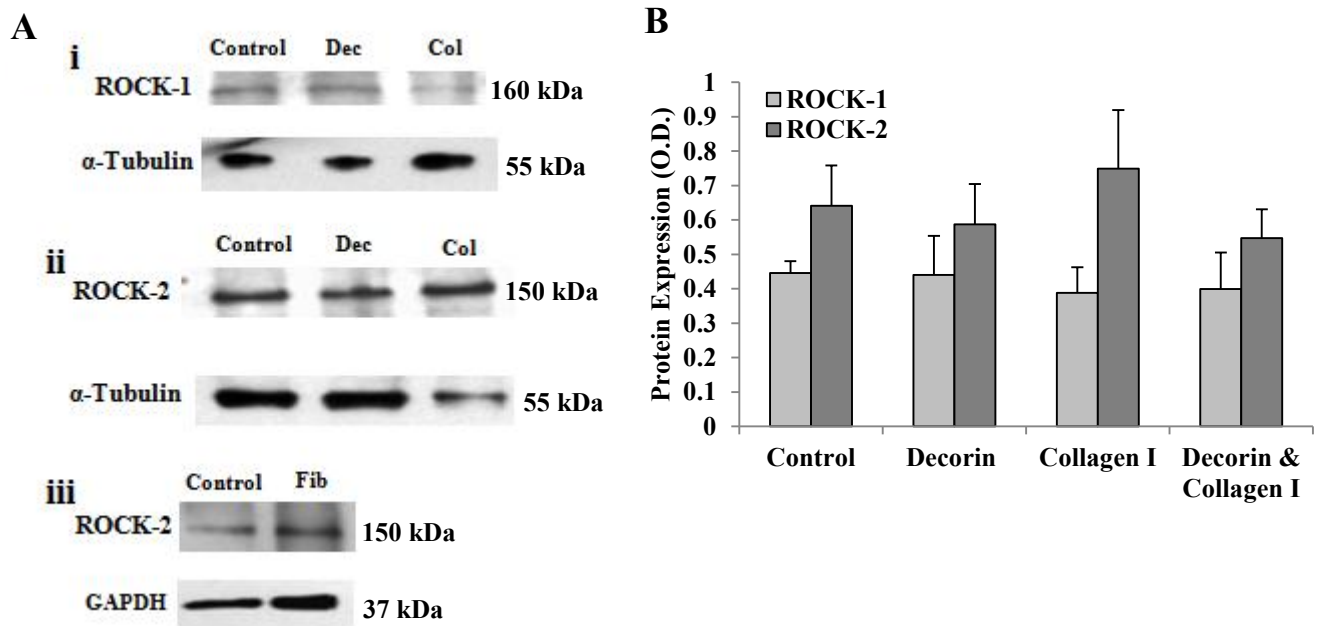
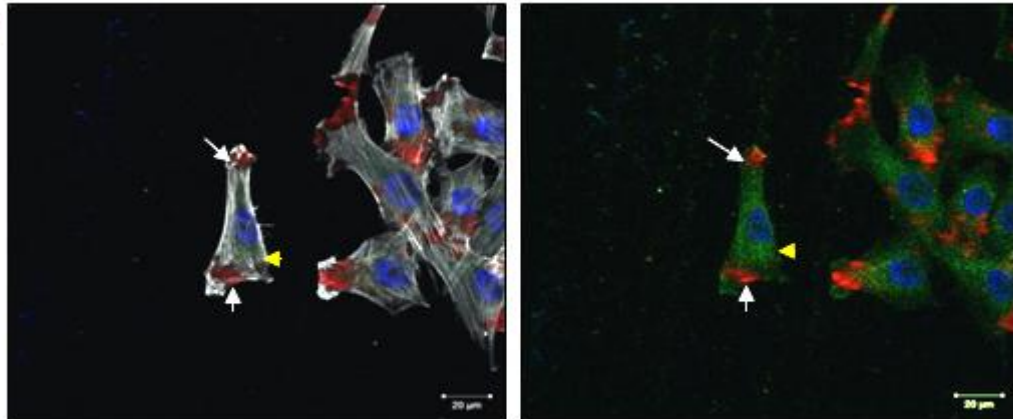


Figure 3.6 ROCK-1 and -2 protein expression in C2C12 myoblasts. **Ai & ii)** Analysis of total ROCK-1 and -2 protein expression within C2C12 myoblasts following the addition of decorin (10 $\mu\text{g/ml}$) and collagen I (25 $\mu\text{g/ml}$), added separately and in combination. Alpha-tubulin was used as an internal loading control. **iii)** Analysis of total ROCK-2 protein expression within C2C12 myoblasts with the addition of fibronectin (5 $\mu\text{g/ml}$). GAPDH was used as the internal loading control. **B)** Densitometric analysis of ROCK-1 and ROCK-2 expression. Growth media was used as the control for all experimental procedures. n=3-6.

3.3.7 ROCK 2, but not ROCK 1, localizes to focal adhesions in C2C12 myoblasts

Co-localization analysis revealed that cells which had migrated into the wound area did not express ROCK-1 and ROCK-2 at the same location. ROCK-1 was found to be expressed at low levels and spread throughout the cytoplasm (observed in migrating myoblasts (five fields of view, n=3), Yellow arrow head, Figure 3.7); whereas ROCK-2 was expressed more strongly and located within the lamellipodia and tail of the migrating cell (white



arrows, Figure 3.7).

Figure 3.7 ROCK-1 and -2 localization in C2C12 myoblasts. Confocal images of migrating C2C12 myoblasts at 7 hours post-migration. ROCK-1 (green, FITC), ROCK-2 (red, Cy5), phalloidin-TRITC conjugated (grey) and Hoechst (blue). The Zeiss 710 LSM microscope was utilized for all confocal images. Scale bar = 20 μ m.

3.3.8 Increased number of ROCK-2-containing focal adhesions during decorin & collagen I facilitated migration

ROCK-2 localization was assessed along the migration front of the wound in response to decorin and collagen I. ROCK-2 was primarily localized to focal points (confirmed with vinculin labeling, see *Chapter 4*) within the lamellipodia of migrating cells under control conditions (arrows, Figure 3.8A). Incubation with decorin did not result in any difference in the number of focal adhesion clusters containing ROCK-2 compared to control, with focal clusters ranged from 2-3 per migrating cell under both conditions (Figure 3.8B). Cells plated and wounded on collagen I showed an increase in the number of ROCK-2 containing focal adhesion clusters (5 focal adhesion clusters per migrating cell), when compared to control (Figure 3.8B); this effect was not significant. However, decorin and collagen I together, significantly increased the number of focal adhesion clusters to a range of 7-8 points per migrating cell (Figure 3.8B).

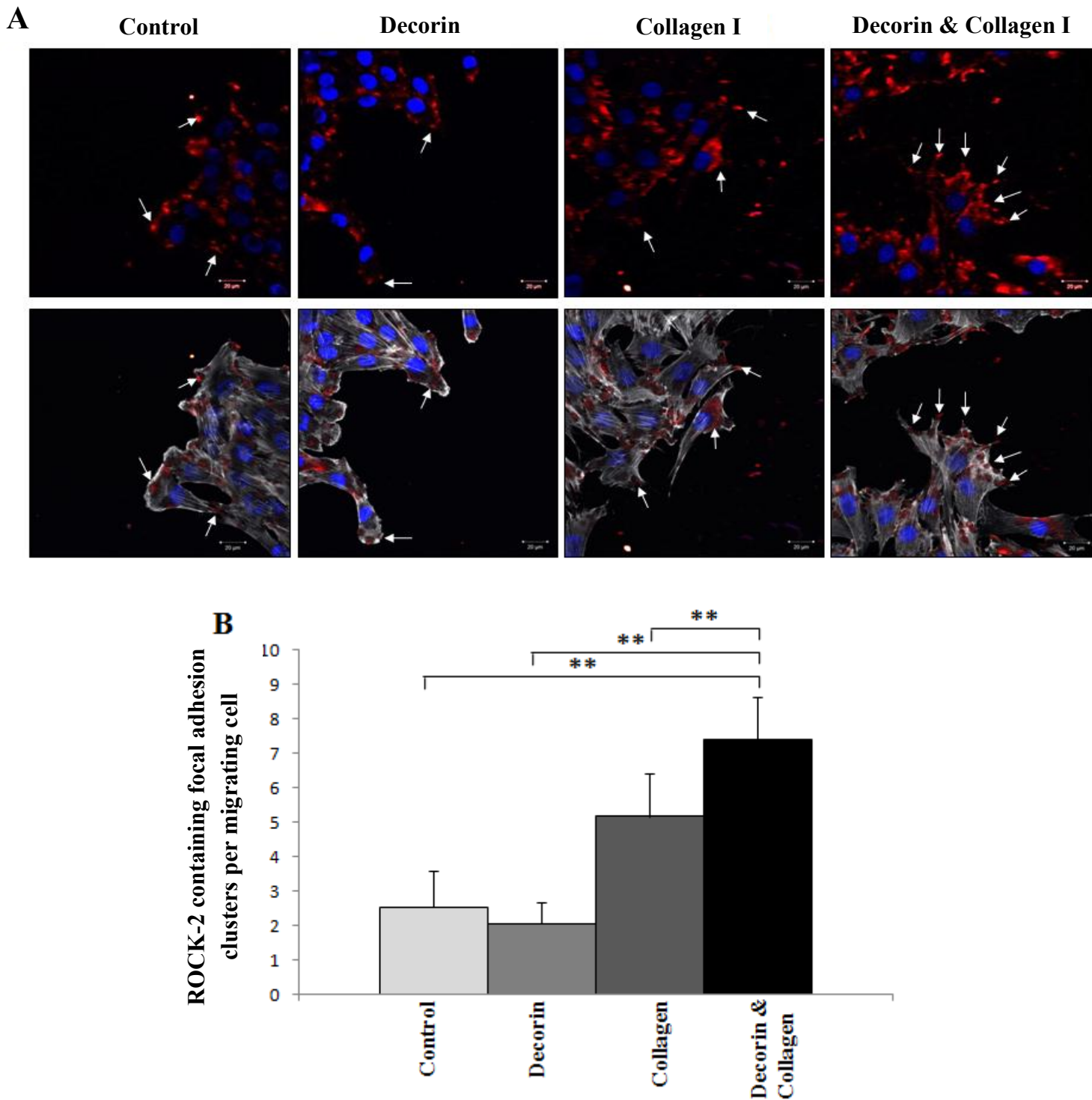


Figure 3.8 ROCK-2 localization in response to incubation with decorin and collagen I during C2C12 myoblast migration. **A)** Confocal images of migrating C2C12 myoblasts at 7 hours post-scratch for decorin (10 μ g/ml) and collagen I (25 μ g/ml). ROCK-2 (red) is localized to focal points within the lamellipodia (arrows). Phalloidin-TRITC (grey) and Hoechst (blue) are utilized as reference stains. **B)** Bar graph representing the number of ROCK-2 containing focal adhesion clusters in response to decorin and collagen I. The Zeiss 710 LSM microscope was utilized for all confocal images. Scale bar = 20 μ m. * p <0.05, ** p <0.005, n =3. All data shown as Mean \pm SEM.

3.3.9 Fibronectin does not increase active ROCK-2 focal adhesions during migration

ROCK-2 localization was assessed along the migration front of the wound in response to fibronectin. Control cells demonstrated low numbers of ROCK-2 positive focal adhesions within the lamellipodia of the migrating myoblasts along the scratch front (arrows, Figure 3.9) which was consistent with the previous control. With the addition of fibronectin the limited localization of ROCK-2 within the lamellipodia at the wound edge is lost (arrows, Figure 3.9). Furthermore, in response to fibronectin, the ROCK-2 appeared to be expressed at greater levels around the nucleus than within the lamellipodia or tail of the cells.

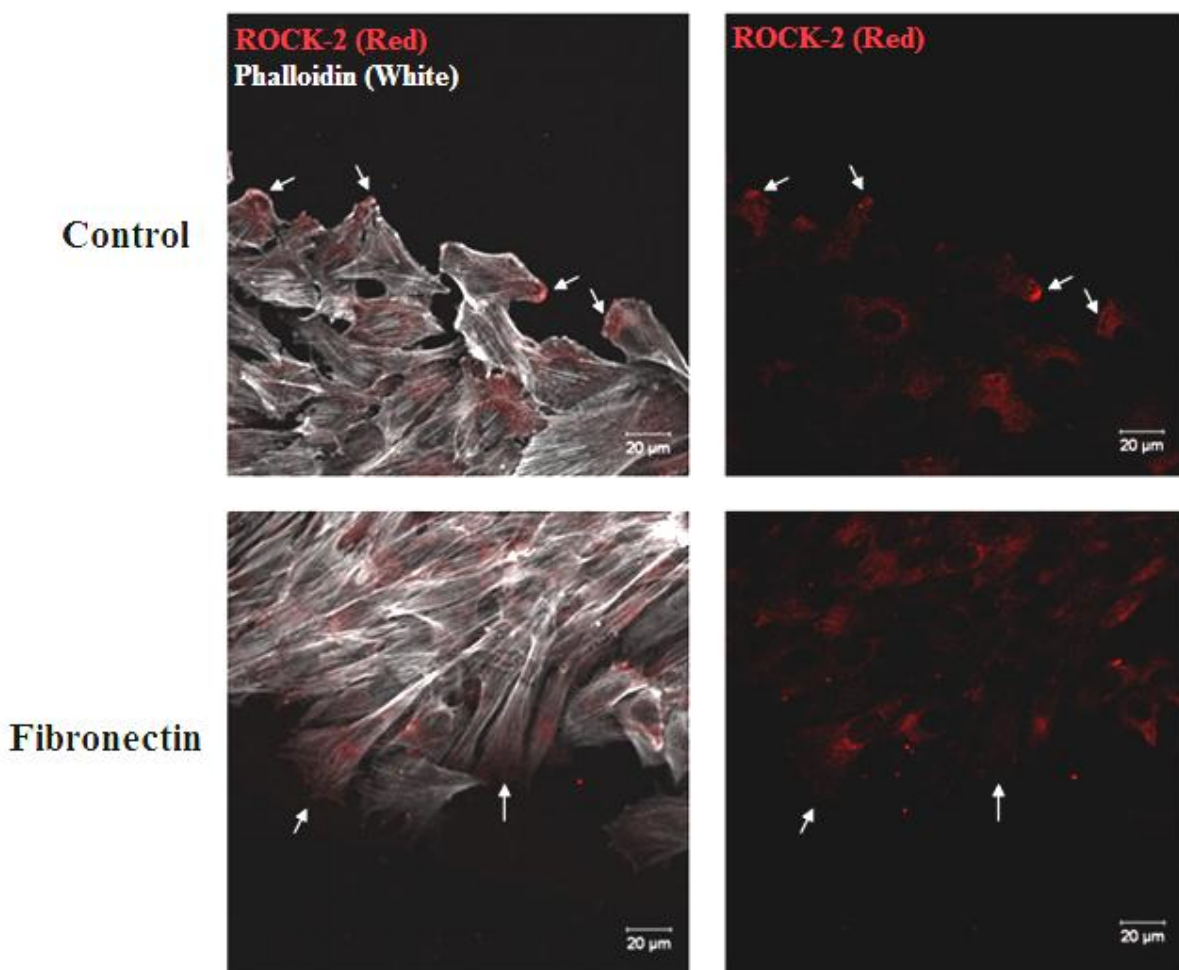


Figure 3.9 ROCK-2 localization within C2C12 myoblasts migrating on fibronectin. Confocal images of migrating C2C12 myoblasts at 7 hours post-scratch on non-coated (control) and fibronectin-coated (5µg/ml) plates. ROCK-2 (red) is localized to lamellipodia within the control (arrows). Phalloidin-TRITC (white). The Zeiss 710 LSM microscope was utilized for all confocal images. Scale bar = 20µm.

3.4 DISCUSSION

Following skeletal muscle injury, two key events take place concurrently in an effort to promote repair. These are the deposition of extracellular matrix components (initially by fibronectin and later replaced by collagen I and III) as well as muscle regeneration via the activation of muscle stem cells (Quintero *et al.*, 2009). Although both processes are required, the deposition of excessive fibrotic scar tissue (containing collagen I) severely hampers the ability of activated myogenic stem cells, termed myoblasts, to facilitate repair. Decorin has been shown to decrease the amount of scar tissue formed during skeletal muscle repair within a rat model, as well as increased the repair rate by several days (Fukushima *et al.*, 2001). However, the mechanism for this is still unclear.

We analysed the effect of collagen I, fibronectin, and decorin on the ability of myoblasts to promote repair via migration. Collagen I and fibronectin were both shown to have significantly increased migration at numerous doses, and demonstrated no negative effect on migration. However, the novel results that will be discussed below include the finding that decorin influenced cell movement in both a positive and negative way, depending on the dose used. Decorin significantly increased collagen I-stimulated migration, but not fibronectin-stimulated migration. The finding that ECM components influenced myoblast function in unexpected ways when assessed in combination, revealed how important it is that *in vitro* model design includes combination studies which mimic the *in vivo* micro-environment. For example, the effect of decorin and collagen I together was greater than the additive effect of decorin and collagen I separately, suggesting an additional interaction between decorin and collagen I. Decorin has been shown to modulate endothelial cell migration *in vitro*, and negatively regulate *in vivo* myoblast migration during *embryonic* development; however the effect of this proteoglycan on *adult* myoblast migration has been unclear to date ((Olguin *et al.*, 2003; Sulochana *et al.*, 2005; Fiedler *et al.*, 2008). Given that embryonic and fetal generation are essentially free of the extensive fibrosis seen in adults, the effect of decorin on post-natal myoblast migration is likely to be different to that seen during embryonic development.

A dose dependent response of decorin revealed that 10 $\mu\text{g/ml}$ increased myoblast migration, whereas at 20 $\mu\text{g/ml}$, migration was decreased. Olguin *et al.*, demonstrated that decorin inhibited myoblast migration at 40 $\mu\text{g/ml}$ which was a necessary step in order for normal muscle differentiation to occur (Olguin *et al.*, 2003). It is therefore important to

keep the dose used in different experiments in mind since this can differentially affect myoblast migration during muscle regeneration.

In order to better understand the current results, it is also pertinent that dose dependent studies are carried out in order to assess any dose dependent effects. It has been shown previously by a number of authors that decorin can bind to collagen I and increase collagen's binding affinity for the $\alpha 2\beta 1$ integrin (Svensson *et al.*, 1995; Keene *et al.*, 2000; Ruhland *et al.*, 2007). Another possible explanation for the increased migration rates with collagen I and decorin may be via "inside-out" signaling. This was proposed by Friedler *et al.*, in a study whereby decorin regulated endothelial migration by binding to the IGF-1 receptor, and through modulation of $\alpha 2\beta 1$ integrin activity, increased the binding affinity within migrating endothelial cells (Fiedler *et al.*, 2008). These studies reveal that there may be several different mechanisms in which decorin is modulating collagen I and subsequently increasing migration rates.

Decorin was not able to significantly modify fibronectin-stimulated wound closure. Fibronectin can be detected immunohistologically as early as 1 hour post-injury during the initial stages of muscle fiber repair, and precedes the deposition of collagen III and subsequently collagen I in the granulation tissue (Lehto and Jarvinen 1985). The secretion of decorin by inflammatory cells and myoblasts coincides with the deposition of collagen and therefore the ability of decorin to modulate collagen I-, but not fibronectin-, stimulated cell movement would coincide correctly with their temporal expression during the physiological stages of repair. Another possible explanation is the attachment strength of a cell to the substratum with maximal migration at an intermediate level of adhesiveness (Goldstein and DiMilla 2003); suggesting that if decorin altered the binding of fibronectin to the cell by either reducing (loss of traction) or increasing (reduced disruption of adhesions), cell motility would be impaired.

The Rho/ROCK pathway is required for actin-myosin cytoskeletal contraction as ROCK regulates actin-myosin cross-linking and the prevention of actin fiber degradation (Watanabe *et al.*, 1999). Collagen I activates the Rho/ROCK pathway via the $\alpha 2\beta 1$ integrin resulting in increased migration (Fiedler *et al.*, 2008). We determined the effect of fibronectin, collagen I and decorin on ROCK isoform expression and localization, in order to begin to elucidate the mechanism by which ECM factors influence myoblast migration.

Total ROCK-1 and -2 protein expression levels were analyzed in C2C12 myoblasts. Our results indicate that ROCK-2 is expressed at higher levels than ROCK-1, suggesting perhaps a more prominent role for ROCK-2 in myoblast migration. ROCK-1 had been shown to be up-regulated during myogenic differentiation and is down-regulated prior to myoblast fusion (Fortier *et al.*, 2008), further emphasizing a role for ROCK-1 in myogenesis rather than migration. We also demonstrate ROCK-1 to be expressed throughout the cytoplasm of migrating myoblasts, rather than being localized at active focal points.

Analysis of total ROCK-2 protein levels revealed no significant change in expression in response to decorin, collagen 1 or fibronectin. However, analysis of focal points containing ROCK-2 (via confocal microscopy) demonstrated these focal points to be localized primarily to the lamellipodia and the tail of migrating myoblasts. The number of focal points positive for ROCK-2 correlated with the change in percentage wound closure for decorin and collagen I, suggesting that ROCK-2 plays a role in mediating the effect of these two factors on myoblast migration. ROCK proteins have recently been shown to be crucial in focal adhesion formation by enabling tension-dependent maturation of the focal adhesions (Papusheva and Heisenberg 2010). Interestingly, ROCK-2-positive focal points did not differ significantly in number between control, collagen I-stimulated, and fibronectin-stimulated cells. These findings suggest that decorin and collagen I *in combination* are working via the Rho/ROCK pathway, whereas fibronectin and collagen I alone may not.

In conclusion we have shown that collagen I and fibronectin can both increase myoblast migration at dose dependent levels. Also, decorin displayed dose-dependent opposing effects on cellular movement, and regulated collagen I-stimulated, but not fibronectin-stimulated migration of C2C12 myoblasts. Finally, the effect of decorin plus collagen I, but not fibronectin or collagen I on their own, is at least in part mediated by the kinase, ROCK-2. These findings tie in with the wound repair process, whereby fibronectin is an early temporary scaffold which does not result in permanent fibrosis and is laid down prior to decorin secretion. However, collagen I is the major fibrotic component and therefore regulation of myoblast migration, via decorin, within this matrix is important to reducing scar tissue formation.

CHAPTER 4

ROCK INHIBITOR (Y-27632) MODULATES MYOBLAST MIGRATION IN A MATRIX-DEPENDENT MANNER

Includes data from:

Goetsch, K. P., Snyman, C., Elliott, E., Niesler, C. U. (2012) Y-27632 modulates mesenchymal and epithelial cell migration in a matrix-dependent manner, *Matrix Biology* - Submitted

4.1 INTRODUCTION

Migration is an essential process undertaken by many cell types in order to facilitate new tissue growth or repair. Key steps in the motility of any cell include the process of polarization and formation of protrusions or lamellipodia (Vicente-Manzanares *et al.*, 2007). This is followed by the assembly of adhesions at the leading front to facilitate interaction with the substratum (Pollard and Borisy 2003; Vicente-Manzanares *et al.*, 2007). In areas of increased tension, scaffold molecules including talin and vinculin, accumulate intracellularly at the integrin cytoplasmic tail, and subsequently recruit and bind to cytoskeletal polymerized actin, which accumulates into stress fiber bundles (Humphries *et al.*, 2006). The morphological behavior of the cell is governed by these adhesion points, with small protrusions forming from established leading edges. The assembly, disassembly and the reorganization of the actin cytoskeleton, which ultimately leads to the retraction of the rear tail, and detachment (Pollard and Borisy 2003), are critical to finally allow the cell to generate forward movement (Raftopoulou and Hall 2004).

The ECM plays a major role in the regulation of cellular migration providing cues to influence velocity and directionality via intracellular signaling pathways. The cell binds to the underlying matrix via integrins and other adhesion molecules gathered within focal adhesion complexes (Humphries *et al.*, 2006). Early focal complexes are groupings of individual integrin-related adhesions within an area, held in complex by activated talin and vinculin (Humphries *et al.*, 2006); which subsequently aggregate and mature into dense focal adhesions. These focal adhesions serve as traction points during migration. The

morphological behavior of the cell is governed by these adhesion points, with small protrusions forming from established leading edges.

The intracellular signaling molecules known to regulate cell migration include Ser/Thr and Tyr kinases, lipid kinases, as well as the Rho GTPases (Nobes and Hall 1995; Raftopoulou and Hall 2004). The Rho proteins are associated with focal adhesion assembly and cell contractility and responsible for cell body contraction and retraction of the rear tail. An important Rho target is the Ser/Thr kinase, ROCK, which is involved in stimulating filament assembly, and therefore is one of the essential steps required for cell body contraction and subsequent motility (Gerthoffer 2007).

The actin stress fibers and focal adhesion complexes in combination with the Rho/ROCK pathway play an important role in regulating cell migration (Nobes and Hall 1995; Ridley 2001; Wehrle-Haller and Imhof 2002; Leboeuf and Henry 2006; O'Neill 2009; Petrie *et al.*, 2009). While two ROCK isoforms have been described, ROCK-2 is thought to be the predominant isoform expressed in migrating skeletal myoblasts (Goetsch *et al.*, 2011). However, it is still not clear exactly what role ROCK plays. In addition to the role in assembling cytoskeletal actin fibers into contractile machinery, it may be involved in focal adhesion turnover and release at the rear of the cell by activating pathways resulting in phosphorylation of focal adhesion kinase (FAK) (Leboeuf and Henry 2006; Iwanicki *et al.*, 2008). In cells that have stress fibers, such as fibroblasts and myoblasts, the high level of substrate adhesion through stress-fibre-associated focal adhesions slows down cell migration. Reducing Rho activity can therefore have two opposing effects: migration is promoted by lowering adhesion to the ECM or decreased by inhibition of cell body contraction (Ridley 2001). Inhibition of ROCK by Y-27632 has been shown to induce a loss of focal adhesions, with cells moving faster and in a straighter line. Y-27632 is a synthetic compound that inhibits ROCK by competing with ATP for its binding site in the active region of this kinase (Ishizaki *et al.*, 2000). Such treatment also stimulates ruffling of the leading front membrane and formation of new low density focal complexes (Small *et al.*, 2002).

In this chapter we investigated the role of ROCK, specifically ROCK-2, in migrating myoblasts. This was carried out on Matrigel, used to mimic the basement membrane, and collagen I and decorin, used to mimic wound conditions. We analysed ROCK-2 and

vinculin expression in focal adhesion complexes to help us understand the role of this kinase during myoblast migration.

4.2 EXPERIMENTAL PROCEDURES

4.2.1 Collagen & Matrigel Coating

Calf skin collagen I (Sigma, Cat.C9791) was utilized for all collagen coating. Matrigel (BD, cat.356231, 10.1 mg/ml) was coated at 60 $\mu\text{g/ml}$. The stock solution (10.1 mg/ml) was diluted with DMEM. Plates were coated for a 1 h period at 37°C after which the excess solution was discarded and plates were U.V. sterilized and stored at 4°C.

4.2.2 Scratch Assay

The scratch assay was adapted from (Goetsch *et al.*, 2011). Briefly, the C2C12 cell line was cultured to 80% confluence in 24-well culture dishes which had either been left uncoated or had been coated with Matrigel (60 $\mu\text{g/ml}$) or collagen I (25 $\mu\text{g/ml}$) prior to seeding. A scratch was made using a sterile pipette tip and the percentage wound closure was assessed over a period of 7 h in the presence or absence of Y-27632 at 10 μM (ROCK Inhibitor, Calbiochem, cat.688001). To determine the percentage wound closure, wounds were photographed at hours 0, 3, 5, and 7 with the Motic 3 megapixel camera linked to an Olympus CKX41 inverted microscope (40X magnification). Percentage wound closure was calculated for all wounds by tracing the area along the border of the wound using the Motic 2.0 image analysis software.

4.2.3 Live Cell Imaging

Cells were cultured until 80% confluence on glass-bottomed culture dishes (Mattek Corporation, cat.P35G-1.5-14-C) that were left either uncoated or coated with Matrigel (60 $\mu\text{g/ml}$) or collagen I (25 $\mu\text{g/ml}$). The cells were wounded as described above and cultured for a further 4 h in fresh media, or media containing 10 μM Y-27632. Over this period, DIC images of cells migrating into the wound were recorded at 2 min intervals using a Zeiss 710 confocal microscope. Four hundred images were recorded and subsequently analysed. Images of cells migrating into the wounded area from the cell monolayer edge were captured as a time-lapse series. The paths of six representative cells (using the nuclei as points of reference) were tracked using the “manual tracking” plug-in in the ImageJ

software (rsbweb.nih.gov/ij). This was repeated in triplicate. Individual tracks were plotted as an overlay onto the final image of the time series and presented as a scatter plot, using the “chemotaxis and migration” tool in ImageJ. Data gathered in this way was applied to the “chemotaxis tool” ImageJ plug-in to generate scatter plots.

4.2.4 Immunocytochemical Analysis of ROCK-2 & Vinculin

C2C12 cells were cultured to 80% confluence in 24-well plates on coverslips that were uncoated or coated with Matrigel (60 µg/ml) or collagen I (25 µg/ml) prior to seeding. Cultures were wounded and after 3 hours cells were washed with PBS and fixed in a 4% paraformaldehyde solution. Cells were incubated in blocking solution [1% BSA in PBS buffer (pH 7.4)] for 1 hour and immunolabelled using primary antibodies to ROCK-2 (1/1000, polyclonal goat anti-rat ROCK-2, Santa Cruz, cat.Sc-1851) and vinculin (1/1000, monoclonal mouse anti-human vinculin, Sigma, cat.V9131) for 4 h at room temperature. Cells were then washed with PBS and incubated (room temperature) with secondary antibodies, Dylight 549 donkey anti-goat (1/800, Jackson Scientific) and Dylight 488 donkey anti-mouse (1/800, Jackson Scientific) for 1 hour. The actin cytoskeleton was visualized using TRITC-conjugated phalloidin (1/20 000, Sigma, cat.P1951) which was added with the secondary antibody. Hoechst (1/4000, Sigma) was used as a nuclear stain for both cell types and added 5 minutes prior to mounting after secondary labeling. Coverslips were mounted with moviol and viewed on the Zeiss 710 confocal microscope.

4.2.5 Statistics

For the scratch assay n=6 data points were obtained for each condition. Data was determined to be non-parametric. The *Mann-Whitney U test* was therefore used to calculate *p*-values for the differences between the means of experimental conditions and control. Image quantification (cell number, length and area) was performed in triplicate and the *Student's t-test* was utilized for statistical analysis. *Genstat* was used for all statistical tests and significance was determined as $p < 0.05$. Results are presented as the mean \pm the standard error of the mean (SEM).

4.3 RESULTS

4.3.1 *Y-27632 differentially affects myoblast morphology and velocity*

Given the key role of ROCK in conventional cell migration, we initially investigated the influence of Y-27632, a ROCK inhibitor, on the morphology and migration patterns of C2C12 myoblasts. Under control conditions (uncoated) migrating C2C12 cells displayed lamellipodia with membrane ruffling at the front of the cell (white arrows) tapering to a pointed tail at the rear (Figure 4.1A). However, inhibition of ROCK generated several lateral protrusions that formed and collapsed quickly on an ongoing basis. A distinct change in myoblast morphology was evident when Y-27632 was added to the media. Scatter plot analysis of migrating C2C12 nuclei's trajectories can be used to determine a track or patterning for migration trajectories (Figure 4.1B). The total distance travelled by C2C12 myoblasts increased when treated with Y-27632 compared to the untreated control (Figure 4.1B). Interestingly, persistence of direction (directionality) of migrating C2C12 myoblasts was evident, indicating that cells continued to migrate uniformly in the same direction.

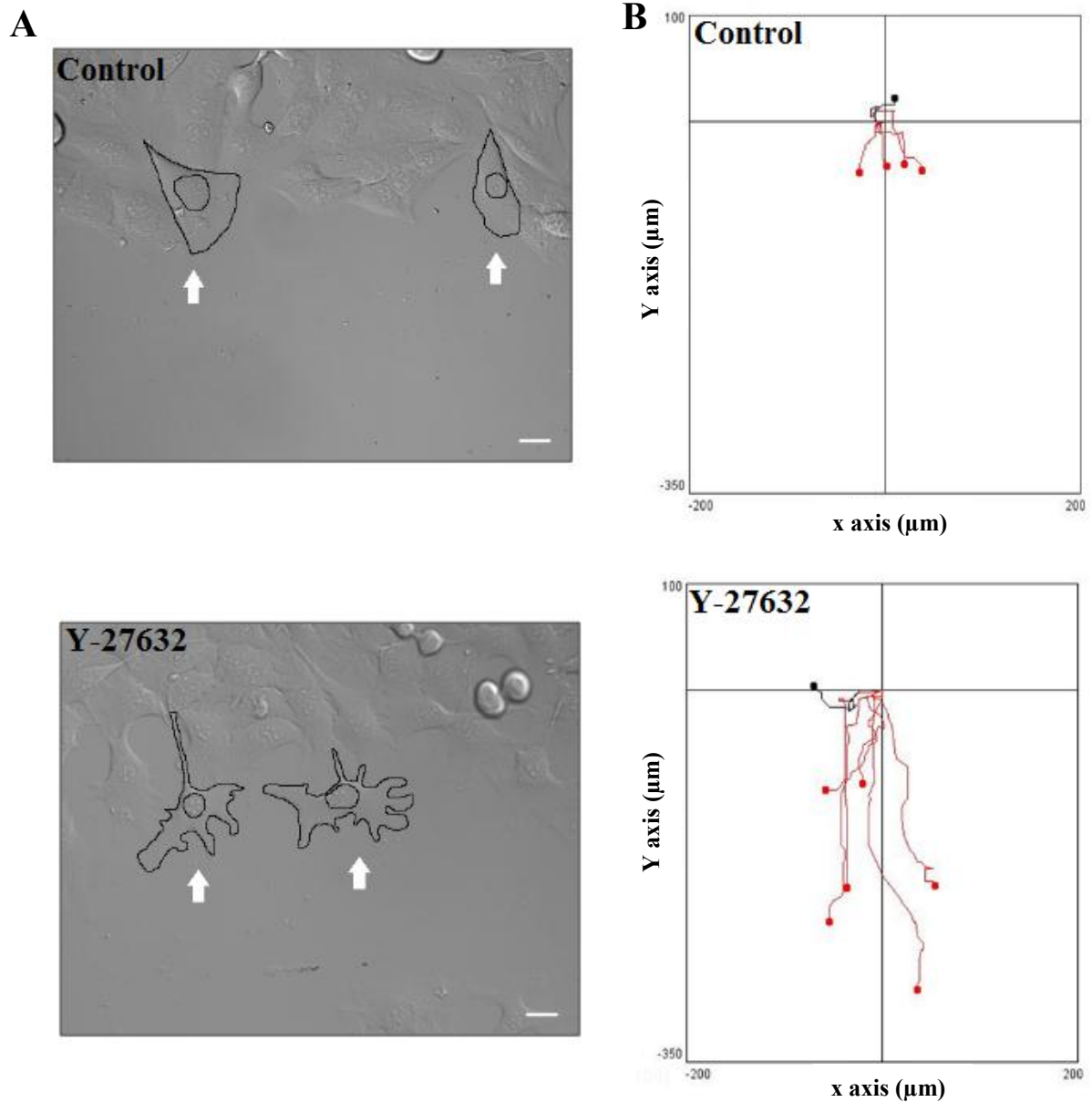


Figure 4.1 Effect of Y-27632 on morphology and migration patterns of C2C12 myoblasts on uncoated plates. **A)** Micrographs of cells within “wounded” monolayers at 4 hours post-injury. Cells were cultured after wounding in growth media with or without Y-27632 (10 μ M) as indicated. Outline of representative cells are shown in black. Leading fronts are designated by white arrows. **B)** Migration pattern of cells over a 4 hour period is illustrated as scatter plots. Y-axis is distance travelled. X-axis is the displacement from original position. Images were taken at 2 minute intervals with the Zeiss 710 confocal microscope. Scale bar = 20 μ m.

4.3.2 Effect of Y-27632 on migration of C2C12 myoblasts cultured on Matrigel

In vivo, activated myoblasts initially migrate along a basement membrane to facilitate wound healing. Matrigel was used to mimic the ECM of the basal lamina in order to determine the effect of ROCK inhibition on myoblasts during the early migration phase of wound repair. Matrigel is a reconstituted basement membrane preparation which contains primarily laminin and collagen IV. Compared to control (uncoated conditions), C2C12 myoblasts migrating on Matrigel showed a significant increase in the percentage wound closure from $34.96 \pm 6.84\%$ to $66.64 \pm 14.07\%$ at 7 hours, a 31.68% increase ($p < 0.026$) (Figure 4.2). As expected, Y-27632 also significantly increased the percentage wound closure at 7 hours to $58.88 \pm 10.59\%$ when compared to untreated control, a 23.93% increase ($p < 0.026$). The combination of Matrigel and Y-27632 maintained this increase in the percentage wound closure of $71.59 \pm 14.27\%$ when compared with control ($p < 0.001$), but did not significantly increase the percentage wound closure when compared to Matrigel or Y-27632 alone (Figure 4.2).

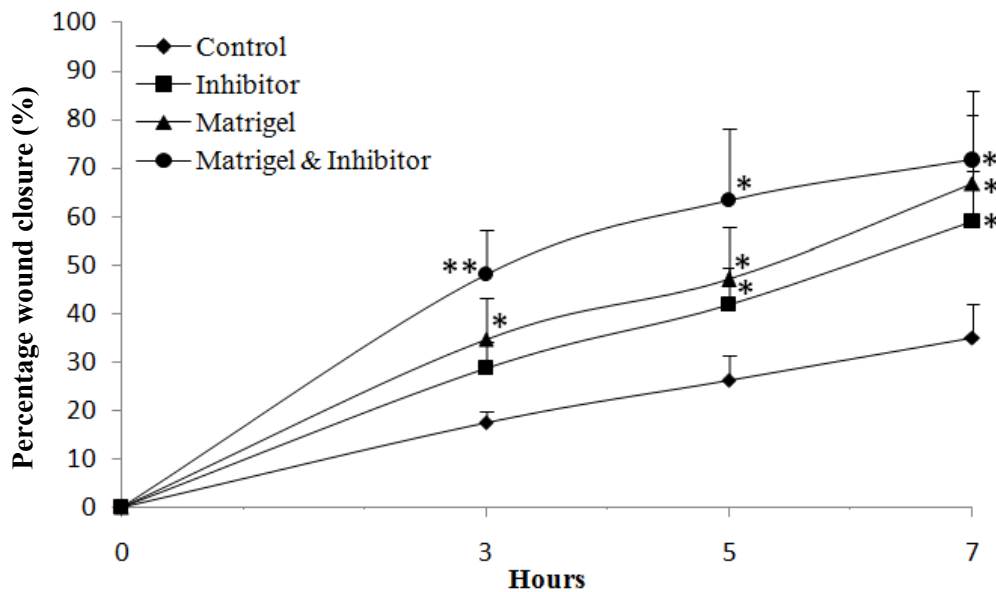


Figure 4.2. Effect of Y-27632 on C2C12 myoblast wound closure when cultured on Matrigel. C2C12 cells were cultured on uncoated or Matrigel-coated (60 $\mu\text{g/ml}$) plates. Cells were wounded (scratch assay) and migration monitored over a 7 hour period in the presence or absence of Y-27632 (10 μM). Percentage wound closure graph for C2C12 myoblasts. Results are presented as Mean \pm SEM. Significance is compared to the control (uncoated and growth media only) unless otherwise indicated. * $p < 0.05$ and ** $p < 0.005$ compared to control, unless otherwise stated. $n=3$.

4.3.3 Effect of Y-27632 on C2C12 myoblast migration cultured on collagen I

Collagen I is a key extracellular matrix protein which is laid down by fibroblasts as a structural scaffold within the skeletal muscle repair site. Therefore, investigating the effect that collagen I has on myoblast migration is important in order to understand the role of the ECM on skeletal muscle regeneration.

Compared to the percentage wound closure of untreated control at 7 hour ($51.37 \pm 7.82\%$), C2C12 myoblasts migrated significantly faster when cultured either on collagen I ($88.87 \pm 8.48\%$; $p < 0.002$) or in the presence of Y-27632 ($76.85 \pm 10.08\%$; $p < 0.026$) (Figure 4.3). A further significant increase was seen when cells migrated on collagen I in the presence of Y-27632 ($97.26 \pm 2.74\%$; $p < 0.009$) compared to both control and inhibitor alone (Figure 4.3). These data highlight that in contrast to Matrigel, collagen I elicits a further increase in migration in Y-27632-treated C2C12 myoblasts. The ROCK inhibitor was not able to increase collagen-induced migration significantly beyond collagen I alone.

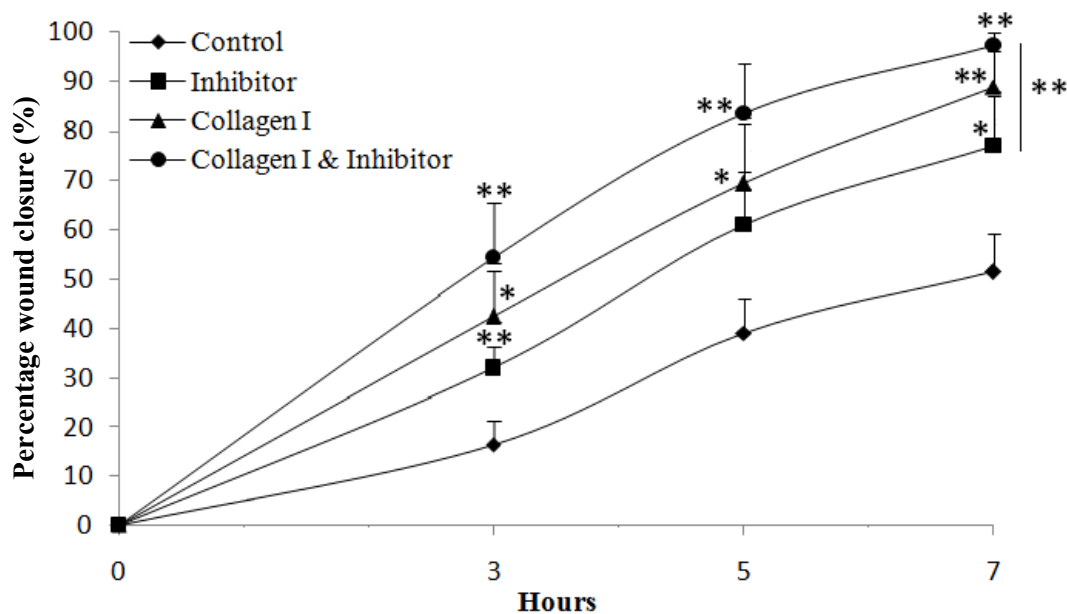


Figure 4.3. Effect of Y-27632 on C2C12 myoblast wound closure when cultured on collagen I. C2C12 cells were cultured on uncoated or collagen I-coated (25 $\mu\text{g/ml}$) plates. Cells were wounded (scratch assay) and migration monitored over a 7 hour period in the presence or absence of Y-27632 (10 μM). Percentage wound closure graph for C2C12 myoblasts. Results are presented as Mean \pm SEM. Significance is compared to the control (uncoated and growth media only) unless otherwise indicated. * $p < 0.05$ and ** $p < 0.005$ compared to control, unless otherwise stated. $n=3$.

4.3.4 Localization of ROCK-2 & vinculin within migrating C2C12 myoblasts cultured on Matrigel and collagen I

We have previously shown that ROCK-2, but not ROCK-1, is the more predominantly expressed isoform during the migration of skeletal myoblasts (see *Chapter 3*) and furthermore that ROCK-2, not ROCK-1, is localized to focal adhesion complexes. In the current study, ROCK-2 localization to focal adhesion sites was confirmed by co-labeling with vinculin, an indicator of integrin-related cell-matrix adhesion points.

Following wounding of C2C12 myoblasts, ROCK-2 expression was observed to correspond with vinculin staining under control, Matrigel, and collagen I conditions (Figure 4.4A); however, no visible changes in ROCK-2 expression levels were evident. Interestingly, irrespective of extracellular matrix factors, the addition of Y-27632 did not decrease the visible ROCK-2 expression in the focal adhesion sites (Figure 4.4A). Vinculin expression levels decreased with collagen I, but not Matrigel. RGB Profiler was utilized to determine localization of ROCK-2 and vinculin within the focal adhesion complexes at the leading front of the “wounded” area (Figure 4.4B). Y-27632 did not prevent or decrease the localization of ROCK-2 at the focal adhesion complex. Notably, a decrease in vinculin expression was seen in response to collagen I, but not Matrigel (Figure 4.4B).

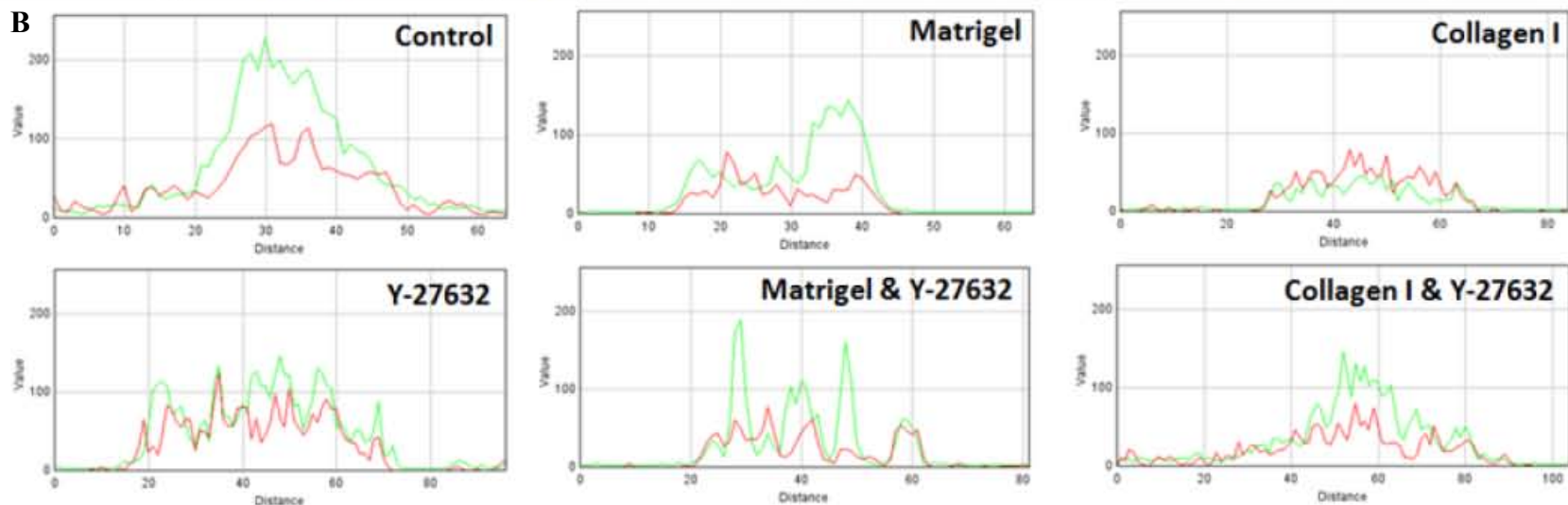
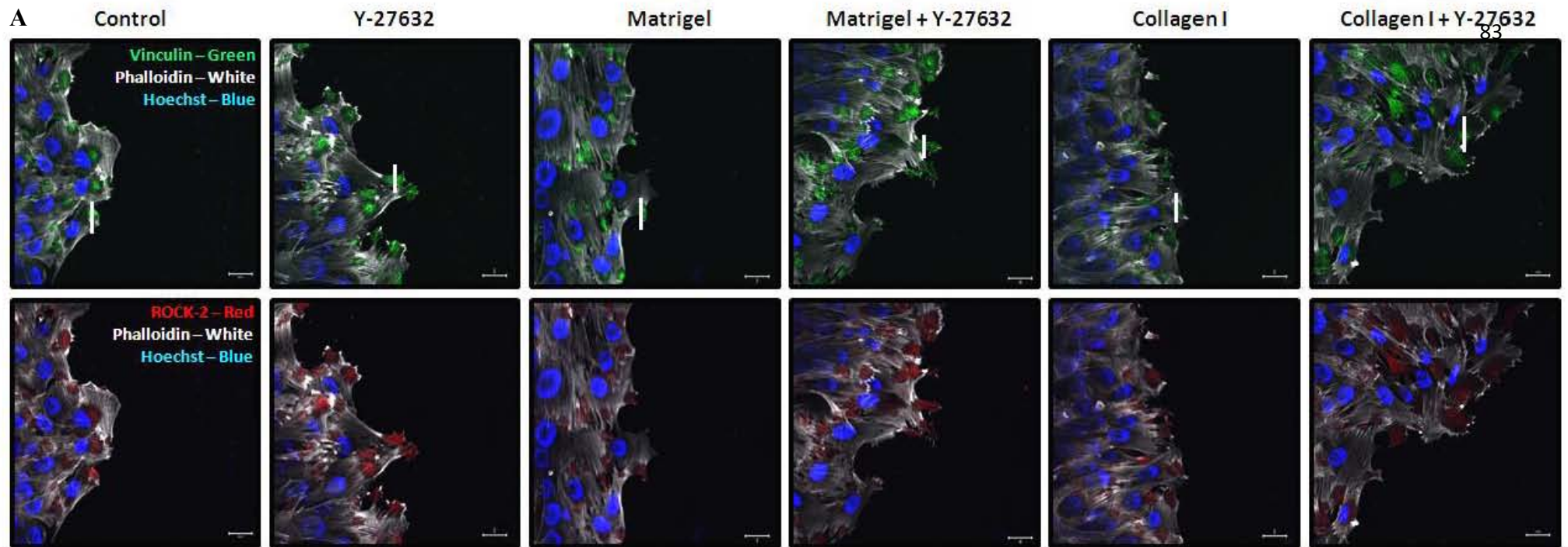


Figure 4.4. Cellular expression of ROCK-2 and vinculin in response to Matrigel and collagen I \pm Y-27632. **A)** Confocal microscopy of ROCK-2 and vinculin expression at the cell-matrix adhesion plane of C2C12 myoblasts. Panel of representative images showing ROCK-2 (red) and vinculin (green) expression. Actin (white) was fluorescently labelled with TRITC-conjugated phalloidin. Nuclei were labelled with Hoechst (blue). **B)** RGB intensity profiles for vinculin (green) and ROCK-2 (red) determined at a focal adhesion complex cluster (white line in (A)). All immunocytochemical labelling was performed at 7 hours post wounding and images were captured along the leading front. Matrigel (60 μ g/ml), collagen I (25 μ g/ml) and Y-27632 (10 μ M) were used. Cells cultured on uncoated plates in the presence of growth media (10% FCS) were used as control. Images were captured using a Zeiss 710 inverted confocal microscope. Scale bar = 20 μ m.

4.3.5 *Y-27632 increases the total area of ROCK-2-containing focal adhesion clusters in C2C12 myoblasts*

Despite the apparent lack of effect of Y-27632 or Matrigel on ROCK-2 or vinculin expression *levels*, a change in the number and size of focal adhesion complexes in C2C12 myoblasts under these conditions was observed. We therefore assessed the number of focal adhesion clusters containing ROCK-2 (white arrow heads, Figure 4.5A) and the area of these clusters at the leading front.

Although both Matrigel and Y-27632 appeared to increase the number of focal adhesion clusters containing ROCK-2 when compared to control (Figure 4.5B), the effect was not significant. However, the addition of Y-27632 to C2C12 cells cultured on Matrigel significantly increased the number of clusters compared to both Matrigel and inhibitor alone ($p < 0.05$). Collagen I significantly increased the number of clusters compared to the untreated control from 1.76 ± 0.20 to 3.95 ± 0.39 , a two-fold difference ($p < 0.05$, Figure 4.5B). However, the addition of Y-27632 to cells cultured on collagen I had a negative effect on cluster number, decreasing the number to 2.71 ± 0.15 when compared to collagen I alone.

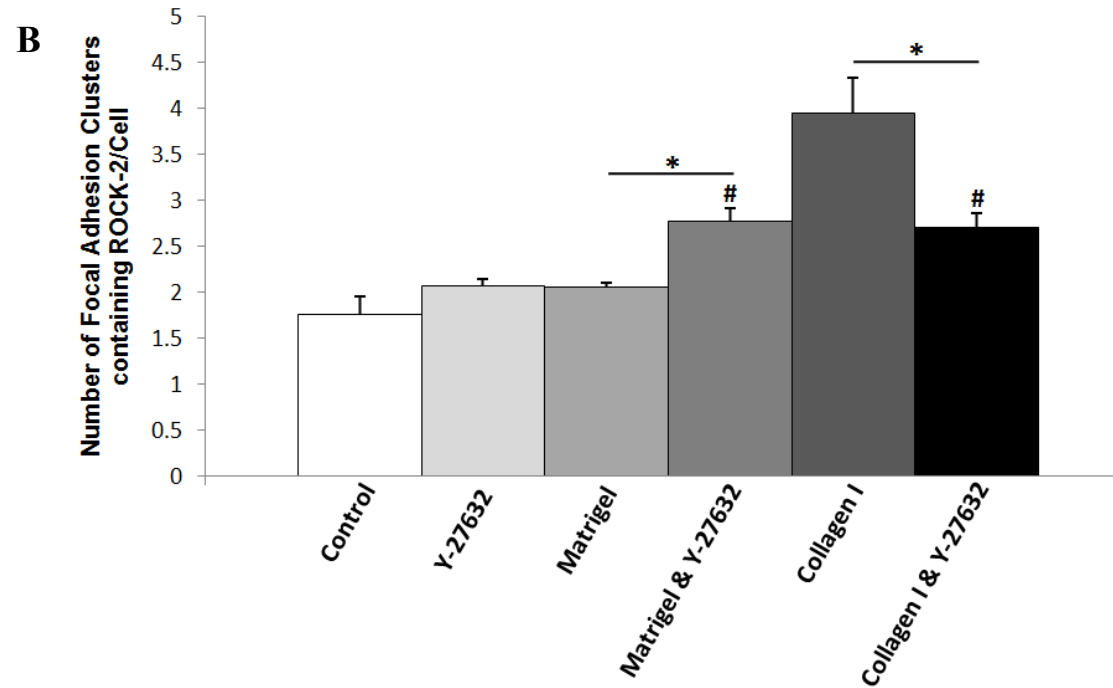
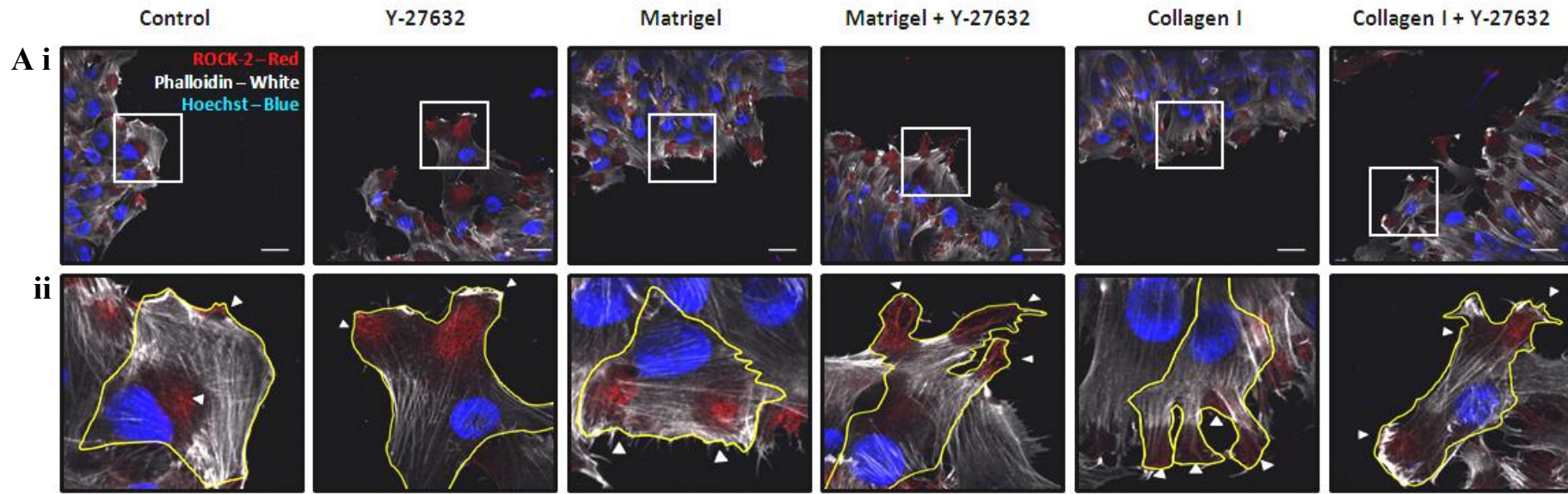


Figure 4.5. Effect of Matrigel and collagen I ± Y-27632 on the number of ROCK-2 containing focal adhesion clusters in C2C12 myoblasts. **Ai)** Confocal microscopy of ROCK-2-positive clusters (red) in migrating cells at the leading front (white box). **ii)** Focal adhesion clusters within the white box from (i) **B)** The number of focal adhesion clusters within the C2C12 cells (white arrow heads in (A)) were counted and represented as a bar graph showing the average number of focal adhesion clusters per migrating cell. All immunocytochemical labelling was performed at 7 hours post wounding and images were captured along the leading front. Matrigel (60 $\mu\text{g/ml}$), collagen I (25 $\mu\text{g/ml}$) and Y-27632 (10 μM) were used. Actin was fluorescently labelled with TRITC-conjugated phalloidin (white) and nuclei were labelled with Hoechst (blue). Images were captured using a Zeiss 710 inverted confocal microscope. Scale bar = 20 μm . * $p < 0.05$, $n = 3$. Results are presented as Mean \pm SEM.

Analysis of vinculin-positive focal adhesion clusters revealed minimal increases in cluster area for Matrigel and collagen I compared to the untreated control (Figure 4.6A). However, an increase in focal adhesion cluster area to $107.41 \pm 5.83 \mu\text{m}^2$ was evident when Y-27632 was added compared to the control ($41.08 \pm 1.87 \mu\text{m}^2$, $p < 0.005$; Figure 4.6B). The effect of Y-27632 was even more prominent when the inhibitor was added to C2C12 cells cultured on collagen I, with clusters covering an average area of $202.20 \pm 26.60 \mu\text{m}^2$ when treated with collagen I and Y-27632 compared to collagen I alone ($58.22 \pm 5.42 \mu\text{m}^2$) ($p < 0.006$) (Figure 4.6B).

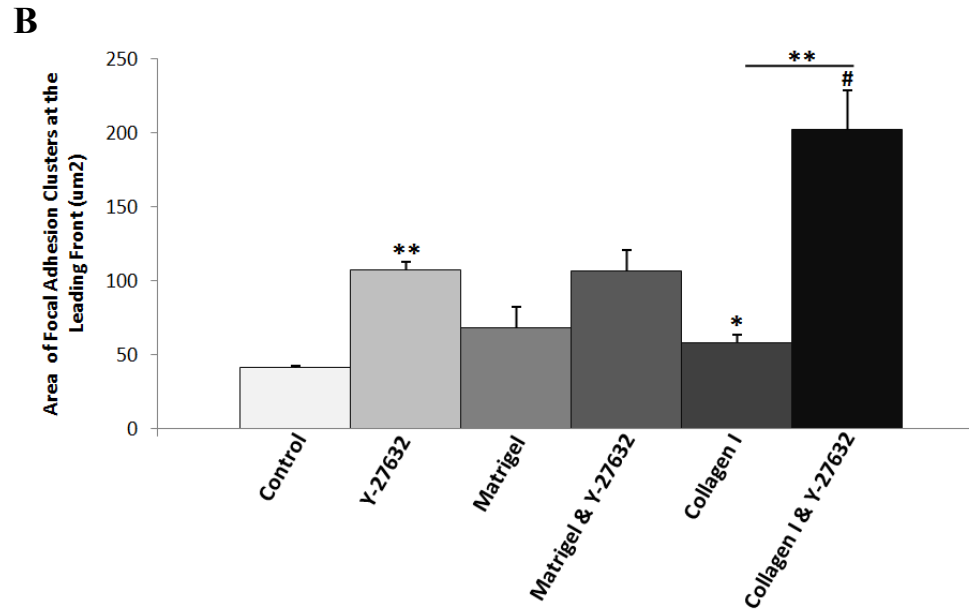
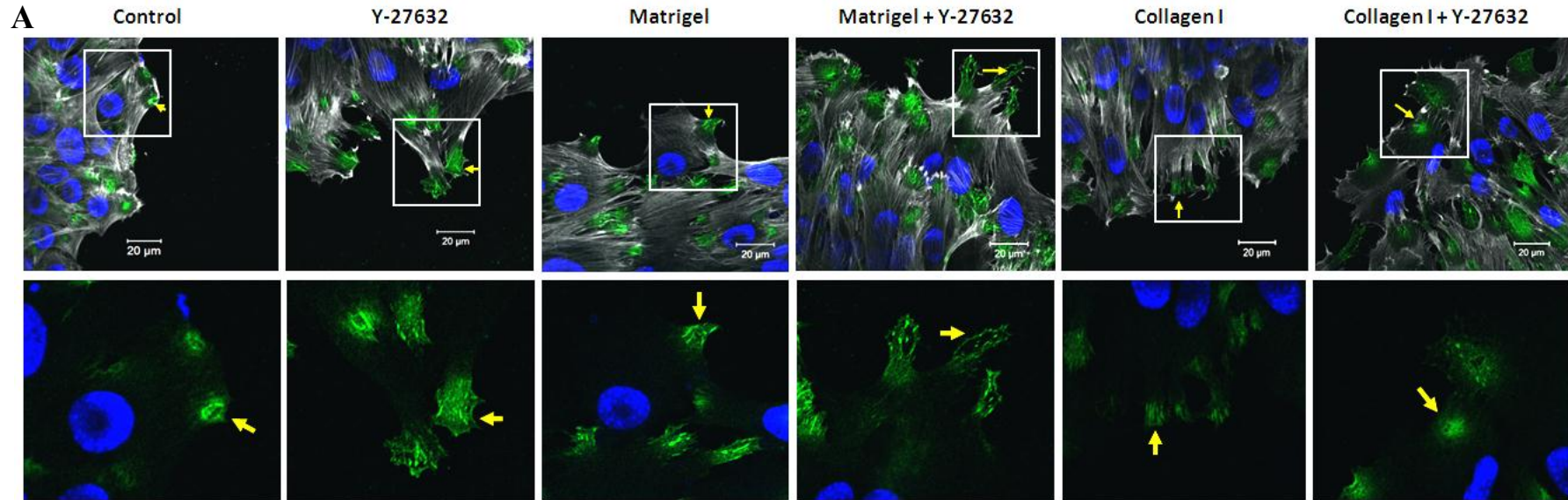


Figure 4.6. Effect of Matrigel and collagen I ± Y-27632 on the area of focal adhesion clusters in C2C12 myoblasts. **A)** Confocal microscopy of vinculin-positive clusters (green) in migrating cells at the leading front (white box). **B)** Bar graph showing the area of focal adhesion clusters per migrating cell. All immunocytochemical labelling was performed at 7 hours post wounding and images were captured along the leading front. Matrigel (60 μg/ml), collagen I (25 μg/ml) and Y-27632 (10 μM) were used. Actin was fluorescently labelled with TRITC-conjugated phalloidin (white) and nuclei were labelled with Hoechst (blue). Images were captured using a Zeiss 710 inverted confocal microscope. Scale bar = 20 μm. * $p < 0.05$, ** $p < 0.05$ compared to control. # $p < 0.05$ compared to Y-27632. $n = 3$. Results are presented as Mean ± SEM.

4.4 DISCUSSION

Cells that have been activated to migrate by “wounding”, use cues from the extracellular environment to influence and guide forward motility. Myoblasts *in vivo* migrate from the niche towards a wound and may therefore be influenced by both the BM components and collagen I secreted at the site of injury by infiltrating fibroblasts (Bentzinger *et al.*, 2012). In order to understand some of the mechanisms influencing myoblast migration in these two distinct environments, this study assessed whether the kinase, ROCK, a major component in the regulation of myoblast migration, was involved differently during *in vitro* migration on different substrata.

In response to injury, the morphology of migrating myoblasts into the scratch area was seen to be affected by experimentally-induced ROCK inhibition. ROCK-inhibited C2C12 myoblasts displayed an increasing number of distinct protrusions at the leading front compared to single lamellipodia in untreated cells. Inhibition of ROCK during migration thus altered cytoskeletal dynamics; this was accompanied by an increased velocity reflected by a faster wound closure. The change in morphology and velocity following inhibition suggests that ROCK may play a restraining role, through increased stress fiber formation and focal adhesions, in myoblast migration. Interestingly, directionality of migration was retained despite the appearance of more lamellipodia in the absence of ROCK activity.

The underlying matrix not only serves as a base to which cells adhere, but supports survival and provides traction influencing forward motility. The experimental substratum that most closely resembled the basement membrane (Matrigel) hastened wound closure *in vitro* compared to the condition without any simulated ECM; however, addition of the ROCK inhibitor did not significantly improve C2C12 myoblast migration into the wound in comparison with Matrigel alone. This suggests that migration along the basement membrane may not be regulated by ROCK, thus limiting the influence of ROCK to earlier events or to less organized niches. An alternative explanation is that ROCK is indirectly inhibited when Matrigel-C2C12 adhesion complexes are formed (possibly by structural constraints: on ATP binding sites on ROCK, or the phosphorylation sites of targets are no longer accessible) so further addition of the ROCK inhibitor would not have an effect.

ROCK may also inhibit the interaction of the laminin $\alpha7\beta1$ integrin since laminin is known to increase myoblast migration rates; and laminin is a major constituent of Matrigel (Crawley *et al.*, 1997). Similar to Matrigel, a substratum of collagen I also significantly enhanced migration of C2C12 cells. Again, the inhibition of ROCK did not further alter the migration of myoblasts on collagen I. This was unexpected as collagen I is known to activate the Rho/ROCK pathway via the $\alpha2\beta1$ integrin of epithelial cells (Friedl *et al.*, 1998; Humphries *et al.*, 2006).

Given that activated ROCK is known to be involved in the process of migration (Nobes *et al.*, 1995; Raftopoulou and Hall 2004), we were not able to properly explain why ROCK inhibition did not affect wound closure in all of the conditions. We also assessed the localization of ROCK-2 in myoblasts migrating on the different ECM components found in the basal lamina and during wound repair. The mechanism by which the extracellular matrix and ROCK may influence stress fibre-related migration was investigated by analyzing the localization of vinculin at adhesion sites. Alterations in vinculin accumulation at cell-matrix adhesion sites reflected the influence of the underlying matrix on the number and strengthening of stress-related adhesions, and thus exhibit control over forward movement. Myoblasts formed several adhesion cluster sites defined by a surrounding layer of actin which contained a number of well-defined vinculin-positive complexes. The defined adhesion cluster sites observed may restrain migration. As a result, C2C12 myoblast migration may be more targeted, as demonstrated in the scatter plot analysis. Also, vinculin-positive focal adhesion clusters in C2C12 myoblasts cultured on collagen I had an enlarged morphology and were increased in number compared to the control, where no matrix was present.

The change in stability of cell-matrix adhesions may, therefore, be an underlying factor in the increased velocity of ROCK inhibited myoblasts. A cohesive contractile mechanism is required to ensure persistence of directionality. However, strengthening of focal adhesion sites and the development of stress fibers during this process may actually restrain the mechanism of forward sliding. It was proposed in 1995 that ROCK-2 coordinates adherence and the connection of adhesion proteins to the cytoskeleton (Nobes and Hall 1995). Cell-matrix adhesion complexes are strengthened through phosphorylation of the myosin light chain, which results in condensation of these intracellular focal complexes into focal adhesions. Such dedicated, well developed sites are related to slower migration,

with retention of directional persistence. Nobes proposed that the advantage might be that these processes result in a more determined, and thereby ultimately faster, mode of migration (Nobes and Hall 1999).

Using this information to explain our results, we observed the non-coated control closed the “wound” area at approximately half the rate of collagen I and Matrigel; however, treatment with the ROCK inhibitor more than doubled the percentage wound closure on non-coated plates (Figure 4.7A). No major change was observed in focal adhesion number with the ROCK inhibitor (uncoated), but an increase in focal adhesion area was observed compared to the non-treated control (Figure 4.7B). This possibly explains the increase in wound closure observed, as the focal adhesion complex sites are not as tightly packed and therefore are not restraining migration as well as tightly packed complexes. ROCK induced focal adhesions with limited size allow for the formation of many stress fibers (reduced migration and increased directionality) rather than only a few large ROCK-induced actin bundles (increased migration, reduced directionality) (Dhawan and Helfman 2004). Collagen I had a relatively large number of tightly packed focal adhesion complexes which would explain the increase in percentage wound closure on collagen I alone. Although the addition of experimentally-induced ROCK inhibition increased the focal adhesion area (on both matrices and uncoated), which would increase migration, focal adhesion cluster number decreased to a level similar to that of the inhibitor alone, leaving less focal adhesion clusters to facilitate myoblast migration. A direct correlation between myoblast adhesion and $\beta 1$ -integrin expression has been shown (Modulevsky *et al.*, 2012) implicating collagen I in cell adhesion regulation. Although addition of ROCK inhibition to cells cultured on Matrigel increased focal adhesion cluster number and focal adhesion area, the effect observed during wound closure was minimal (Figure 4.7). This supports the idea that Matrigel is regulating myoblast migration via integrin specific mechanisms and not directly via the ROCK pathway.

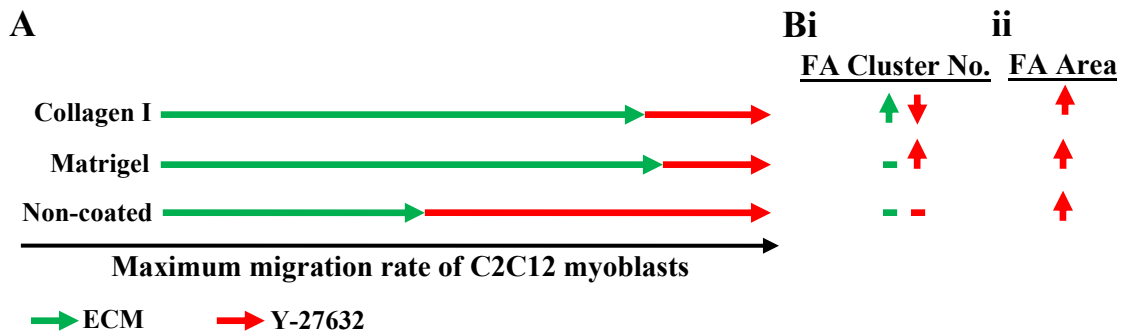


Figure 4.7. Effect of Y-27632 on myoblast migration in relation to untreated ECM-coated plates. A) Maximum migration rates of Y-27632 over and above the effect of untreated collagen I, Matrigel, and the non-coated control. **Bi)** Effect of Y-27632 and ECM on focal adhesion (FA) number. **ii)** Effect of Y-27632 on focal adhesion area compared the respective control. Green arrow – ECM effect, red arrow – Y-27632 effect. Arrow length refers to migration rates.

Myoblasts rely on mechanical cues from the ECM. This requires robust cell adhesion to the microenvironment via integrins and focal adhesion sites for the transmission and conversion of mechanical information into biochemical signaling (Modulevsky *et al.*, 2012). The mechanisms of migration during wound repair are complex, involving changing microenvironments, cytokines and cell types. However, these external changes facilitate a highly regulated and controlled mode of migration by regulating cellular velocity and directionality.

CHAPTER 5

THE TGF- β /DECORIN COMPLEX DIFFERENTIALLY INFLUENCES MYOBLAST MIGRATION IN A ECM DEPENDANT MANNER

Contains data from:

Goetsch, K. P., Myburgh, K.H., Niesler, C. U. (2012) The TGF- β /decorin complex differentially influences myoblast migration in a ECM dependant manner– **in preparation**

5.1 INTRODUCTION

In vivo, muscular injuries that destroy the basal lamina result in a poor functional recovery of the skeletal muscle compared to injuries that minimally disrupt the muscular integrity and orientation (Sanes 2003). This is due in part, to the presence of pro-inflammatory cytokines, such as TGF- β , which promote the deposition of collagen I by infiltrating fibroblasts (Serrano *et al.*, 2011). During tissue repair, collagen forms the tensile strength of the healing wound, while fibronectin forms a scaffold to which cells migrating into the wound area can attach. TGF- β increases the accumulation of these matrix proteins at the injury site, resulting in increased connective tissue formation and subsequent scarring (Roberts *et al.*, 1992). *In vivo* studies have highlighted the negative role of TGF- β on functional skeletal muscle repair, whereby an increase in TGF- β 1 signaling increased muscular fibrosis and muscle fibre degeneration (Mezzano *et al.*, 2007; Mendias *et al.*, 2011).

Decorin and biglycan are proteoglycans that bind TGF- β , as well as ECM proteins, such as collagens (Yamaguchi *et al.*, 1990; Ameye *et al.*, 2002). Decorin constitutes an attractive candidate for the modulation of TGF- β bio-availability, as it has a high affinity for TGF- β and the decorin/TGF- β complex is rapidly endocytosed (Hausser *et al.*, 1996). Studies of TGF- β /decorin interactions have focused primarily on understanding the anti-fibrotic effect of decorin against TGF- β and have found that decorin decreases fibrotic scar tissue formation by sequestering TGF- β (Cabello-Verrugio *et al.*, 2012). However, the effect of this complex on myoblast migration is not well characterized (Li *et al.*, 2008).

We have previously shown that decorin increases the rate of migration of C2C12 myoblasts on collagen I and fibronectin compared to an uncoated control (Goetsch *et al.*, 2011). Also, Marmotti *et al.*, (2012) recently reported that primary chondrocyte migration was increased with TGF- β 1 exposure (Marmotti *et al.*, 2012), while Finnson *et al.*, (2012) indicated that keratinocyte migration was increased by TGF- β 3 (Finnson *et al.*, 2012). However, this may be a cell-specific response since the dermis and cartilage ECM compositions and cell-types differ from that of the skeletal myofiber micro-environment. This was seen in the interaction between ECM and TGF- β on cell migration of liver microvascular endothelial cells which were influenced by substrate rigidity but not by TGF- β (Tian *et al.*, 2012).

In this chapter, we investigate the combined effect of TGF- β & decorin on migration of C2C12 murine myoblasts and primary cultured human skeletal muscle myoblasts. We also further investigate whether ECM components such as, collagen IV & laminin (Matrigel), collagen I and fibronectin modulate the response of myoblasts to the TGF- β /decorin complex.

5.2 EXPERIMENTAL PROCEDURES

5.2.1 General

All chemicals used were of an analytical grade and were purchased from either Sigma or Merck unless otherwise stipulated. All cell culture was carried out under sterile conditions in a level II lamina flow hood (ESCO class II BSC) and incubated in a CO₂ incubator (Innova CO-170) at 37°C, 5% CO₂. Brightfield images were captured using the Motic 3.0 MP camera on the Olympus CKX41 microscope. The Zeiss 710 confocal microscope was utilized for all fluorescence microscopy.

5.2.2 Cell Culture

The C2C12 cell line was donated by the Cape Heart Center, University of Cape Town. Primary cultured human skeletal myoblasts (HSKM) were purchased from Lonza. Growth media contained Dulbecco's Modified Eagle Serum (DMEM, Highveld, cat.CN3193-9), L-glutamine (2% v/v, Cambrex, cat.17-605E), Penstrep (2% v/v, Cambrex, cat.17-602E), fetal calf serum (10% v/v, Invitrogen, cat.10108165). Human culture media contained HAMS-F10 (Gibco, cat.15140), FCS (20% v/v), Pentrep (2% v/v), L-glutamine (2% v/v), fibroblast growth factor (FGF, 2.5 ng/ml, Promega, cat.G507A).

5.2.3 Scratch Assay

The scratch assay was adapted from (Goetsch *et al.*, 2011). Briefly, the C2C12 and HSKM cells were cultured to 80% confluence in 24-well culture dishes which had either been left uncoated or had been coated with Matrigel (60 µg/ml), collagen I (25 µg/ml) or fibronectin (5 µg/ml) prior to seeding (see *Chapter 3, Section 3.2.2* for detailed coating methods). Briefly, a scratch was made using a sterile pipette tip and the percentage wound closure was assessed over a period of 7 hours in the presence or absence of TGF-β2 (10 ng/ml, Sigma) and/or decorin (10 µg/ml, Sigma, cat.D8428). To determine the percentage wound closure, wounds were photographed at hours 0, 3, 5, and 7 with the Motic 3 megapixel camera linked to an Olympus CKX41 inverted microscope (40X magnification). Percentage wound closure was calculated for all wounds by tracing the area along the border of the wound using the Motic 2.0 image analysis software. The rate of migration was determined by calculating the gradient of the percentage wound closure for each treatment group.

5.2.4 Immunocytochemical Analysis of ROCK-2 & Vinculin

C2C12 and HSKM cells were cultured to 80% confluence in 24-well plates on coverslips that were uncoated or coated with Matrigel (60 µg/ml), collagen I (25 µg/ml) or fibronectin (5 µg/ml) prior to seeding. Cultures were wounded and after 7 hours cells were washed with PBS and fixed in a 4% paraformaldehyde solution. Cells were incubated in blocking solution [1% BSA in PBS buffer (pH 7.4)] for 1 hour and immunolabelled using primary antibodies to ROCK-2 (1/1000, polyclonal goat anti-rat ROCK-2, Santa Cruz, cat.Sc-1851) and vinculin (1/1000, monoclonal mouse anti-human vinculin, Sigma, cat.V9131) for 4 h at room temperature. Cells were then washed with PBS and incubated (room temperature) with secondary antibodies, Dylight 549 donkey anti-goat (1/800, Jackson Scientific) and Dylight 488 donkey anti-mouse (1/800, Jackson Scientific) for 1 h. Hoechst (1/4000, Sigma) was used as a nuclear stain for both cell types and added 5 minutes prior to mounting after secondary labeling. Coverslips were mounted with moviol and viewed on the Zeiss 710 confocal microscope.

5.2.5 Statistics

The *Mann-Whitney U test* was used to calculate *p*-values for the differences between the means of experimental conditions and control. *Genstat* was used for all statistical tests and significance was determined at $p < 0.05$. Results are presented as the mean \pm the standard error of the mean (SEM).

5.3 RESULTS

5.3.1 Decorin modulates the inhibitory effect of TGF- β on myoblast migration

To study the effect of decorin & TGF- β on myoblast migration, we incubated the C2C12 cell line and HSKM primary cultured myoblasts with decorin (10 $\mu\text{g/ml}$) and/or TGF- β 2 (10 ng/ml). In C2C12 cells, TGF- β 2 ($12.67 \pm 2.69\%$) caused a perceived decrease, of 3.06%, in the percentage wound closure compared to control ($15.73 \pm 1.87\%$) at 7 hours, whereas decorin increased migration to 21% (Figure 5.1A). When decorin was added together with TGF- β 2 ($29.37 \pm 4.75\%$), a significant increase in percentage wound closure was observed compared to control, with an increase of 14% ($p < 0.05$, Figure 5.1A). This effect was also observed when looking at the rate of migration, whereby decorin and TGF- β 2 in combination ($4.14 \pm 0.67\%/hr$) significantly increased the rate of migration over TGF- β 2 ($1.77 \pm 0.39\%/hr$, $p < 0.005$) and the control ($2.17 \pm 0.28\%/hr$, $p < 0.05$, Figure 5.1B).

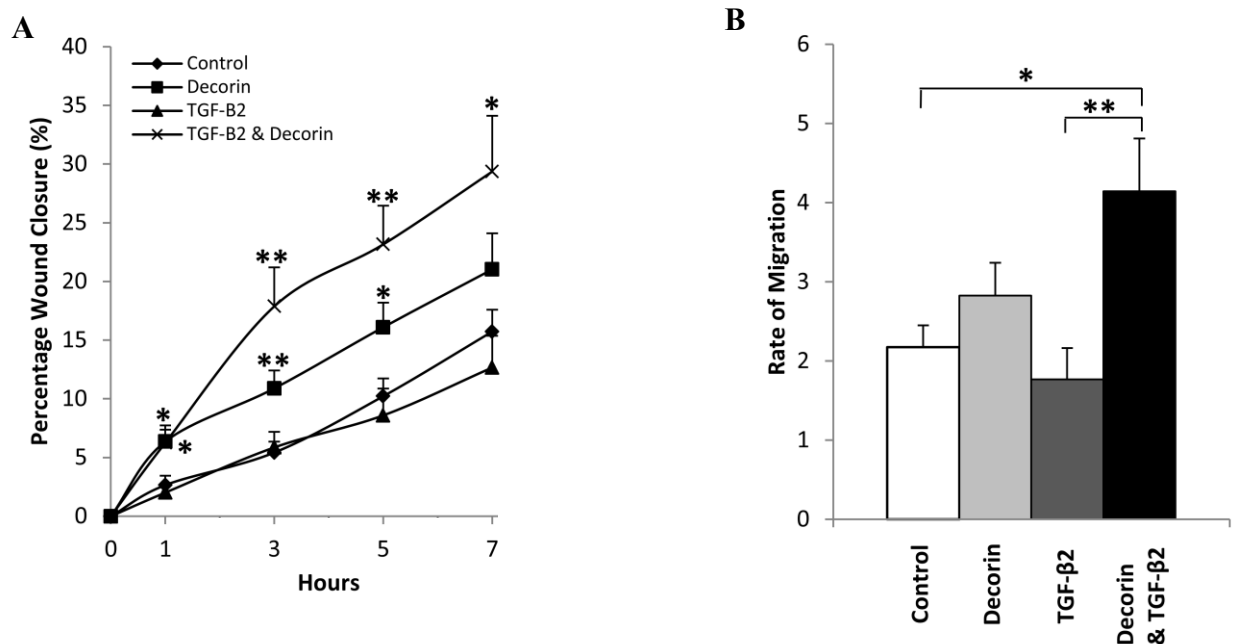


Figure 5.1 Decorin & TGF- β 2 enhance C2C12 myoblast migration. (A) Percentage wound closure of cells in response to decorin (10 $\mu\text{g/ml}$), TGF- β 2 (10 ng/ml), and decorin & TGF- β 2. Growth media containing 10% foetal calf serum served as the control. Cells were analyzed at 0, 1, 5 & 7 hours. Decorin and TGF- β 2 in combination significantly increased the percentage wound closure compared to the control at 7 hours post-injury. (B) Decorin and TGF- β 2 in combination significantly increased the rate of migration compared to TGF- β 2 and control. * $p < 0.05$, ** $p < 0.005$, $n=3$. All data shown as Mean \pm S.E.M.

In human skeletal myoblasts, TGF- β 2 significantly ($p < 0.032$) reduced the wound closure at 7 hours post-wounding, to almost half of what was achieved in the absence of the growth factor (15% and 31%, respectively). In real terms, this difference amounted to 16.06% of the wound area (Figure 5.2i). Decorin ($33.67 \pm 3.84\%$) had no significant effect on the percentage wound closure which was consistent with the C2C12 data at 7 hours (Figure 5.1A). Decorin & TGF- β 2 in combination increased the percentage wound closure at the 5 hour time point ($55.71 \pm 9.56\%$). The improvement was approximately of 14% better compared with control and 23% compared with TGF- β 2. At 7 hours post-wounding the increase in percentage wound closure in response to decorin & TGF- β 2 was even greater when compared to the control (increase of 25%), decorin (increase of 22%), and TGF- β 2 (increase of 41%) (Figure 5.2i). The rate of migration decreased significantly ($2.19 \pm 0.85\%/hr$, $p < 0.035$) when treated with TGF- β 2 compared to control and increased significantly with the combination treatment, TGF- β 2 & decorin ($8.09 \pm 1.38\%/hr$) compared to control ($4.41 \pm 0.42\%/hr$, $p < 0.032$) (Figure 5.2ii). This difference was even greater when comparing TGF- β 2 ($2.19 \pm 0.85\%/hr$) with TGF- β 2 & decorin ($8.10 \pm 1.38\%/hr$, $p < 0.015$).

Analysis of vinculin and ROCK-2 localization and expression revealed no differences in intensity and localization of ROCK-2 in myoblasts incubated with TGF- β 2 and/or decorin where compared with control. However, an increase in vinculin intensity and distribution within the cell could be seen in response to TGF- β 2, in the presence or absence of decorin (Figure 5.2iii).

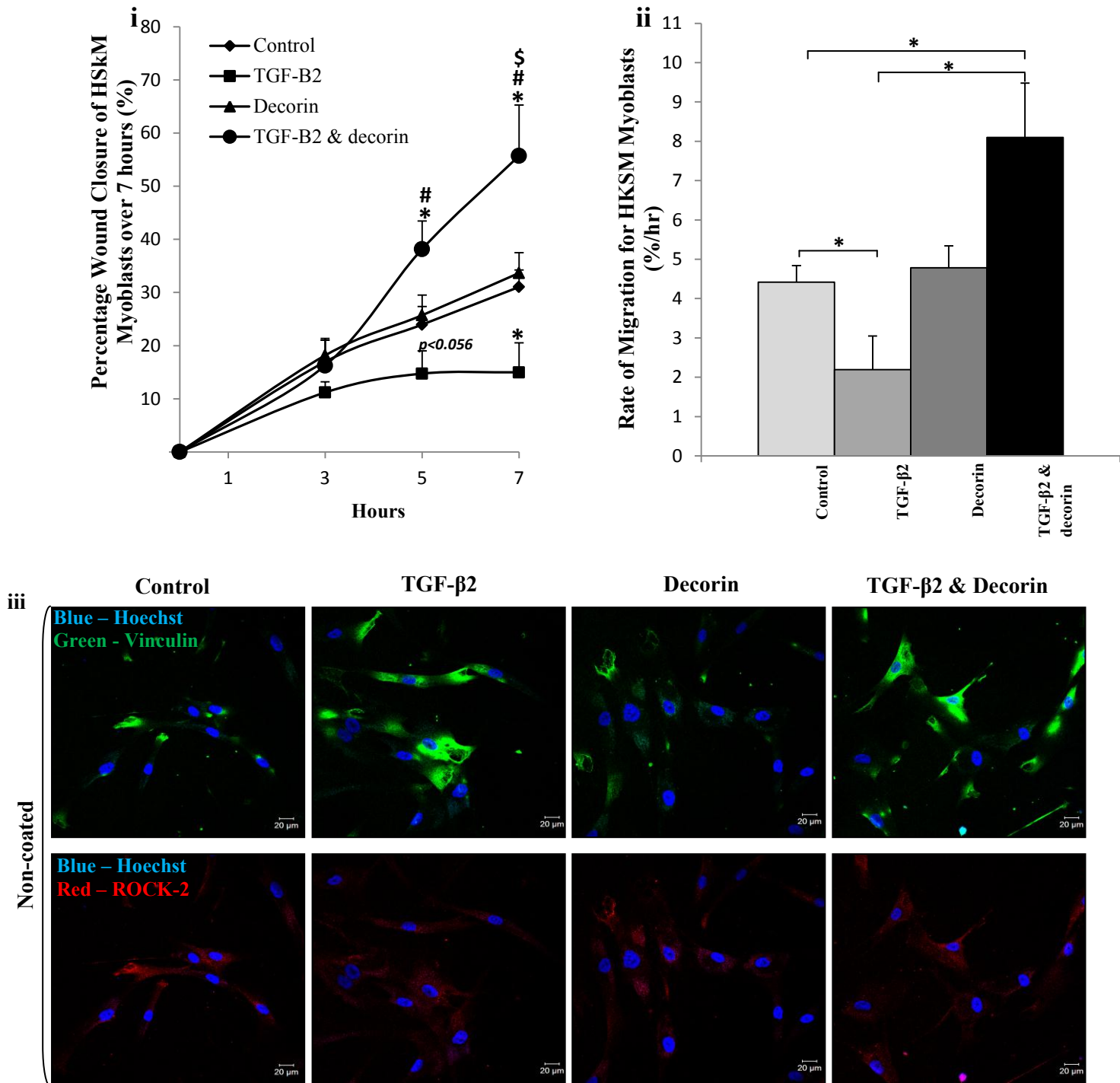


Figure 5.2 Decorin and TGF-β2 in combination promote the migration of HSKM myoblasts. i) Percentage wound closure at 0, 3, 5 & 7 hours for decorin (10 μg/ml), TGF-β2 (10 ng/ml). Growth media containing 10% fetal calf serum served as the control. **ii)** Rate of migration. **iii)** Expression of vinculin, (green) ROCK-2 (red), and nuclei (blue). Cells were fixed at 7 hours post-wounding utilizing the scratch assay. * $p < 0.05$ compared to control, # $p < 0.05$ compared to TGF-β2, \$ $p < 0.05$ compared to decorin. $n = 4$. All data shown as Mean \pm S.E.M. Scale Bar = 20 μm.

5.3.2 Decorin and TGF- β promote HSKM cell migration in the presence of Matrigel

To determine whether *basal lamina* ECM components modulate the effect of decorin and TGF- β on HSKM myoblasts we cultured cells on Matrigel (to mimic the *basal lamina* which consists primarily of collagen IV and laminin) (Roberts *et al.*, 1992).

Percentage wound closure of myoblasts on Matrigel-coated plates was decreased by 14% in the response to TGF- β 2 ($26.88 \pm 4.89\%$) when compared to Matrigel control ($40.68 \pm 5.30\%$, $p < 0.056$) at 7 hours post-wounding. In response to both decorin + TGF- β 2, human myoblasts migrating on Matrigel significantly increased migration at 7 hours by 8% to 49% compared to control ($p < 0.016$) (Figure 5.3i). TGF- β 2 significantly decreased the rate of migration ($3.83 \pm 0.66\%/hr$, $p < 0.031$), however when decorin was added in combination with TGF- β 2 to cells on Matrigel, a significant increase (6.95 ± 0.74 , $p < 0.013$) in the rate of migration was observed (Figure 5.3ii). No specific focal adhesion sites could be identified despite clear expression of vinculin. In addition, no distinct differences were observed for ROCK-2 expression and localization in cells cultured on Matrigel and treated with TGF- β 2 and/or decorin (Figure 5.3iii). However, an increase in vinculin expression levels was observed in cells on Matrigel when treated with TGF- β 2 (in the presence or absence of decorin) compared to the Matrigel control (Figure 5.2iii).

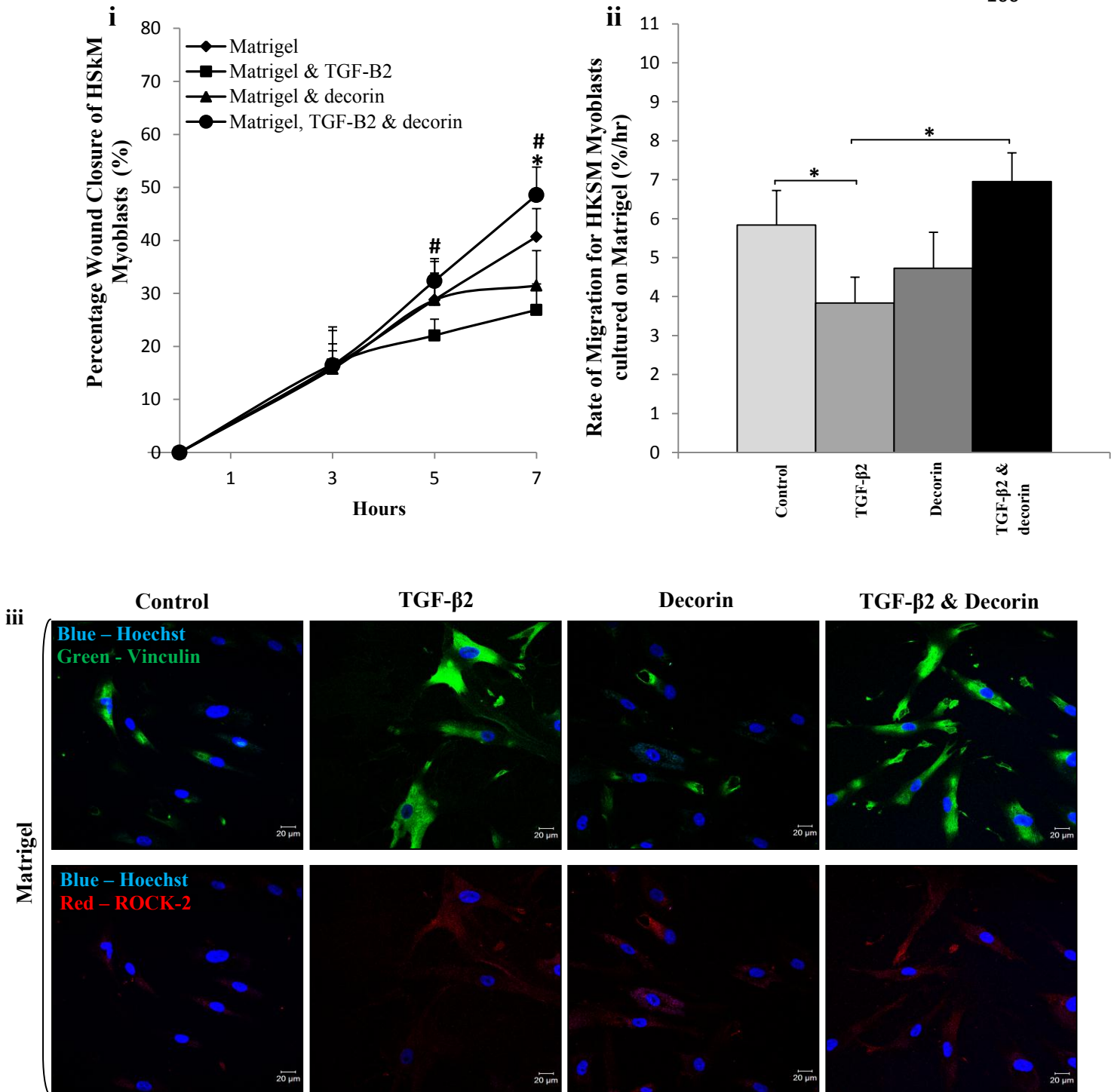


Figure 5.3 Decorin and TGF-β2 in combination promote the migration of HSKM myoblasts on Matrigel-coated plates. **i**) Percentage wound closure at 0, 3, 5 & 7 hours for decorin (10 μg/ml), TGF-β2 (10 ng/ml) and Matrigel (60 μg/ml). Growth media contains 10% fetal calf serum. **ii**) Rate of migration. **iii**) Fluorescent labeling for vinculin (green), ROCK-2 (red), and nuclei (blue). Cells were fixed at 7 hours post-wounding utilizing the scratch assay. * $p < 0.05$ compared to matrigel, # $p < 0.05$ compared to TGF-β2. $n = 4$. All data shown as Mean ± S.E.M. Scale Bar = 20 μm.

5.3.3 Decorin and TGF-β promote HSKM cell migration in the presence of collagen I, but not fibronectin

In the presence of collagen I, TGF- β did not decrease the percentage wound closure ($40.42 \pm 5.28\%$) or the rate of migration ($5.75 \pm 0.75\%/hr$) compared to the collagen I control ($42.27 \pm 3.83\%$ and $6.08 \pm 0.50\%/hr$, respectively) (Figure 5.4i & ii). However, the addition of TGF- β 2 + decorin to cells migrating on collagen I significantly ($66.28 \pm 7.20\%$, $p < 0.016$) increased the percentage wound closure by 26% (7 hours) compared to collagen I with ($40.42 \pm 5.28\%$) or without ($42.27 \pm 3.83\%$) the addition of TGF- β 2. The rate of migration of myoblasts in response to TGF- β 2 + decorin + collagen I ($9.23 \pm 0.97\%/hr$) was significantly increased compared to collagen I ($6.08 \pm 0.50\%/hr$) and TGF- β 2-treated collagen I ($5.75 \pm 0.75\%/hr$). A significant increase was also observed when cells cultured on collagen I were treated with decorin ($7.66 \pm 0.77\%/hr$), compared to collagen I (Figure 5.4ii). An increase in the localization and intensity of vinculin expression following TGF- β 2 treatment was observed when compared to cells cultured on collagen I alone. No difference in ROCK-2 localization or intensity was apparent following either TGF- β 2 or decorin incubation in the presence of collagen I (Figure 5.4iii).

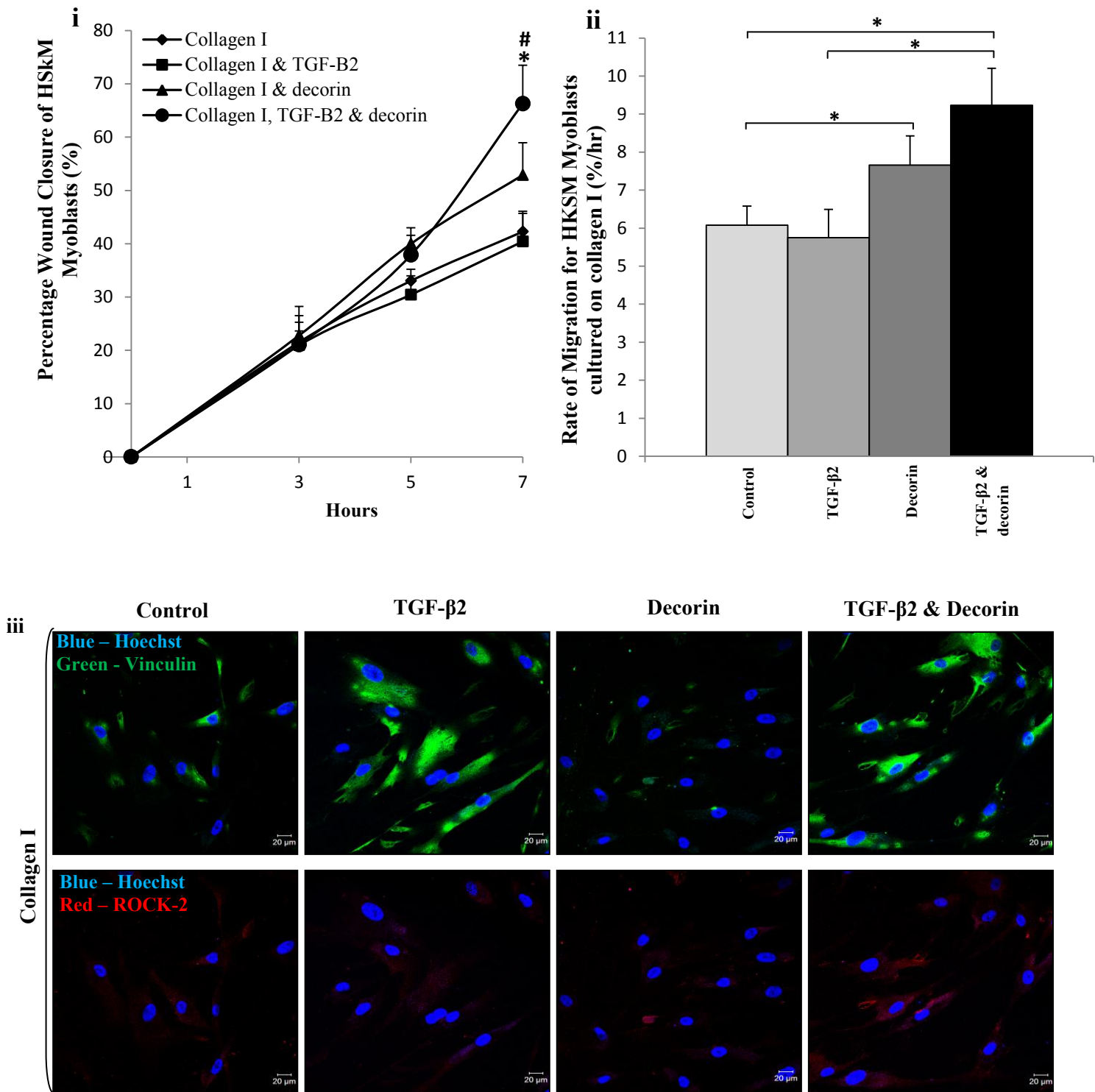


Figure 5.4 Decorin and TGF-β2 in combination promote the migration of HSKM myoblasts on collagen I-coated plates. i) Percentage wound closure at 0, 3, 5 & 7 hours for decorin (10μg/ml), TGF-β2 (10ng/ml) and collagen I (25μg/ml). Growth media contains 10% fetal calf serum. ii) Rate of migration. iii) Expression and localization of vinculin (green), ROCK-2 (red), and nuclei (blue). Cells were fixed at 7 hours post-wounding utilizing the scratch assay. * $p < 0.05$ compared to collagen I, # $p < 0.05$ compared to TGF-β2. n=4. All data shown as Mean ± S.E.M. Scale Bar = 20μm.

In the presence of fibronectin, TGF- β 2 significantly ($32.29 \pm 2.73\%$, $p < 0.016$) decreased the percentage wound closure compared to fibronectin ($46.86 \pm 5.34\%$) by 15% at 7 hours post-injury (Figure 5.5i). However, decorin & TGF- β 2 ($46.47 \pm 7.48\%$) were not able to significantly increase the percentage wound closure compared to fibronectin alone ($46.86 \pm 5.34\%$), or even fibronectin treated with TGF- β 2 ($32.29 \pm 2.73\%$) (Figure 5.5i & ii). Only a minor increase of 0.39% (TGF- β 2 + decorin) for the percentage wound closure was observed. The rate of migration results also did not show any significant change when comparing the treatment and control groups (Figure 5.5ii).

Immuno-fluorescent labeling for vinculin revealed an increase in intensity and localization within TGF- β 2 treatment groups (\pm decorin addition) which is consistent with matrigel and collagen I findings (Figure 5.5iii). An increase in intensity of vinculin staining in cells treated with fibronectin and decorin was also observed compared to fibronectin alone which differed from the other matrix factors. ROCK-2 expression levels appeared to be higher when TGF- β 2 or decorin was present compared to the fibronectin control (Figure 5.5iii).

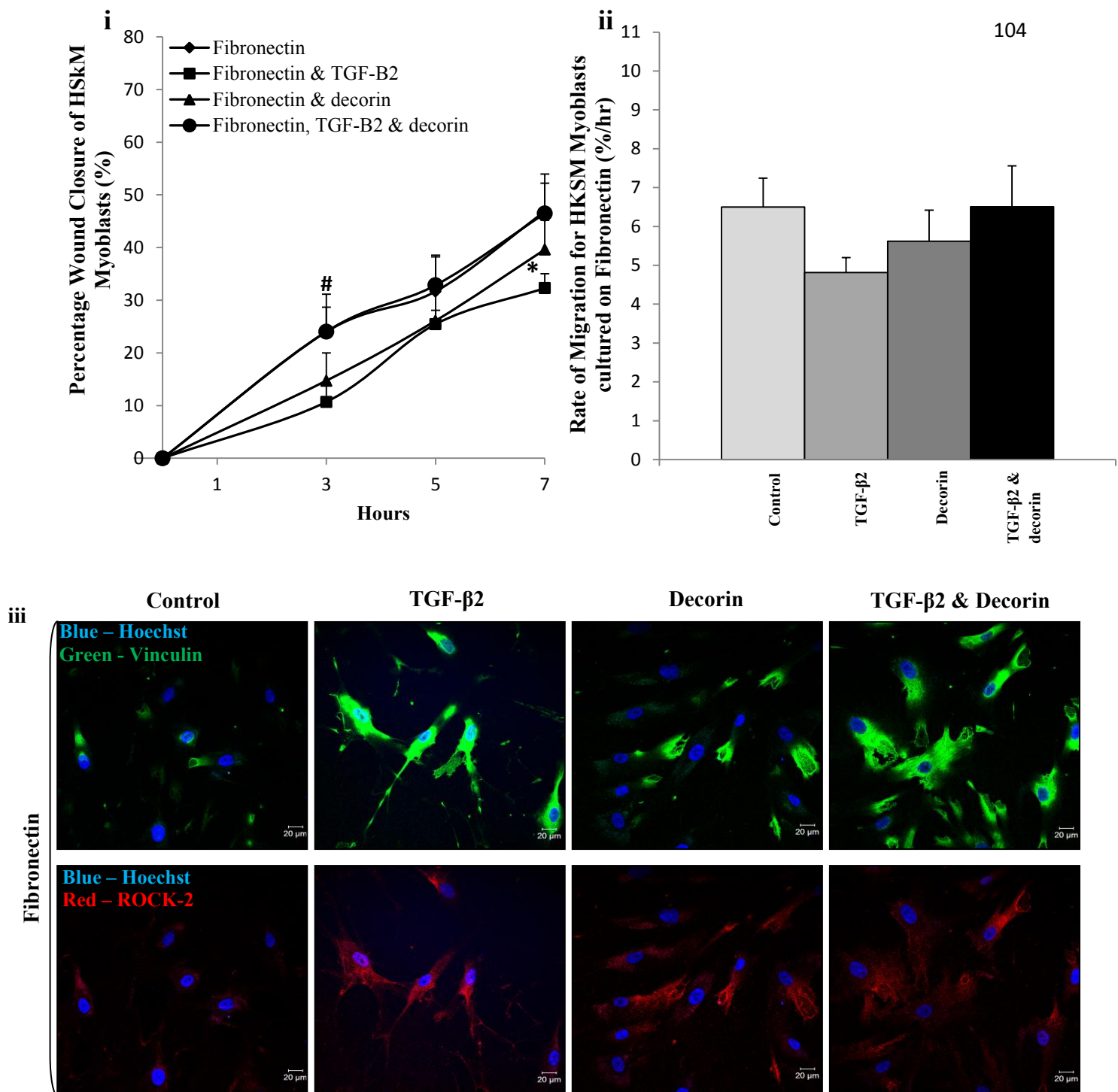


Figure 5.5 Decorin and TGF-β2 in combination do not promote the migration of HSKM myoblasts on fibronectin-coated plates. i) Percentage wound closure at 0, 3, 5 & 7 hours for decorin (10μg/ml), TGF-β2 (10ng/ml) and fibronectin (5μg/ml). Growth media contains 10% fetal calf serum. **ii)** Rate of migration. **iii)** Expression of vinculin (green), ROCK-2 (red), and nuclei (blue). Cells were fixed at 7 hours post-wounding utilizing the scratch assay. * $p < 0.05$ compared to fibronectin, # $p < 0.05$ compared to TGF-β2. n=4. All data shown as Mean ± S.E.M. Scale Bar = 20μm.

5.3 DISCUSSION

Decorin is known to act as an anti-fibrotic and pro-myogenic agent in skeletal muscle (Fukushima *et al.*, 2001; Droguett *et al.*, 2006; Miura *et al.*, 2006; Zhu *et al.*, 2007; Brandan *et al.*, 2008; Kishioka *et al.*, 2008). *In vivo* studies, where decorin was injected directly into lacerated muscle, revealed that this proteoglycan could promote the complete regeneration of the injured murine skeletal muscle with minimal fibrotic scar tissue formation (Fukushima *et al.*, 2001; Fukushima *et al.*, 2006). This effect may be due to its modulation of collagen fibrillogenesis and its ability to reduce myofibroblast proliferation *in vitro* (Fukushima *et al.*, 2001; Fukushima *et al.*, 2006). However, decorin is able to bind members of the TGF- β super-family, such as TGF- β 1, 2, 3 and myostatin, thereby antagonizing their activities and acting as an antifibrotic agent (Verrecchia and Mauviel 2007; Cabello-Verrugio *et al.*, 2012). In this way decorin would indirectly enhance muscle regeneration.

This study provides evidence that the interaction between decorin and TGF- β 2 can have a direct effect on myoblast migration. Specifically, in the presence of decorin, TGF- β 2 was shown to promote myoblast migration and could in this way positively influence skeletal muscle regeneration. A critical observation is that the addition of decorin to TGF- β 2 (in the presence or absence of Matrigel, collagen I or fibronectin) resulted in a significant increase in migration (compared to treatment with TGF- β 2 alone). This is *despite* the fact that treatment with decorin did not have a significant effect in increasing migration rates, and TGF- β 2 was predominantly anti-migratory, decreasing migration rates.

A possible explanation for this phenomenon involves mechanisms that attenuate TGF- β -dependent signaling. This could occur in part via a reduction in TGF- β bioavailability due to the presence of decorin, limiting its access to specific receptors and resulting in a diminished cellular response (Droguett *et al.*, 2006). However, the increase in migration suggests the activation of either alternate pathways or changes in signaling behavior caused by the TGF- β /decorin complex binding to TGF- β and decorin receptors. The TGF- β /decorin complex has been shown by others to result in a greater biological activity compared with the growth factor alone (Riquelme *et al.*, 2001). This supports the premise that a specific response is being induced due to the biological constellation (i.e. the TGF- β /decorin complex), which is now presented to TGF- β or decorin signaling receptors (Schonherr *et al.*, 2001). Within this study we suggest that not only is the binding of TGF-

β -to decorin acting as a TGF- β antagonist, but the subsequent complex enhances myoblast migration by altering the interaction with cell surface receptors.

TGF- β is present during skeletal muscle formation and regeneration. Therefore it is not surprising that mechanisms controlling bio-availability to regulate the modulatory effect TGF- β on myogenesis evolved. Interestingly, in the presence of fibronectin, TGF- β 2 plus decorin were not able to significantly increase the migration rate compared with either TGF- β 2, decorin or the untreated fibronectin control. A possible explanation for this is the binding of TGF- β to the latent TGF- β binding protein (LTBP-1). LTBP-1 has been shown to co-localize and physically interact with fibronectin (Schlotzer-Schrehardt *et al.*, 2000; Kottler *et al.*, 2005). Therefore, fibronectin may sequester TGF- β via LTBP-1 and reduce the effect of both TGF- β 2 and the TGF- β /decorin complex by reducing its bio-availability. However, localization of the TGF- β /decorin complex to different areas within the ECM during wound repair may have an inhibitory effect or result in greater biological activity (Schonherr *et al.*, 2001). Independent binding sites of decorin for collagen I and TGF- β exist, allowing decorin to simultaneously bind collagen I and TGF- β (Schonherr *et al.*, 1998). Furthermore, decorin bound to collagen I via its core protein has the ability to sequester TGF- β (Markmann *et al.*, 2000). Downstream effects of temporary decorin-induced sequestering of TGF- β within the ECM, was suggested in 1998 by Schonherr to be a result of modulating the interaction of TGF- β with its signaling receptors (Schonherr *et al.*, 1998). Since then the responses of signaling pathways, gene expression and associated protein synthesis have been studied in various contexts.

TGF- β affects integrin-mediated cell adhesion and migration by regulating the expression of integrins, their ligands and integrin-associated proteins (Margadant and Sonnenberg 2010). In a study utilizing human peritoneal fibroblasts, TGF- β 1 facilitated vinculin expression and localization, primarily to the focal adhesion contacts of the cells, which caused distortion of F-actin structure. TGF- β may promote adhesion formation by altering expression levels and patterns of specific integrin subunits, vinculin, and F-actin (Rout *et al.*, 2002). The increased expression of vinculin upon TGF- β addition was apparent within our findings. However, there appeared to be no direct correlation between TGF- β and vinculin localization within migrating myoblasts.

Another interesting observation was the delayed onset of the TGF- β /decorin complex effect in HSKM myoblasts compared to C2C12 myoblasts, which did not display a delay

in the percentage wound closure. This would seem to point to a signaling effect and a “wait” for the protein that is having the effect to be expressed, which differs in murine and human skeletal muscle.

In summary, in this study we demonstrate a unique mechanism for increased muscle regeneration (through increased migration rates) via the regulation of TGF- β signaling. We propose that the interaction of decorin with TGF- β 2 alters the signaling effects by forming the TGF- β /decorin complex, which can either sequester or promote alternate signaling pathways. Investigations into the mechanistic process causing this effect are underway.

CHAPTER 6

3D SKELETAL MUSCLE TISSUE DEVELOPMENT & FUTURE WORK

6.1 INTRODUCTION

The ability of cells to migrate within an extracellular matrix depends on the physical and biochemical characteristics of the particular matrix as well as on the properties of the migrating cells. Analysing changes in migration patterns within different matrices is vital for our understanding of how mobility and homing is influenced by physiological and pathological conditions. *In vivo*, cells migrate through different types of extracellular matrix: dense connective tissue, loose connective tissue or basement membrane tightly packed as an acellular layer (Wang *et al.*, 2012). The different environments affect the ability of a cell to migrate, its mode of migration and its directionality. Mesenchymal cell migration is triggered in response to either mechanical or biochemical cues and is characterised by the following steps: extension of the leading edge, cellular attachment to the ECM, maturation of adhesions, advancement of the cellular body, and release of the rear adhesions (Cukierman *et al.*, 2001; Modulevsky *et al.*, 2012).

Although direct experimentation *in vivo* would be favourable, it is necessary to isolate and define the specific contribution of single factors to migration in order to understand the overall process; therefore *in vitro* models are indispensable. The mechanism and regulation of cell migration has been studied extensively in 2-dimensional models. However, discrepancies between cell behaviour in *in vitro* versus *in vivo* have led many research groups to develop 3D models in order to better mimic the natural micro-environment (Even-Ram and Yamada 2005).

3-Dimensional models have obvious advantages over 2-dimensional cultures in mimicking *in vivo* conditions, such as allowing for the study of dimensionality, cellular architecture and cell polarity. However, the complexity and diversity of *in vivo* ECM organisation is difficult to mimic *in vitro*. Although collagens contribute the major component of the ECM, other components are also important (Friedl *et al.*, 1998).

Several different types of gel constructs have been utilized to achieve a desired ECM architecture *in vitro*. Important characteristics of these constructs include molecular composition and concentration, macromolecular orientation, and the degree of cross-linking (Even-Ram and Yamada 2005). Collagen and laminin are able to polymerize and spontaneously form 3D gels, whereas fibronectin fibrillogenesis is an active, cell-dependent process involving integrin translocation to facilitate polymerization (Pankov *et al.*, 2000). Nonetheless, fibronectin is an important component since it promotes fibroblast migration in 3D matrices and the addition of fibronectin to collagen I substrates has been shown to enhance the migration of these cells (Cukierman *et al.*, 2001).

In vitro preparations of collagen are limited by the maximal concentration of the stock solution (3-5 mg/ml). Yet the *in vivo* concentration of the epidermis is nearly 140 mg/ml collagen in wet weight and is nearly 100 times higher than what can be utilized within the *in vitro* model (Robins *et al.*, 2000). The tumor basement membrane extract (Matrigel) produced by Engelbrecht-Holm-Swarm sarcoma cells, which is used to mimic the *in vivo* basement membrane, differs from normal basement membranes *in vivo*. It is significantly less cross-linked and is therefore more susceptible to proteolysis, remodelling and turnover. However, Matrigel can promote 3D tissue organization and is often added with collagen I to form 3D gel constructs (Kalluri 2003). Fibrin gels are also commonly used for the study of mesenchymal cell migration studies. Thrombin cleavage of fibrinogen generates fibrin, which assembles into a tight meshwork of fibers; cells must therefore be able to degrade the ECM in order to migrate through the gel. Within our study we have focused on several different types of gel constructs and assessed how they affect skeletal muscle tissue development.

6.2 EXPERIMENTAL PROCEDURES

6.2.1 General

All chemicals used were of an analytical grade and were purchased from either Sigma or Merck unless otherwise stipulated. All cell culturing was carried out under sterile conditions in a level II lamina flow hood (ESCO class II BSC) and incubated in a CO₂ incubator (Innova CO-170) at 37°C, 5% CO₂. Brightfield images were captured using the Motic 3.0 MP camera on the Olympus CKX41 microscope. The Zeiss 710 confocal microscope was utilized for all fluorescence microscopy.

6.2.2 Cell Culture

The C2C12 cell line was donated by the Cape Heart Center, University of Cape Town. Primary cultured human skeletal myoblasts (HSKM) were purchased from Lonza. Growth media contained Dulbecco's Modified Eagle Serum (DMEM) (Highveld, cat.CN3193-9), L-glutamine (2% v/v) (Cambrex, cat.17-605E), PenStrep (2% v/v) (Cambrex, cat.17-602E), fetal calf serum (10% v/v) (Invitrogen, cat.10108165). Differentiation media contained DMEM, L-glutamine (2% v/v), PenStrep (2% v/v) and horse serum (HS; 1% v/v) (Invitrogen cat.16050-130). Human culture media contained HAMS-F10 (Gibco, cat.15140), FCS (20% v/v), Pentrep (2% v/v), L-glutamine (2% v/v), fibroblast growth factor (FGF, 2.5 ng/ml, Promega, cat.G507A).

6.2.3 MC-8 chamber

MC-8 chambers were obtained from *In vivo Sciences*. A 10% FBS solution was added to each well 30 minutes prior to the addition of the gel construct and incubated at 37 °C. This created a favourable condition of cell attachment on the stainless steel pins. 225 µl cell/gel solution was added per MC-8 cell (for details on each gel construct refer to *Section 6.2.5 – 6.2.8*). MC-8 chamber sterility was maintained by keeping the chambers within 10 cm culture dishes. Either growth media or differentiation media was added directly after seeding on experimental application.

6.2.4 Silicone chamber

Biological grade silicone tubing was utilized for all the silicone models. The tubing was cut to fit a well within a 24-well plate. The stainless steel pins were cut and inserted into the silicone tubing to achieve a distance of 8 mm between pins. The tubes containing the pin inserts were glued within the wells with SYLGARD 182 (Figure 6.1). The plates were cured overnight under an ultraviolet light to maintain sterile conditions. A 10% FBS solution was added to each well 30 minutes prior to the addition of the gel construct and incubated at 37 °C. This created a favourable condition for cell attachment on the stainless steel pins.

6.2.5 Collagen I Gel Construct

Calf skin collagen I (Sigma, cat. C9791) was dissolved in 0.1% acetic acid to give a final concentration of 5 mg/ml. A 280 µl volume of collagen I (5 mg/ml) was neutralized with 11.2 µl of a 2% NaOH solution. A 5X DMEM solution (72.8 µl) and a cell suspension (730 µl) containing 800 000 cells were added to the collagen I solution prior to plating within the MC-8 chamber or silicone tubes. The gel/cell suspension polymerized after a 20 minute incubation period at 37 °C. A 350 µl volume of growth media was added to each well after complete polymerization had occurred.

6.2.6 Collagen I/Matrigel Construct

Calf skin collagen I was dissolved in 0.1% acetic acid to give a collagen I concentration of 2 mg/ml. 10X DMEM, reconstitution buffer (50 ml distilled water, 1.1 g sodium bicarbonate, and 2.4 g HEPES), and collagen I solution (2 mg/ml) were added at a ratio of 1:1:12 (i.e. 167 µl 10X DMEM, 167 µl reconstitution buffer, and 2 ml collagen I). The solution was neutralized by 10% NaOH (30 µl). A cell suspension (120 µl) containing 800 000 cells was added to the collagen I solution along with 20 µl Matrigel (10.1 mg/ml, BD Biosciences, cat.356231). The subsequent cell/gel suspension was plated into either MC-8 chamber wells or silicone tubes and incubated at 37 °C for 20 minutes to allow for complete gel polymerization to occur. Following complete polymerization the wells were supplemented with 350 µl growth media.

6.2.7 Fibrin Gel Construct

A 20 μ l thrombin (10 Units, Sigma, cat. T4648) solution was added to 180 μ l growth media containing 800 000 myoblasts (determined by cell count) per MC-8 chamber well or per silicone tube. Gel polymerization occurred ~10 minutes after the addition of 80 μ l fibrinogen (20 μ g/ml, Sigma, cat.F8630) and incubation at 37 °C. The fibrin gel/cell suspension was supplemented with 350 μ l growth media every 24 hours.

6.2.8 Hydrogel Construct

For the hydrogel construct, QGel (QGelSA, ref.1001) was utilized. We used the soft I and soft III gel constructs were used. The QGel powder was resuspended in 400 μ l PBS buffer. 200 μ l QGel solution and 50 μ l cell suspension containing 500 000 cells were added per silicone tube for the soft III gel construct. For the soft I gel construct, 200 μ l QGel solution, 80 μ l PBS buffer, and 70 μ l cell suspension containing 500 000 cells were added per silicone tube. Gel polymerization occurred 5-6 minutes after incubation at 37 °C. Growth media (500 μ l) was added per well following gel polymerization.

6.3 RESULTS

6.3.1 Development of an *in vitro* 3-Dimensional Skeletal Muscle Tissue Model

To develop a 3D model of skeletal muscle *in vitro*, we resuspended myoblasts in a variety of gel constructs within both a commercially available tissue chamber (MC-8, *in vivo Sciences*) as well as a silicone chamber constructed within our lab (Figure 6.1).

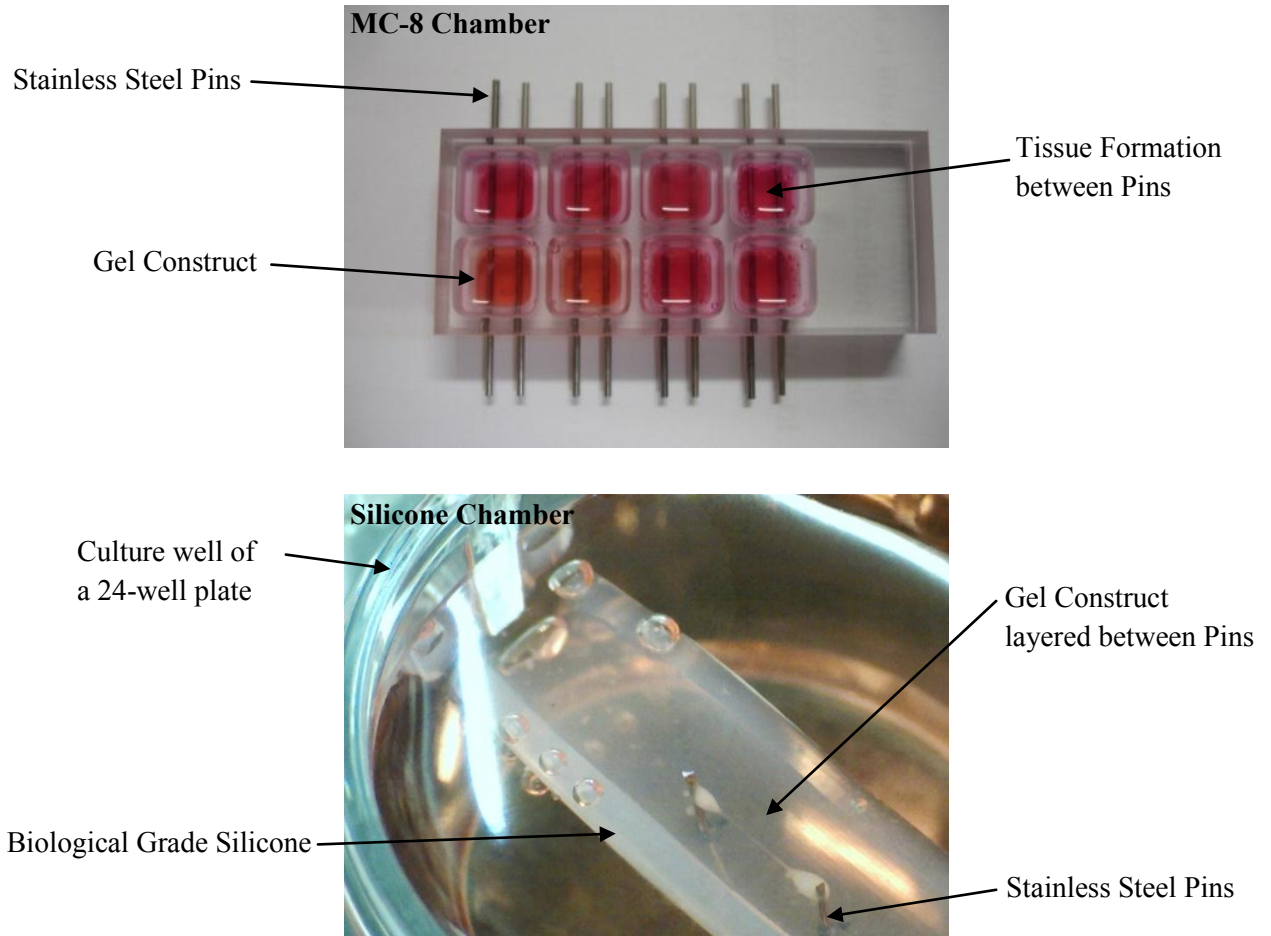


Figure 6.1 MC-8 and customized silicone chamber for the development of *in vitro* 3D skeletal muscle. MC-8 chambers were purchased from *in vivo Sciences*. Silicone chambers were created within our laboratory. For detailed information on both models and tissue constructs utilized within these models see section 6.2 *Experimental Procedures*.

Four different gel constructs (Collagen I, Matrigel/collagen I, fibrin, and hydrogel) were used within the MC-8 and silicone chambers with cell number, cell type and media variations to optimize skeletal muscle tissue development between the two anchor points. Attachment of the gel construct to the pins and tissue formation spanning the two anchor points were both assessed (Table 6.1). Better attachment of the myoblasts to the pins was seen within the silicone chamber compared to the MC-8 chamber for the collagen I/Matrigel, collagen I and fibrin gel constructs (Table 6.1). Tissue formation between the two anchor points was only achieved with the silicone chamber utilizing the collagen I construct for both murine C2C12 and human myoblasts (HSKM).

The media did not appear to play a direct role in the initial attachment and spanning between the pins. However, continued use of the differentiation media (DM) resulted in sustained spanning of the tissue between the pins (Table 6.1). The fibrin construct presented numerous difficulties as the addition of the thrombin to the fibrinogen caused the gel to set very rapidly, not giving the cells enough time to spread evenly throughout the gel. The hydrogel construct did not result in any tissue formation; this was primarily due to low viscosity levels which prevented the cells from being held in suspension.

Table 6.1: Optimization of 3D construct model within two different chamber systems

Gel Construct	Chamber	Cell Number	Media	Successful Pin Attachment	Tissue Formation
Collagen I / Matrigel	MC-8,	1.6 million (C2C12)	DM,	MC-8, Silicone	Tissue clumping around pins
	Silicone	800 000 (C2C12)	GM,	All cell numbers tested	No tissue formation across pins
		1.3 million (HSKM)	SkGM	All media tested	
		800 000 (HSKM)			
Collagen I	MC-8,	1.6 million (C2C12)	DM,	MC-8, Silicone	MC-8 tissue clumping around pins and within gel
	Silicone	800 000 (C2C12)	GM,	All cell numbers tested	Silicone – tissue formation across pins for 800 000 C2C12 with GM or DM media.
		1.3 million (HSKM)	SkGM	All media tested	
		800 000 (HSKM)			
Fibrin	MC-8,	1.6 million (C2C12)	DM, GM	MC-8	MC-8 tissue formation around pins
	Silicone	800 000 (C2C12)		All cell numbers tested	Silicone – less tissue formation and no attachment to pins
					All media tested
Hydrogel (QGel)	Silicone	800 000 HSKM cells	SkGM	No attachment	No attachment of cells to pins or tissue formation due to insufficient gel viscosity

HSKM – Human Skeletal Myoblasts, GM – Growth Media, DM – Differentiation Media, SkGM – HSKM Growth Media. For detailed information, such as gel concentrations or incubation periods see section 6.2 *Experimental Procedures*.

6.3.2 MC-8 Chamber

The MC-8 chamber did not allow for spanning of the skeletal muscle tissue between the pins, furthermore visualization of the 3-dimensional attachment and tissue formation was difficult due to the chamber design. Attachment of the cells to the MC-8 pins was achieved with the collagen I/Matrigel, collagen I and the fibrin gel constructs (Figure 6.2A). However, the pin angle resulted in the cells, especially within the collagen I/Matrigel construct, attaching and aggregating along the stainless steel pins instead of spanning the space between them. The collagen I gel construct allowed spanning of the gel construct between the pins in a sheet-like manner when utilizing 1.6 million C2C12 cells (Figure 6.2A). When analyzing the spanning of the cells within the collagen I gel construct (1.6 million C2C12 cells, 1% HS) clumping was observed instead of continuous spanning across the pins (Figure 6.2B&C, white arrows). Tube formation was observed between the clumps showing that the cells were capable of differentiation into myotubes, but not in an evenly spread manner (Figure 6.2C black arrows). The fibrin construct resulted in reduced clumping and better alignment of the myotubes in a linear formation. However, the directionality was not consistent, with myotubes aligning in different directions within the same construct (Figure 6.2D&E).

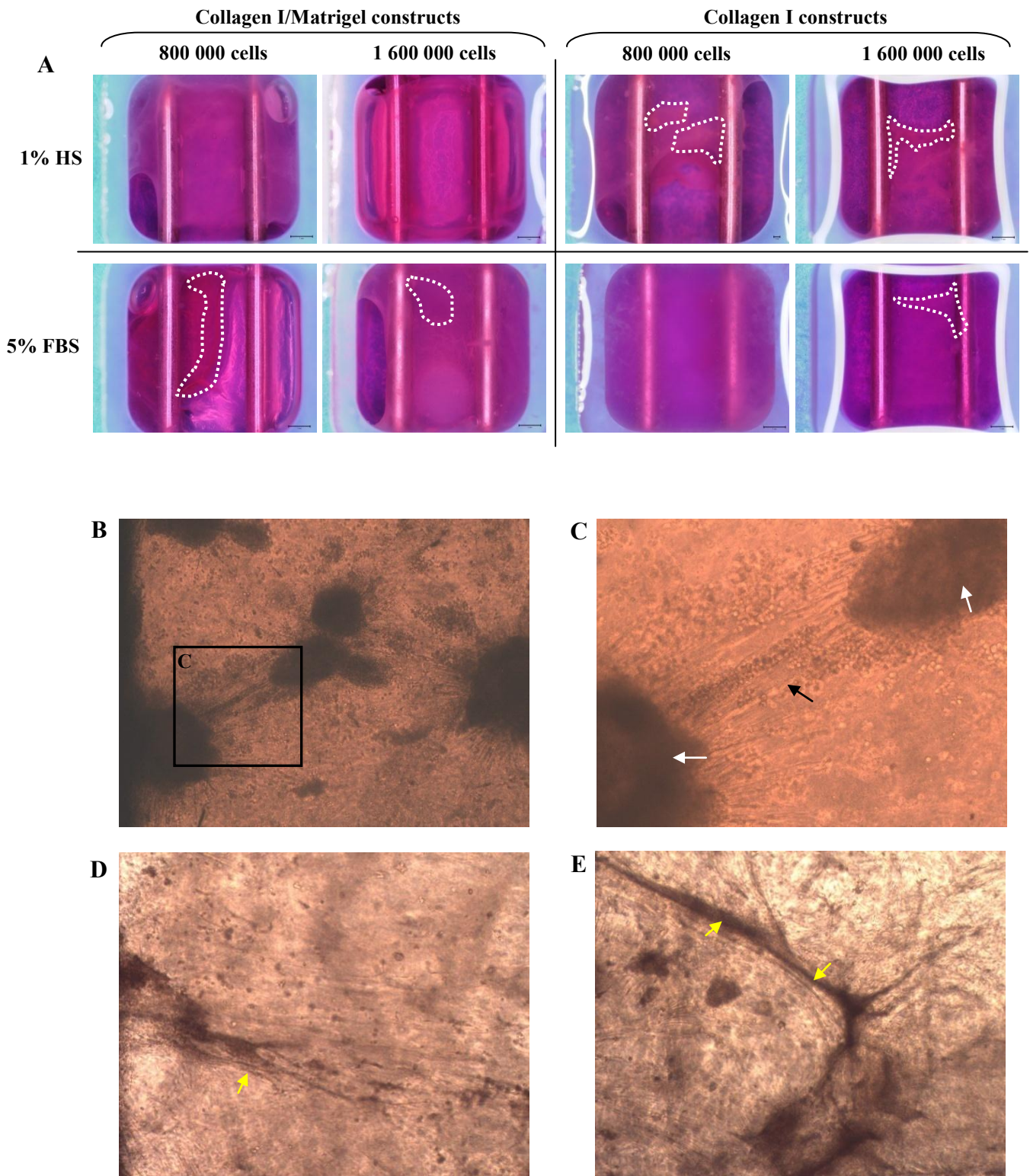


Figure 6.2 Development of a 3D *in vitro* muscle tissue model utilizing the MC-8 chamber system. A) Collagen I/Matrigel gel construct versus Collagen I gel construct within the MC-8 chamber. 800 000 and 1.6 million C2C12 cells were used within both gel constructs with either differentiation media (1 % horse serum) or growth media containing 5 % foetal calf serum. The cells were incubated within these media solutions for 3 days. Media was changed daily. Dashed lines indicate visible tissue formation. **B)** 1.6 million cells within the collagen I gel construct supplemented with 1 % HS. **C)** Magnification of black box in **B**. Myotube formation (black arrow) between cellular clumps (white arrows). **D & E)** Reduced clumping of cells (yellow arrows) within fibrin gel constructs supplemented with 1.6 million cells and 1 % HS.

6.3.3 Silicone Chamber

The use of a silicone-based model was determined by: biological grade silicone being readily available, ability to shape silicone to existing culture dishes and chambers within our laboratory, the relative ease of pin insertion, and subsequent tissue manipulation. The distance between pins published by other researchers ranged from 8-20 mm, depending on the model being used (Powell *et al.*, 2002; Huang *et al.*, 2005). We utilized 8 mm for all initial studies as this should result in tissue formation due to the close proximity of the pins. SYLGARD 182 was used as biological glue (Huang *et al.*, 2005) to seal the silicone tube into place within the 24-well plates and prevent any leaking of the gel construct before setting the gels at 37°C (Figure 6.3).

The silicone tube-based model proved to have many advantages over the MC-8 chamber for skeletal muscle formation. The vertical positioning of the pins (rather than horizontally in the MC-8 model) allowed for better attachment and anchoring of the cell/gel suspension during the setting stage at 37°C (Figure 6.4 A). Furthermore, the utilization of the collagen I gel construct resulted in the cell formation across the pins once the collagen I gel had dissipated into the media (Figure 6.4C). The fibrin and collagen I/Matrigel constructs formed clumps of cells around the pins and did not span across the pins as observed with the collagen I gel construct (*data not shown*). Successful tissue formation was achieved between the pins within the silicone tube model for both C2C12 and HSKM cells on repeated occasions (Figure 6.4 C&D).

Biological grade silicone tubing is cut to the length of the well and an opening is cut across the top of the tube.

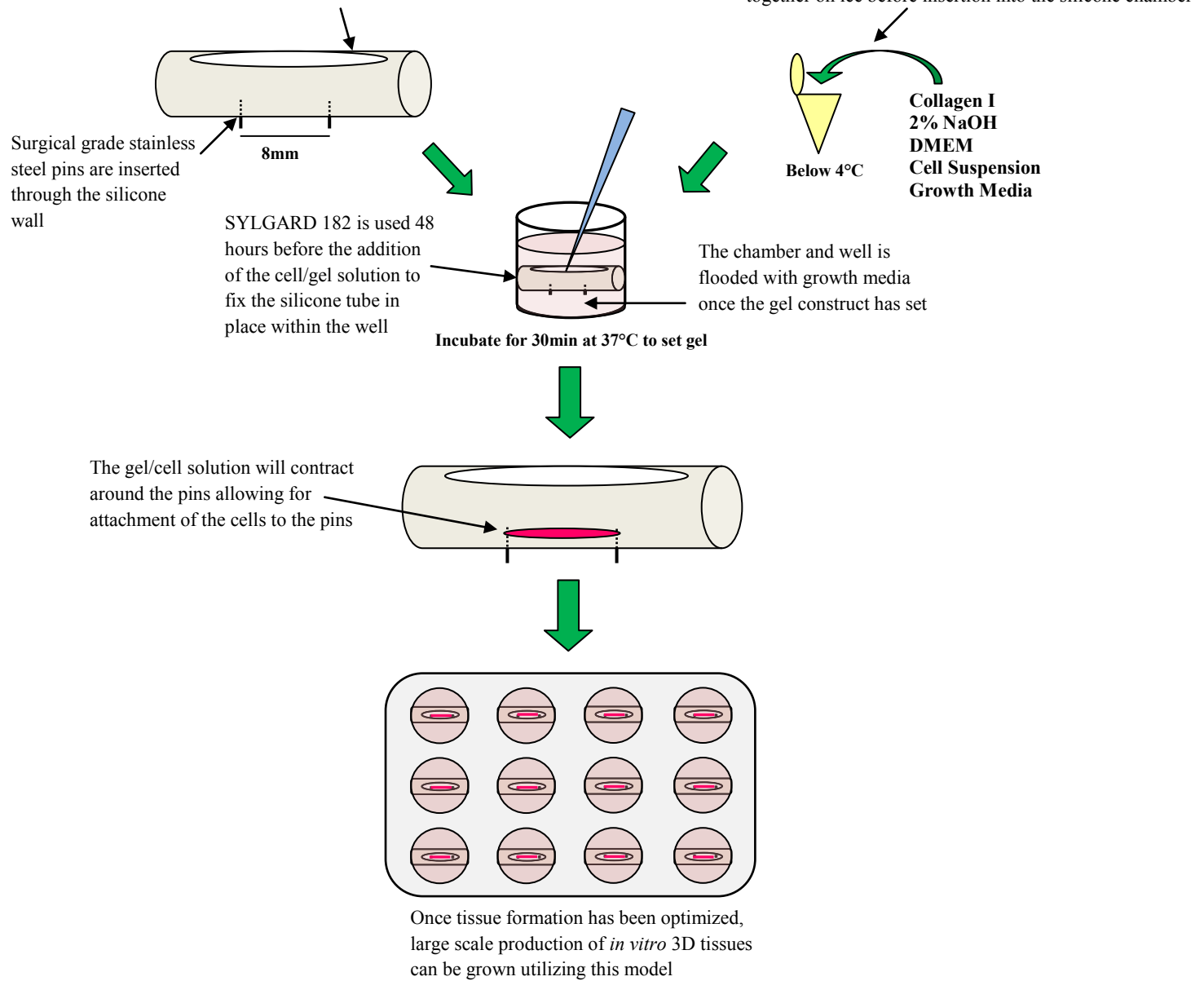


Figure 6.3 Skeletal muscle formation using a silicone tube model. This model was developed due to the lack of adaptability within other commercially available models, as well as the high expense in continually purchasing these models. Within our model, several different gel constructs can be utilized and pin diameter, pin type, pre-coating, and media exchange can all be adapted. For a detailed description on the silicone model assembly see section 6.2 *Experimental Procedures*.

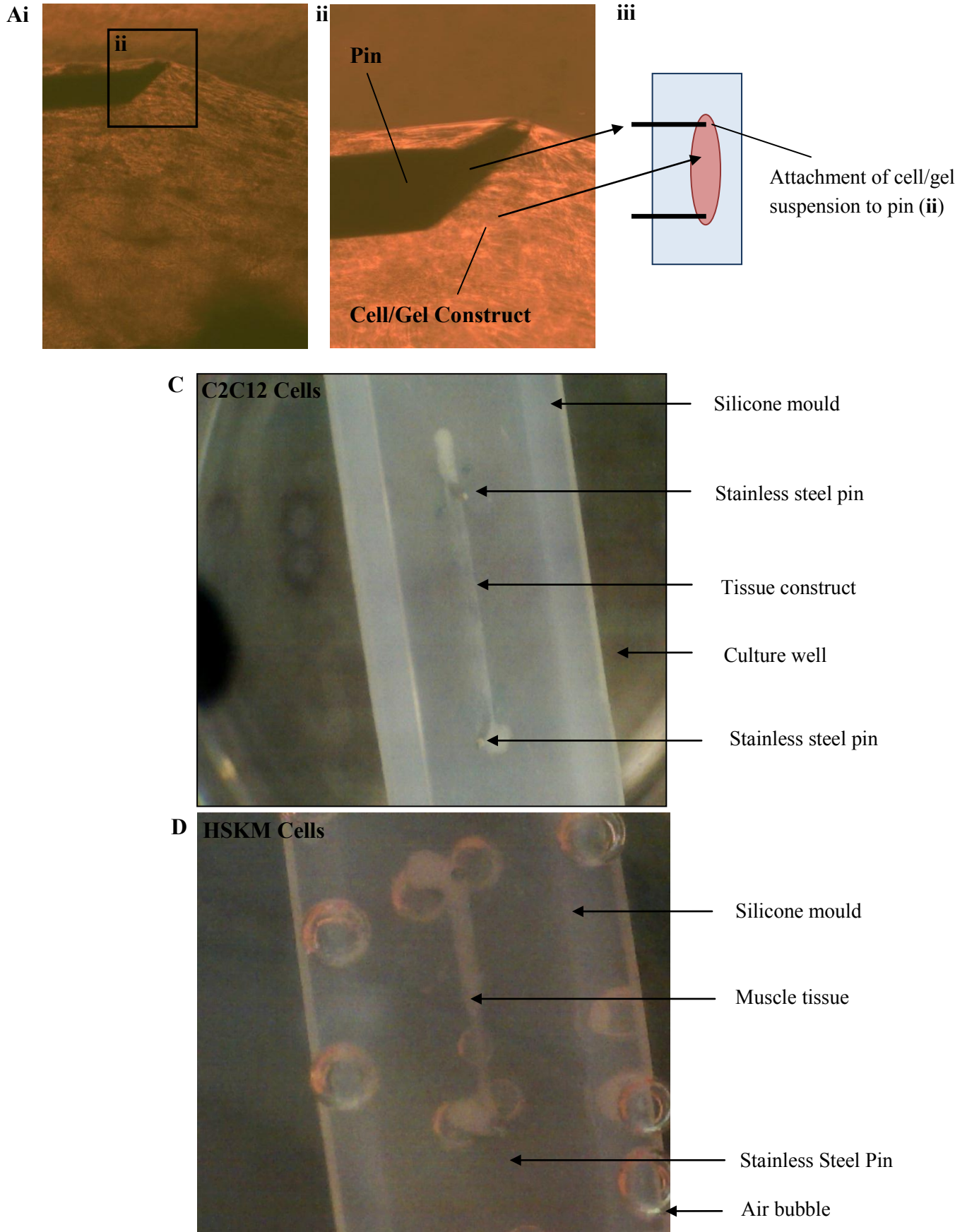


Figure 6.4 Development of a 3D in vitro muscle tissue model utilizing the silicone tube system. **Ai & ii**) Gel/cell suspension (collagen I gel) attachment to a stainless steel pin. **iii**) Orientation of pin and gel construct. **C**) Gel/cell suspension spanning between pins for C2C12 myoblasts within collagen I construct. **D**) Gel/cell suspension spanning between pins for HSKM cells within collagen I construct.

6.3.4 Conclusion

Contractile skeletal muscle tissue engineered from myoblasts has a number of potential applications, such as, therapeutic protein delivery, tissue repair, and *in vitro* drug screening (Vandenburgh 2010). In a 3-dimensional setting, naturally derived hydrogels (e.g. collagen I, Matrigel, fibrin) have been employed as a microenvironment for the growth and differentiation of skeletal myoblasts because they support: a high density and even spreading of myoblasts, positive unidirectional cell alignment, and muscle-specific tissue contractions (Hinds *et al.*, 2011). These hydrogels have been used to successfully engineer muscle-based tissues which contain striated and aligned myotubes. However, the contractile forces of these tissues have been limited to several hundred μN (one to two orders of magnitude less than measured in normal adult muscle). This loss in contractile force has been attributed to inadequate myotube diameter, volume density, and the level of functional differentiation (Vandenburgh *et al.*, 2008).

In order to address these issues we will employ the use of an electrical stimulator (Purchased from *Ion Optix*). This will aid in the alignment of myoblasts prior to differentiation and increase myotube formation by simulating the polarized environment in which muscle fibers and axons form junctions (Langelaan *et al.*, 2011). The use of short electrical pulses will also be used to simulate nerve impulse-induced calcium release and sarcomere shortening, thus preconditioning the newly formed muscle tissue for increased contractile force generation. In combination with electrical stimulation we will introduce other cell types present during muscle regeneration in a controlled manner. We aim to add fibroblasts to the base of our wells which will allow the interaction of secreted cytokines/growth factors to aid in 3D tissue formation. We suspect the combination of electrical stimulation along with a co-cultured microenvironment will increase the contractile force of the *in vitro* grown muscle tissue which will better mimic *in vivo* muscle functionality.

Within this chapter we have optimized culture conditions within our silicone chamber for *in vitro* muscle tissue formation. This platform will work as part of our *in vitro* testing platform where initial testing in 2-dimensional assays will be followed by testing in the 3-dimensional model.

CHAPTER 7

CONCLUDING REMARKS

Stem cell transplantation is an innovative therapy for tissue regeneration and repair after an injury or during disease. Optimal cell therapy would be autologous transplantation to circumvent the need for immune-suppression. Satellite cells function as the major myogenic precursors for muscle growth and repair (Ferrari *et al.*, 1998; Asakura and Rudnicki 2002). Studies, where either single intact myofibers (containing a pure uncommitted satellite cell population) or individual satellite cells were isolated and transplanted into radiation-ablated muscle, demonstrated rapid satellite cell proliferation and new myofiber formation (Collins *et al.*, 2005; Sacco *et al.*, 2008). As few as seven satellite cells within one myofiber were reported to generate over 100 new myofibers containing thousands of nuclei; furthermore, the satellite cells had a high self-renewal potential, repopulating the host muscle satellite cells (Collins *et al.*, 2005).

When cultured *in vitro*, the lack of niche components leads to a loss of proliferative capacity and results in defective regeneration when implanted back into a muscle defect (Boonen and Post 2008; Cosgrove *et al.*, 2009). Changes in the muscle microenvironment, rather than modification of the satellite cells themselves, also appears to be the main factor responsible for the declining regenerative response seen in aged muscle tissue (Shefer *et al.*, 2006; Collins *et al.*, 2007; LaBarge *et al.*, 2009). This highlights the importance of maintaining satellite cell populations within their niche microenvironment prior to transplantation (Zammit 2008).

Rapid loss of stem cell properties once removed from the muscle fiber, presents a major limitation to the study and clinical application of satellite cells. This is further confounded by our poor comprehension of niche composition and the regulation it imposes when guiding the behavior and fate of satellite cells (Bentzinger *et al.*, 2012). Due to this, there is a need to create novel *in vitro* microenvironments that allow for the maintenance and propagation of satellite cells while retaining their potential to function as muscle stem cells.

Standard tissue culture protocols typically supplement growth factors and cytokines within the media, while in tissues these secreted factors are most commonly presented to the cells tethered to the ECM (Griffith and Swartz 2006). Attachment of secreted growth factors to

biomaterial surfaces (such as Matrigel, collagen I, and fibronectin utilized within our study) have demonstrated improved stability of proteins and persistent signaling resulting in long-term maintenance of signaling without further supplementation required (Alberti *et al.*, 2008). Also, when comparing ligand presentation, soluble factors result in divergent effects on cell fate compared to factors tethered to the ECM (Beckstead *et al.*, 2006; Mehta *et al.*, 2010). This was demonstrated within our own study whereby the addition of TGF- β or decorin or the TGF- β /decorin complex on different biomaterials resulted in distinctly different effects on myoblast migration.

Approaches utilizing biomaterials in a 2-dimensional manner (i.e. coating tissue culture plates with collagen I) are well suited for the study of cellular and molecular mechanisms involved in cell fate regulation (Ravin *et al.*, 2008). While 2-dimensional assays enable controlled platforms for analyzing single niche elements on cell fate, they do not take into account the fact that many stem cells are embedded within a complex 3-dimensional matrix. Three-dimensional tissue engineering attempts to reconstruct the complex architecture of the tissue to achieve a physiologically relevant structure (Gilbert and Blau 2011). By extending the design principles established in 2-dimensional assays and building on these assays towards a 3-dimensional model, these complexities can be systematically expanded in order to increase our understanding of *in vivo* tissue function.

The integration of cell biology with bioengineering approaches has the potential to substantially change the practice of applied science and medicine in the future. Both 2- or 3-dimensional biomaterial approaches are changing the way scientists think about the stem cell microenvironment. In order to accelerate the impact of biomaterials towards the treatment of human disease or injury, emphasis should also be placed on utilizing human stem cells. In this respect, our study has shown some differences between murine and primary human cell cultures. Ultimately, the development of 2- and 3-dimensional *in vitro* microenvironments in which niche features can be systematically modulated will be instrumental in future therapeutic approaches to muscle regeneration caused by injury, disease, and aging.

PUBLICATIONS

K.P. Goetsch, K. Kallmeyer & C.U. Niesler (2011) Decorin modulates collagen I-stimulated, but not fibronectin-stimulated, migration of C2C12 myoblasts, *Matrix Biology*, 30, pp 109-117

K.P. Goetsch & C.U. Niesler (2011) Optimisation of the scratch assay for *in vitro* skeletal muscle wound healing analysis, *Analytical Biochemistry*, 411, pp 158-160

CONFERENCE ATTENDENCE

1) Postgraduate Research Day, Faculty of Science & Agriculture, UKZN (2009)

The Extracellular Matrix Factors, Decorin and Collagen I, Play an Essential Role in C2C12 Myoblast Migration

Goetsch, K.P. & Niesler, C.U.

School of Biochemistry, Microbiology and Genetics

Skeletal muscle repair is facilitated by activated muscle progenitor cells, termed myoblasts. Following injury these cells migrate towards the wound area where they differentiate and fuse to form new myotubes. Interactions between myoblasts and the extracellular matrix allow the cellular environment to regulate the rate and direction of migration; understanding these interactions provides a tool for improving wound repair. The proteoglycan decorin, a soluble extracellular matrix component, along with other matrix components, such as collagen, activate cellular pathways by binding to specific cell surface receptors. These pathways have been shown to modulate migration in endothelial cells, but very little is known about their effect in muscle cells.

In the current study we utilize the C2C12 myoblast cell line to determine the effect of decorin, TGF- β 2, and collagen I on migration *in vitro*. Dose responses for both decorin and collagen I at 7 hours showed optimal concentrations of 10 μ g/ml and 25 μ g/ml for decorin and collagen I, respectively. Higher concentrations of decorin and collagen I had a negative effect on cell motility, demonstrating the sensitivity of the cellular response to its environment. An *in vitro* wound assay was developed to analyze the effect of the matrix components on migration during wound closure.

Decorin and collagen I increased the percentage wound closure by 6% and 13%, respectively (compared to control). However, in combination decorin and collagen I had a synergistic effect and increased the percentage wound closure by 25% after 7 hours. TGF- β 2, a cytokine known to interact with decorin, increased the effect on wound closure by 17%. The exact mechanisms for this increase are not yet fully understood and the signaling pathways mediating these effects are currently being investigated. These studies will help to show how interactions between the cell and matrix factors are pivotal in regulating cellular processes.

2) 37th Annual Congress of the Physiological Society of Southern Africa (2009)

The Extracellular Matrix Factors, Decorin and Collagen I, are Essential for Myoblast Migration

Goetsch, K.P. & Niesler, C.U

School of Biochemistry, Microbiology and Genetics

Skeletal muscle repair is facilitated by activated muscle progenitor cells, termed myoblasts. Following tissue injury these cells migrate towards the wound area where they differentiate and fuse to form new myotubes. Interactions between myoblasts and the extracellular matrix allow the cellular environment to regulate the rate and direction of migration; understanding these interactions provides a tool for improving wound repair. The proteoglycan decorin, a soluble extracellular matrix component, along with other matrix components, such as collagen, activate intracellular pathways and influence cellular migration. The Rho activated Kinase (ROCK) pathway is of particular interest as its activation controls actin fibre contraction and pulls the cell forward during migration. The ROCK pathway is mediated by ROCK1 and 2, and has been shown to be activated by collagen I. However, the effect of decorin and collagen I on this pathway and on myoblast migration is unclear.

In the current study we utilize the C2C12 myoblast cell line to determine the effect of decorin and collagen I on migration *in vitro*. A wound assay was developed to analyse the effect of the matrix components on migration during wound closure. Dose responses after 7 hours showed optimal concentrations of 10µg/ml and 25µg/ml for decorin and collagen I, respectively. Higher concentrations of decorin and collagen I had a negative effect on cell motility, demonstrating the sensitivity of the cellular response to its environment. Decorin and collagen I increased the percentage wound closure by 6% and 13%, respectively (compared to control). However, in combination, decorin and collagen I had a synergistic effect and increased the percentage wound closure by 25% after 7 hours. Analysis of ROCK-1 protein expression in response to decorin, collagen I or a combination of both showed no significant difference to control. However, ROCK-2 protein expression showed a significant increase in response to Collagen I as well the Collagen I and decorin combination.

These results show that decorin and collagen together play a significant role in regulating myoblast migration and that the pathway by which this is achieved appears to be directly linked to the ROCK pathway, and specifically using ROCK-2 to enhance migration.

3) 2nd School Postgraduate Research Day, School of Biochemistry, Genetics & Microbiology, UKZN (2009)

The wise man built his house on ROCK

Goetsch, K.P, Snyman C. & Niesler, C.U.

Department of Biochemistry, University of KwaZulu-Natal, Pietermaritzburg

Skeletal muscle repair is facilitated by activated muscle progenitor cells, termed myoblasts. Following tissue injury these cells migrate towards the wound area where they differentiate and fuse to form new myotubes. The proteoglycan decorin, a soluble extracellular matrix component, along with other matrix components, such as collagen, activate intracellular pathways and influence cellular migration. The Rho activated Kinase (ROCK) pathway is of particular interest as its activation controls actin fibre contraction and pulls the cell forward during migration. The effect of decorin and collagen I on expression of the two isoforms of ROCK (ROCK-1 and -2) and on myoblast migration is unclear and requires further investigation.

In the current study we developed a wound assay to analyse the effect of decorin and collagen I on *in vitro* migration of the C2C12 myoblast cell line. Dose responses following 7 hours migration showed optimal concentrations of 10µg/ml and 25µg/ml for decorin and collagen I, respectively. At these concentrations, decorin and collagen I increased wound closure by 6% and 13% respectively when compared to control. Interestingly, decorin and collagen in combination had a synergistic effect, increasing wound closure by 25%. Analysis of ROCK revealed isoforms-specific differences in both their level of protein expression and localisation in response to decorin and collagen. Furthermore, inhibition studies revealed a key role of these isoforms in myoblast migration.

4) 39th Annual Congress of the Physiological Society of Southern Africa (2011)

Myoblast migration is facilitated by essential extracellular matrix components

Skeletal muscle repair is facilitated by activated muscle progenitor cells, termed myoblasts. Following tissue injury these cells migrate towards the wound area where they differentiate and fuse to form new myotubes. Interactions between myoblasts and the extracellular matrix allow the cellular environment to regulate the rate and direction of migration; understanding these interactions provides a tool for improving wound repair. The proteoglycan decorin, a soluble extracellular matrix component, along with other matrix components, such as collagen, activate intracellular pathways and influence cellular migration. The Rho activated Kinase (ROCK) pathway is of particular interest as its activation controls actin fibre contraction and pulls the cell forward during migration. The ROCK pathway is mediated by ROCK1 and 2, and has been shown to be activated by collagen I. However, the effect of decorin and collagen I on this pathway and on myoblast migration is unclear.

In the current study we utilize the C2C12 myoblast cell line to determine the effect of decorin and collagen I on migration *in vitro*. A wound assay was developed to analyse the effect of the matrix components on migration during wound closure. Dose responses after 7 hours showed optimal concentrations of 10µg/ml and 25µg/ml for decorin and collagen I, respectively. Higher concentrations of decorin and collagen I had a negative effect on cell motility, demonstrating the sensitivity of the cellular response to its environment. Decorin and collagen I increased the percentage wound closure by 6% and 13%, respectively (compared to control). However, in combination, decorin and collagen I had a synergistic effect and increased the percentage wound closure by 25% after 7 hours. Analysis of ROCK-1 protein expression in response to decorin, collagen1 or a combination of both showed no significant difference to control. However, ROCK-2 protein expression showed a significant increase in response to Collagen I as well the Collagen I and decorin combination. These results show that decorin and collagen together play a significant role in regulating myoblast migration and that the pathway by which this is achieved appears to be directly linked to the ROCK pathway, and specifically using ROCK-2 to enhance migration.

Currently, we are repeating this experimental procedure utilizing primary cultured mouse myoblasts. The method of primary culture isolation is varied and outcomes are not guaranteed. However, the use of primary culture is a far better model and mimics *in vivo* conditions to a greater extent than an immortalized cell line. Furthermore, we will be developing a 3-dimensional model based on *in vitro* muscle tissue which will be grown in our lab. We will then analyse the effect of ECM components on muscle repair within the new model and compare this artificially grown muscle with *in vivo* conditions.

5) Swiss-South African Joint Business Development Program (2011)

In vitro cell models are currently being used for drug discovery and screening within the biotech and pharmaceutical community. However, many of the cellular assays use cell lines or tumor derived cells which are “abnormal” and differ substantially from *in vivo* tissue. As a result, data derived from these models is often difficult to translate into animal and human drug trials contributing to the current high attrition rate of drug trials.

The model we are developing involves the use of both animal and human stem cells to bioengineer functional 3D skeletal muscle *in vitro*. Minimal modifications to stem cells are made prior to *in vitro* tissue formation. Mechanical and electrical systems for muscle stimulation are also being developed to ensure optimal skeletal muscle formation. Endpoints to be measured include, but are not limited to, contractile response, rate of fatigue, utilization of glucose and rate of repair following damage.

The development of functional three dimensional skeletal muscle *in vitro* represents a cell based assay which mimics *in vivo* conditions closely and can be used to test new or existing pharmaceutical or biotech compounds. This method would be adapted and developed to allow for high through-put screening of multiple compounds at varying concentrations within a short period of time. It is envisaged that the pharmaceutical and biotech (local and international) would be very interested in this type of assay system.

6) SASBMB FASBMB Congress (2012)**Effect of extracellular matrix factors on myoblast migration****Kyle P. Goetsch**¹, Kathy Myburgh², Carola Niesler¹

¹Department of Biochemistry, University of KwaZulu-Natal, Pietermaritzburg, South Africa; ²Department of Physiological Sciences, University of Stellenbosch, Stellenbosch, South Africa

Email: 205508050@ukzn.ac.za / kpgoetsch@gmail.com

Skeletal muscle regeneration is facilitated by satellite cells located between the basal lamina and sarcolemma of a mature myofiber. In response to injury, activated satellite cells (myoblasts) migrate to the wound area, differentiate and fuse to facilitate repair. Myoblast migration is regulated by several extracellular matrix (ECM) and growth factors, which have different effects on the morphology and rate of migration. One of the major regulatory pathways for migration involves Rho/ROCK, which facilitates correct tubule alignment and contraction during migration. Previously, we have shown that decorin, a proteoglycan secreted during severe muscle injury, significantly enhances myoblast migration when added in combination with collagen I, the major structural protein laid down during muscle regeneration. We have now expanded our study to include other key ECM and growth factors that myoblasts will encounter during migration. C₂C₁₂ myoblasts were grown on matrigel, laminin, collagen IV, fibronectin and TGF- β 2. The rate of migration was assessed and results showed that the ECM factors increased migration at different rates, whereas TGF- β 2 decreased the rate of migration. Unexpectedly, inhibition of ROCK using the Y-27632 inhibitor increased the rate of migration. To try and understand this we assessed the localization of ROCK-2 and vinculin, a marker for focal adhesion sites, as well as investigated the effect of the inhibitor on directional migration of the cells. Preliminary results suggest that ROCK-2 plays a role in directional migration through the regulation of focal adhesions. Primary cultured murine and human myoblast studies to confirm these results are underway.

REFERENCES

- Abd-Elgaliel, W. R. and C. H. Tung (2012).** "Exploring the structural requirements of collagen-binding peptides." *Biopolymers*.
- Alberti, K., R. E. Davey, K. Onishi, S. George, K. Salchert, F. P. Seib, M. Bornhauser, T. Pompe, A. Nagy, C. Werner and P. W. Zandstra (2008).** "Functional immobilization of signaling proteins enables control of stem cell fate." *Nat Methods* **5**(7): 645-650.
- Ameys, L., D. Aria, K. Jepsen, A. Oldberg, T. Xu and M. F. Young (2002).** "Abnormal collagen fibrils in tendons of biglycan/fibromodulin-deficient mice lead to gait impairment, ectopic ossification, and osteoarthritis." *FASEB J* **16**(7): 673-680.
- Armand, A. S., I. Laziz and C. Chanoine (2006).** "FGF6 in myogenesis." *Biochim Biophys Acta* **1763**(8): 773-778.
- Asakura, A. and M. A. Rudnicki (2002).** "Side population cells from diverse adult tissues are capable of in vitro hematopoietic differentiation." *Exp Hematol* **30**(11): 1339-1345.
- Attisano, L. and J. L. Wrana (2002).** "Signal transduction by the TGF-beta superfamily." *Science* **296**(5573): 1646-1647.
- Austin, L. and A. W. Burgess (1991).** "Stimulation of myoblast proliferation in culture by leukaemia inhibitory factor and other cytokines." *J Neurol Sci* **101**(2): 193-197.
- Avery, N. C. and A. J. Bailey (2005).** "Enzymic and non-enzymic cross-linking mechanisms in relation to turnover of collagen: relevance to aging and exercise." *Scand J Med Sci Sports* **15**(4): 231-240.
- Beauchamp, J. R., L. Heslop, D. S. Yu, S. Tajbakhsh, R. G. Kelly, A. Wernig, M. E. Buckingham, T. A. Partridge and P. S. Zammit (2000).** "Expression of CD34 and Myf5 defines the majority of quiescent adult skeletal muscle satellite cells." *J Cell Biol* **151**(6): 1221-1234.
- Beauchamp, J. R., J. E. Morgan, C. N. Pagel and T. A. Partridge (1999).** "Dynamics of myoblast transplantation reveal a discrete minority of precursors with stem cell-like properties as the myogenic source." *J Cell Biol* **144**(6): 1113-1122.
- Beckstead, B. L., D. M. Santosa and C. M. Giachelli (2006).** "Mimicking cell-cell interactions at the biomaterial-cell interface for control of stem cell differentiation." *J Biomed Mater Res A* **79**(1): 94-103.
- Bentzinger, C. F., Y. X. Wang and M. A. Rudnicki (2012).** "Building muscle: molecular regulation of myogenesis." *Cold Spring Harb Perspect Biol* **4**(2).
- Bentzinger, C. F., Y. X. Wang, J. von Maltzahn and M. A. Rudnicki (2012).** "The emerging biology of muscle stem cells: Implications for cell-based therapies." *Bioessays*.
- Bernal, F., H. P. Hartung and B. C. Kieseier (2005).** "Tissue mRNA expression in rat of newly described matrix metalloproteinases." *Biol Res* **38**(2-3): 267-271.
- Birchmeier, C. and E. Gherardi (1998).** "Developmental roles of HGF/SF and its receptor, the c-Met tyrosine kinase." *Trends Cell Biol* **8**(10): 404-410.
- Birkedal-Hansen, H. (1995).** "Proteolytic remodeling of extracellular matrix." *Curr Opin Cell Biol* **7**(5): 728-735.
- Bishop, J. R., M. Schuksz and J. D. Esko (2007).** "Heparan sulphate proteoglycans fine-tune mammalian physiology." *Nature* **446**(7139): 1030-1037.
- Black, R. A. and J. M. White (1998).** "ADAMs: focus on the protease domain." *Curr Opin Cell Biol* **10**(5): 654-659.
- Bonnemann, C. G. and N. G. Laing (2004).** "Myopathies resulting from mutations in sarcomeric proteins." *Curr Opin Neurol* **17**(5): 529-537.
- Boonen, K. J. and M. J. Post (2008).** "The muscle stem cell niche: regulation of satellite cells during regeneration." *Tissue Eng Part B Rev* **14**(4): 419-431.
- Booth, F. (2006).** "The many flavors of IGF-I." *J Appl Physiol* **100**(6): 1755-1756.
- Border, W. A. and N. A. Noble (1994).** "Transforming growth factor beta in tissue fibrosis." *N Engl J Med* **331**(19): 1286-1292.
- Boyden, S. (1962).** "The chemotactic effect of mixtures of antibody and antigen on polymorphonuclear leucocytes." *J Exp Med* **115**: 453-466.

- Brack, A. S., M. J. Conboy, S. Roy, M. Lee, C. J. Kuo, C. Keller and T. A. Rando (2007).** "Increased Wnt signaling during aging alters muscle stem cell fate and increases fibrosis." *Science* **317**(5839): 807-810.
- Brandan, E., C. Cabello-Verrugio and C. Vial (2008).** "Novel regulatory mechanisms for the proteoglycans decorin and biglycan during muscle formation and muscular dystrophy." *Matrix Biol* **27**(8): 700-708.
- Bretscher, M. S. (1996).** "Moving membrane up to the front of migrating cells." *Cell* **85**(4): 465-467.
- Brooks, P. C. (1996).** "Cell adhesion molecules in angiogenesis." *Cancer Metastasis Rev* **15**(2): 187-194.
- Burridge, K. and K. Wennerberg (2004).** "Rho and Rac take center stage." *Cell* **116**(2): 167-179.
- Cabello-Verrugio, C. and E. Brandan (2007).** "A novel modulatory mechanism of transforming growth factor-beta signaling through decorin and LRP-1." *J Biol Chem* **282**(26): 18842-18850.
- Cabello-Verrugio, C., C. Santander, C. Cofre, M. J. Acuna, F. Melo and E. Brandan (2012).** "The internal region leucine-rich repeat 6 of decorin interacts with low density lipoprotein receptor-related protein-1, modulates transforming growth factor (TGF)-beta-dependent signaling, and inhibits TGF-beta-dependent fibrotic response in skeletal muscles." *J Biol Chem* **287**(9): 6773-6787.
- Caswell, P. T. and J. C. Norman (2006).** "Integrin trafficking and the control of cell migration." *Traffic* **7**(1): 14-21.
- Catlow, K., J. A. Deakin, M. Delehedde, D. G. Fernig, J. T. Gallagher, M. S. Pavao and M. Lyon (2003).** "Hepatocyte growth factor/scatter factor and its interaction with heparan sulphate and dermatan sulphate." *Biochem Soc Trans* **31**(2): 352-353.
- Chakkalakal, J. V., K. M. Jones, M. A. Basson and A. S. Brack (2012).** "The aged niche disrupts muscle stem cell quiescence." *Nature* **490**(7420): 355-360.
- Chakravarthy, M. V., T. W. Abraha, R. J. Schwartz, M. L. Fiorotto and F. W. Booth (2000).** "Insulin-like growth factor-I extends in vitro replicative life span of skeletal muscle satellite cells by enhancing G1/S cell cycle progression via the activation of phosphatidylinositol 3'-kinase/Akt signaling pathway." *J Biol Chem* **275**(46): 35942-35952.
- Chen, X. and Y. Li (2009).** "Role of matrix metalloproteinases in skeletal muscle: migration, differentiation, regeneration and fibrosis." *Cell Adh Migr* **3**(4): 337-341.
- Chiquet-Ehrismann, R. (2004).** "Tenascins." *Int J Biochem Cell Biol* **36**(6): 986-990.
- Chiquet-Ehrismann, R. and R. P. Tucker (2004).** "Connective tissues: signalling by tenascins." *Int J Biochem Cell Biol* **36**(6): 1085-1089.
- Chrzanowska-Wodnicka, M. and K. Burridge (1996).** "Rho-stimulated contractility drives the formation of stress fibers and focal adhesions." *J Cell Biol* **133**(6): 1403-1415.
- Chua, F., P. D. Sly and G. J. Laurent (2005).** "Pediatric lung disease: from proteinases to pulmonary fibrosis." *Pediatr Pulmonol* **39**(5): 392-401.
- Collins, C. A., I. Olsen, P. S. Zammit, L. Heslop, A. Petrie, T. A. Partridge and J. E. Morgan (2005).** "Stem cell function, self-renewal, and behavioral heterogeneity of cells from the adult muscle satellite cell niche." *Cell* **122**(2): 289-301.
- Collins, C. A., P. S. Zammit, A. P. Ruiz, J. E. Morgan and T. A. Partridge (2007).** "A population of myogenic stem cells that survives skeletal muscle aging." *Stem Cells* **25**(4): 885-894.
- Cooper, O. and O. Isacson (2004).** "Intrastriatal transforming growth factor alpha delivery to a model of Parkinson's disease induces proliferation and migration of endogenous adult neural progenitor cells without differentiation into dopaminergic neurons." *J Neurosci* **24**(41): 8924-8931.
- Cornelison, D. D. (2008).** "Context matters: in vivo and in vitro influences on muscle satellite cell activity." *J Cell Biochem* **105**(3): 663-669.
- Cornelison, D. D. and B. J. Wold (1997).** "Single-cell analysis of regulatory gene expression in quiescent and activated mouse skeletal muscle satellite cells." *Dev Biol* **191**(2): 270-283.

- Cosgrove, B. D., A. Sacco, P. M. Gilbert and H. M. Blau (2009).** "A home away from home: challenges and opportunities in engineering in vitro muscle satellite cell niches." *Differentiation* **78**(2-3): 185-194.
- Crawley, S., E. M. Farrell, W. Wang, M. Gu, H. Y. Huang, V. Huynh, B. L. Hodges, D. N. Cooper and S. J. Kaufman (1997).** "The alpha7beta1 integrin mediates adhesion and migration of skeletal myoblasts on laminin." *Exp Cell Res* **235**(1): 274-286.
- Cukierman, E., R. Pankov, D. R. Stevens and K. M. Yamada (2001).** "Taking cell-matrix adhesions to the third dimension." *Science* **294**(5547): 1708-1712.
- Dhawan, J. and D. M. Helfman (2004).** "Modulation of acto-myosin contractility in skeletal muscle myoblasts uncouples growth arrest from differentiation." *J Cell Sci* **117**(Pt 17): 3735-3748.
- Droguett, R., C. Cabello-Verrugio, C. Riquelme and E. Brandan (2006).** "Extracellular proteoglycans modify TGF-beta bio-availability attenuating its signaling during skeletal muscle differentiation." *Matrix Biol* **25**(6): 332-341.
- Dunkman, A. A., M. R. Buckley, M. J. Mienaltowski, S. M. Adams, S. J. Thomas, L. Satchell, A. Kumar, L. Pathmanathan, D. P. Beason, R. V. Iozzo, D. E. Birk and L. J. Soslowky (2013).** "Decorin expression is important for age-related changes in tendon structure and mechanical properties." *Matrix Biol* **32**(1): 3-13.
- Ehrhardt, J. and J. Morgan (2005).** "Regenerative capacity of skeletal muscle." *Curr Opin Neurol* **18**(5): 548-553.
- Emsley, J., C. G. Knight, R. W. Farndale, M. J. Barnes and R. C. Liddington (2000).** "Structural basis of collagen recognition by integrin alpha2beta1." *Cell* **101**(1): 47-56.
- Engert, J. C., E. B. Berglund and N. Rosenthal (1996).** "Proliferation precedes differentiation in IGF-I-stimulated myogenesis." *J Cell Biol* **135**(2): 431-440.
- Even-Ram, S. and K. M. Yamada (2005).** "Cell migration in 3D matrix." *Curr Opin Cell Biol* **17**(5): 524-532.
- Fabbri, M., E. Bianchi, L. Fumagalli and R. Pardi (1999).** "Regulation of lymphocyte traffic by adhesion molecules." *Inflamm Res* **48**(5): 239-246.
- Fedorov, Y. V., N. C. Jones and B. B. Olwin (1998).** "Regulation of myogenesis by fibroblast growth factors requires beta-gamma subunits of pertussis toxin-sensitive G proteins." *Mol Cell Biol* **18**(10): 5780-5787.
- Ferrari, G., G. Cusella-De Angelis, M. Coletta, E. Paolucci, A. Stornaiuolo, G. Cossu and F. Mavilio (1998).** "Muscle regeneration by bone marrow-derived myogenic progenitors." *Science* **279**(5356): 1528-1530.
- Fiedler, L. R. and J. A. Eble (2009).** "Decorin regulates endothelial cell-matrix interactions during angiogenesis." *Cell Adh Migr* **3**(1).
- Fiedler, L. R., E. Schonherr, R. Waddington, S. Niland, D. G. Seidler, D. Aeschlimann and J. A. Eble (2008).** "Decorin regulates endothelial cell motility on collagen I through activation of insulin-like growth factor I receptor and modulation of alpha2beta1 integrin activity." *J Biol Chem* **283**(25): 17406-17415.
- Finnson, K. W., Y. Chi, G. Bou-Gharios, A. Leask and A. Philip (2012).** "TGF-b signaling in cartilage homeostasis and osteoarthritis." *Front Biosci (Schol Ed)* **4**: 251-268.
- Fluck, M., M. Chiquet, S. Schmutz, M. H. Mayet-Sornay and D. Desplanches (2003).** "Reloading of atrophied rat soleus muscle induces tenascin-C expression around damaged muscle fibers." *Am J Physiol Regul Integr Comp Physiol* **284**(3): R792-801.
- Fortier, M., F. Comunale, J. Kucharczak, A. Blangy, S. Charrasse and C. Gauthier-Rouviere (2008).** "RhoE controls myoblast alignment prior fusion through RhoA and ROCK." *Cell Death Differ* **15**(8): 1221-1231.
- Friedl, P. and E. B. Brocker (2000).** "The biology of cell locomotion within three-dimensional extracellular matrix." *Cell Mol Life Sci* **57**(1): 41-64.
- Friedl, P., K. S. Zanker and E. B. Brocker (1998).** "Cell migration strategies in 3-D extracellular matrix: differences in morphology, cell matrix interactions, and integrin function." *Microsc Res Tech* **43**(5): 369-378.

- Fukushima, H., M. Ohsawa, Y. Ikura, T. Naruko, Y. Sugama, T. Suekane, C. Kitabayashi, T. Inoue, M. Hino and M. Ueda (2006).** "Mast cells in diffuse large B-cell lymphoma; their role in fibrosis." *Histopathology* **49**(5): 498-505.
- Fukushima, K., N. Badlani, A. Usas, F. Riano, F. Fu and J. Huard (2001).** "The use of an antifibrosis agent to improve muscle recovery after laceration." *Am J Sports Med* **29**(4): 394-402.
- Gelse, K., E. Poschl and T. Aigner (2003).** "Collagens--structure, function, and biosynthesis." *Adv Drug Deliv Rev* **55**(12): 1531-1546.
- Gerthoffer, W. T. (2007).** "Mechanisms of vascular smooth muscle cell migration." *Circ Res* **100**(5): 607-621.
- Gharaibeh, B., A. Lu, J. Tebbets, B. Zheng, J. Feduska, M. Crisan, B. Peault, J. Cummins and J. Huard (2008).** "Isolation of a slowly adhering cell fraction containing stem cells from murine skeletal muscle by the preplate technique." *Nat Protoc* **3**(9): 1501-1509.
- Gilbert, P. M. and H. M. Blau (2011).** "Engineering a stem cell house into a home." *Stem Cell Res Ther* **2**(1): 3.
- Goetsch, K. P., K. Kallmeyer and C. U. Niesler (2011).** "Decorin modulates collagen I-stimulated, but not fibronectin-stimulated, migration of C2C12 myoblasts." *Matrix Biol* **30**(2): 109-117.
- Goetsch, K. P. and C. U. Niesler (2011).** "Optimization of the scratch assay for in vitro skeletal muscle wound healing analysis." *Anal Biochem* **411**(1): 158-160.
- Goldstein, A. S. and P. A. DiMilla (2003).** "Examination of membrane rupture as a mechanism for mammalian cell detachment from fibronectin-coated biomaterials." *J Biomed Mater Res A* **67**(2): 658-666.
- Goodpaster, T., A. Legesse-Miller, M. R. Hameed, S. C. Aisner, J. Randolph-Habecker and H. A. Collier (2008).** "An immunohistochemical method for identifying fibroblasts in formalin-fixed, paraffin-embedded tissue." *J Histochem Cytochem* **56**(4): 347-358.
- Gorshkova, I., D. He, E. Berdyshev, P. Usatuyk, M. Burns, S. Kalari, Y. Zhao, S. Pandyala, J. G. Garcia, N. J. Pyne, D. N. Brindley and V. Natarajan (2008).** "Protein kinase C-epsilon regulates sphingosine 1-phosphate-mediated migration of human lung endothelial cells through activation of phospholipase D2, protein kinase C-zeta, and Rac1." *J Biol Chem* **283**(17): 11794-11806.
- Griffith, L. G. and M. A. Swartz (2006).** "Capturing complex 3D tissue physiology in vitro." *Nat Rev Mol Cell Biol* **7**(3): 211-224.
- Grounds, M. D., L. Sorokin and J. White (2005).** "Strength at the extracellular matrix-muscle interface." *Scand J Med Sci Sports* **15**(6): 381-391.
- Guerette, B., K. Wood, R. Roy and J. P. Tremblay (1997).** "Efficient myoblast transplantation in mice immunosuppressed with monoclonal antibodies and CTLA4 Ig." *Transplant Proc* **29**(4): 1932-1934.
- Hausser, H., P. Wedekind, T. Sperber, R. Peters, A. Hasilik and H. Kresse (1996).** "Isolation and cellular localization of the decorin endocytosis receptor." *Eur J Cell Biol* **71**(4): 325-331.
- Heino, J. (1996).** "Biology of tumor cell invasion: interplay of cell adhesion and matrix degradation." *Int J Cancer* **65**(6): 717-722.
- Hinds, S., W. Bian, R. G. Dennis and N. Bursac (2011).** "The role of extracellular matrix composition in structure and function of bioengineered skeletal muscle." *Biomaterials* **32**(14): 3575-3583.
- Hocking, D. C., P. A. Titus, R. Sumagin and I. H. Sarelius (2008).** "Extracellular matrix fibronectin mechanically couples skeletal muscle contraction with local vasodilation." *Circ Res* **102**(3): 372-379.
- Huang, Y. C., R. G. Dennis, L. Larkin and K. Baar (2005).** "Rapid formation of functional muscle in vitro using fibrin gels." *J Appl Physiol* **98**(2): 706-713.
- Huard, J., Y. Li and F. H. Fu (2002).** "Muscle injuries and repair: current trends in research." *J Bone Joint Surg Am* **84-A**(5): 822-832.

- Huard, J., R. Roy, B. Guerette, S. Verreault, G. Tremblay and J. P. Tremblay (1994).** "Human myoblast transplantation in immunodeficient and immunosuppressed mice: evidence of rejection." *Muscle Nerve* **17**(2): 224-234.
- Humphries, J. D., A. Byron and M. J. Humphries (2006).** "Integrin ligands at a glance." *J Cell Sci* **119**(Pt 19): 3901-3903.
- Hynes, R. O., J. C. Lively, J. H. McCarty, D. Taverna, S. E. Francis, K. Hodivala-Dilke and Q. Xiao (2002).** "The diverse roles of integrins and their ligands in angiogenesis." *Cold Spring Harb Symp Quant Biol* **67**: 143-153.
- Irintchev, A., M. Zeschnigk, A. Starzinski-Powitz and A. Wernig (1994).** "Expression pattern of M-cadherin in normal, denervated, and regenerating mouse muscles." *Dev Dyn* **199**(4): 326-337.
- Ishizaki, T., M. Uehata, I. Tamechika, J. Keel, K. Nonomura, M. Maekawa and S. Narumiya (2000).** "Pharmacological properties of Y-27632, a specific inhibitor of rho-associated kinases." *Mol Pharmacol* **57**(5): 976-983.
- Ispanovic, E., D. Serio and T. L. Haas (2008).** "Cdc42 and RhoA have opposing roles in regulating membrane type 1-matrix metalloproteinase localization and matrix metalloproteinase-2 activation." *Am J Physiol Cell Physiol* **295**(3): C600-610.
- Iwanicki, M. P., T. Vomastek, R. W. Tilghman, K. H. Martin, J. Banerjee, P. B. Wedegaertner and J. T. Parsons (2008).** "FAK, PDZ-RhoGEF and ROCKII cooperate to regulate adhesion movement and trailing-edge retraction in fibroblasts." *J Cell Sci* **121**(Pt 6): 895-905.
- Jarvinen, T. A., T. L. Jarvinen, M. Kaariainen, V. Aarimaa, S. Vaittinen, H. Kalimo and M. Jarvinen (2007).** "Muscle injuries: optimising recovery." *Best Pract Res Clin Rheumatol* **21**(2): 317-331.
- Jarvinen, T. A., T. L. Jarvinen, P. Kannus, L. Jozsa and M. Jarvinen (2004).** "Collagen fibres of the spontaneously ruptured human tendons display decreased thickness and crimp angle." *J Orthop Res* **22**(6): 1303-1309.
- Jasper, H. and B. K. Kennedy (2012).** "Niche science: the aging stem cell." *Cell Cycle* **11**(16): 2959-2960.
- Jayo, A., M. Parsons and J. C. Adams (2012).** "A novel Rho-dependent pathway that drives interaction of fascin-1 with p-Lin-11/Isl-1/Mec-3 kinase (LIMK) 1/2 to promote fascin-1/actin binding and filopodia stability." *BMC Biol* **10**: 72.
- Jenniskens, G. J., J. H. Veerkamp and T. H. van Kuppevelt (2006).** "Heparan sulfates in skeletal muscle development and physiology." *J Cell Physiol* **206**(2): 283-294.
- Kalamajski, S., A. Aspberg and A. Oldberg (2007).** "The decorin sequence SYIRIADTNIT binds collagen type I." *J Biol Chem* **282**(22): 16062-16067.
- Kalluri, R. (2003).** "Basement membranes: structure, assembly and role in tumour angiogenesis." *Nat Rev Cancer* **3**(6): 422-433.
- Kanagawa, M., D. E. Michele, J. S. Satz, R. Barresi, H. Kusano, T. Sasaki, R. Timpl, M. D. Henry and K. P. Campbell (2005).** "Disruption of perlecan binding and matrix assembly by post-translational or genetic disruption of dystroglycan function." *FEBS Lett* **579**(21): 4792-4796.
- Karalaki, M., S. Fili, A. Philippou and M. Koutsilieris (2009).** "Muscle regeneration: cellular and molecular events." *In Vivo* **23**(5): 779-796.
- Kastner, S., M. C. Elias, A. J. Rivera and Z. Yablonka-Reuveni (2000).** "Gene expression patterns of the fibroblast growth factors and their receptors during myogenesis of rat satellite cells." *J Histochem Cytochem* **48**(8): 1079-1096.
- Kawada, K., G. Upadhyay, S. Ferandon, S. Janarthanan, M. Hall, J. P. Vilardaga and V. Yajnik (2009).** "Cell migration is regulated by platelet-derived growth factor receptor endocytosis." *Mol Cell Biol* **29**(16): 4508-4518.
- Kawano, Y., Y. Fukata, N. Oshiro, M. Amano, T. Nakamura, M. Ito, F. Matsumura, M. Inagaki and K. Kaibuchi (1999).** "Phosphorylation of myosin-binding subunit (MBS) of myosin phosphatase by Rho-kinase in vivo." *J Cell Biol* **147**(5): 1023-1038.

- Keene, D. R., J. D. San Antonio, R. Mayne, D. J. McQuillan, G. Sarris, S. A. Santoro and R. V. Iozzo (2000).** "Decorin binds near the C terminus of type I collagen." *J Biol Chem* **275**(29): 21801-21804.
- Keese, C. R., J. Wegener, S. R. Walker and I. Giaever (2004).** "Electrical wound-healing assay for cells in vitro." *Proc Natl Acad Sci U S A* **101**(6): 1554-1559.
- Kemp, L. E., B. Mulloy and E. Gherardi (2006).** "Signalling by HGF/SF and Met: the role of heparan sulphate co-receptors." *Biochem Soc Trans* **34**(Pt 3): 414-417.
- Kherif, S., C. Lafuma, M. Dehaupas, S. Lachkar, J. G. Fournier, M. Verdiere-Sahuque, M. Fardeau and H. S. Alameddine (1999).** "Expression of matrix metalloproteinases 2 and 9 in regenerating skeletal muscle: a study in experimentally injured and mdx muscles." *Dev Biol* **205**(1): 158-170.
- Kinoshita, I., J. T. Vilquin and J. P. Tremblay (1995).** "Pretreatment of myoblast cultures with basic fibroblast growth factor increases the efficacy of their transplantation in mdx mice." *Muscle Nerve* **18**(8): 834-841.
- Kiselyov, V. V., E. Bock, V. Berezin and F. M. Poulsen (2006).** "NMR structure of the first Ig module of mouse FGFR1." *Protein Sci* **15**(6): 1512-1515.
- Kishioka, Y., M. Thomas, J. Wakamatsu, A. Hattori, M. Sharma, R. Kambadur and T. Nishimura (2008).** "Decorin enhances the proliferation and differentiation of myogenic cells through suppressing myostatin activity." *J Cell Physiol* **215**(3): 856-867.
- Kjaer, M. (2004).** "Role of extracellular matrix in adaptation of tendon and skeletal muscle to mechanical loading." *Physiol Rev* **84**(2): 649-698.
- Kottler, U. B., A. G. Junemann, T. Aigner, M. Zenkel, C. Rummelt and U. Schlotzer-Schrehardt (2005).** "Comparative effects of TGF-beta 1 and TGF-beta 2 on extracellular matrix production, proliferation, migration, and collagen contraction of human Tenon's capsule fibroblasts in pseudoexfoliation and primary open-angle glaucoma." *Exp Eye Res* **80**(1): 121-134.
- Kozma, R., S. Ahmed, A. Best and L. Lim (1995).** "The Ras-related protein Cdc42Hs and bradykinin promote formation of peripheral actin microspikes and filopodia in Swiss 3T3 fibroblasts." *Mol Cell Biol* **15**(4): 1942-1952.
- Kresse, H., C. Liszio, E. Schonherr and L. W. Fisher (1997).** "Critical role of glutamate in a central leucine-rich repeat of decorin for interaction with type I collagen." *J Biol Chem* **272**(29): 18404-18410.
- LaBarge, M. A., C. M. Nelson, R. Villadsen, A. Fridriksdottir, J. R. Ruth, M. R. Stampfer, O. W. Petersen and M. J. Bissell (2009).** "Human mammary progenitor cell fate decisions are products of interactions with combinatorial microenvironments." *Integr Biol (Camb)* **1**(1): 70-79.
- Langelaan, M. L., K. J. Boonen, K. Y. Rosaria-Chak, D. W. van der Schaft, M. J. Post and F. P. Baaijens (2011).** "Advanced maturation by electrical stimulation: Differences in response between C2C12 and primary muscle progenitor cells." *J Tissue Eng Regen Med* **5**(7): 529-539.
- Leboeuf, D. and N. Henry (2006).** "Molecular bond formation between surfaces: anchoring and shearing effects." *Langmuir* **22**(1): 127-133.
- Lehto, M. and M. Jarvinen (1985).** "Collagen and glycosaminoglycan synthesis of injured gastrocnemius muscle in rat." *Eur Surg Res* **17**(3): 179-185.
- Leshem, Y., I. Gitelman, C. Ponzetto and O. Halevy (2002).** "Preferential binding of Grb2 or phosphatidylinositol 3-kinase to the met receptor has opposite effects on HGF-induced myoblast proliferation." *Exp Cell Res* **274**(2): 288-298.
- Li, X., D. C. McFarland and S. G. Velleman (2008).** "Extracellular matrix proteoglycan decorin-mediated myogenic satellite cell responsiveness to transforming growth factor-beta1 during cell proliferation and differentiation Decorin and transforming growth factor-beta1 in satellite cells." *Domest Anim Endocrinol* **35**(3): 263-273.
- Li, Y., W. Foster, B. M. Deasy, Y. Chan, V. Prisk, Y. Tang, J. Cummins and J. Huard (2004).** "Transforming growth factor-beta1 induces the differentiation of myogenic cells into fibrotic cells in injured skeletal muscle: a key event in muscle fibrogenesis." *Am J Pathol* **164**(3): 1007-1019.

- Liang, C. C., A. Y. Park and J. L. Guan (2007).** "In vitro scratch assay: a convenient and inexpensive method for analysis of cell migration in vitro." *Nat Protoc* **2**(2): 329-333.
- Liu, H., A. Niu, S. E. Chen and Y. P. Li (2011).** "Beta3-integrin mediates satellite cell differentiation in regenerating mouse muscle." *FASEB J* **25**(6): 1914-1921.
- Machesky, L. M. (1997).** "Cell motility: complex dynamics at the leading edge." *Curr Biol* **7**(3): R164-167.
- Machesky, L. M. and A. Hall (1997).** "Role of actin polymerization and adhesion to extracellular matrix in Rac- and Rho-induced cytoskeletal reorganization." *J Cell Biol* **138**(4): 913-926.
- Machida, S., E. E. Spangenburg and F. W. Booth (2004).** "Primary rat muscle progenitor cells have decreased proliferation and myotube formation during passages." *Cell Prolif* **37**(4): 267-277.
- Mackey, A. L., U. R. Mikkelsen, S. P. Magnusson and M. Kjaer (2012).** "Rehabilitation of muscle after injury - the role of anti-inflammatory drugs." *Scand J Med Sci Sports* **22**(4): e8-14.
- Margadant, C. and A. Sonnenberg (2010).** "Integrin-TGF-beta crosstalk in fibrosis, cancer and wound healing." *EMBO Rep* **11**(2): 97-105.
- Markmann, A., H. Hausser, E. Schonherr and H. Kresse (2000).** "Influence of decorin expression on transforming growth factor-beta-mediated collagen gel retraction and biglycan induction." *Matrix Biol* **19**(7): 631-636.
- Marmotti, A., D. E. Bonasia, M. Bruzzone, R. Rossi, F. Castoldi, G. Collo, C. Realmuto, C. Tarella and G. M. Peretti (2012).** "Human cartilage fragments in a composite scaffold for single-stage cartilage repair: an in vitro study of the chondrocyte migration and the influence of TGF-beta1 and G-CSF." *Knee Surg Sports Traumatol Arthrosc*.
- Massague, J. and D. Wotton (2000).** "Transcriptional control by the TGF-beta/Smad signaling system." *Embo J* **19**(8): 1745-1754.
- Mathews, K. D., C. M. Stephan, K. Laubenthal, T. L. Winder, D. E. Michele, S. A. Moore and K. P. Campbell (2011).** "Myoglobinuria and muscle pain are common in patients with limb-girdle muscular dystrophy 2I." *Neurology* **76**(2): 194-195.
- Matsumoto, K. and T. Nakamura (1997).** "Hepatocyte growth factor (HGF) as a tissue organizer for organogenesis and regeneration." *Biochem Biophys Res Commun* **239**(3): 639-644.
- Mauro, A. (1961).** "Satellite cell of skeletal muscle fibers." *J Biophys Biochem Cytol* **9**: 493-495.
- McLennan, R., L. Dyson, K. W. Prather, J. A. Morrison, R. E. Baker, P. K. Maini and P. M. Kulesa (2012).** "Multiscale mechanisms of cell migration during development: theory and experiment." *Development* **139**(16): 2935-2944.
- Mehta, V., R. Suri, J. Arora, G. Rath and S. Das (2010).** "Anomalous constitution of the brachioradialis muscle: a potential site of radial nerve entrapment." *Clin Ter* **161**(1): 59-61.
- Melrose, J., E. S. Fuller, P. J. Roughley, M. M. Smith, B. Kerr, C. E. Hughes, B. Caterson and C. B. Little (2008).** "Fragmentation of decorin, biglycan, lumican and keratocan is elevated in degenerate human meniscus, knee and hip articular cartilages compared with age-matched macroscopically normal and control tissues." *Arthritis Res Ther* **10**(4): R79.
- Mendias, C. L., E. Kayupov, J. R. Bradley, S. V. Brooks and D. R. Claffin (2011).** "Decreased specific force and power production of muscle fibers from myostatin-deficient mice are associated with a suppression of protein degradation." *J Appl Physiol* **111**(1): 185-191.
- Meyvantsson, I. and D. J. Beebe (2008).** "Cell culture models in microfluidic systems." *Annu Rev Anal Chem (Palo Alto Calif)* **1**: 423-449.
- Mezzano, V., D. Cabrera, C. Vial and E. Brandan (2007).** "Constitutively activated dystrophic muscle fibroblasts show a paradoxical response to TGF-beta and CTGF/CCN2." *J Cell Commun Signal* **1**(3-4): 205-217.
- Midwood, K. S. and G. Orend (2009).** "The role of tenascin-C in tissue injury and tumorigenesis." *J Cell Commun Signal* **3**(3-4): 287-310.
- Miller, R. J., G. Banisadr and B. J. Bhattacharyya (2008).** "CXCR4 signaling in the regulation of stem cell migration and development." *J Neuroimmunol* **198**(1-2): 31-38.
- Miura, T., Y. Kishioka, J. Wakamatsu, A. Hattori, A. Hennebry, C. J. Berry, M. Sharma, R. Kambadur and T. Nishimura (2006).** "Decorin binds myostatin and modulates its activity to muscle cells." *Biochem Biophys Res Commun* **340**(2): 675-680.

- Modulevsky, D. J., D. Tremblay, C. Gullekson, N. V. Bukoresthliev and A. E. Pelling (2012).** "The Physical Interaction of Myoblasts with the Microenvironment during Remodeling of the Cytoarchitecture." *PLoS One* **7**(9): e45329.
- Moissoglu, K. and M. A. Schwartz (2006).** "Integrin signalling in directed cell migration." *Biol Cell* **98**(9): 547-555.
- Moon, S. Y. and Y. Zheng (2003).** "Rho GTPase-activating proteins in cell regulation." *Trends Cell Biol* **13**(1): 13-22.
- Moss, F. P. and C. P. Leblond (1971).** "Satellite cells as the source of nuclei in muscles of growing rats." *Anat Rec* **170**(4): 421-435.
- Moyer, A. L. and K. R. Wagner (2011).** "Regeneration versus fibrosis in skeletal muscle." *Curr Opin Rheumatol* **23**(6): 568-573.
- Murphy, M. M., J. A. Lawson, S. J. Mathew, D. A. Hutcheson and G. Kardon (2011).** "Satellite cells, connective tissue fibroblasts and their interactions are crucial for muscle regeneration." *Development* **138**(17): 3625-3637.
- Musaro, A. and L. Barberi (2010).** "Isolation and culture of mouse satellite cells." *Methods Mol Biol* **633**: 101-111.
- Nagata, Y., H. Kobayashi, M. Umeda, N. Ohta, S. Kawashima, P. S. Zammit and R. Matsuda (2006).** "Sphingomyelin levels in the plasma membrane correlate with the activation state of muscle satellite cells." *J Histochem Cytochem* **54**(4): 375-384.
- Nakagawa, O., K. Fujisawa, T. Ishizaki, Y. Saito, K. Nakao and S. Narumiya (1996).** "ROCK-I and ROCK-II, two isoforms of Rho-associated coiled-coil forming protein serine/threonine kinase in mice." *FEBS Lett* **392**(2): 189-193.
- Neuhaus, P., S. Oustanina, T. Loch, M. Kruger, E. Bober, R. Dono, R. Zeller and T. Braun (2003).** "Reduced mobility of fibroblast growth factor (FGF)-deficient myoblasts might contribute to dystrophic changes in the musculature of FGF2/FGF6/mdx triple-mutant mice." *Mol Cell Biol* **23**(17): 6037-6048.
- Nicolas, N., J. C. Mira, C. L. Gallien and C. Chanoine (2000).** "Neural and hormonal control of expression of myogenic regulatory factor genes during regeneration of *Xenopus* fast muscles: myogenin and MRF4 mRNA accumulation are neurally regulated oppositely." *Dev Dyn* **218**(1): 112-122.
- Nizamutdinova, I. T., Y. M. Kim, J. I. Chung, S. C. Shin, Y. K. Jeong, H. G. Seo, J. H. Lee, K. C. Chang and H. J. Kim (2009).** "Anthocyanins from black soybean seed coats stimulate wound healing in fibroblasts and keratinocytes and prevent inflammation in endothelial cells." *Food Chem Toxicol* **47**(11): 2806-2812.
- Nizamutdinova, I. T., Y. M. Kim, H. J. Kim, H. G. Seo, J. H. Lee and K. C. Chang (2009).** "Carbon monoxide (from CORM-2) inhibits high glucose-induced ICAM-1 expression via AMP-activated protein kinase and PPAR-gamma activations in endothelial cells." *Atherosclerosis* **207**(2): 405-411.
- Nobes, C. D. and A. Hall (1995).** "Rho, rac, and cdc42 GTPases regulate the assembly of multimolecular focal complexes associated with actin stress fibers, lamellipodia, and filopodia." *Cell* **81**(1): 53-62.
- Nobes, C. D. and A. Hall (1999).** "Rho GTPases control polarity, protrusion, and adhesion during cell movement." *J Cell Biol* **144**(6): 1235-1244.
- Nobes, C. D., P. Hawkins, L. Stephens and A. Hall (1995).** "Activation of the small GTP-binding proteins rho and rac by growth factor receptors." *J Cell Sci* **108** (Pt 1): 225-233.
- O'Neill, G. M. (2009).** "The coordination between actin filaments and adhesion in mesenchymal migration." *Cell Adh Migr* **3**(4): 355-357.
- Oberringer, M., C. Meins, M. Bubel and T. Pohlemann (2007).** "A new in vitro wound model based on the co-culture of human dermal microvascular endothelial cells and human dermal fibroblasts." *Biol Cell* **99**(4): 197-207.
- Ohuchi, E., K. Imai, Y. Fujii, H. Sato, M. Seiki and Y. Okada (1997).** "Membrane type 1 matrix metalloproteinase digests interstitial collagens and other extracellular matrix macromolecules." *J Biol Chem* **272**(4): 2446-2451.

- Olguin, H. C., C. Santander and E. Brandan (2003).** "Inhibition of myoblast migration via decorin expression is critical for normal skeletal muscle differentiation." *Dev Biol* **259**(2): 209-224.
- Ornitz, D. M. (2005).** "FGF signaling in the developing endochondral skeleton." *Cytokine Growth Factor Rev* **16**(2): 205-213.
- Ornitz, D. M. and N. Itoh (2001).** "Fibroblast growth factors." *Genome Biol* **2**(3): REVIEWS3005.
- Pankov, R., E. Cukierman, B. Z. Katz, K. Matsumoto, D. C. Lin, S. Lin, C. Hahn and K. M. Yamada (2000).** "Integrin dynamics and matrix assembly: tensin-dependent translocation of alpha(5)beta(1) integrins promotes early fibronectin fibrillogenesis." *J Cell Biol* **148**(5): 1075-1090.
- Papusheva, E. and C. P. Heisenberg (2010).** "Spatial organization of adhesion: force-dependent regulation and function in tissue morphogenesis." *EMBO J* **29**(16): 2753-2768.
- Park, H. J., J. Lee, M. J. Kim, T. J. Kang, Y. Jeong, S. H. Um and S. W. Cho (2012).** "Sonic hedgehog intradermal gene therapy using a biodegradable poly(beta-amino esters) nanoparticle to enhance wound healing." *Biomaterials* **33**(35): 9148-9156.
- Peault, B., M. Rudnicki, Y. Torrente, G. Cossu, J. P. Tremblay, T. Partridge, E. Gussoni, L. M. Kunkel and J. Huard (2007).** "Stem and progenitor cells in skeletal muscle development, maintenance, and therapy." *Mol Ther* **15**(5): 867-877.
- Petrie, R. J., A. D. Doyle and K. M. Yamada (2009).** "Random versus directionally persistent cell migration." *Nat Rev Mol Cell Biol* **10**(8): 538-549.
- Pollard, T. D. and G. G. Borisy (2003).** "Cellular motility driven by assembly and disassembly of actin filaments." *Cell* **112**(4): 453-465.
- Poujade, M., E. Grasland-Mongrain, A. Hertzog, J. Jouanneau, P. Chavrier, B. Ladoux, A. Buguin and P. Silberzan (2007).** "Collective migration of an epithelial monolayer in response to a model wound." *Proc Natl Acad Sci U S A* **104**(41): 15988-15993.
- Powell, C. A., B. L. Smiley, J. Mills and H. H. Vandenberg (2002).** "Mechanical stimulation improves tissue-engineered human skeletal muscle." *Am J Physiol Cell Physiol* **283**(5): C1557-1565.
- Pownall, M. E., M. K. Gustafsson and C. P. Emerson, Jr. (2002).** "Myogenic regulatory factors and the specification of muscle progenitors in vertebrate embryos." *Annu Rev Cell Dev Biol* **18**: 747-783.
- Puri, P. L., S. Iezzi, P. Stiegler, T. T. Chen, R. L. Schiltz, G. E. Muscat, A. Giordano, L. Kedes, J. Y. Wang and V. Sartorelli (2001).** "Class I histone deacetylases sequentially interact with MyoD and pRb during skeletal myogenesis." *Mol Cell* **8**(4): 885-897.
- Quintero, A. J., V. J. Wright, F. H. Fu and J. Huard (2009).** "Stem cells for the treatment of skeletal muscle injury." *Clin Sports Med* **28**(1): 1-11.
- Raftopoulou, M. and A. Hall (2004).** "Cell migration: Rho GTPases lead the way." *Dev Biol* **265**(1): 23-32.
- Rando, T. A. and H. M. Blau (1994).** "Primary mouse myoblast purification, characterization, and transplantation for cell-mediated gene therapy." *J Cell Biol* **125**(6): 1275-1287.
- Rando, T. A., G. K. Pavlath and H. M. Blau (1995).** "The fate of myoblasts following transplantation into mature muscle." *Exp Cell Res* **220**(2): 383-389.
- Ranzato, E., V. Balbo, F. Boccafoschi, L. Mazzucco and B. Burlando (2009).** "Scratch wound closure of C2C12 mouse myoblasts is enhanced by human platelet lysate." *Cell Biol Int* **33**(9): 911-917.
- Ratajczak, M. Z., M. Majka, M. Kucia, J. Drukala, Z. Pietrzowski, S. Peiper and A. Janowska-Wieczorek (2003).** "Expression of functional CXCR4 by muscle satellite cells and secretion of SDF-1 by muscle-derived fibroblasts is associated with the presence of both muscle progenitors in bone marrow and hematopoietic stem/progenitor cells in muscles." *Stem Cells* **21**(3): 363-371.
- Ravin, R., D. J. Hoeppner, D. M. Munno, L. Carmel, J. Sullivan, D. L. Levitt, J. L. Miller, C. Athaide, D. M. Panchision and R. D. McKay (2008).** "Potency and fate specification in CNS stem cell populations in vitro." *Cell Stem Cell* **3**(6): 670-680.

- Reigle, K. L., G. Di Lullo, K. R. Turner, J. A. Last, I. Chervoneva, D. E. Birk, J. L. Funderburgh, E. Elrod, M. W. Germann, C. Surber, R. D. Sanderson and J. D. San Antonio (2008).** "Non-enzymatic glycation of type I collagen diminishes collagen-proteoglycan binding and weakens cell adhesion." *J Cell Biochem* **104**(5): 1684-1698.
- Ricard-Blum, S. and F. Ruggiero (2005).** "The collagen superfamily: from the extracellular matrix to the cell membrane." *Pathol Biol (Paris)* **53**(7): 430-442.
- Richler, C. and D. Yaffe (1970).** "The in vitro cultivation and differentiation capacities of myogenic cell lines." *Dev Biol* **23**(1): 1-22.
- Ridley, A. J. (2001)a.** "Rho family proteins: coordinating cell responses." *Trends Cell Biol* **11**(12): 471-477.
- Ridley, A. J. (2001)b.** "Rho GTPases and cell migration." *J Cell Sci* **114**(Pt 15): 2713-2722.
- Ridley, A. J. and A. Hall (1992).** "Distinct patterns of actin organization regulated by the small GTP-binding proteins Rac and Rho." *Cold Spring Harb Symp Quant Biol* **57**: 661-671.
- Ridley, A. J. and A. Hall (1992).** "The small GTP-binding protein rho regulates the assembly of focal adhesions and actin stress fibers in response to growth factors." *Cell* **70**(3): 389-399.
- Riquelme, C., J. Larrain, E. Schonherr, J. P. Henriquez, H. Kresse and E. Brandan (2001).** "Antisense inhibition of decorin expression in myoblasts decreases cell responsiveness to transforming growth factor beta and accelerates skeletal muscle differentiation." *J Biol Chem* **276**(5): 3589-3596.
- Roberts, A. B., B. K. McCune and M. B. Sporn (1992).** "TGF-beta: regulation of extracellular matrix." *Kidney Int* **41**(3): 557-559.
- Rout, U. K., G. M. Saed and M. P. Diamond (2002).** "Transforming growth factor-beta1 modulates expression of adhesion and cytoskeletal proteins in human peritoneal fibroblasts." *Fertil Steril* **78**(1): 154-161.
- Ruhland, C., E. Schonherr, H. Robenek, U. Hansen, R. V. Iozzo, P. Bruckner and D. G. Seidler (2007).** "The glycosaminoglycan chain of decorin plays an important role in collagen fibril formation at the early stages of fibrillogenesis." *FEBS J* **274**(16): 4246-4255.
- Rushton, I. (2007).** "Understanding the role of proteases and pH in wound healing." *Nurs Stand* **21**(32): 68, 70, 72 passim.
- Rushton, J. L., I. Davies, M. A. Horan, M. Mahon and R. Williams (1997).** "Production of consistent crush lesions of murine skeletal muscle in vivo using an electromechanical device." *J Anat* **190** (Pt 3): 417-422.
- Sacco, A., R. Doyonnas, P. Kraft, S. Vitorovic and H. M. Blau (2008).** "Self-renewal and expansion of single transplanted muscle stem cells." *Nature* **456**(7221): 502-506.
- Sahai, E. and C. J. Marshall (2003).** "Differing modes of tumour cell invasion have distinct requirements for Rho/ROCK signalling and extracellular proteolysis." *Nat Cell Biol* **5**(8): 711-719.
- Saihara, R., H. Komuro, Y. Urita, K. Hagiwara and M. Kaneko (2009).** "Myoblast transplantation to defecation muscles in a rat model: a possible treatment strategy for fecal incontinence after the repair of imperforate anus." *Pediatr Surg Int* **25**(11): 981-986.
- Sanders, L. C., F. Matsumura, G. M. Bokoch and P. de Lanerolle (1999).** "Inhibition of myosin light chain kinase by p21-activated kinase." *Science* **283**(5410): 2083-2085.
- Sanes, J. R. (2003).** "The basement membrane/basal lamina of skeletal muscle." *J Biol Chem* **278**(15): 12601-12604.
- Sato, M., M. Markiewicz, M. Yamanaka, A. Bielawska, C. Mao, L. M. Obeid, Y. A. Hannun and M. Trojanowska (2003).** "Modulation of transforming growth factor-beta (TGF-beta) signaling by endogenous sphingolipid mediators." *J Biol Chem* **278**(11): 9276-9282.
- Schabort, E. J., M. van der Merwe, B. Loos, F. P. Moore and C. U. Niesler (2009).** "TGF-beta's delay skeletal muscle progenitor cell differentiation in an isoform-independent manner." *Exp Cell Res* **315**(3): 373-384.
- Schlotzer-Schrehardt, U., M. Kuchle, C. Hofmann-Rummelt, A. Kaiser and T. Kirchner (2000).** "[Latent TGF-beta 1 binding protein (LTBP-1); a new marker for intra- and extraocular PEX deposits]." *Klin Monbl Augenheilkd* **216**(6): 412-419.

- Schmidt, G., H. Hausser and H. Kresse (1991).** "Interaction of the small proteoglycan decorin with fibronectin. Involvement of the sequence NKISK of the core protein." *Biochem J* **280** (Pt 2): 411-414.
- Schmitz, A. A., E. E. Govek, B. Bottner and L. Van Aelst (2000).** "Rho GTPases: signaling, migration, and invasion." *Exp Cell Res* **261**(1): 1-12.
- Schonherr, E., M. Broszat, E. Brandan, P. Bruckner and H. Kresse (1998).** "Decorin core protein fragment Leu155-Val260 interacts with TGF-beta but does not compete for decorin binding to type I collagen." *Arch Biochem Biophys* **355**(2): 241-248.
- Schonherr, E., B. Levkau, L. Schaefer, H. Kresse and K. Walsh (2001).** "Decorin-mediated signal transduction in endothelial cells. Involvement of Akt/protein kinase B in up-regulation of p21(WAF1/CIP1) but not p27(KIP1)." *J Biol Chem* **276**(44): 40687-40692.
- Scott, J. E. and M. Haigh (1985).** "Small'-proteoglycan:collagen interactions: keratan sulphate proteoglycan associates with rabbit corneal collagen fibrils at the 'a' and 'c' bands." *Biosci Rep* **5**(9): 765-774.
- Seale, P. and M. A. Rudnicki (2000).** "A new look at the origin, function, and "stem-cell" status of muscle satellite cells." *Dev Biol* **218**(2): 115-124.
- Seale, P., L. A. Sabourin, A. Girgis-Gabardo, A. Mansouri, P. Gruss and M. A. Rudnicki (2000).** "Pax7 is required for the specification of myogenic satellite cells." *Cell* **102**(6): 777-786.
- Serrano, A. L., C. J. Mann, B. Vidal, E. Ardite, E. Perdiguero and P. Munoz-Canoves (2011).** "Cellular and molecular mechanisms regulating fibrosis in skeletal muscle repair and disease." *Curr Top Dev Biol* **96**: 167-201.
- Shapiro, S. D. (1998).** "Matrix metalloproteinase degradation of extracellular matrix: biological consequences." *Curr Opin Cell Biol* **10**(5): 602-608.
- Shefer, G., D. P. Van de Mark, J. B. Richardson and Z. Yablonka-Reuveni (2006).** "Satellite-cell pool size does matter: defining the myogenic potency of aging skeletal muscle." *Dev Biol* **294**(1): 50-66.
- Sheffer, Y., O. Leon, J. H. Pinthus, A. Nagler, Y. Mor, O. Genin, M. Iluz, N. Kawada, K. Yoshizato and M. Pines (2007).** "Inhibition of fibroblast to myofibroblast transition by halofuginone contributes to the chemotherapy-mediated antitumoral effect." *Mol Cancer Ther* **6**(2): 570-577.
- Shi, J. and L. Wei (2007).** "Rho kinase in the regulation of cell death and survival." *Arch Immunol Ther Exp (Warsz)* **55**(2): 61-75.
- Shi, Y. and J. Massague (2003).** "Mechanisms of TGF-beta signaling from cell membrane to the nucleus." *Cell* **113**(6): 685-700.
- Siegel, A. L., K. Atchison, K. E. Fisher, G. E. Davis and D. D. Cornelison (2009).** "3D timelapse analysis of muscle satellite cell motility." *Stem Cells* **27**(10): 2527-2538.
- Small, J. V., T. Stradal, E. Vignal and K. Rottner (2002).** "The lamellipodium: where motility begins." *Trends Cell Biol* **12**(3): 112-120.
- Smith, J. A., L. A. Samayawardhena and A. W. Craig (2010).** "Fps/Fes protein-tyrosine kinase regulates mast cell adhesion and migration downstream of Kit and beta1 integrin receptors." *Cell Signal* **22**(3): 427-436.
- Strachan, L. R. and M. L. Condic (2004).** "Cranial neural crest recycle surface integrins in a substratum-dependent manner to promote rapid motility." *J Cell Biol* **167**(3): 545-554.
- Streuli, C. H. and N. Akhtar (2009).** "Signal co-operation between integrins and other receptor systems." *Biochem J* **418**(3): 491-506.
- Suelves, M., B. Vidal, V. Ruiz, B. Baeza-Raja, A. Diaz-Ramos, I. Cuartas, F. Lluís, M. Parra, M. Jardí, R. Lopez-Aleman, A. L. Serrano and P. Munoz-Canoves (2005).** "The plasminogen activation system in skeletal muscle regeneration: antagonistic roles of urokinase-type plasminogen activator (uPA) and its inhibitor (PAI-1)." *Front Biosci* **10**: 2978-2985.
- Sulochana, K. N., H. Fan, S. Jois, V. Subramanian, F. Sun, R. M. Kini and R. Ge (2005).** "Peptides derived from human decorin leucine-rich repeat 5 inhibit angiogenesis." *J Biol Chem* **280**(30): 27935-27948.

- Suzuki, S., K. Yamanouchi, C. Soeta, Y. Katakai, R. Harada, K. Naito and H. Tojo (2002).** "Skeletal muscle injury induces hepatocyte growth factor expression in spleen." Biochem Biophys Res Commun **292**(3): 709-714.
- Svensson, L., D. Heinegard and A. Oldberg (1995).** "Decorin-binding sites for collagen type I are mainly located in leucine-rich repeats 4-5." J Biol Chem **270**(35): 20712-20716.
- Takaguri, A., K. Kimura, A. Hinoki, A. M. Bourne, M. V. Autieri and S. Eguchi (2011).** "A disintegrin and metalloprotease 17 mediates neointimal hyperplasia in vasculature." Hypertension **57**(4): 841-845.
- Tamada, M., T. D. Perez, W. J. Nelson and M. P. Sheetz (2007).** "Two distinct modes of myosin assembly and dynamics during epithelial wound closure." J Cell Biol **176**(1): 27-33.
- Tatsumi, R., J. E. Anderson, C. J. Nevoret, O. Halevy and R. E. Allen (1998).** "HGF/SF is present in normal adult skeletal muscle and is capable of activating satellite cells." Dev Biol **194**(1): 114-128.
- Ten Broek, R. W., S. Grefte and J. W. Von den Hoff (2010).** "Regulatory factors and cell populations involved in skeletal muscle regeneration." J Cell Physiol **224**(1): 7-16.
- Thorrez, L., J. Shansky, L. Wang, L. Fast, T. VandenDriessche, M. Chuah, D. Mooney and H. Vandenburgh (2008).** "Growth, differentiation, transplantation and survival of human skeletal myofibers on biodegradable scaffolds." Biomaterials **29**(1): 75-84.
- Tian, W., B. Li, X. Zhang, W. Dang, X. Wang, H. Tang, L. Wang, H. Cao and T. Chen (2012).** "Suppression of tumor invasion and migration in breast cancer cells following delivery of siRNA against Stat3 with the antimicrobial peptide PR39." Oncol Rep **28**(4): 1362-1368.
- Tidball, J. G. (2005).** "Inflammatory processes in muscle injury and repair." Am J Physiol Regul Integr Comp Physiol **288**(2): R345-353.
- Tremblay, L., F. Valenza, S. P. Ribeiro, J. Li and A. S. Slutsky (1997).** "Injurious ventilatory strategies increase cytokines and c-fos m-RNA expression in an isolated rat lung model." J Clin Invest **99**(5): 944-952.
- Usas, A., J. Maciulaitis, R. Maciulaitis, N. Jakuboniene, A. Milasius and J. Huard (2011).** "Skeletal muscle-derived stem cells: implications for cell-mediated therapies." Medicina (Kaunas) **47**(9): 469-479.
- Valluru, M., C. A. Staton, M. W. Reed and N. J. Brown (2011).** "Transforming Growth Factor-beta and Endoglin Signaling Orchestrate Wound Healing." Front Physiol **2**: 89.
- Vandenburgh, H. (2010).** "High-content drug screening with engineered musculoskeletal tissues." Tissue Eng Part B Rev **16**(1): 55-64.
- Vandenburgh, H., J. Shansky, F. Benesch-Lee, V. Barbata, J. Reid, L. Thorrez, R. Valentini and G. Crawford (2008).** "Drug-screening platform based on the contractility of tissue-engineered muscle." Muscle Nerve **37**(4): 438-447.
- Velnar, T., T. Bailey and V. Smrkolj (2009).** "The wound healing process: an overview of the cellular and molecular mechanisms." J Int Med Res **37**(5): 1528-1542.
- Verrecchia, F. and A. Mauviel (2007).** "Transforming growth factor-beta and fibrosis." World J Gastroenterol **13**(22): 3056-3062.
- Vicente-Manzanares, M., J. Zareno, L. Whitmore, C. K. Choi and A. F. Horwitz (2007).** "Regulation of protrusion, adhesion dynamics, and polarity by myosins IIA and IIB in migrating cells." J Cell Biol **176**(5): 573-580.
- Wagers, A. J. (2008).** "Wnt not, waste not." Cell Stem Cell **2**(1): 6-7.
- Wang, X. B., X. Y. Tian, Y. Li, B. Li and Z. Li (2012).** "Elevated expression of macrophage migration inhibitory factor correlates with tumor recurrence and poor prognosis of patients with gliomas." J Neurooncol **106**(1): 43-51.
- Watanabe, N., T. Kato, A. Fujita, T. Ishizaki and S. Narumiya (1999).** "Cooperation between mDia1 and ROCK in Rho-induced actin reorganization." Nat Cell Biol **1**(3): 136-143.
- Weber, I. T., R. W. Harrison and R. V. Iozzo (1996).** "Model structure of decorin and implications for collagen fibrillogenesis." J Biol Chem **271**(50): 31767-31770.
- Wehrle-Haller, B. and B. Imhof (2002).** "The inner lives of focal adhesions." Trends Cell Biol **12**(8): 382-389.

- Wennerberg, K., M. A. Forget, S. M. Ellerbroek, W. T. Arthur, K. Burrige, J. Settleman, C. J. Der and S. H. Hansen (2003).** "Rnd proteins function as RhoA antagonists by activating p190 RhoGAP." Curr Biol **13**(13): 1106-1115.
- Yamaguchi, Y., D. M. Mann and E. Ruoslahti (1990).** "Negative regulation of transforming growth factor-beta by the proteoglycan decorin." Nature **346**(6281): 281-284.
- Young, M. F., Y. Bi, L. Ameye, T. Xu, S. Wadhwa, A. Heegaard, T. Kilts and X. D. Chen (2006).** "Small leucine-rich proteoglycans in the aging skeleton." J Musculoskelet Neuronal Interact **6**(4): 364-365.
- Zammit, P. S. (2008).** "All muscle satellite cells are equal, but are some more equal than others?" J Cell Sci **121**(Pt 18): 2975-2982.
- Zammit, P. S., J. P. Golding, Y. Nagata, V. Hudon, T. A. Partridge and J. R. Beauchamp (2004).** "Muscle satellite cells adopt divergent fates: a mechanism for self-renewal?" J Cell Biol **166**(3): 347-357.
- Zanotti, S., T. Negri, C. Cappelletti, P. Bernasconi, E. Canioni, C. Di Blasi, E. Pegoraro, C. Angelini, P. Ciscato, A. Prella, R. Mantegazza, L. Morandi and M. Mora (2005).** "Decorin and biglycan expression is differentially altered in several muscular dystrophies." Brain **128**(Pt 11): 2546-2555.
- Zengel, P., A. Nguyen-Hoang, C. Schildhammer, R. Zantl, V. Kahl and E. Horn (2011).** "mu-Slide Chemotaxis: a new chamber for long-term chemotaxis studies." BMC Cell Biol **12**(1): 21.
- Zhang, Z., T. M. Garron, X. J. Li, Y. Liu, X. Zhang, Y. Y. Li and W. S. Xu (2009).** "Recombinant human decorin inhibits TGF-beta1-induced contraction of collagen lattice by hypertrophic scar fibroblasts." Burns **35**(4): 527-537.
- Zhu, J., Y. Li, W. Shen, C. Qiao, F. Ambrosio, M. Lavasani, M. Nozaki, M. F. Branca and J. Huard (2007).** "Relationships between transforming growth factor-beta1, myostatin, and decorin: implications for skeletal muscle fibrosis." J Biol Chem **282**(35): 25852-25863.
- Zicha, D., G. A. Dunn and A. F. Brown (1991).** "A new direct-viewing chemotaxis chamber." J Cell Sci **99** (Pt 4): 769-775.
- Zigmond, S. H. (1988).** "Orientation chamber in chemotaxis." Methods Enzymol **162**: 65-72.